Low fluence UV-B as a positive regulator of photosynthesis in *Arabidopsis thaliana*

A thesis presented in partial fulfilment of the requirements for the degree of

Doctor of Philosophy in Agriculture and Horticulture

At Massey University, Palmerston North, New Zealand

Rixta F. T. Sievers

2019

Abstract

UV-B radiation can induce a wide range of developmental responses in plants, and magnitudes of UV-B exposure can also vary greatly. Historically, research into the effects of UV-B radiation on photosynthetic processes has often utilised high fluence rates of UV-B, which have been frequently shown to impede photosynthetic performance and induce photosystem damage. More recently, a number of studies have focused on the impact of low fluence UV-B exposure, and have found that such treatments can be beneficial to photosynthesis by upregulating photosynthetic performance. The aim of this PhD was to understand the consequences of low fluence UV-B exposure on net photosynthetic rate and underlying mechanistic responses. We characterised the photosynthetic response to 0.5 µmol m^{-2} s^{-1} of UV-B and established that net photosynthetic rate increased by 12% in wild type *Arabidopsis* plants at 24hrs of UV-B exposure. Through analysis of knockout lines for the UV-B photoreceptor UVR8, we determined that the photosynthesis phenotype is dependent on the presence of UVR8. To determine how low fluence UV-B exposure mediates the increase in photosynthetic rate, transcriptomic analysis via RNA-seq was undertaken. Our analysis showed that UV-B exposure results in the upregulation of photosynthesis-associated genes during the initial exposure period. The most highly upregulated genes were related to chloroplast biogenesis and synthesis of photosynthetic proteins within the chloroplast, as well as chloroplastic oxidoreductase activity. We further investigated three of these candidates: *RBF1, TOC33* and *TFP*, and found that each of those genes plays a role in the UV-B mediated increase of photosynthetic rate at 24hrs and that the upregulation of these genes in response to UV-B exposure is regulated by UVR8. Taken together, we describe here for the first time, that low fluence UV-B increases net photosynthetic rate through UVR8-mediated upregulation of key genes, resulting in increased synthesis of chloroplastic photosynthesis-associated proteins and chloroplastic oxidoreductase activity. This further extends our knowledge of UV-B plant-response and offers further potential for exploitation of UV-B photomorphogenesis in agriculture.

Acknowledgements

Foremost, I would like to thank my supervisor Dr Jason Wargent, for his continued support and input throughout my PhD, as well as his patience, motivation, and enthusiasm throughout this endeavour. I would also like to thank Professor Gareth Jenkins, for his guidance, insightful inputs, and support. Furthermore, I would like to thank Dr Paul Dijkwel for his inputs and the use of his lab for all of my experimental work.

I would also like to acknowledge the Marsden Fund, administered by the Royal Society of New Zealand; for the funding of this PhD project. I would also like to thank BioLumic Ltd for the use of the LED arrays allowing me to undertake this work. Furthermore, I would like to thank Professor Peter Lockhart for the use of the IRGA. As well as Dr Dave Wheeler for all the help with the RNA-seq data.

I would like to thank the members of the lab D5.13, and the staff at the PGU for all the support along the way.

To the friends who have helped me along the way and have helped me through this - thank you.

Lastly, I would like to thank my family for their continued love and support; none of this would have been possible without you. Danke.

Contents

Abbreviations

+UVB	UV-B exposure
-UVB	no UV-B exposure
6-4 PPs	Pyrimidine (6-4) Pyrimidinone dimers
ABC transporter	ATP-Binding Cassette transporter
ABCB13	ATP-BINDING CASSETTE B13
ABRC	Arabidopsis Biological Resource Center
APG3	ALBINO AND PALE GREEN 3
BLRP	Blue Light Responsive Promoter
bp	base pairs
BPG3	BRZ-INSENSITIVE-PALE GREEN 3
CAB proteins	CHLOROPHYLL A-B BINDING proteins
CFCs	Chlorofluorocarbons
CHO metabolism	Carbohydrate metabolism
CHS	CHALCONE SYNTHASE
Col-0	Columbia-0
COP1	CONSTITUTIVELY PHOTOMORPHOGENIC 1
CPDs	Cyclobutane pyrimidine dimers
CRY	Cryptochrome
DAS	Days After Sowing
DEGs	Differentially expressed genes
ELIP1	EARLY LIGHT-INDUCIBLE PROTEIN 1
ELIP2	EARLY LIGHT-INDUCIBLE PROTEIN 2
FAD	Flavin Adenine Dinucleotide
FDR	False Discovery Rate
FMN	Flavin Mononucleotide
FtsH	ATP-dependent metalloproteases
GM	Genetic modification
HY5	ELONGATED HYPOCOTYL 5
HYH	HY5 HOMOLOG
IR	Infrared light
IRGA	Infra-Red Gas Analyzer
LEDs	Light Emitting Diodes
L*er*	Landsberg erecta
LFC	log2foldchange
LHCII	LIGHT HARVESTING CHLOROPHYLL protein complex II
LOV domains	LIGHT, OXYGEN OR VOLTAGE domains
lug444	*leunig-444*
luh4	*leunig-like-4*
mt	Mutant
MTHF	Methenyltetrahydrofolate
NZGL	New Zealand Genomics Limited
OEC	OXYGEN EVOLVING COMPLEX
padj	p adjusted value

PAR	Photosynthetically Active Radiation
PIF	PHYTOCHROME INTERACTING FACTOR
PCR	POLYMERASE CHAIN REACTION
PDE327	PIGMENT DEFECTIVE 327
PDIL1-2	PROTEIN DISULFIDE ISOMERASE 1-2
PEP	Plastid-encoded Polymerase
PHY	Phytochrome
ppi1	*plastid protein import 1*
PS I	Photosystem I
PS II	Photosystem II
PSB28	PHOTOSYSTEM II REACTION CENTRE PSB28
PTAC14	PLASTID TRANSCRIPTIONALLY ACTIVE 14
qRT-PCR	Quantitative Real-Time Polymerase Chain Reaction
RBF1	RIBOSOME-BINDING FACTOR 1
rbf1-1	*ribosome-binding factor 1-1*
rbf1-2	*ribosome-binding factor 1-2*
RbfA	Ribosome binding factor A
RNA-seq	RNA sequencing
RNEE/G	RNASE E/G-LIKE
ROS	Reactive Oxygen Species
RuBisCO	Ribulose-1,5-bisphosphate carboxylase/oxygenase
RUP1	REPRESSOR OF UV-B PHOTOMORPHOGENESIS 1
rup1,2	*repressor of UV-B photomorphogenesis 1,2*
RUP2	REPRESSOR OF UV-B PHOTOMORPHOGENESIS 2
RUS1	ROOT UV-B SENSITIVE 1
seu-4	*seuss-4*
SIG5	SIGMA FACTOR 5
sig5-1 (sig5.1)	*sigma factor 5-1*
sig5-2	*sigma factor 5-2*
TAC	Transcriptionally Active Chromosome
TFP	Thioredoxin Family Protein
TOC	Translocon At The Outer Envelope Membrane Of Chloroplast
TOC33	TRANSLOCON AT THE OUTER ENVELOPE MEMBRANE OF CHLOROPLAST 33
Trp	Tryptophan
UV	Ultraviolet light
UV-B	Ultraviolet light B
UVR8	ULTRAVIOLET-B RESISTANCE LOCUS 8
uvr8-1	*UV-B resistance locus 8-1*
uvr8-6	*UV-B resistance locus 8-6*
WL	White Light
wt	wild type
ZTL proteins	Zeitlupe proteins

List of Figures

List of Tables

1 Introduction & Literature Review

1.1 Introduction

The population of earth is currently estimated to be 7.6 billion people (UN, 2017). Although the rate of population growth has slowed, it is estimated that the population will rise to 8.6 billion by 2030; and increase to 10 billion by 2050 (FAO, 2017; UN, 2017). The growing population brings with it many challenges. Not only does it pose the question as to how to regulate the increase in population, but also as to how to keep up with the increasing demand for food. At present global food production is sufficient to feed the global population (FAO et al., 2012). This is due to a striking increase in food production over the last fifty years, despite the global population nearly doubling in size at the same time (Godfray et al., 2010). However, global food demand is projected to be 60% higher in 2050 than it was in 2006 (FAO, 2016), therefore food security remains an issue.

In 2016 there were an estimated 815 million undernourished people (FAO et al., 2017). Calorific undernourishment is not the only problem; further problems are caused when people suffer from micronutrient deficiencies, as well as having insufficient protein supply in their diet, due to limited access to diverse food sources (FAO, 2014). Nevertheless, these numbers are a marked decrease from the turn of the century when 14.9% of the population were undernourished (FAO et al., 2015). However, as much as has been done to combat food insecurity, over the coming decades global demand for food is going to increase further, and food security will remain an issue, especially in the face of global climate and environmental changes.

The increase in population requires innovative ways to keep up with demand for food as well as ways to improve food security and prevent malnourishment. Key to increasing food production further is the ability to produce food environmentally and socially sustainably. Traditionally, in order to produce more food, new land was cleared for agricultural purposes (Godfray et al., 2010). While food production has increased by over 50%, land use has only increased by 9%

(Pretty, 2008), which suggests that more land would be available for agricultural purposes. However, the amount of available land is likely to decrease in the coming years due to soil degradation (Nellemann et al., 2009), global climate change (IPCC, 2007) and the demand for land for other human activities as well as the need to protect carbon sinks (such as the rainforests) and biodiversity (Balmford et al., 2005).

One way of increasing food production is through the use of traditional plant breeding. Many of the high yield crops used today have been produced by selecting for increased yield under specific conditions (Tester and Langridge, 2010). However, traditional breeding faces some key difficulties, including a lack of resources, capability and genetic diversity present, as well as the lengthy time spans involved in these breeding programs (Godfray et al., 2010; Tester and Langridge, 2010).

Therefore, the development of other plant molecular methods for increasing food production are necessary. One potential solution is the use of genetically modified crop species. Use of genetic modification (GM) allows for the generation of novel variation in populations (Table 1.1). Common applications are the use of GM to introduce to proteinaceous toxins into crop species to increase pest resistance (Tester and Langridge, 2010), as well as using GM to increase photosynthetic efficiency (Godfray et al., 2010). However, in many parts of society opposition to GM has become the norm, and thus in many countries, the access and use of GM has been severely restricted (Tester and Langridge, 2010), which limits the potential of GM to increase crop production. Hence, it is likely that over the next decade traditional breeding approaches will continue to be used in order to improve crop yields. Furthermore, the development and use of CRISPR/Cas9 genome editing to enhance abiotic and biotic stress tolerance in crops will likely play an important role in the future development of non GM crops (Haque et al., 2018; Jaganathan et al., 2018). It is also likely that more research into GM will eventually allow for a wider acceptance of the technology and modified crop species (Tester and Langridge, 2010).

Table 1.1 Potential uses of GM technology to further improve target crop species by the manipulation of key traits of the plant over the next twenty years. Adapted from Godfray et al. (2010)

Target traits	Potential Target Crops
Increased tolerance to herbicides	Maize and Soybean
Increased resistance to insects and pests	Cotton and Oilseed Brassica
Nutritional bio-fortification	Staple cereal crops
Increased resistance against fungus and viruses	Fruits and Vegetables
Improved storage capacity	Rice, Fruits, and Vegetables
Drought, temperature and salinity tolerance	Wheat
Increased nitrogen use and nitrogen fixation efficiency	Staple cereal and tuber crops
Increased photosynthetic efficiency	Staple cereal and tuber crops

The use of breeding technologies are not the only possible mechanisms of increasing food crop production as well as there is evidence to suggest that crop yield optimisation through breeding is nearing its biological limit (Zhu et al., 2010). Consequently, improving crop yields through environmental influences is of arguably greater importance than ever before. Possible avenues of exploration include the improving of photosynthetic performance through manipulation of the light environment to increase agricultural yields. A possible approach is through the addition of UV-B (Ultraviolet light B) to spectrum to improve crop stress tolerance (Wargent and Jordan, 2013).

The research presented in this thesis focuses on the addition of low fluence rate UV-B radiation to the spectrum to alter photosynthetic performance. The focus being on developing a better understanding of the regulatory effects of UV-B radiation on photosynthetic function.

1.2 Understanding light

The sun emits a spectrum of electromagnetic radiation; most of which is absorbed by the earth's atmosphere (Aphalo et al., 2012). The wavelengths that reach the earth's surface range from the high energy ultraviolet (UV) wavelengths (100 – 400 nm), through the visible light wavelengths (400 – 700 nm) to the lower energy infrared (IR) wavelengths (> 700 nm). Light particles, known as photons, in the visible part of the spectrum are perceived by photosynthetic apparatus (Aphalo et al., 2012). In plants, the perception of light begins a photochemical event,

which results in a number of different downstream responses specific to the type of light perceived. The different responses to different types and wavelengths of light have been closely studied, and have provided much insight into the complexity of light-mediated effects on plant growth and development, or 'photomorphogenesis'.

Plants have the ability to perceive UV light, which makes up approximately 7% of the electromagnetic radiation emitted by the sun (Frohnmeyer and Staiger, 2003). UV light is split into three distinctive parts; UV-C (100 – 280 nm), UV-B (280 – 315 nm) and UV-A (315 – 400 nm) (Frohnmeyer and Staiger, 2003). The ozone layer affects the transmission of UV light to the earth's surface and changes the composition of UV light reaching the surface (Frohnmeyer and Staiger, 2003). UV-C is completely absorbed by the ozone layer, and only limited amounts of UV-B pass through, it severely reduces the amounts of UV-B that reach the surface, whereas UV-A passes through the ozone layer unaffected (Frohnmeyer and Staiger, 2003), but is limited by the presence of pollutants in the troposphere.

1.3 UV-B – Ultraviolet light B

Due to their sessile nature, plants are routinely exposed to UV-B radiation. There is a great deal of variation in the amounts and quality of UV radiation that the plants are exposed to; as both amounts and quality are affected by latitude, altitude, seasons, cloud and canopy cover as well as the presence of pollutants in the air (Jenkins, 2009; Aphalo et al., 2012). Thus plants can use UV-B radiation as a way to determine where they are situated within a particular environment; similarly to the way plants use the ratio of red to far-red light to grow as to avoid shading by other plants and determining the time of day (Aphalo et al., 2012).

UV-B wavelengths are the highest energy wavelengths to reach the earth's surface. Due to the high energy, these wavelengths can have a detrimental effect on exposed cells, such as impairing cellular process, damaging macromolecules such as DNA and creating reactive oxygen species (ROS) (Jansen et al., 1998; Britt, 1999; Brosché et al., 2002). During the earth's evolution much

higher levels of UV-B used to reach the earth's surface and thus organisms have had to evolve mechanisms to protect against or repair UV damage; such as producing phenolic compounds, which act as a sunscreen of sort (Jordan, 1996; Bornman et al., 1997), as well as producing DNA photolyases to protect against UV-dependent DNA damage (Chen et al., 1994; Ahmad et al., 1997). The formation of the ozone layer greatly reduced the amount of UV-B reaching the surface. However, in 1985, researchers discovered a thinning of the ozone layer above the Antarctic during the summer months (Farman et al., 1985), later to be commonly known as the hole in the ozone layer. As early as 1970 it was known that nitrogen oxides present in the atmosphere, due to both natural processes and human activity, have the ability to decompose the stratospheric ozone (Crutzen, 1970). By 1974, more man-made pollutants, especially chlorofluorocarbons (CFCs) were found to destroy ozone (Molina and Rowland, 1974). CFCs are reduced by UV light in the stratosphere, and the resulting free chlorine atoms which catalytically destroy ozone (Molina and Rowland, 1974). The combination of all these factors resulted in the thinning of the ozone layer, and in the last 50 years, ozone levels have decreased by approximately 5% (Pyle, 1997); leading to more UV-B reaching the surface. Continued increases in UV-B radiation reaching the surface could have serious implications for all living organisms (Xiong and Day, 2001; Caldwell et al., 2003). The prospect of further loss of ozone resulted in the Montreal Protocol being signed in 1987 to reduce the release of CFCs and protect the atmospheric ozone layer.

The loss of ozone in the atmosphere resulted in an increase in UV-B related research from the 1980s onwards, as increasing the ambient UV-B levels would have had possibly catastrophic effects of plant life (Caldwell, 1971; Caldwell et al., 1989; Caldwell and Flint, 1994). As time went on it became clear that the interactions between different wavebands of the solar spectrum are very important as to how plants respond to high levels of certain wavelengths. And since the 1990s there has been an increased interest in studying "normal" levels of UV-B radiation to learn

more about the photomorphogenic response of UV-B rather than the stress responses studied (Paul, 2001; Aphalo, 2003; Jansen and Bornman, 2012).

1.3.1 Effects of UV-B radiation on plants

Despite making up less than 1% of the sun's radiation that reaches earth (Rastogi et al., 2010), at high fluence rates UV-B can be highly damaging to plants. Some of the potential targets of UV-B radiation on plants are summarised in Table 1.2.

Table 1.2 Possible targets of high fluence UV-B radiation and plant response. Adapted from Jordan (1996); Jansen et al. (1998); Jenkins (2017)

Targets of UV-B radiation in plants
DNA: Formation of photoproducts - cyclobutane pyrimidine dimers (CPDs) and pyrimidine (6-4) pyrimidinone dimers (6-4 PPs)
Photosynthetic apparatus: Inactivation of photosystem II (PS II) and degradation of the D1 and D2 proteins Reduced activity of RuBisCO and other key enzymes as well as decreased levels of chlorophyll Changes in chloroplast ultrastructure
Secondary metabolism: Activation of UV-B photoreceptor – UV-B resistance locus 8 (UVR8) Accumulation of flavonoids and anthocyanins Accumulation of alkaloids and cuticle waxes Decreased levels of carotenoids
Production of free radicals: Production of Reactive Oxygen Species
Physiological effects: Thicker leaves Reduced growth Reduction of pollen fertility Inhibition of shade avoidance Inhibition of thermomorphogenesis

One of the major targets of damage by high fluence UV-B is DNA (Britt et al., 1993; Jansen et al., 1998). The absorption of UV-B by DNA causes phototransformations, resulting in the production of cyclobutane pyrimidine dimers (CPDs) and pyrimidine (6-4) pyrimidinone dimers (6-4 PPs) (Britt and May, 2003; Britt, 2004). To avoid the cytotoxic effects of these photoproducts, they need to be repaired prior to replication (Britt and May, 2003). One way is the use of photolyases, which bind to the photoproducts and restore the DNA integrity via electron transfer (Hoffman

et al., 1996; Ahmad et al., 1997). *Arabidopsis thaliana* has two types of photolyases, specific for either CPDs or 6-4 PPs (Hoffman et al., 1996; Ahmad et al., 1997). While the 6-4 PP photolyase protein is constitutively expressed, the CPD photolyase is induced by UV-B exposure (Waterworth et al., 2002). DNA damage can also be repaired through nucleotide excision repair in darkness (Liu et al., 2000) as well as homologous recombination (Ries et al., 2000b).

When treated with high fluence rates of UV-B, plants are found to be reduced in growth as well having thicker leaves and higher amounts of cuticular waxes. Furthermore, a reduction in photosynthetic activity can be seen, as the D1 and D2 proteins of photosystem II (PS II) are degraded; as well as a reduction in pollen fertility (Jansen et al., 1998; Caldwell et al., 2003; Caldwell et al., 2007). Higher plants have evolved several protective mechanisms, such as the generation of flavonoid and anthocyanin compounds in epidermal cells, which act as a sunscreen by absorbing the UV light and protecting the deeper cell levels, and the development of cellular antioxidant system and cuticle waxes (Jordan, 1996; Bornman et al., 1997; Jansen et al., 1998).

However, UV-B also plays an important role in the photomorphogenic development of plants. When the UV-B photoreceptor in the plants detects UV-B, a large number of genes are differentially regulated in response to UV-B, affecting plant morphology (Wu et al., 2013). Plants respond differently to different levels of UV-B radiation; stimulating varying levels of protection and repair mechanisms to mitigate the stress produced. Low fluence rates may be beneficial to the plant as it promotes cotyledon opening, inhibits stem extension and promotes the synthesis of flavonoids, some of which may be involved in deterring pathogens and are thus beneficial to the plant (Kim et al., 1998; Frohnmeyer et al., 1999; Boccalandro et al., 2001; Brosché and Strid, 2003; Suesslin and Frohnmeyer, 2003; Ulm et al., 2004).

UV-B further modulates the photomorphogenic response in plants by inhibiting the shade avoidance response through enhancing the degradation and inhibition of PIF (PHYTOCHROME INTERACTING FACTORS) function (Hayes et al., 2014; Mazza and Ballare, 2015). PIFs stimulate

auxin biosynthesis leading to hypocotyl extension (Hornitschek et al., 2012; Li et al., 2012). UV-B has also been shown to inhibit the thermomorphogenic response by inhibiting hypocotyl and petiole extension, as well as leaf elevation in response to higher temperatures (Hayes et al., 2017).

1.4 Photoreception

The interest in the effects of UV-B radiation on plants and potential applications kick-started the search for the UV-B photoreceptor. The nature of plant responses to light is complex, and for a long time, the nature of the UV-B photoreceptor remained elusive as no protein could be found which resembled the previously identified photoreceptors and was UV-B responsive.

The two most well-known photoreceptor families, phytochrome (PHY; 600 – 750 nm) and cryptochrome (CRY; 320 – 500 nm) are light-sensitive proteins; which typically consist of a protein functional group and a photopigment known as the chromophore (Li et al., 2011a). In higher plants, multiple forms of the phytochrome (PHYA to PHYE) and cryptochrome (CRY1, CRY2) exist, as well as other photoreceptors such as phototropin and the Zeitlupe (ZTL) proteins, which also absorb blue light (Kim et al., 2007; Li et al., 2011a).

Phytochromes are made up of the phytochromobilin apoprotein, which is synthesised in the cytosol and is a linear tetrapyrrole chromophore (Li et al., 2011a) (Fig 1.1). The chromophore is attached to the apoprotein via thioether linkage through a series of enzymatic steps (Terry, 1997; Li et al., 2011a). Phytochromes exist in two interconvertible forms, which absorb red (maximally absorbed at 660 nm) and far-red light (maximally absorbed at 730 nm) (Quail, 1997). The different forms play an important role in the shade avoidance response of the plants. Chlorophyll and carotenoids absorb red and blue wavelengths for photosynthesis; this reduces the ratio of red to far-red light in light that has passed through or reflected from other plants (Li et al., 2011a). The phytochromes perceive this difference, changing between the two isoforms, which results in different responses, depending on the level of shading. For instance, in shade,

the shade avoidance response initiated by phytochrome will result in the leaves bending towards unfiltered daylight (Smith and Whitelam, 1997). Phytochromes are also involved in stem elongation and seed germination (Li et al., 2011a), as well as playing a role in temperature sensing (Jung et al., 2016; Legris et al., 2016) and entrainment of the circadian rhythm (Somers et al., 1998) and flowering (Reed et al., 1993; Kendrick and Kronenberg, 1994). PHYB is the primary high red light photoreceptor (Somers et al., 1998), and has been shown to be involved in both the flowering response and entrainment of circadian rhythm through direct interaction, with several downstream signalling components directly involved in the control of the circadian clock (Somers et al., 1998). PhyB plays a key role in temperature sensing as it interacts with key genes involved in the thermomorphogenic response in a temperature dependent manner (Jung et al., 2016; Legris et al., 2016), showing that phytochromes act both as light and temperature sensors.

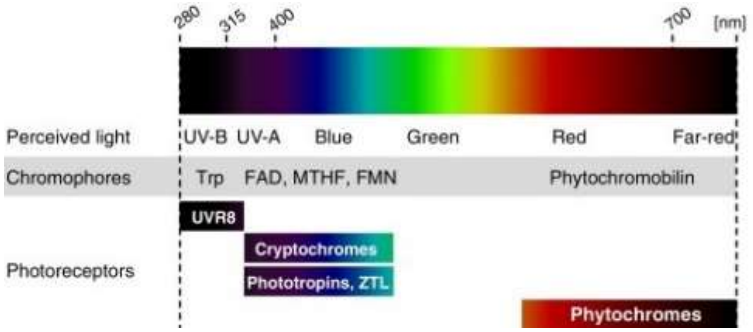

Figure 1.1 The different classes of photoreceptors identified in *Arabidopsis thaliana*. The photoreceptors use the perceived light to give them information about the general light spectrum found in their environment, resulting in changes to the plant morphology. Phytochromes absorb red/far-red light, the chromophore is the plant specific phytochromobilin. Blue light and UV-A are absorbed by several different photoreceptors; cryptochromes, phototropins and the Zeitlupe (ZTL) proteins. Cryptochromes bind Flavin Adenine Dinucleotide (FAD) and Methenyltetrahydrofolate (MTHF) as chromophores, while phototropins and the ZTL proteins bind Flavin Mononucleotide (FMN) chromophore through their LOV (Light, Oxygen or Voltage) domains. UVR8 absorbs UV-B through intrinsic Tryptophans (Trp). From Heijde and Ulm (2012).

In *Arabidopsis thaliana*, UV-A and blue light are perceived by several different receptors, by cryptochromes, phototropins and ZTL proteins. Cryptochromes bind Flavin Adenine Dinucleotide (FAD) and Methenyltetrahydrofolate (MTHF) as chromophores (Yu et al., 2010) (Fig

1.1). Cryptochromes undergo phosphorylation when perceiving light, and are involved in a number of blue light responses, such as mediating the inhibition of hypocotyl elongation and stomatal opening (Yu et al., 2010). Cryptochromes are also involved in the photoperiodic control of flowering, as well as being involved in entrainment of the circadian clock (Li et al., 2011b; Christie et al., 2015). The other blue light receptors, phototropins and the ZTL proteins bind to Flavin Mononucleotide (FMN) as a chromophore through their LOV (Light, Oxygen or Voltage) domains (Heijde and Ulm, 2012). Phototropins are primarily involved in blue light-mediated stomatal opening, while ZTL proteins are mostly involved in the circadian rhythm (Yu et al., 2010) (Fig 1.1).

While each group of photoreceptors mediates various downstream signalling pathways individually, there is also cross talk among the signalling pathways allowing the plant to determine day length and control flowering in response (Endo et al., 2016; Kong and Okajima, 2016; Pedmale et al., 2016).

1.4.1 UVR8: The UV-B photoreceptor

The UV-B photoreceptor, UV-B RESISTANCE LOCUS 8 (UVR8), was first identified through a mutant screen looking at UV-B sensitivity in *Arabidopsis thaliana.* Kliebenstein et al. (2002) identified the mutant *uvr8-1* (*UV-B resistance locus 8-1*) as altered in response to UV-B, but behaving like wild type (*wt*) in the absence of UV-B. *uvr8-1* is altered in the UV-B induced accumulation of flavonoids, anthocyanins and CHALCONE SYNTHASE (CHS) (Kliebenstein et al., 2002; Brown et al., 2005). CHS had been previously identified as the key enzyme in both the flavonoid and anthocyanin pathway and is known to be positively regulated by UV-B exposure (Christie and Jenkins, 1996). Expression of *CHS* is also controlled by a number of photoreceptors in response to different types of light; such as the upregulation of CHS in response to UV-A exposure is mediated by cryptochrome 1 (Kaiser and Batschauer, 1995; Wade et al., 2001).

When wild type plants are exposed to UV-B a continual increase of CHS can be seen, while in *uvr8-1* the UV-B mediated induction of CHS does not occur although other stress response genes are still induced. All of which suggested that UVR8 is needed for the transduction of the UV-B response signal (Kliebenstein et al., 2002). When 10-day old *uvr8-1* plants were exposed to 3 days of constant UV-B exposure, necrosis of the first true leaves and cotyledons was seen, as well as folding of the young leaves (Kliebenstein et al., 2002). Brown et al. (2005) determined that UVR8 is UV-B specific as the CHS response in *uvr8-1* is only absent in the presence of UV-B, but the CHS response to other wavelengths remained the same. Transcriptome analysis of *uvr8-1* in comparison to wild type, when exposed to high doses of UV-B, identified 72 UV-B induced genes regulated by UVR8 (Brown et al., 2005).

UVR8 has also been shown to be involved in the suppression of the shade avoidance response; when UV-B is detected by UVR8 it inhibits the increase in auxin biosynthesis and other signalling genes involved in the shade avoidance response elicited by reduced red: far-red ratio (Hayes et al., 2014). Under UV-B exposure the thermomorphogenic response to elevated temperatures is inhibited by UVR8 (Hayes et al., 2017).

Orthologues of UVR8 have been found in many other species; such as green algae, bryophytes, lycophytes, and angiosperms (Fernández et al., 2016; Soriano et al., 2018). The UVR8 protein sequence is strongly conserved (Rizzini et al., 2011; Fernández et al., 2016; Soriano et al., 2018); and Soriano et al. (2018) showed that the UVR8 homolog in *Physcomitrella patens* and *Marchantia polymorpha* was sufficiently conserved to complement the Arabidopsis *uvr8* mutant. The conservation of UVR8 sequence and structure throughout the plant lineage illustrate the important role of UVR8 in UV-B protection; and adds support to the hypothesis that UVR8 evolved at a time when higher levels of UV-B reached the surface around 400-700 million years ago (Cnossen et al., 2007; Jenkins, 2009; Fernández et al., 2016).

1.4.2 Photoreception and gene regulation

UVR8 essentially behaves as a light responsive pigment at the top of a transduction chain, which regulates over 100 genes (Aphalo et al., 2012). In the absence of UV-B, UVR8 exists as a symmetrical homodimer, which monomerises when exposed to UV-B (Rizzini et al., 2011) (Fig 1.2). Each of the two subunits is made up of seven β-propeller blades (Wu et al., 2012). Each blade is connected with the N and C termini of the blade before and after it, which may allow for a more flexible conformation (Christie et al., 2012), resulting in a round shape with a central tunnel (Fig 1.2). The homodimer is stabilised by the interaction of acidic and basic patches as well as hydrogen bonds on the surface of each of the core domains (Wu et al., 2012). The dimer is further stabilised by the interaction of arginine residues with the tryptophan residues at the dimer interface (Rizzini et al., 2011). The monomerisation is reversible, as, after the end of exposure to UV-B, the dimer reassembles without the need for a cofactor, indicating that the dimeric state is an intrinsic property of the protein (Fig 1.2) (Christie et al., 2012).

Instead of a chromophore, UVR8 uses a 'tryptophan pyramid' to detect UV-B. UV-B is detected by the tryptophan (Trp) residues, as these absorb UV-B and have an absorption maximum of 300 nm and in the protein environment is likely to extend even further (Rizzini et al., 2011) and thus should be able to detect even higher wavelengths of UV-B. Trp285 and Trp233 have been identified as the most important tryptophan residues, as when they are mutated to phenylalanine they ceased to dissociate into monomers in the presence of UV-B (Wu et al., 2012). The arrangement of the tryptophans was termed a tryptophan pyramid by Christie et al. (2012), and the overlap between the UV-B absorbing residues produces a distinct signature in the far UV circular dichroism spectrum. It is thought that UVR8 detects UV-B by using these tryptophans as a chromophore; when UV-B hits the salt bridges between the arginine and the tryptophan, specifically R286-W285, it causes an excited electron to move from the tryptophan to the arginine, causing the neutralization and breaking of the salt bridge and thus the dimer

becomes destabilized and dissociates (Christie et al., 2012). The *uvr8-1* mutant has a 15bp deletion in the *UVR8* gene, causing it to lose its ability to transmit the UV-B signal (Kliebenstein et al., 2002).

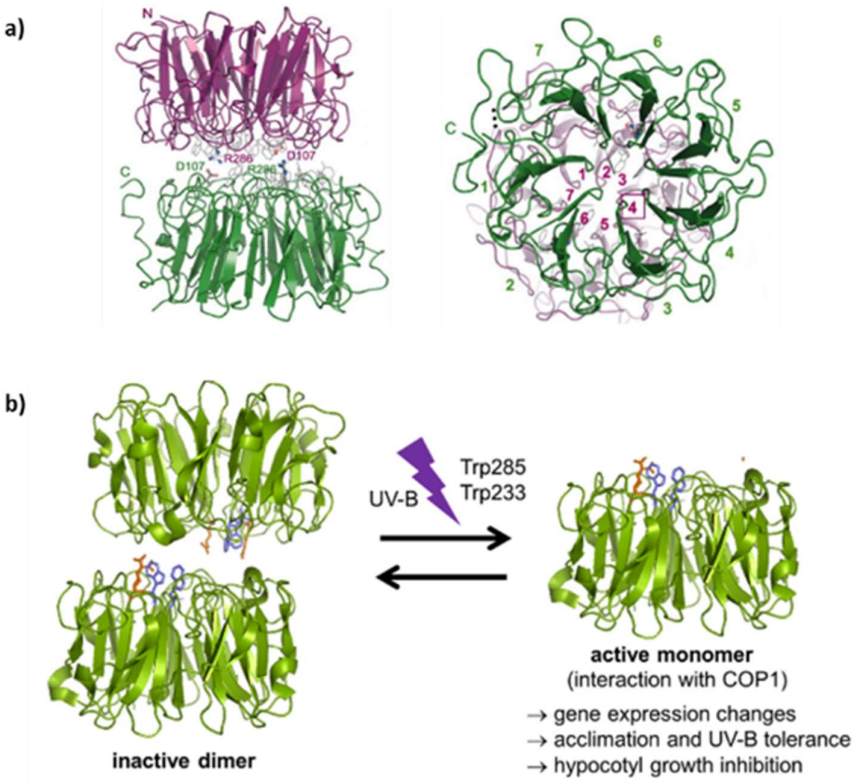

Figure 1.2 The structure of the UVR8 photoreceptor. a) Shows the symmetrical homodimer of seven-bladed β-proper subunits, from the side and the end. The key salt bridges are shown in the side view; the numbers indicate the blade pairing at blade 4. From Christie et al. (2012). **b)** UVR8 protein model showing the UV-B dependent monomerisation into the UVR8 monomer. Arginine (Arg, orange) residues at position 286 and 338 form hydrogen bonds that hold the homodimer together while tryptophan (Trp, blue) residues at position 285 and 233 serve as chromophores to perceive UV-B. From Tilbrook et al. (2013).

1.4.2.1 After monomerization: Interaction with COP1

The UVR8 monomer then interacts with the E3 ubiquitin ligase COP1 (CONSTITUTIVELY PHOTOMORPHOGENIC 1). The 27 amino acids on the C terminus of UVR8 interact with the WD40-repeat domain in COP1 (Gruber et al., 2010; Wu et al., 2013). COP1 is a protein made up of a RING finger, coiled-coil and WD40 domains, each of mediate the interaction with other proteins or aid in self-dimerisation (Yi and Deng, 2005). COP1 is a central regulator of light-dependent plant photomorphogenesis by impairing the transcriptional activation of the *HY5*

(*ELONGATED HYPOCOTYL 5*) gene, which encodes a bZIP transcription factor that plays an important role in the UV-B signalling pathway (Gruber et al., 2010). Thus, the interaction between COP1 and UVR8 is essential for the acclimation of the plant to UV-B as COP1 acts a positive regulator of UV-B photomorphogenesis (Heijde et al., 2013). COP1 represses light signalling by targeting downstream transcription factors involved in photoreception for ubiquitylation and degradation (Yi and Deng, 2005) and thus acts as a negative regulator of photomorphogenic development. Its sequence contains nuclear import and export signals, and its localisation is controlled by light (Yi and Deng, 2005). In darkness, COP1 is localised to the nucleus, where ubiquitylation and degradation of the photomorphogenic transcription factors occurs, and thus repressing photomorphogenic genes. In light, COP1 is excluded from the nucleus, and the transcription factors accumulate again, and thus the plants can undergo photomorphogenic development (Yi and Deng, 2005).

In response to light HY5 activates a number of genes leading to photomorphogenic development. HY5 accumulates in light-grown plants and is degraded in dark-grown plants through proteasome-mediated proteolysis, which requires the ubiquitylation by COP1 (Yi and Deng, 2005). COP1 is a negative regulator of HY5 and has been shown to interact and co-localize with HY5 to subnuclear speckles in the plant (Yi and Deng, 2005). HY5 is stabilised in white light, as then COP1 is excluded from the nucleus, HYH (HY5 HOMOLOG) is also degraded by COP1 and is involved in blue light signalling (Yi and Deng, 2005). COP1 also targets other transcription factors involved in other light signalling responses, and thus COP1 can be considered to be the master switch as it ubiquitylates all the transcription factors involved in light signalling when in the dark and thus targets them for degradation leading to a stop in photomorphogenic development (Yi and Deng, 2005).

1.4.2.2 Gene regulation

UVR8 is found both in the nucleus and the cytoplasm, and its levels do not change when exposed to different light conditions, however upon irradiation by UV-B the levels of UVR8 in the nucleus increase, indicating redistribution from the cytoplasm into the nucleus (Kaiserli and Jenkins, 2007; Heijde and Ulm, 2012). Once in the nucleus, it is hypothesised that the UVR8-COP1 complex interacts with the chromatin of UV-B regulated genes by binding to the histones (Cloix and Jenkins, 2008; Christie et al., 2012). Studies have shown that the chromatin of the promoter regions of a UV-B upregulated gene is enriched with diacetylhistone H3 (K9/K14), showing a link between histone modification and transcriptional activity in a UV-B stressed environment (Cloix and Jenkins, 2008). It then initiates the transcriptional response to the UV-B stress. Transcriptome analysis has identified over 100 genes that are regulated by UVR8 under UV-B exposure (Brown et al., 2005; Christie et al., 2012).

Under UV-B conditions *HY5* transcription is activated, and the COP1 dependent degradation is inhibited, most likely due to the binding of the UVR8 monomer to COP1 preventing the ubiquitylation and subsequent degradation (Gruber et al., 2010). The transcription factor HY5 and its homolog HYH regulate a number of genes under UV-B stress, several of which are involved in protection against UV radiation. Mutant studies of *hy5* and *hyh* have shown that HYH is less important than HY5 as the *hyh* mutant is less sensitive to UV-B; indicating that the lack of the HY5 transcription factor is vital to UV-B acclimation and protection (Ulm et al., 2004; Brown et al., 2005; Oravecz et al., 2006). In wild type plants, both transcription factors are involved in the regulation of UV-B pathway-specific genes and play a key role in the downstream effect of UVR8 signalling.

RUP1 (REPRESSOR OF UV-B PHOTOMORPHOGENESIS 1) and RUP2 interact with UVR8 to negatively regulate the photomorphogenic response elicited by UVR8 (Gruber et al., 2010). Both are transcriptionally activated by UVR8, COP1 and HY5 (Gruber et al., 2010). The *rup1,rup2*

double mutant showed a stronger response to UV-B stress and was better acclimated, and overexpression of *RUP2* showed a reduced photomorphogenesis when under UV-B stress (Gruber et al., 2010). Thus indicating that both proteins are involved in repressing the UVR8 regulated UV-B response and can be seen as negative feedback regulators, which are needed to balance the need for UV-B damage response and plant growth. The regulation of RUP1 and RUP2 is critical, and data suggests that a rapid increase in RUP1 and RUP2 is necessary to prevent overstimulation under UV-B stress (Gruber et al., 2010). Mutants of either *rup1* or *rup2* show a hypersensitivity to UV-B and *HY5* and *CHS* exhibit higher expression levels in the mutants; indicating the RUP1 and RUP2 interact with UVR8 or COP1 to prevent overstimulation (Gruber et al., 2010). RUP1 and RUP2 are also activated by other light wavelength indicating a general role in light response; however, in other light responses, they do not seem to affect HY5 or CHS (Gruber et al., 2010). Thus, their major negative regulatory role is UV-B specific. Overexpression of RUP1 or RUP2 results in blockage of UV-B specific signalling (Gruber et al., 2010). Fig 1.3 shows a model of the UVR8 mediated UV-B response to the extent it is known so far.

1.4.2.3 Other possible pathways:

Other pathways in UV-B signalling have been identified, but little about them is known. One pathway involved the RUS1 (ROOT UV-B SENSITIVE 1) protein, which is believed to negatively regulate the UV-B response pathway in roots (Gruber et al., 2010). It is thought that other pathways and proteins that inhibit and promote UV-B induced signalling and differ from the COP1/UVR8 pathway must exist (Gruber et al., 2010).

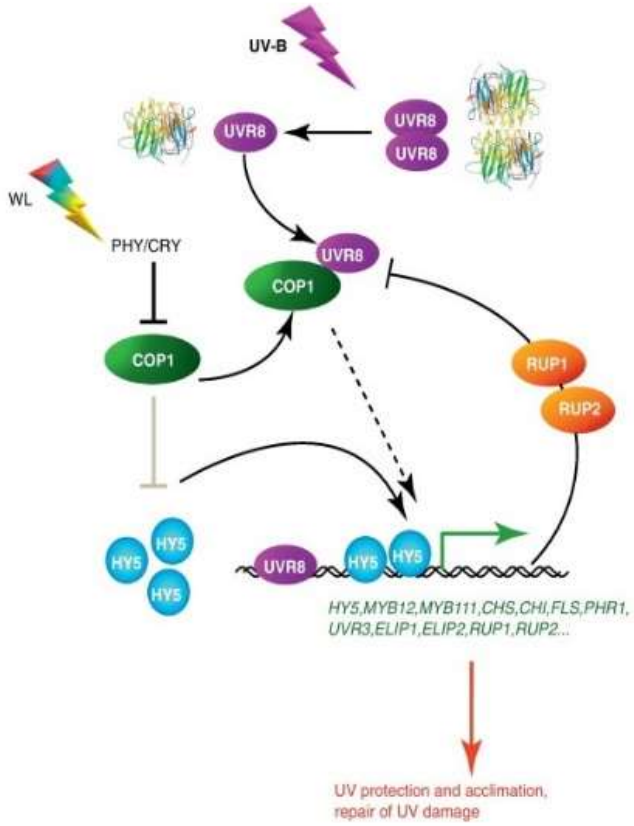

Figure 1.3 Model of UVR8 mediated UV-B signalling as currently understood. In the absence of UV-B (white light - WL), UVR8 is primarily a homodimer, and COP1 represses photomorphogenesis by promoting degradation of HY5. In the presence of UV-B, UVR8 monomerises and interacts with COP1. The bZIP transcription factor HY5 is stabilised and UV-B responsive genes are activated. These include genes encoding proteins of importance for UV protection (e.g. *CHS*), but also the RUP1 and RUP2 proteins, which constitute negative feedback on UVR8 activity involving direct protein–protein interaction. From Heijde and Ulm (2012).

1.4.3 UV-B interaction with other wavelengths:

In a natural environment, plants are exposed to the entire electromagnetic spectrum of sunlight, rather than only a particular set of wavebands. While the stress response to high levels of UV-B has been extensively studied, there has been little research into understanding how other wavebands, wavelengths, and groups of wavebands, particularly Photosynthetically Active Radiation (PAR), and UV-A interact with UV-B, and how this affects the photomorphogenic response.

While there have been several studies examining the effect of UV-B radiation on both the photomorphogenic response as well as effects on photosynthetic apparatus, there has been little research into the effects of UV-A. UV-A radiation is perceived by the plants through cryptochromes, and studies have revealed the dual nature of UV-A radiation on plants. It activates the expression of PS II proteins (Christopher and Mullet, 1994), but it also damages photosynthetic machinery (Joshi et al., 1997; Turcsányi and Vass, 2000). While the primary target of UV-A radiation is PS II, it is also damaging to PS I (Photosystem I) (Turcsányi and Vass, 2000), and there is some evidence to suggest that UV-A radiation results in the increase in the amounts of UV absorbing compounds (Rozema et al., 2002). Of further interest is the combined effects of UV-A and UV-B radiation on plants. It has been shown that the presence of UV-A moderately protects the photosynthetic apparatus against the effects of UV-B (Gartia et al., 2003). Furthermore, it has been demonstrated that seedlings exhibit differences when exposed to different wavebands of UV, particularly in terms of the carotenoid composition, which are protective agents against UV damage (Gartia et al., 2003).

Evidence also suggests that a mixture of UV-B, UV-A, blue and red light is required to maintain plant function under stress as well as being needed for the repair of damage caused by high doses of UV-B (Christie and Jenkins, 1996; Wade et al., 2001). The combination of different wavebands, such as PAR and UV-A, together with UV-B radiation have a strong influence on the effect of UV-B radiation on plants (Fuglevand et al., 1996). It has been shown that high levels of PAR reduce the effects of UV-B, and that pre-treating plants with PAR prior to exposing them to UV-B, mediates the effects of UV irradiation, thus limiting the damage done to the plants. High doses of PAR result in gene expression changes; inducing the accumulation of phenolic compounds (Rossel et al., 2002). Thus, pre-treating plants with high doses of PAR prior to irradiation of UV-B provides plants with added protection in terms of UV-B absorbing compounds as well as increasing leaf thickness (Wargent et al., 2011). A high UV-B/high PAR

ratio resulted in the accumulation of flavonoids, while a high UV-B/low PAR resulted in a much lower accumulation, which suggests that the balance between PAR and UV-B in the spectrum is important in the plant adaptation to UV-B stress (Götz et al., 2010). While low levels of PAR and UV-A, exasperate the effects of UV-B (Caldwell and Flint, 1994), the presence of both PAR and UV-A in higher quantities is beneficial to the plant as both are required for photoreactivation.

Both UV-A and PAR are not absorbed by ozone, meaning that their relative intensities are typically constant. However, the ratio of PAR/UV-A to UV-B is determined by the ozone layer (Götz et al., 2010). The different ratios result in changes in both the transcriptomic and phenotypic response. The PAR/UV-B ratio has also been shown to affect photoinhibition and the turnover of the D1 protein in PS II (Bornman, 1994). UV-B induced DNA damage is repaired by photoreactivation, which is dependent on the energy provided by UV-A and blue light (Britt, 1999; Ries et al., 2000a). Interestingly, there is also evidence showing that illuminating a plant with red light after UV-B exposure rapidly increases the net rate of photosynthesis, which suggest that photosynthesis may be affected by the PAR/UV-B ratio (Ries et al., 2000a). Also of interest is evidence suggesting that UVR8 may be interacting with other photoreceptors when exposed to ambient PAR and high UV-A exposure; as under such conditions, it may act as a regulator of gene expression (Morales et al., 2013). Understanding how PAR/UV-A and UV-B wavebands interact is key to understanding in how to improve plant response in a high UV-B environment, as well as furthering the understanding of how these wavebands affect morphology as well as photosynthesis.

1.5 UV-B and photosynthesis

Although light drives primary productivity in plants via photosynthesis, the addition of UV-B to the spectrum also has an effect on photosynthesis. The severity of the reaction depends on the dose and irradiance scheme administered; high fluence rates will elicit a more severe effect than lower doses (Teramura and Sullivan, 1994; Takahashi et al., 2010; Davey et al., 2012). High

fluence rates of UV-B have been defined as fluence rates higher than 3 μmol m^{-2} s^{-1} of UV-B, as this represents the fluence rate measured at midday in summer in the UK. Low fluence rates have been defined as < 1 μmol m^{-2} s^{-1} of UV-B (Frohnmeyer and Staiger, 2003; Jenkins, 2009). As many historical experiments were performed in the presence of high fluence rate UV-B and low fluence rates of PAR, photosynthetic responses to high fluence UV-B is well characterised (Teramura, 1983).

1.5.1 Impact of high fluence rates of UV-B

High fluence rates of UV-B have been shown to impede photosynthetic performance (Allen et al., 1997; Mackerness et al., 1998; Takahashi et al., 2010). High fluence rates of UV-B have been shown to result in damage to the photosystems (PS I and PS II) and lower photosynthetic efficiency (Tyystjärvi, 2008; Davey et al., 2012; Dobrikova et al., 2013) as well as lower chlorophyll content (Surabhi et al., 2009) and inhibition of net photosynthetic rate (Jansen et al., 1998).

1.5.1.1 Photosystem II

UV-B has been shown to affect PS II to a much greater extent than PS I (Hollósy, 2002). PS II is the key supramolecular complex in the photosynthetic machinery and has been identified as one of the main targets of UV-B radiation (Booij-James et al., 2000). PS II is found in the chloroplast and is a pigment-protein complex which catalyses the light-induced transfer of electrons from water to plastoquinone (Booij et al., 1999). The photosynthetic machinery; made up of the OXYGEN EVOLVING COMPLEX (OEC), the LIGHT HARVESTING COMPLEX (LHCII) and the reaction centre, is made up of over 25 different polypeptides (Mattoo et al., 1999). While the reaction of water splitting in the OEC is damaging to the proteins and pigments involved; photodamage occurs in several parts of the complex, such as the manganese cluster through the direct photoexcitation of manganese as it absorbs UV-B (Sarvikas et al., 2006; Takahashi et al., 2010).

The PS II reaction centre is composed of the D1 and D2 proteins, α and β subunits of cytochrome b559 and a few low molecular mass polypeptides (Mattoo et al., 1989). The D2 and D1 proteins form a backbone for the binding of cofactors and prosthetic groups, which are involved in charge separation and electron flow (Loll et al., 2007). The two electron acceptor plastoquinones Qa and Qb bind to D2 and D1 respectively (Booij et al., 1999). The D1 and D2 proteins have structural and functional similarities, but they differ in stability (Mattoo et al., 1989). The D1 protein is rapidly degraded by light; the degradation is specifically driven by UV-C, UV-B, UV-A, PAR and far-red light, and the rate at which it degrades exceeds that of all other PS II proteins, while in comparison the D2 protein is relatively stable and long-lived under physiological fluence rates of PAR (Booij-James et al., 2000). It has been shown that UV-B targets the D2-D1 heterodimer and accelerates degradation with the greatest effect being on the D2 protein (Booij-James et al., 2000). The ratio of D2 degradation/D1 degradation is wavelength dependent; rates of D2 degradation are lowest in the visible part of the spectrum and highest in the UV-B/UV-C region of the spectrum (Booij-James et al., 2000). In the UV-A and blue light part of the spectrum, the relative rate of D2 gradation is also higher; degradation is driven by UV-B fluence rates as a low as 1 µmol m^{-2} s^{-1} (Booij-James et al., 2000). It has been shown that chronic exposure to low levels of UV-B has little effect on the maximal photosynthetic efficiency of PS II, suggesting that acclimation to UV-B is possible (Hectors et al., 2007).

1.5.2 Impact of low fluence rates of UV-B on photosynthesis

There is now growing evidence suggesting that lower fluence rates of UV-B can be beneficial to photosynthesis. Visible light supplemented with low fluence UV-B has been shown to protect the plant against high light damage (Bolink et al., 2001) and may even enhance recovery from a photoprotected state (Xu and Gao, 2010). Furthermore, chlorophyll content of plants grown under low fluence UV-B has been shown to be higher than the no UV-B control (Poulson et al., 2006).

Under low fluence rates of UV-B, Davey et al. (2012) showed an increase in photosynthetic performance, and analysis of the Favory et al. (2009) microarray data by Wargent and Jordan (2013) showed an upregulation of photosynthesis-associated genes. Further studies in other plant species have shown that presence of low levels of UV-B may stimulate photosynthesis (Vidović et al., 2015), as well as studies indicating that ambient levels of UV-B have little effect on photosynthesis (Hectors et al., 2007; Ballaré et al., 2011; Hideg et al., 2013). In summary, a number of studies have highlighted the potential for UV-B to positively influence photosynthetic competency and performance, but there is very little mechanistic understanding of such responses, particularly at the gene expression level.

1.6 Aims of this work

This work will focus on mechanistically characterising the photosynthesis response to low fluence rate UV-B exposure in *Arabidopsis thaliana.* High UV-B fluence rates have been shown to damage the photosynthetic apparatus and lower PS II efficiency (Tyystjärvi, 2008; Davey et al., 2012; Dobrikova et al., 2013), as well as inhibit photosynthetic rate (Jansen et al., 1998). Little is known about the effect of low fluence UV-B on photosynthesis; but microarray analysis has shown that in response to low fluence UV-B photosynthesis-associated genes are upregulated (Favory et al., 2009) suggesting that there may be a positive impact on photosynthesis.

As the response to low fluence rate UV-B is not well understood this PhD project aims to:

- Characterise the impact of low fluence UV-B exposure on the net photosynthetic rate of wild type and the *uvr8* mutants.
- To determine the differences in gene expression in *wt* and *uvr8* mutants in response to low fluence UV-B exposure, and identify possible candidate genes that may be involved in the UV-B dependent photosynthesis response.

- To gain a better understanding as to how the candidate genes identified affect the UV-B dependent photosynthesis response and how these candidates may interact with one another.

Ultimately, the aim of this work is to gain more insight into the photosynthesis response of *Arabidopsis thaliana* to low fluence rate UV-B exposure. These insights may then be applied to gain a better understanding of UV-B response in *Arabidopsis* overall and may in the long term be useful in manipulating photosynthetic efficacy in agricultural plants.

2 Materials and Methods

2.1 Plant material

Arabidopsis thaliana wild type ecotypes used in the research presented were *Columbia-0* (Col-0) and *Landsberg erecta* (L*er*). *uvr8* mutant lines used where *uvr8-1* (L*er*) and *uvr8-6* (Col). Wild type L*er*, *uvr8-1* (L*er*) and *rup1,rup2* (Col) (henceforth referred to as *rup1,2*) seed lines were provided with the assistance of Professor Gareth Jenkins, University of Glasgow, Scotland. Wild type Col-0 ecotype, *uvr8-6* (Col) and all other mutant seed lines were obtained through the Arabidopsis Biological Resource Center (ABRC, The Ohio State University, Ohio, USA). All mutant lines used are listed and described in Table 2.1.

Table 2.1 Mutant lines used in the research presented

Mutant line name	Background	Gene ID	Stock name
uvr8-1	L*er*	AT5G63860	
uvr8-6	Col	AT5G63860	SALK_033468
lug444	Col	AT4G32551	SALK_126444
luh4	Col	AT2G32700	SALK_097509
seu-4	Col	AT1G43850	SALK_069303
sig5-1 (sig5.1)	Col	AT5G24120	SALK_049021
sig5-2	Col	AT5G24120	SAIL_1232_H11
elip1	Col	AT3G22840	CS321141
elip2	Col	AT4G14690	SALK_105392C
rup1,2	Col	AT5G52250 AT5G23730	
rbf1-1	Col	AT4G34730	SALK_008178
rbf1-2	Col	AT4G34730	SALK_058490
toc33	Col	AT1G02280	SALK_122849
tfp	Col	AT1G52990	SALK_009687C

Prior to all experimental work, all T-DNA insertion mutant lines were screened for homozygosity of the T-DNA insertion; see section 2.5.1 for details.

2.2 Growth Conditions

All seeds, apart from *rbf1-2* (Col), were germinated directly on sieved soil (Daltons Premium Seed Mix, Matamata, New Zealand) in detachable seedling pots (each pot is 45 mm by 45 mm). The pot trays were placed inside of a holding tray (420 x 310 mm) into which 500 ml of water

was poured every 2nd day. In each pot, two seeds were germinated and were thinned to 1 seedling per pot after successful germination.

Plants were germinated and grown in controlled environment growth rooms at the Plant Growth Unit, Massey University, Palmerston North or at the Plant Growth Facility at the Institute of Fundamental Sciences, Massey University, Palmerston North. Environmental conditions in the rooms were maintained at 10:14hrs day/night length; 20 °C ± 2 temperature; 75% ± 10 relative humidity. The 10:14hrs day/night length cycle was selected to allow for sufficient growth of plant for the IRGA measurements but avoiding without green biomass development without driving the plant to flowering. PAR light sources were made up of using a mixture of cool white fluorescent tubes (Philips 54W T5, Eindhoven, Netherlands) and Gro-Lux fluorescent tubes (Sylvania F58W T8 Gro-lux, Seneca Falls, NY, USA) (Fig 2.1a). The two types of fluorescent tubes were selected as this provided the desired quantity of PAR and desired ratio of red: far-red. PAR intensity was measured using an Optronic OL-756 UV-VIS Spectroradiometer (Optronic Laboratories, Gooch and Housego, Orlando, FL, USA) equipped with integrating sphere and set to 220 µmol m^{-2} s^{-1} at plant canopy height. Plants were grown under these conditions between 28 to 35 days after sowing (DAS) depending on the experiment.

2.2.1 Growth medium for *rbf1-2* (SALK_058490)

Due to the nature of the *rbf1-2* mutation the seedlings needed to be germinated on a Murashige and Skoog medium (Murashige and Skoog, 1962), supplemented with 0.8% Suc, for 2 weeks as described in Fristedt et al. (2014); under the same environmental conditions as all other mutants. After 2 weeks (14 DAS), the seedlings were transferred onto the same soil mix as all other seedlings and grown under the same conditions.

2.3 Experimental setup

Experimental set up varied between experiments as different UV-B fluence rates as well as different UV-B sources were used. The details of all experiments undertaken in this thesis can be seen in Table 2.

Table 2.2 Experimental set up

UV-B experimental dose		Propagation	PAR acclimation period (prior to UV-B exposure)	UV-B exposure
1.5 µmol m^{-2} s^{-1} UV-B using LEDs	Age of plants	From sowing	No PAR Acclimation Period	35 DAS
	Time period	35 days		5 days
	Day length (Day/Night)	10:14hrs		12:12hrs
	Light conditions	WL - 220 µmol m^{-2} s^{-1} PAR		PAR LEDs 220 µmol m^{-2} s^{-1} UV-B LEDs 1.5 µmol m^{-2} s^{-1}
	Relative Humidity	75% ± 10		70% ± 10
	Temperature	20 °C ± 2		20 °C ± 2
0.5 µmol m^{-2} s^{-1} UV-B using LEDs	Age of plants	From sowing	28 DAS	35 DAS
	Time period	28 days	7 days	48hrs
	Day length (Day/Night)	10:14hrs	12:12hrs	12:12hrs
	Light conditions	WL - 220 µmol m^{-2} s^{-1} PAR	PAR LEDs - 220 µmol m^{-2} s^{-1}	PAR LEDs 220 µmol m^{-2} s^{-1} UV-B LEDs 0.5 µmol m^{-2} s^{-1}
	Relative Humidity	75% ± 10	75% ± 10	75% ± 10
	Temperature	20 °C ± 2	20 °C ± 2	20 °C ± 2

Table continues on next page

0.5 µmol m^{-2} s^{-1} Broadband UV-B using UV-B fluorescent tubes	Age of plants	From sowing	28 DAS	35 DAS
	Time period	28 days	7 days	48hrs
	Day length (Day/Night)	10:14hrs	12:12hrs	12:12hrs
	Light conditions	WL - 220 µmol m^{-2} s^{-1} PAR	WL - 220 µmol m^{-2} s^{-1} PAR	WL - 220 µmol m^{-2} s^{-1} PAR UV-B tubes - 0.5 µmol m^{-2} s^{-1}
	Relative Humidity	75% ± 10	75% ± 10	75% ± 10
	Temperature	20 °C ± 2	20 °C ± 2	20 °C ± 2
3 µmol m^{-2} s^{-1} Broadband UV-B using UV-B fluorescent tubes	Age of plants	From sowing	No PAR Acclimation Period	21 DAS
	Time period	21 days		5 days
	Day length (Day/Night)	10:14hrs		12:12hrs
	Light conditions	WL - 220 µmol m^{-2} s^{-1} PAR		WL - 220 µmol m^{-2} s^{-1} PAR UV-B tubes - 3 µmol m^{-2} s^{-1}
	Relative Humidity	75% ± 10		75% ± 10
	Temperature	20 °C ± 2		20 °C ± 2

DAS – Days after sowing;

WL – White light – Cool White (Philips 54W T5, Eindhoven, Netherlands) and Gro-Lux fluorescent tubes (Sylvania F58W T8 Gro-Lux, Seneca Falls, NY, USA);

PAR LEDs – 665 nm (red light) and 460 nm (blue light) emitting LEDs (BioLumic Ltd, Palmerston North, New Zealand);

UV-B LEDs – narrowband UV-B emitting LEDs (peak at 295 nm) (BioLumic Ltd, Palmerston North, New Zealand);

UV-B tubes – Broadband UV-B metal halide bulbs (Phillips HPI T Plus, Eindhoven, the Netherlands

2.3.1 Experimental Chamber set up

For the PAR acclimation period prior to UV-B exposure and for UV-B exposure, plants were moved from the propagation environment and placed into a modified controlled environment chamber (Contherm 630; Contherm Scientific Ltd, Petone, New Zealand). Environmental conditions in the chamber were maintained at 12:12hrs day/night length; 20 °C ± 2 temperature; 75% ± 10 relative humidity. Light intensity varied based on the experimental conditions; light intensity for PAR and UV-B were measured at plant canopy height using an Optronic OL-756 UV-VIS Spectroradiometer (Optronic Laboratories, Gooch and Housego, Orlando, FL, USA) equipped with integrating sphere.

2.3.1.1 Narrowband UV-B experiments using LEDs

2.3.1.1.1 1.5 µmol m^{-2} s^{-1} of UV-B

At 35 DAS, plants were moved from propagation environment into the modified controlled environment chamber (Contherm 630; Contherm Scientific Ltd, Petone, New Zealand). The chamber was equipped with proprietary commercial light modules, consisting of UV-B and PAR emitting LEDs (BioLumic Ltd, Palmerston North, New Zealand). The UV-B LEDs emitted narrowband UV-B between 290 nm and 305 nm of UV-B with a spike at 295 nm (Fig 2.1b) and the PAR emitting LEDs showed a spike at 665 nm (red light) and 460 nm (blue light) (Fig 2.1c). Intensity of UV-B was set to 1.5 µmol m^{-2} s^{-1}; intensity of PAR was set to 220 µmol m^{-2} s^{-1}.

The chamber was split into a +UVB (UV-B exposure) and a –UVB (no UV-B exposure) zone; separated by a central curtain of UV-B opaque film (Lumivar; BPI Visqueen, Ardeer, UK), allowing air to circulate between the zones. In the +UVB zone both UV-B and PAR emitting LEDs were present and in the -UVB zone only PAR emitting LEDs where present. The plants were in this environment for 5 days.

2.3.1.1.2 0.5 µmol m^{-2} s^{-1} of UV-B

At 28 DAS, plants were moved from the propagation environment to the modified controlled environment chamber (Contherm 630; Contherm Scientific Ltd, Petone, New Zealand) equipped with the same LEDs as described before (section 2.3.1.1.1). For 7 days, plants were exposed to 220 µmol m^{-2} s^{-1} of PAR only (the PAR acclimation period).

After the 7-day PAR acclimation period, the chamber was split into the +UVB and –UVB zones; as before, separated by a central curtain of UV-B opaque film (Lumivar; BPI Visqueen, Aberdeer, UK), and UV-B was turned on; at a fluence rate of 0.5 µmol m^{-2} s^{-1} of UV-B. Plants were in this environment for 48hrs.

2.3.1.2 Broadband UV-B experiments using UV-B fluorescent tubes

2.3.1.2.1 0.5 µmol m^{-2} s^{-1} of broadband UV-B

At 28 DAS, plants were moved from the propagation environment to the modified controlled environment chamber (Contherm 630; Contherm Scientific Ltd, Petone, New Zealand). The chamber was equipped with white light emitting metal halide bulbs (Phillips HPI T Plus, Eindhoven, the Netherlands); which were set to emit of 220 µmol m^{-2} s^{-1} of PAR. For 7 days plants were exposed to 220 µmol m^{-2} s^{-1} of PAR only (the PAR acclimation period).

A specifically designed frame was placed into the chamber to hold the UV-B emitting fluorescent tubes (Q-Panel 313; Q-Lab Corp, Cleveland, OH, USA); which were set to emit 0.5 µmol m^{-2} s^{-1} of UV-B. The UV-B emitting tubes were wrapped with 0.13 mm thick cellulose diacetate (Clarifoil; Courtaulds Ltd, Derby, UK) to filter out wavelengths < 290 nm. The chamber was split into a +UVB and a –UVB zone, separated by a central curtain of UV-B opaque film (Lumivar; BPI Visqueen, Aberdeer, UK). For the –UVB side, the lengths of UV-B tubes were wrapped with the same UV-B opaque film.

After the 7-day PAR acclimation period, the UV-B fluorescent tubes were turned on, and the plants were in this environment for 48hrs.

2.3.1.2.2 3 µmol m^{-2} s^{-1} of broadband UV-B

At 21 DAS, plants were moved from the nursery environment to the modified controlled environment chamber (Contherm 630; Contherm Scientific Ltd, Petone, New Zealand). The chamber was set up the same way as it was for the 0.5 µmol m^{-2} s^{-1} of broadband UV-B experiments. As there was no acclimation period, plants were exposed to of 3 µmol m^{-2} s^{-1} of broadband UV-B for 5 days (Fig 2.1d).

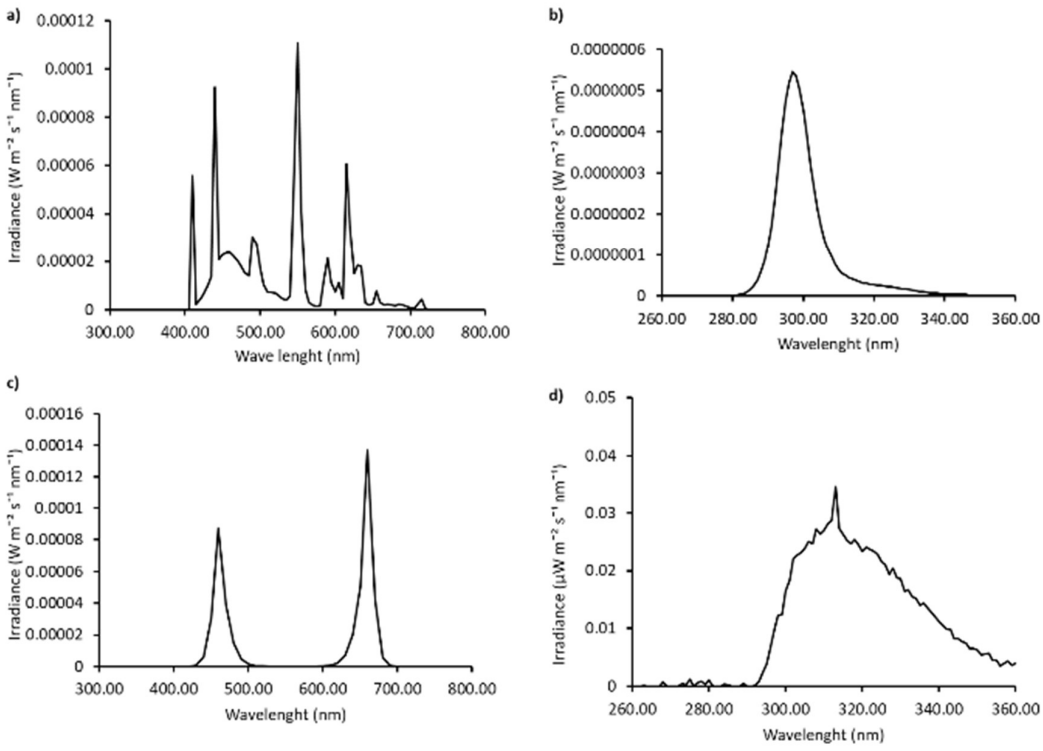

Figure 2.1 Spectral qualities of the different light sources. a) Spectral irradiance in propagation environment - 220 µmol m^{-2} s^{-1} of PAR using a mixture cool white fluorescent tubes (Philips 54W T5, Eindhoven, the Netherlands) and Gro-Lux fluorescent tubes (Sylvania 58W T8 Gro-Lux, Seneca Falls, NY, USA). **b)** Spectral irradiance of 295 nm UV-B emitting LEDs (Biolumic Ltd, Palmerston North, New Zealand) - 0.5 µmol m^{-2} s^{-1} UV-B. **c)** Spectral irradiance of PAR emitting LEDs (Biolumic Ltd, Palmerston North, New Zealand) - 220 µmol m^{-2} s^{-1} of PAR (red peak at 665 nm, blue peak at 460 nm). **d)** Spectral irradiance of UV-B emitting fluorescent tubes (Q-Panel 313; Q-Lab Corp, Cleveland, OH, USA) - 3 µmol m^{-2} s^{-1}. All irradiances were measured at plant canopy height with an Optronic OL-756 UV-VIS Spectroradiometer (Optronic Laboratories, Gooch and Housego, Orlando, FL, USA) equipped with integrating sphere.

2.4 Physiological measurements

2.4.1 Net photosynthetic rate

Photosynthetic rate was measured using the infra-red gas analyzer (IRGA) LI-6400XT Portable Photosynthesis System (Li-Cor Biosciences, Lincoln, Nebraska, USA), with the 6400-17 Whole Plant Arabidopsis Camber and 6400-18 RGB Light Source as attachments. Basic set up and warm-up procedures were followed as per the instructions provided. For photosynthetic rate measurements chamber conditions were maintained at 400 µmol m^{-2} s^{-1} PAR, 75% relative humidity, 20 °C chamber temperature and 400 ppm of CO_2.

Each plant was placed with the pot into the whole plant chamber and left for 5 minutes to allow a steady state to be reached. Net photosynthetic rate (µmol CO_2 m^{-2} s^{-1}) was noted, and afterwards plants where returned to the experimental environment. All measurements took place at around the middle of the day as plants are the most active then.

2.4.2 Leaf Area

Due to the limited number of samples available in each experiment, leaf area was measured non-destructively through the use of ImageJ (ImageJ 1.52a, https://imagej.nih.gov/ij/) (Abramoff et al., 2003; Schneider et al., 2012). Pictures were taken of each plant just after the plant had been removed from the IRGA, at a height of 10 cm above plant canopy. The image was loaded in ImageJ, and leaf area was determined following the protocol for leaf area determination provided on the ImageJ website (https://imagej.nih.gov/ij/docs/pdfs/examples.pdf) (Reinking, 2007).

To determine green leaf area rather than whole leaf area, the protocol was adjusted. Rather than converting the image into binary, the colour threshold was adjusted by going to Image → Adjust → Colour threshold. Within the Threshold Colour menu, the colour space “HSB” was selected, and dark background was unselected. “Hue” was set between the 50 and 115, while “Saturation” and “Brightness” were set to 0 and 225. After exiting the menu, area was

determined through going to Analyse → Analyse Particles. This allows for the determination of green leaf area as other colours are excluded from the calculation.

2.4.3 Dry weight measurements

Dry weights were measured to assess changes in biomass in response to UV-B exposure at the end of the experiment. Plants were harvested after the last IRGA measurement; the whole rosette was cut away from the roots at the soil level, and fresh weight was measured. Afterwards, the samples were dried at 70 °C for one week until constant mass was reached. Once constant mass was reached, dry weight of each sample was measured.

2.4.4 Photosystem II quantum efficiency (Fv/Fm)

Chlorophyll fluorescence analysis of maximum quantum efficiency of PS II (Fv/Fm) was spot measured using a plant efficiency analyzer (Pocket PEA, Hansatech, Norfolk, UK). After the IRGA measurement, the clip was attached to the second true leaf allowed to dark adapt for 20 min before measurement. After the measurement, the plant was returned to the experimental environment.

2.4.5 Secondary metabolite measurements

Quantification of foliar flavonoid and chlorophyll content was carried out non-destructively using the Dualex Scientific+ (Force-A, Paris, France). Both chlorophyll and flavonoids were measured as arbitrary units (Cerovic et al., 2012). The Dualex device was used on one leaf per plant at a time; immediately after the IRGA measurements. Following this, the plant was returned to the experimental environment.

2.4.6 Statistical Analysis

All statistical analysis was performed using Microsoft Office Excel 2016 and IBM SPSS Statistics (SPSS Statistics v25; v25; IBM, Armonk, NY, USA). To determine statistical significance, the following tests were used:

- Two-Sample T-test – to determine significance between two genotypes at a given time point and treatment
- One-way ANOVA – to determine significance between two treatments (+UVB and –UVB) at a given time point in a single genotype
- Repeated measures – to determine significance between time points in a single genotype and treatment.

Throughout this thesis $P < 0.05$ indicates significance, and "n" refers to the number of biological repeats per genotype, unless otherwise indicated.

A replicate in the physiological measurements refers to one plant. After plants were measured for photosynthetic rate and/or leaf metabolites and secondary metabolism, the plants were returned to the experimental growth chamber in a different position from where they were taken from initially.

2.5 Molecular biology protocols

2.5.1 Verification of mutant lines

2.5.1.1 Sample harvesting and preparation

To confirm the T-DNA insertion in the mutant lines, two leaves were harvested from growing plants, and snap frozen in liquid N_2 and placed into -80°C until further use. Samples were ground into a fine powder in liquid N_2. DNA was isolated from 50 mg of sample using the Plant Genomic DNA Extraction Miniprep System (Viogene, Tapei, Taiwan), following the protocol provided.

2.5.1.2 Polymerase Chain Reaction (PCR)

2.5.1.2.1 Primer Design

For PCR analysis primers were designed using Primer-BLAST (Ye et al., 2012) and obtained from Macrogen Inc. (Seoul, South Korea); and are listed in Supplemental information Table 9.1.

2.5.1.2.2 Protocol for PCR amplification

PCR was performed using the GoTaq Hot Start Master Mix (Promega, Madison, WI, USA) following the protocol provided (Supplemental information Table 9.2). The PCR was run in the

Eppendorf Mastercycler Pro (Eppendorf, Hamburg, Germany) using a pre-set program (Supplemental information Table 9.3).

2.5.1.2.3 Agarose gel electrophoresis

PCR products were analysed by gel electrophoresis using a 1% agarose gel (x1 TAE) with 3 µL SYBR Safe DNA Gel Stain (Invitrogen, Carlsbad, CA, USA) at 120V for 30 minutes and visualised on a UV transilluminator.

If the correct bands were present, identifying the T-DNA insertion, the plants were grown to maturity and seeds were harvested; and used in further experiments.

2.5.2 RNA sequencing (RNA-seq)

2.5.2.1 Sample harvesting and preparation

For RNA-seq the youngest four leaf pairs were cut from the plant and snap frozen in liquid N_2 and placed into -80°C until further use. Samples were ground into a fine powder in liquid N_2. RNA was isolated from 50 mg of sample using the RNeasy Plant Mini Kit (Qiagen, Hilden, Germany) following the protocol provided. The only modification to the protocol was that the DNase treatment step was not carried out to prevent degradation of the RNA.

Sampling consisted of 4 biological replicates (independent repeated trials), and in each trial, two wild type plants (*wt*) and two *uvr8-1* (*mt*) plants were harvested at each time point and treatment. RNA extracted from these plants was pooled to generate a single sample per time point per genotype (Table 2.3).

Table 2.3 Samples collected for RNA-seq for a single biological repeat. In total, there were four biological repeats.

Genotype	Treatment	Time point		
		0hrs	**6hrs**	**24hrs**
Wild type (L*er*)	+UVB	2 plants harvested - 1 pooled sample	2 plants harvested - 1 pooled sample	2 plants harvested - 1 pooled sample
Wild type (L*er*)	-UVB		2 plants harvested - 1 pooled sample	2 plants harvested - 1 pooled sample
uvr8-1 (L*er*)	+UVB	2 plants harvested - 1 pooled sample	2 plants harvested - 1 pooled sample	2 plants harvested - 1 pooled sample

2.5.2.2 RNA quantification and quality control

RNA quantity and quality were determined using Agilent 2100 Bioanalyzer (Agilent Technologies, Palo Alto, CA, USA).

2.5.2.3 RNA-sequencing

The samples (500ng/sample) were then submitted to New Zealand Genomics Limited (NZGL; Otago, New Zealand) for further processing and sequencing. RNA-seq was performed by paired-end sequencing of three lanes of Illumina HiSeq2500. The sequencing generated a total of > 1 000 000 000 reads, with an average of > 40 000 000 reads per biological replicate.

2.5.2.4 RNA-seq analysis

Initial analysis was performed by NZGL. The analysis was performed as follows: reads were mapped to the TAIR10 release of the *A. thaliana* genome using tophat2; which generated an average concordant mapping rate of 86.5%. Gene counts were generated from each aligned BAM file using the software HTSeq-count package. Differential expression was detected using the R-package DESeq2 (Love et al., 2014). Key comparisons can be seen in Table 2.4.

Table 2.4 Key comparisons investigated in through RNA-seq.

Wild type comparisons (wt – L*er*)	*wt* 6hrs +UVB versus *wt* 6hrs -UVB
	wt 24hrs +UVB versus *wt* 24hrs -UVB
Mutant versus wild type comparisons (mt - *uvr8-1* (L*er*) : wt – L*er*)	*mt* 0hrs -UVB versus *wt* 0hrs -UVB
	mt 6hrs +UVB versus *wt* 6hrs -UVB
	mt 24hrs +UVB versus *wt* 24hrs -UVB

To validate the RNA-seq results, 6 differentially expressed were selected for analysis using Quantitative Real-Time Polymerase Chain Reaction (qRT-PCR) (see Section 2.5.3 for methods).

2.5.2.5 Overrepresentation analysis

GO enrichment analysis used the differential expression analysis files generated through DESeq2 to further analyse the differentially expressed genes (DEGs) for functionality. Significantly changed genes (p-adjusted; padj < 0.05) in key comparisons were uploaded to PANTHER version 11 (http://www.pantherdb.org/) (Mi et al., 2013; Mi et al., 2017). GO enrichment analysis was performed using GO-slim molecular function, biological process, and cellular location. PANTHER overrepresentation test was performed at $P < 0.05$ with P-values determined by binomial statistics (Cho and Campbell, 2000).

2.5.2.6 MapMan and PageMan analysis

MapMan and PageMan analysis (MapMan 3.6.0, http://mapman.gabipd.org/web/guest/mapman) (Thimm et al., 2004; Usadel et al., 2009) allows for the visualisation of the transcriptomic data at a process and pathway level. MapMan uses hierarchical BIN based ontology, were specific bins are allocated to biological functions, and sub-bins are allocated to individual steps of that particular function. This minimises redundancy usually found in GO enrichment analysis.

All differentially expressed genes found in the key comparisons through DeSeq2 was analysed through MapMan version 3.6.0, focusing in particular on the photosynthesis-associated pathways. All the data for the differentially expressed genes (padj < 1) were arranged in with

their unique locus identifiers and Log2FoldChange and saved in a tab-delimited format in Excel. These files were then mapped against the Arabidopsis "Ath_AGI_LOCUS_TAIR10_Aug2012.m02" database in MapMan and subjected to Wilcoxon Wilcoxon Rank-Sum testing within MapMan, as well as Benjamini & Hochberg-corrected (P-value < 0.05). The generated maps can be seen in Chapter 4.

2.5.3 Quantitative Real-Time Polymerase Chain Reaction (qRT-PCR)

2.5.3.1 Sample harvesting and preparation

For qRT-PCR the youngest 4 leaf pairs were cut from the plant and snap frozen in liquid N_2 and placed into -80°C until further use. Samples were ground into a fine powder in liquid N_2. RNA was isolated from 50 mg of sample using the RNeasy Plant Mini Kit (Qiagen, Hilden, Germany) following the protocol provided. The only modification to the protocol was that the in column DNase treatment step was skipped and performed after RNA quantification and quality control.

Sampling consisted of 3 biological replicates (independent trials), in each trial there were 2 wild type plants (*wt,* Col -0) and 2 mutant plants harvested at each time point and the RNA extracted from these plants was pooled to generate a single sample per time point per genotype.

2.5.3.2 RNA quantification and quality control

RNA was quantified and quality controlled using the Nanodrop ND-1000 (Thermo Fisher Wilmington, DE, Scientific, USA) following the protocol provided.

2.5.3.3 DNase treatment

5 µg of RNA from each sample needed to be re-suspended with DNA/RNA free water for DNase treatment using RNase-free recombinant DNase I (Roche, Mannheim, Germany), following the protocol provided. Prior to cDNA synthesis absence of contaminating DNA was confirmed using the control Actin primers described in the general PCR protocol (Section 2.5.1.2) and subsequent gel electrophoresis.

2.5.3.4 cDNA synthesis

1 µg of the DNase treated RNA sample was resuspended in DEPC-treated water for cDNA synthesis using the Transcriptor First Strand cDNA Synthesis Kit (Roche, Mannheim, Germany), using the Oligo $(dT)_{18}$ primer.

After cDNA synthesis, the presence of cDNA was confirmed using the control Actin primers described in the general PCR protocol and subsequent gel electrophoresis (Section 2.5.1.2).

2.5.3.5 qRT-PCR

2.5.3.5.1 Primer design

For qRT-PCR analysis primers were designed using Primer-BLAST (Ye et al., 2012) according to the requirements of qRT-PCR:

- Melting point is between 55 °C and 60 °C
- GC content is ~50%
- Primer length is ~20 bp
- Amplicon length is between 100 – 200 nucleotides

Primers were obtained from Macrogen Inc. (Seoul, South Korea), and are listed in Supplemental information Table 9.4.

2.5.3.5.2 Protocol for qRT-PCR amplification

qRT-PCR was performed using the Light Cycler 480 SYBR Green I Master kit (Roche Diagnostics, Indianapolis, IN, USA) following the protocol provided. The only adjustment was the halving the reagents to ensure a final volume of 10 µL (Supplemental information Table 9.5). The final dilution was 1:100. The plates were run in the Light Cycler 480 (Roche Diagnostics, Indianapolis, IN, USA) using a pre-set program (Supplemental information Table 9.6).

Three technical replicates were performed for each cDNA sample, and overall three biological repeats per time point and genotype were used.

2.5.3.6 Analysis of qRT-PCR data

Output from the Roche Light Cycler 480 was converted to a readable format using:

- Convert Light Cycler 480 Raw Data text file into Input Format for LinREG PCR (version 2)
- LinREG PCR: Analysis of quantitative RT-PCR Data (version 2014.4)

Downloaded from https://www.medischebiologie.nl/files/?main=files&sub=LinRegPCR (Ruijter et al., 2009).

The data was then transformed into a reportable format following the protocol from Schmittgen and Livak (2008), generating Delta Ct values allowing us to determine fold change. To determine statistical significance between treatments and between genotypes the transformed data was analysed through a one-way ANOVA in IBM SPSS Statistics (SPSS Statistics v25; IBM, Armonk, NY, USA).

3 Identification of photosynthesis phenotype in response to low fluence rates of UV-B

3.1 Introduction

In the coming decades, the global population will continue to increase and to keep up with the global demand for food; crop production will have to continue to increase. Evidence suggests that conventional plant breeding in terms of optimising crop yields is near its biological limit (Zhu et al., 2010); however, the conversion of solar energy by plants to further increase crop yields can still be improved (Zhu et al., 2008, 2010). Much research has gone into trying to improve photosynthetic performance to improve agricultural yields (Murchie and Niyogi, 2011; Ort et al., 2015). Being able to manipulate photosynthesis through altering the light spectrum may be a sustainable way of improving crop production without the use of gene manipulation; given its negative perception by the public.

Most studies have looked at the impact of high fluence rates of UV-B on photosynthesis; and have shown that high fluence rates of UV-B result in damage to PS II and lower photosynthetic efficiency (Tyystjärvi, 2008; Davey et al., 2012; Dobrikova et al., 2013) as well as lower chlorophyll content (Surabhi et al., 2009) and inhibition of net photosynthetic rate (Jansen et al., 1998). Given the negative impact of high UV-B doses, understanding the impact of lower UV-B fluence rates is vital. Recently, more studies have examined the impact of low fluence UV-B on the plants, such as the work by Favory et al. (2009), which examined the impact of 1.5 µmol m^{-2} s^{-1} of narrowband UV-B on photomorphogenesis. The analysis of the Favory et al. (2009) microarray data by Wargent and Jordan (2013) using PageMan showed upregulation of photosynthesis-associated genes in plants exposed to 1.5 µmol m^{-2} s^{-1} of narrowband UV-B versus no UV-B; which was not present under high UV-B fluence rates (3 µmol m^{-2} s^{-1}) (Brown et al., 2005; Wargent and Jordan, 2013). This upregulation of photosynthesis-associated genes indicates that on a transcriptome level low fluence rates of UV-B may be beneficial to

photosynthesis. Further studies in other plant species have shown that presence of low levels of UV-B may stimulate photosynthesis (Vidović et al., 2015), as well as studies indicating that ambient levels of UV-B have little effect on photosynthesis (Ballaré et al., 2011; Hideg et al., 2013). The series of experiments presented in this chapter looks at the impact of low fluence rate UV-B on net photosynthetic rate to determine if UV-B can indeed be beneficial to photosynthetic performance.

3.2 Net photosynthetic rate of *wt* decreases after 48 hours of 1.5 µmol m^{-2} s^{-1} UV-B exposure

The starting point for initial experiments was based on the Wargent and Jordan (2013) analysis of the Favory et al. (2009) microarray data using PageMan, which showed the upregulation of photosynthesis-associated genes at 6 hours of 1.5 µmol m^{-2} s^{-1} narrowband UV-B in 4-day old L*er Arabidopsis* seedlings. The experiment was designed to test if 1.5 µmol m^{-2} s^{-1} narrowband UV-B would cause a change in net photosynthetic rate in both *wt* (L*er*) and *uvr8-1* (L*er*).

In their experiment, Favory et al. (2009) used a narrowband filter on UV-B emitting fluorescent tubes; in this experiment UV-B emitting LEDs were used instead. These LEDs emit a very specific and narrow dose of UV-B; the wavelengths emitted ranged from 290 nm to 305 nm, peaking at 295 nm. Also, in order to measure net photosynthetic rate using the IRGA, the plants were grown to 35 days after sowing (DAS), rather than using very young seedlings. At 35 DAS the plants were placed in a UV-B environment of 1.5 µmol m^{-2} s^{-1} UV-B and 220 µmol m^{-2} s^{-1} of PAR (+UVB), as well as the control no UV-B environment of 220 µmol m^{-2} s^{-1} of PAR only (-UVB). Net photosynthetic rate (µmol CO_2 m^{-2} s^{-1}) was measured prior to commencement of UV-B exposure (0hrs) and then every 24 hours over the course over 5 days, with only the first 48hrs of exposure shown in Fig 3.1.

Net photosynthetic rate of wild type was altered in response to UV-B exposure compared to no UV-B over 48hrs. At 24hrs the photosynthetic rate did not differ between UV-B and no UV-B (Fig

3.1), and at 48hrs there was a significant decrease in net photosynthetic rate under UV-B ($P < 0.05$, Fig 3.1) compared to no UV-B. The decrease in photosynthetic rate suggests that low fluence UV-B may be mildly impeding or damaging to the function of photosynthetic apparatus over longer exposure times.

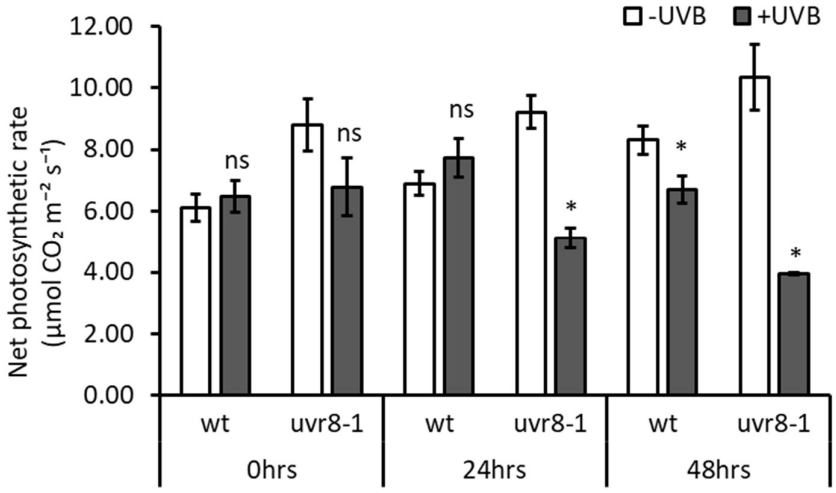

Figure 3.1 Changes in net photosynthetic rate (µmol CO_2 m^{-2} s^{-1}) in *wt* (L*er*) and *uvr8-1* (L*er*) in response to irradiation with 1.5 µmol m^{-2} s^{-1} of UV-B (+UVB, dark grey) or without (-UVB, white) over 48 hours of exposure. 0hrs is 35 DAS and is the net photosynthetic rate prior to commencement of illumination with UV-B, while 24hrs is after 24 hours of exposure and so forth. In the +UVB condition the plants are exposed to 1.5 µmol m^{-2} s^{-1} and 220 µmol m^{-2} s^{-1} of PAR, in the -UVB condition the plants are exposed to 220 µmol m^{-2} s^{-1} of PAR only. *uvr8-1 - UV-B resistance locus 8-1*. Error bars represent ± S.E. (n = 8 biological repeats). Asterisks indicate statistically significant means ($P < 0.05$) between +UVB and -UVB treatments for a given time point and genotype; ns indicates not significant means.

It is worth noting while there was no significant difference in net photosynthetic rate between 0hrs and 24hrs of UV-B, as well as between 0hrs and 48hrs of UV-B; there is a significant decrease in the photosynthetic rate of wild type exposed to UV-B at 24hrs *versus* photosynthetic rate at 48hrs exposed to UV-B ($P < 0.05$, Fig 3.1). The decrease in rate suggests that long-term exposure may cause damage; resulting in the decrease in photosynthetic rate over time. Further photosynthetic rate measurements, over the course of 5 days, showed that longer exposure of wild type to UV-B led to greater reductions in photosynthetic rate (Supplementary information Fig 9.1). At the end of 5 days of exposure, plants mirrored the loss in photosynthetic rate seen in *uvr8-1* in response to UV-B exposure. Wild type plants exposed to PAR only (-UVB) also

showed an increase in photosynthetic rate, suggesting that PAR exposure could be underpinning the upregulation of photosynthesis. It may also be explained by an increase in biomass (e.g. leaf thickness) over time, as the biomass data revealed that -UVB treated plants accrued more biomass than +UVB treated ones (Supplementary information Fig 9.2).

The photosynthesis phenotype observed in *uvr8-1* is different from the wild type phenotype. In *uvr8-1,* exposure to UV-B resulted in an immediate decrease in photosynthetic rate at 24hrs; with the rate of photosynthesis being significantly lower at 24hrs +UVB when compared to the rate under –UVB ($P < 0.01$, Fig 3.1). Photosynthetic rate was further decreased at 48hrs of UV-B exposure compared to no UV-B ($P < 0.01$, Fig 3.1). *uvr8-1* plants exposed to PAR only showed no change in photosynthetic rate; confirming that it is the presence of UV-B which causes the decrease in photosynthetic rate in UV-B exposed plants and that the presence of PAR does not lessen the negative impact of UV-B exposure. The screen confirms the phenotype seen in previous research suggesting that the loss of functional UVR8 makes *uvr8-1* more susceptible to UV-B mediated damage (Brown et al., 2005).

Over the course of the 48 hours of UV-B exposure, there was an observable change in phenotype, as both wild type and *uvr8-1* plants, showed signs of purpling after 24hrs of exposure to UV-B exposure (data not shown). Purpling occurs when flavonoids and anthocyanin accumulate in the plants; and occurs as a response to UV-B exposure, and is seen as a response to UV-B stress (Hahlbrock and Scheel, 1989; Frohnmeyer, 1999; Jenkins et al., 2001).

In summary, exposure to 1.5 µmol m^{-2} s^{-1} UV-B leads to a decrease in net photosynthetic rate over 48 hours, as well as being perceived as a stressor by the plants.

3.3 Net photosynthetic rate of *wt* increases after 24 hours of 0.5 µmol m^{-2} s^{-1} UV-B exposure

Due to the reduction in net photosynthetic rate observed at 1.5 µmol m^{-2} s^{-1} of UV-B, we then chose to characterise the photosynthesis response to 0.5 µmol m^{-2} s^{-1} of UV-B, using the same

set up as before (Chapter 2: Materials and Methods). Also, to eliminate the addition of PAR upon transference from the propagation environment into the growth cabinet as the cause of changes in photosynthetic rate; the plants were given a 7-day PAR acclimation period prior to the start of exposure to UV-B. The acclimation period was under PAR only (-UVB conditions). Net photosynthetic rate (μmol CO_2 m^{-2} s^{-1}) was measured every 24hrs during both the PAR acclimation period and under UV-B exposure; net photosynthetic rate was then normalised to leaf area to allow for changes in biomass (Chapter 2: Materials and Methods).

At 24hrs of UV-B exposure, there was a 10% increase in net photosynthetic rate in wild type when compared to no UV-B ($P < 0.01$, Fig 3.2), indicating that the addition of 0.5 μmol m^{-2} s^{-1} UV-B to the light spectrum results in the increase in photosynthetic rate. Also of note is the significant increase in photosynthetic rate in wild type when comparing 0hrs and 24hrs UV-B ($P < 0.001$, Fig 3.2), which further confirms that the presence of UV-B upregulates photosynthetic rate. Furthermore, there was a significant decrease in photosynthetic rate between *wt* under UV-B at 24hrs and at 48hrs ($P < 0.001$, Fig 3.2); which shows that while the initial exposure to UV-B results in the increase of net photosynthetic rate; longer exposure to UV-B results in photosynthetic rate decreasing. All of which suggests that the initial exposure to low fluence UV-B may be beneficial to the plant in terms of upregulating photosynthetic rate.

At 0hrs, both wild type and *uvr8-1* mutant have similar net photosynthetic rates (Table 3.1), and they do not respond differently from each other under PAR only conditions; suggesting that the two genotypes do not differ in photosynthetic rate. However, after 24hrs of UV-B exposure *wt* has a significantly higher photosynthetic rate than *uvr8-1* ($P < 0.001$, Fig 3.2), which suggests that functional UVR8 is required for the increase in net photosynthetic rate and that UVR8 may play a role in the photosynthesis pathway, perhaps by being involved in the regulation of a number of genes required for photosynthesis.

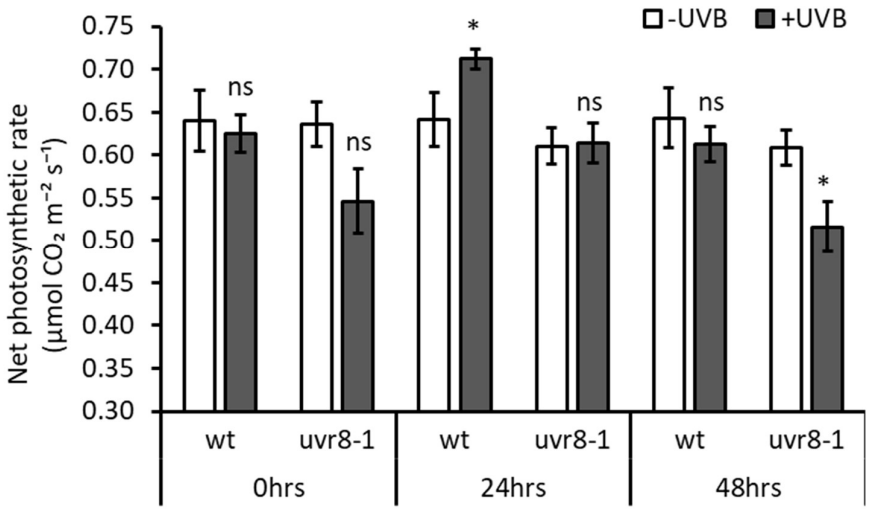

Figure 3.2 Changes in net photosynthetic rate (µmol CO_2 m^{-2} s^{-1}) normalised to leaf area in *wt* (L*er*) and *uvr8-1* (L*er*) in response to irradiation with 0.5 µmol m^{-2} s^{-1} of UV-B (+UVB, dark grey) or without (-UVB, white) over 48 hours of exposure. 0hrs is 35 DAS and is the net photosynthetic rate prior to the commencement of illumination with UV-B, while 24hrs is after 24 hours of exposure and so forth. In the +UVB condition the plants are exposed to 0.5 µmol m^{-2} s^{-1} and 220 µmol m^{-2} s^{-1} of PAR, in the -UVB condition the plants are exposed to 220 µmol m^{-2} s^{-1} of PAR only. *uvr8-1 - UV-B resistance locus 8-1*. Error bars represent ± S.E. (n = 13 biological repeats). Asterisks indicate statistically significant means ($P < 0.05$) between +UVB and -UVB treatments for a given time point and genotype; ns indicates not significant means.

In summary, exposure to 0.5 µmol m^{-2} s^{-1} UV-B leads to a net increase in photosynthetic rate at 24hrs in wild type, while it does not affect *uvr8-1*. After 48hrs, the initial increase is lost in *wt,* and photosynthetic rate begins to decline. To better understand what may cause this phenotype, we characterised the changes in flavonoid and chlorophyll content as well as changes in PS II efficiency.

Table 3.1 Changes in net photosynthetic rate (µmol CO_2 m^{-2} s^{-1}) normalised to leaf area in *wt* (L*er*) and *uvr8-1* (L*er*) in response to irradiation with 0.5 µmol m^{-2} s^{-1} of UV-B over 48 hours of exposure. Averages of photosynthetic rate in -UVB (220 µmol m^{-2} s^{-1} PAR) and +UVB (0.5 µmol m^{-2} s^{-1} UV-B and 220 µmol m^{-2} s^{-1} PAR) ± S.E. Two-sample T-test shows the statically significant difference in net photosynthetic rate between *wt* (L*er*) and *uvr8-1* at 0hrs, 24hrs and 48hrs under –UVB and +UVB.

Normalised data			**Net photosynthetic rate normalised to leaf area (µmol CO_2 m^{-2} s^{-1})**		
Genotype	**Treatment**	**n**	**0hrs**	**24hrs**	**48hrs**
L*er*	-UVB	13	0.64±0.04	0.64±0.03	0.64±0.03
uvr8-1	-UVB	13	0.64±0.03 NS	0.61±0.02 NS	0.61±0.02 NS
L*er*	+UVB	13	0.62±0.02	0.71±0.01	0.61±0.02
uvr8-1	+UVB	13	0.55±0.04 NS	0.61±0.02 **	0.52±0.03 **

*$P < 0.05$, **$P < 0.01$, ***$P < 0.001$, NS - not significant

3.3.1 Chlorophyll content of *wt* does not change in response to UV-B exposure

A possible explanation for the increase in net photosynthetic rate seen at 24hrs could be if there was an increase in chlorophyll at the same time. Studies have shown that low fluence UV-B supplementation does not affect chlorophyll content (Vidović et al., 2015) and under high UV-B stress chlorophyll content is reduced (Gao et al., 2004; Hu et al., 2013). Studies have further shown that the presence of UV-B can inhibit chlorophyll production (Yao et al., 2006). To determine the effect of low fluence UV-B, chlorophyll content was assessed using a Polyphenol Meter (Dualex Scientific+) at 0hrs and 48hrs of UV-B exposure (Chapter 2: Materials and Methods).

There was no significant change in chlorophyll content between +UVB and -UVB at 48hrs (Fig 3.3), which suggests that the increase in net photosynthetic rate under UV-B is not due an increase in chlorophyll content. However, there was a significant increase in chlorophyll content in wild type between 0hrs and 48hrs ($P < 0.01$, Fig 3.3), but this occurs both in the absence and presence of UV-B. As this happens in both light environments it suggests that the addition of UV-B is not a factor in the increase in chlorophyll. There is evidence that PAR supplementation increases chlorophyll *a* and *b* content (Vidović et al., 2015), however, measurements of chlorophyll content during the PAR acclimation period (Data not shown) showed no significant increase. The cause of the increase in chlorophyll content is unknown.

Of further interest is that *uvr8-1* had a significantly lower chlorophyll content compared to wild type at 48hrs in the absence of UV-B, while at 0hrs the chlorophyll contents of both wild type and *uvr8-1* did not differ. This would suggest that the absence of functional UVR8 might affect chlorophyll content as the plants age.

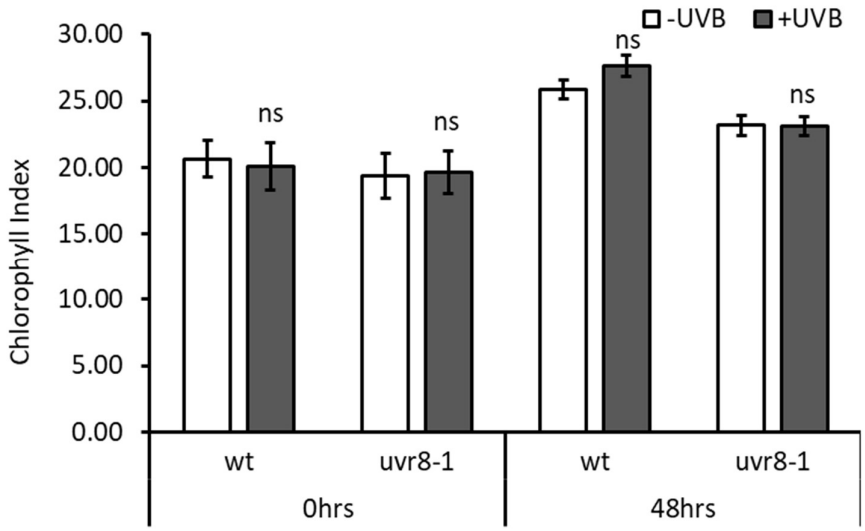

Figure 3.3 Changes in chlorophyll content in *wt* (L*er*) and *uvr8-1* (L*er*) in response to irradiation with 0.5 µmol m^{-2} s^{-1} of UV-B (+UVB, dark grey) or without (-UVB, white) over 48 hours of exposure. Chlorophyll content was measured with the Dualex scientific+ Polyphenol Meter. 0hrs is 35 DAS and is chlorophyll content prior to commencement of illumination with UV-B, while 48hrs is after 48 hours of exposure. In the +UVB condition the plants are exposed to 0.5 µmol m^{-2} s^{-1} and 220 µmol m^{-2} s^{-1} of PAR, in the -UVB condition the plants are exposed to 220 µmol m^{-2} s^{-1} of PAR only. *uvr8-1 - UV-B resistance locus 8-1*. Error bars represent ± S.E. (n = 13 biological repeats). Asterisks indicate statistically significant means ($P < 0.05$) between +UVB and -UVB treatments for a given time point and genotype; ns indicates not significant means.

3.3.2 Flavonoid content of *wt* increases after 48 hours of UV-B exposure

The accumulation of flavonoids in response to UV-B is ubiquitous (Searles et al., 2001), as flavonoids and other phenolic compounds are involved in UV-B protection (Braun and Tevini, 1993). In *Arabidopsis*, flavonoid content in leaves is an indicator of plant response to high light; as flavonoid content increases under UV-B (Mazza et al., 2000; Kliebenstein et al., 2002) and high PAR (Götz et al., 2010). Under UV-B exposure, UVR8 regulates *CHS* in response to UV-B, which in turn regulates flavonoid biosynthesis (Brown et al., 2005).

Flavonoid content was measured to determine if 0.5 µmol m^{-2} s^{-1} UV-B is perceived as a stress to the plant. Flavonoid content was measured non-destructively at 0hrs and 48hrs after UV-B exposure (Fig 3.4) using a Polyphenol Meter (Dualex Scientific+) (Chapter 2: Materials and Methods).

Flavonoid content increased significantly in wild type exposed to UV-B for 48hrs compared to no UV-B ($P < 0.001$, Fig 3.4), but did not increase in *uvr8-1*. The increase in flavonoid content after 48hrs of UV-B exposure suggests that the plants start responding to the presence of UV-B. In *uvr8-1,* flavonoid content does not increase after exposure to UV-B, as expected as the absence of functional UVR8 results in the loss of the increase in flavonoids (Brown et al., 2005).

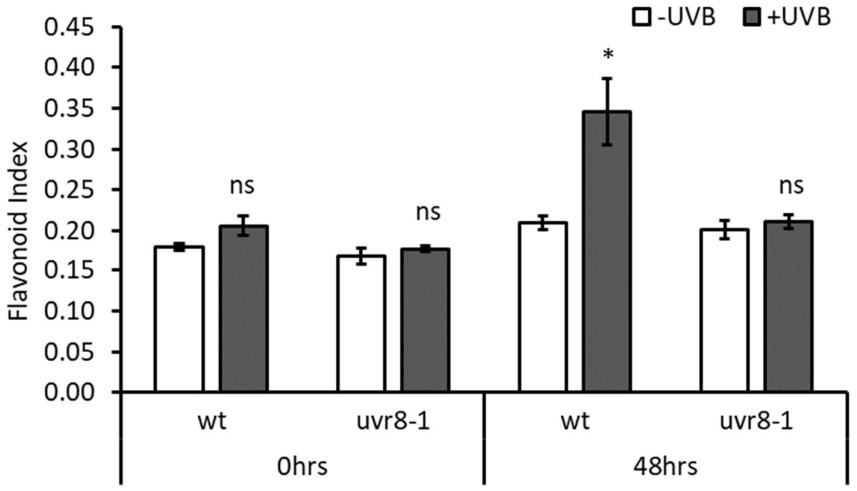

Figure 3.4 Changes in flavonoid content in *wt* (L*er*) and *uvr8-1* (L*er*) in response to irradiation with 0.5 µmol m^{-2} s^{-1} of UV-B (+UVB, dark grey) or without (-UVB, white) over 48 hours of exposure. Flavonoid content was measured with the Dualex scientific+ Polyphenol Meter. 0hrs is 35 DAS and is flavonoid content prior to the commencement illumination with UV-B, while 48hrs is after 48 hours of exposure. In the +UVB condition the plants are exposed to 0.5 µmol m^{-2} s^{-1} and 220 µmol m^{-2} s^{-1} of PAR, in the -UVB condition the plants are exposed to 220 µmol m^{-2} s^{-1} of PAR only. *uvr8-1 - UV-B resistance locus 8-1*. Error bars represent ± S.E. (n = 13 biological repeats). Asterisks indicate statistically significant means ($P < 0.05$) between +UVB and -UVB treatments for a given time point and genotype; ns indicates not significant means.

3.3.3 UV-B exposure does not deleteriously affect PS II efficiency in *wt* L*er*

PS II is a major component of the photosynthetic machinery, and shifts in Fv/Fm indicate changes in the photochemical conversion and possible photoinhibition of photosynthesis (Ranjbarfordoei et al., 2011). Studies have shown that high fluence rates of UV-B lowers PS II efficiency (Davey et al., 2012; Yu et al., 2012; Hu et al., 2013), as it damages the PS II reaction center. In order to determine if low fluence rate had an impact on PS II efficiency, Fv/Fm was

spot measured using a Rapid Screening Chlorophyll Fluorimeter (Pocket PEA) (Chapter 2: Materials and Methods) at 0hrs and 48hrs of exposure (Fig 3.5).

The normal range for PS II efficiency in healthy plants is at Fv/Fm > 0.8 (Schoefs, 2005) which was observed for all plants in the experiments (Fig 3.5). This suggests that the increase in photosynthetic rate is not the result of changes in PS II quantum efficiency nor does the exposure to UV-B negatively affect PS II during the initial exposure.

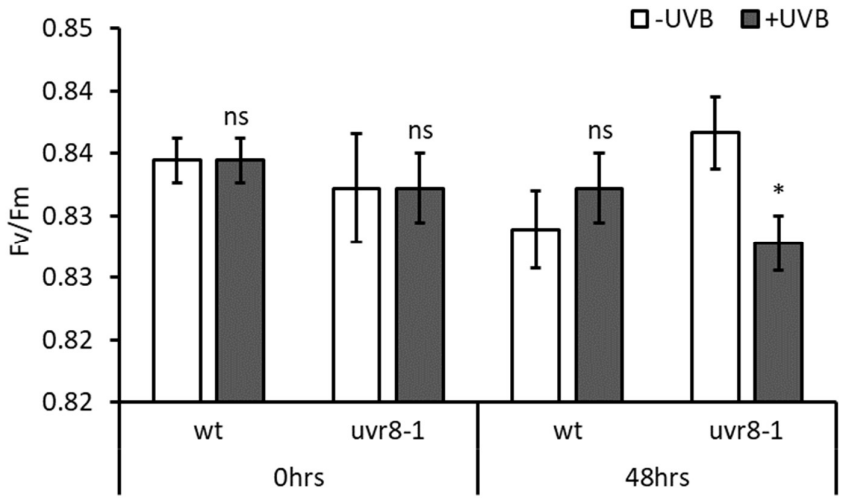

Figure 3.5 Changes in PS II quantum efficiency (Fv/Fm) in *wt* (L*er*) and *uvr8-1* (L*er*) in response to irradiation with 0.5 µmol m^{-2} s^{-1} of UV-B (+UVB, dark grey) or without (-UVB, white) over 48 hours of exposure. Fv/Fm was measured using a Rapid Screening Chlorophyll Fluorimeter. 0hrs is 35 DAS and is the PS II quantum efficiency rate prior to the commencement of illumination with UV-B, while 48hrs is after 48 hours of exposure. In the +UVB condition the plants are exposed to 0.5 µmol m^{-2} s^{-1} and 220 µmol m^{-2} s^{-1} of PAR, in the -UVB condition the plants are exposed to 220 µmol m^{-2} s^{-1} of PAR only. *uvr8-1 - UV-B resistance locus 8-1*. Error bars represent ± S.E. (n = 13 biological repeats). Asterisks indicate statistically significant means ($P < 0.05$) between +UVB and -UVB treatments for a given time point and genotype; ns indicates not significant means.

3.4 Confirmation of UV-B photosynthesis phenotype

3.4.1 Increase in photosynthetic rate is due to exposure to 0.5 µmol m^{-2} s^{-1} UV-B exposure

To determine that the increase in net photosynthetic rate at 24hrs of UV-B exposure was due to the addition of 0.5 µmol m^{-2} s^{-1} UV-B and not due to the addition of PAR upon transference from the propagation environment into the growth chamber, plants were given a 7-day PAR

acclimation period prior to exposure to UV-B. The PAR acclimation period was the same as the -UVB light conditions (Chapter 2: Materials and Methods), and photosynthetic rate was measured every 24hrs over the course of the 7 days.

In both wild type and *uvr8-1* photosynthetic rate increased gradually over the course of the 7 days (Fig 3.6). Moreover, although there is a significant increase between Day 0 and Day 7 in both wild type and *uvr8-1* ($P < 0.01$, Fig 3.6) there were no significant increases in photosynthetic rate between one day to the next as seen in *wt* when exposed to UV-B. The absence of the highly significant increase in photosynthetic rate further indicates that it is the addition of UV-B to the spectrum that results in the abrupt upregulation of photosynthetic rate, following this acclimation period.

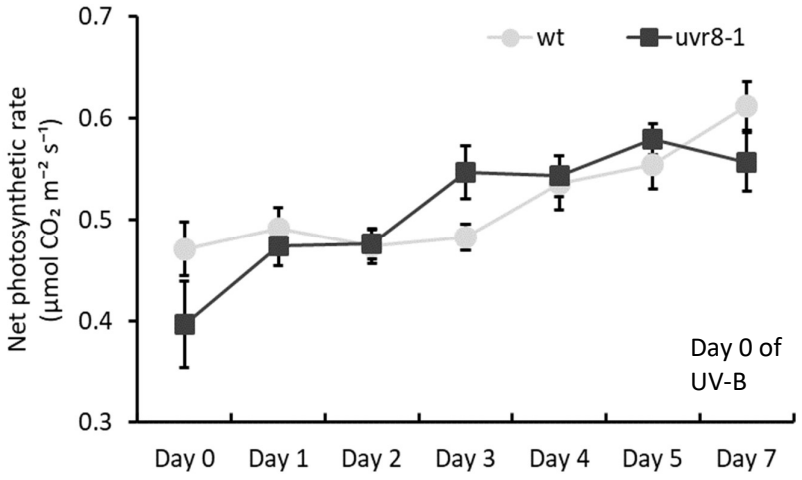

Figure 3.6 Changes in net photosynthetic rate (µmol CO_2 m^{-2} s^{-1}) normalised to leaf area in *wt* (L*er*) and *uvr8-1* (L*er*) in response to irradiation with 220 µmol m^{-2} s^{-1} of PAR (-UVB). Day 0 is 28 DAS and is the net photosynthetic rate prior to commencement of illumination with PAR, while Day 1 is after 24 hours of exposure and so forth. *wt* (L*er*) is represented as the light grey circles, while *uvr8-1* (L*er*) is represented as dark grey squares. *uvr8-1* - *UV-B resistance locus 8-1*. Error bars represent ± S.E. (n = 13 biological repeats).

3.4.2 Net photosynthetic rate of Col-0 increases after 24 hours of UV-B exposure

To determine the robustness of the photosynthesis phenotype seen in L*er* across multiple *Arabidopsis* ecotypes, the Columbia wild type (Col-0) was chosen to test under identical

experimental conditions as L*er*. The Columbia ecotype was also of interest since a large number of photosynthesis mutants exist in the Col ecotype. The Landsberg and Columbia ecotypes vary widely from each other, on both a genotypic and phenotypic level. L*er* and Col-0 have extensive DNA polymorphisms (Nordborg et al., 2005; Ziolkowski et al., 2009), as well as Col-0 having a larger rosette size to L*er*, and a later flowering time (Passardi et al., 2007). Studies examining the chloroplast movement response in both L*er* and Col-0 (Königer et al., 2008), showed that L*er* had a stronger accumulation response to low blue irradiation than Col-0, while Col-0 showed a stronger avoidance response under high blue light irradiation. This suggests that Col-0 and L*er* could respond differently in photosynthetic rate under UV-B irradiation.

At 24hrs of UV-B exposure net photosynthetic rate of Col-0 plants was 12% higher under UV-B compared to no UV-B ($P < 0.001$, Fig 3.7). Furthermore, when comparing Col-0 at 0hrs and 24hrs UV-B, there was a significant increase in net photosynthetic rate ($P < 0.001$, Fig 3.7). At 48hrs of UV-B, there was a significant decrease in photosynthetic rate compared to 24hrs UV-B ($P < 0.001$, Fig 3.7). This is very similar to the phenotype seen in L*er*, suggesting that the photosynthesis phenotype is not limited to L*er*. The increase in photosynthetic rate at 24hrs of UV-B exposure is significantly larger in Col-0 than in L*er* ($P < 0.05$), which suggests Col-0 may be more capable of responding to UV-B exposure. In the absence of UV-B the photosynthetic rate of both ecotypes was very similar, thus suggesting that there is no inherent difference in photosynthetic rate, but the response to UV-B differs between the two.

The absence of the photosynthesis phenotype seen in *uvr8-1* is also seen in the *uvr8* mutant in Columbia, *uvr8-6* (Supplementary information Fig 9.3).

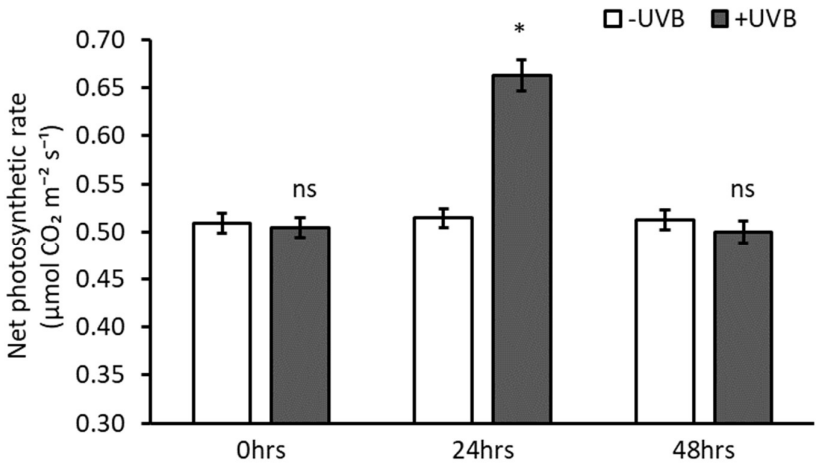

Figure 3.7 Changes in net photosynthetic rate (µmol CO_2 m^{-2} s^{-1}) normalised to leaf area in Col-0 in response to irradiation with 0.5 µmol m^{-2} s^{-1} of UV-B (+UVB, dark grey) or without (-UVB, white) over 48 hours of exposure. All Col-0 samples pooled together. 0hrs is 35 DAS and is the net photosynthetic rate prior to commencement of illumination with UV-B, while 24hrs is after 24 hours of exposure and so forth. In the +UVB condition the plants are exposed to 0.5 µmol m^{-2} s^{-1} and 220 µmol m^{-2} s^{-1} of PAR, in the -UVB condition the plants are exposed to 220 µmol m^{-2} s^{-1} of PAR only. Error bars represent ± S.E. (n = 160 biological repeats). Asterisks indicate statistically significant means ($P < 0.05$) between +UVB and -UVB treatments for a given time point and genotype; ns indicates not significant means.

3.4.3 Photosynthesis phenotype occurs under multiple UV-B light sources

To determine if the photosynthesis phenotype was limited to the specific waveband of 295 nm to 305 nm produced by the LEDs in the main experimental setup, the phenotype was tested using UV-B emitting fluorescent tubes, which emit broadband UV-B; while the remainder of the experimental set up remained the same (Chapter 2: Materials and Methods).

When Col-0 was exposed to a fluence rate of 0.5 µmol m^{-2} s^{-1} of broadband UV-B, net photosynthetic rate increased significantly after 24hrs under UV-B compared to no UV-B ($P <$ 0.001, Fig 3.8). There was a significant increase in photosynthetic rate when comparing 0hrs and 24hrs of UV-B ($P < 0.001$, Fig 3.8). This confirms that the photosynthesis phenotype is not limited to the narrow waveband emitted by the LEDs, but can be reproduced using broadband UV-B emitting fluorescent tubes. It is also worth noting that there is no significant difference between the increases in photosynthetic rate at 24hrs under the LEDs versus the fluorescent tubes.

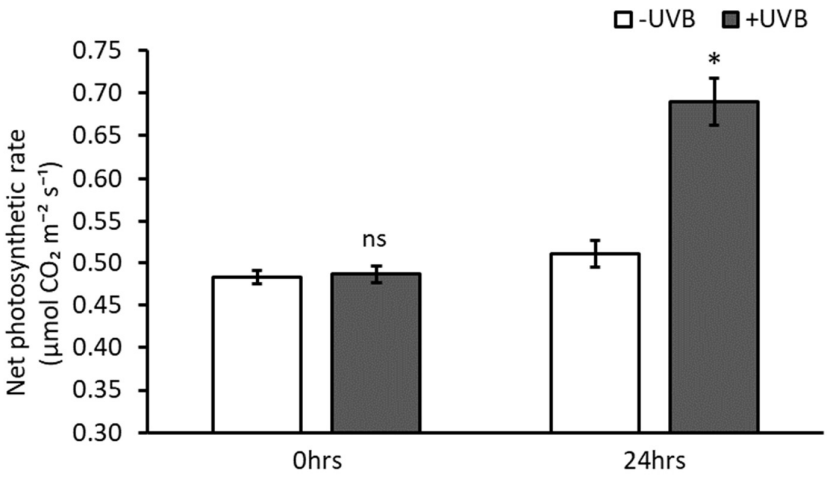

Figure 3.8 Changes in net photosynthetic rate (µmol CO_2 m^{-2} s^{-1}) normalised to leaf area in Col-0 in response to irradiation with 0.5 µmol m^{-2} s^{-1} of UV-B (+UVB, dark grey) or without (-UVB, white) over 24 hours of exposure under UV-B emitting fluorescent tubes. 0hrs is 35 DAS and is the net photosynthetic rate prior to commencement of illumination with UV-B, while 24hrs is after 24 hours of exposure. In the +UVB condition the plants are exposed to 0.5 µmol m^{-2} s^{-1} and 220 µmol m^{-2} s^{-1} of PAR, in the -UVB condition the plants are exposed to 220 µmol m^{-2} s^{-1} of PAR only. Error bars represent ± S.E. (n = 12 biological repeats). Asterisks indicate statistically significant means ($P < 0.05$) between +UVB and -UVB treatments for a given time point and genotype; ns indicates not significant means.

3.4.4 Photosynthesis phenotype occurs in other mutants of UV-B signalling and unrelated photosynthesis genes

To further test the robustness of the phenotype, the effect of UV-B exposure on the photosynthesis response in mutants of genes not known to be affected by UV-B, and not related to photosynthesis, was tested using the same conditions. For this purpose, three floral morphogenesis mutants were chosen: *lug444* (AT4G32551), *luh4* (AT2G32700) and *seu-4* (AT1G43850). Each of these are mutants in genes that are expressed in the later stages of floral development. Thus, the mutations should not affect the net photosynthetic rate and thus are expected to behave like wild type under the screening conditions.

All three mutants tested showed a significant increase in net photosynthetic rate after 24hrs of exposure to UV-B compared to no UV-B ($P < 0.001$, Fig 3.9). The data also showed that each of the mutants exhibited a similar photosynthetic rate to wild type prior to UV-B exposure, as well as having similar photosynthetic rates to the *wt* after 24hrs of UV-B exposure. This suggests that the absence of the photosynthesis phenotype observed in wild type at 24hrs of UV-B is limited

to mutants which have mutations in genes related to UV-B photomorphogenesis, such as *uvr8-1,* or photosynthesis.

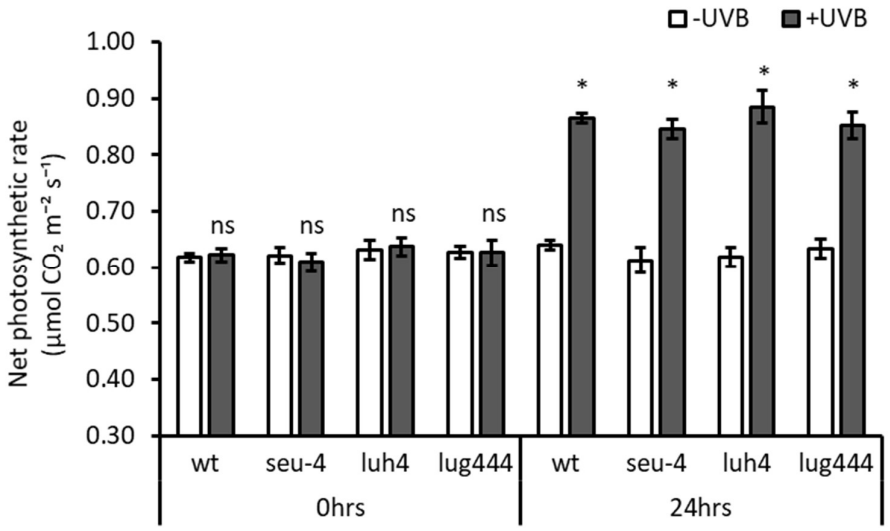

Figure 3.9 Changes in net photosynthetic rate (µmol CO_2 m^{-2} s^{-1}) normalised to leaf area in *wt* (Col-0), *seu-4* (Col), *luh4* (Col) and *lug444* (Col) in response to irradiation with 0.5 µmol m^{-2} s^{-1} of UV-B (+UVB, dark grey) or without (-UVB, white) over 48 hours of exposure. 0hrs is 35 DAS and is the net photosynthetic rate prior to commencement of illumination with UV-B, while 24hrs is after 24 hours of exposure. In the +UVB condition the plants are exposed to 0.5 µmol m^{-2} s^{-1} and 220 µmol m^{-2} s^{-1} of PAR, in the -UVB condition the plants are exposed to 220 µmol m^{-2} s^{-1} of PAR only. *seu-4 - seuss-4*, *luh4 - leunig-like-4*, *lug444* - *leunig-444*. Error bars represent ± S.E. (n = 16 biological repeats). Asterisks indicate statistically significant means ($P < 0.05$) between +UVB and -UVB treatments for a given time point and genotype; ns indicates not significant means.

3.5 Chapter Summary

In this chapter, the upregulated photosynthesis phenotype in response to a low UV-B fluence rate (0.5 µmol m^{-2} s^{-1} UV-B) has been established, and the experimental set up is tested for robustness. The data shows that when exposed to 0.5 µmol m^{-2} s^{-1} UV-B, both L*er* and Col-0 show an increase in net photosynthetic rate at 24hrs; which is accompanied by a subsequent decrease in rate at 48hrs. The exposure to UV-B does not lead to increases in chlorophyll content and PS II efficiency; leading to the question: 'What occurs on a transcriptomic and proteomic level that causes the initial 24hrs increase in photosynthesis?' In the *uvr8* null mutant, *uvr8-1,* the photosynthesis phenotype is absent, suggesting that the phenotype may be UVR8

dependent. Moreover, the phenotype was confirmed in unrelated mutants and using alternative UV-B exposure sources.

Recently, a number of photosynthesis-related genes that are regulated by the UVR8 signalling cascade have been identified; such as *SIG5 (SIGMA FACTOR 5), ELIP1 (EARLY LIGHT-INDUCIBLE PROTEIN 1)* and *ELIP2* (Kanamaru and Tanaka, 2004; Brown et al., 2005). These three genes have been associated with the photomorphogenic response to UV-B exposure, and have been associated with photosynthesis in response to UV-B (Brown et al., 2005; Brown and Jenkins, 2008; Davey et al., 2012). Hence, these genes could be involved in the increase in photosynthetic rate observed at 24hrs +UVB. In Chapter 4, the focus is on these genes as well as the negative regulators of UVR8, *RUP1* and *RUP2*, and how the loss of these genes affects photosynthetic rate. Furthermore, in order to determine what happens in the initial 24hrs of UV-B exposure transcriptomic analysis was undertaken, the results and analysis of which are presented in Chapter 5.

4 Response to low fluence UV-B in mutants of pre-defined candidate regulators of photosynthesis phenotype

4.1 Introduction

In Chapter 3, the photosynthesis response to 0.5 µmol m^{-2} s^{-1} of UV-B in wild type *Arabidopsis* was characterised. In the absence of functional UVR8, the increase in photosynthetic rate is absent, indicating that UVR8 is involved in mediating the increase in photosynthetic rate. As UVR8 is involved in the regulation of a large number of genes in response to UV-B exposure, it may be that UVR8 is involved in gene regulation specific to the photosynthesis response.

A number of photosynthesis-related genes which can be regulated in response to UV-B by the UVR8 signalling cascade have been identified; such as *SIG5, ELIP1* and *ELIP2* (Kanamaru and Tanaka, 2004; Brown et al., 2005). These genes are also associated with the photomorphogenic response under UV-B exposure and have been associated with photosynthesis in response to UV-B (Brown et al., 2005; Brown and Jenkins, 2008; Davey et al., 2012). There is evidence to suggest that these genes are also involved in maintaining photosynthetic efficiency under high visible light stress (Montané and Kloppstech, 2000; Adamska et al., 2001; Onda et al., 2008; Belbin et al., 2017) and hence could be implicated in the photosynthesis phenotype. To determine if this is the case, the UV-B photosynthetic responses were assayed in mutants of these genes, in addition to characterising the green leaf area growth response following UV-B exposure.

In terms of other UV-B related signalling regulators, which have not been previously linked to photosynthesis *per se*, RUP1 and RUP2 are negative regulators of the UVR8 signalling (Gruber et al., 2010), and are involved in maintaining a balance between stress response and plant growth (Gruber et al., 2010; Vanhaelewyn et al., 2016). In the absence of both RUPs, *Arabidopsis* has a heightened acclimation response to UV-B (Gruber et al., 2010), and understanding if such regulators affect the photosynthesis phenotype was also of interest. Here, all of these pre-

defined candidate regulators of the photosynthetic phenotype were studied, prior to the use of RNA-seq to screen for hitherto unidentified candidate regulators (Chapter 5).

4.2 SIGMA FACTOR 5 – SIG5 (AT5G24120)

SIG5 is a nuclear-encoded stress responsive sigma factor involved in chloroplast transcription (Tsunoyama et al., 2002; Nagashima et al., 2004; Tsunoyama et al., 2004). It encodes the plastid RNA polymerase sigma factor that regulates the expression of *psbA* and *psbD* via the Blue Light Responsive Promoter (BLRP) (Tsunoyama et al., 2002; Kanamaru and Tanaka, 2004; Nagashima et al., 2004; Davey et al., 2012). *psbA* and *psbD* encode the D1 and D2 proteins in PS II (Tsunoyama et al., 2002; Kanamaru and Tanaka, 2004; Nagashima et al., 2004). *SIG5* is induced by blue light, high light stress and several other stresses (Tsunoyama et al., 2002; Kanamaru and Tanaka, 2004; Nagashima et al., 2004; Tsunoyama et al., 2004). *SIG5* induction is thus regulated by phytochrome, cryptochrome and UVR8 (Monte et al., 2004; Brown and Jenkins, 2008; Onda et al., 2008; Mellenthin et al., 2014). Expression is also regulated by photosynthesis (Mellenthin et al., 2014), and evidence suggests that photosynthetic gene expression and chloroplast transcription are regulated by the sigma factors, SIG5 in particular, in response to light intensity (Onda et al., 2008; Belbin et al., 2017). The response to high light intensity is suggested to allow the plant to maintain high synthesis rates of D2 and PS II activity as well as increasing the turnover rate of damaged PS II reaction center proteins under those conditions (Tsunoyama et al., 2002; Nagashima et al., 2004; Tsunoyama et al., 2004; Davey et al., 2012; Chi et al., 2015).

UV-B induces upregulation of *SIG5* under both high and low fluence rates (Davey et al., 2012; Morales et al., 2015). Transcript levels of *SIG5* increase when exposed to low doses of UV-B, and UVR8 regulates its expression (Favory et al., 2009; Davey et al., 2012; Wargent and Jordan, 2013). Furthermore, expression of *psbD-BLRP* increased with the duration and fluence rate of UV-B treatment (Davey et al., 2012). SIG5 mediates the increase of *psbD-BLRP*, as the *sig5* null mutant lacked the increase of *psbD-BLRP* (Davey et al., 2012). However, the loss of SIG5 does

not reduce photosynthetic efficiency under UV-B, and it does not affect the overall survival of the plant under UV-B conditions (Davey et al., 2012). This suggests that it is possible that other mechanisms may stimulate *psbD* expression to UV-B, or perhaps that the increase in *psbD* transcript levels as a result of UV-B is not important in maintaining photosynthetic efficiency (Davey et al., 2012). Hence, the role of SIG5 in response to UV-B and its role in photosynthesis is not fully understood.

Here the photosynthesis response of *sig5-1* and *sig5-2* to 0.5 µmol m^{-2} s^{-1} UV-B was characterised under identical conditions as before (Chapter 2: Materials and Methods). Both mutants lack *SIG5* transcription and do not show the increase in *psbD*-BLRP under UV-B that is observed in wild type (Davey et al., 2012). *sig5-1* is a T-DNA insertion mutant; the insertion being in the last exon, which results in SIG5 being non-functional, which in turn severely reduces transcript levels of *psbD*-BLRP (Tsunoyama et al., 2004). In *sig5-2*, SIG5 is unable to function as a sigma factor. *sig5-2* is T-DNA insertion mutant, with the insertion in exon 2, resulting in the protein missing all the conserved regions (Yao et al., 2003), and has no visible mutant phenotype under normal growth conditions, but is more sensitive to stress (Nagashima et al., 2004).

4.2.1 The UV-B dependent photosynthesis phenotype was altered in *sig5* mutants

The UV-B dependent increase in photosynthetic rate at 24hrs was altered in the *sig5* mutants. At 24hrs of UV-B exposure, there was an 8% increase in photosynthetic rate in *sig5-1* compared to no UV-B ($P < 0.001$, Fig 4.1), as well as an 8% increase in rate between 0hrs and 24hrs of UV-B ($P < 0.001$, Fig 4.1). However, *sig5-2* exhibited a different response; as at 24hrs +UVB there was a 3% decrease compared to –UVB at 24hrs ($P < 0.001$, Fig 4.1), but the photosynthetic rate at 24hrs did not differ significantly from the rate measured at 0hrs. The changes in response show that functional SIG5 plays a role in the observed photosynthesis phenotype at 24hrs in wild type. As *sig5-1* showed a lesser increase in rate compared to wild type, it suggests that functional SIG5 is important to the increase in rate and involved in the increase in rate, but is

not key to the increase, as it occurs even in its absence albeit reduced. The decrease in rate observed in *sig5-2* versus the increase observed in both *wt* and *sig5-1* showed that the sigma factor activity of SIG5 plays a role in maintaining photosynthesis efficiency under UV-B exposure. As to why specifically the mutants differ in response, and why the inactivation of sigma factor activity makes such a difference is unknown.

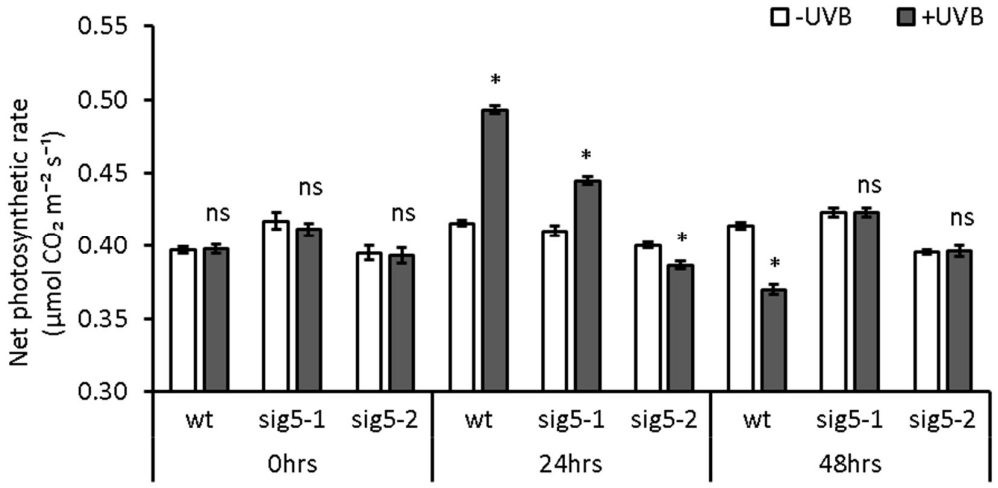

Figure 4.1 Changes in net photosynthetic rate (µmol CO_2 m^{-2} s^{-1}) normalised to leaf area in *wt* (Col-0), *sig5-1* (Col) and *sig5-2* (Col) in response to irradiation with 0.5 µmol m^{-2} s^{-1} of UV-B (+UVB, grey) or without (-UVB, white) over 48 hours of exposure. 0hrs is 35 DAS and is the net photosynthetic rate prior to illumination with UV-B, while 24hrs is after 24 hours of exposure and so forth. In the +UVB condition the plants are exposed to 0.5 µmol m^{-2} s^{-1} and 220 µmol m^{-2} s^{-1} of PAR, in the –UVB condition the plants are exposed to 220 µmol m^{-2} s^{-1} of PAR only. *sig5-1 – sigma factor 5-1, sig5-2 - sigma factor 5-2*. Error bars represent ± S.E. (n = 16 biological repeats). Asterisks indicate statistically significant means ($P < 0.05$) between +UVB and –UVB treatments for a given time point and genotype; ns indicates not significant means.

At 48hrs of UV-B, the absence of SIG5 has less of an impact on photosynthetic rate, as both *sig5* mutants showed no significant change in rate between +UVB and –UVB at 48hrs (Fig 4.1). However, *sig5-1* showed a 5% decrease in rate between 24hrs +UVB and 48hrs –UVB ($P < 0.001$, Fig 4.1), whereas *sig5-2* did not show any difference in rate. The decrease observed in *sig5-1* over time is similar to the response observed in wildtype, suggesting that the absence of functional SIG5 does not have a negative impact on photosynthetic rate in the presence of UV-B, as the absence does not exacerbate the decrease in rate.

Interestingly, in terms of photosynthetic rate, the two mutants behaved slightly differently from one another, both in the presence and absence of UV-B. Prior to UV-B exposure, at 0hrs, *sig5-1* exhibited a significantly higher photosynthetic rate than *sig5-2* ($P < 0.001$, Fig 4.1). This trend continued in the absence of UV-B over 48hrs as the photosynthetic rate of *sig5-1* continued to be higher than the rate of *sig5-2*, which suggests that the sigma factor activity of SIG5 plays a role in maintaining photosynthetic rate even in the absence of UV-B. Interestingly, in the absence of UV-B, neither mutant exhibited significantly different photosynthesis rates from wild type (Fig 4.1). The absence of a significant difference suggests that loss of functional SIG5 does not have an impact on photosynthetic rate in terms of differing from the wild type. This further confirms the phenotype observed by Nagashima et al. (2004) and Tsunoyama et al. (2004) that in the absence of stress the *sig5* mutants have *wt* phenotypes, but that does not explain the differences in rate observed between *sig5-1* and *sig5-2*.

Nagashima et al. (2004) demonstrated that SIG5 is involved in the protection of chloroplast and contributes to the repair of damaged PS II under various stress conditions. The difference in photosynthesis response under UV-B by the *sig5* mutants suggests that SIG5 is involved in the photosynthesis response to UV-B and may mediate the response through involvement in protection of the chloroplast and repair of PS II. It further suggests that the sigma factor functionality of SIG5 plays a role in maintaining photosynthesis even in the absence of UV-B, but also plays a part in the increase in photosynthetic rate at 24hrs.

4.2.2 Exposure to low fluence UV-B slows increase in leaf area in *sig5* mutants

Green leaf area size was assayed to determine if the presence of UV-B limited leaf growth in a predictable photomorphogenic manner, as well as being used as a visual indicator of UV-B stress, as UV-B stress would likely induce purpling of the leaves, and/or may lead to a distortion of the leaf area response.

In wild type green leaf area increased significantly between 0hrs, 24hrs and 48hrs both in the absence and in the presence of UV-B ($P < 0.001$, Fig 4.2). However, under UV-B the increase in green leaf area is lower than the increase observed in the absence of UV-B; indicating a photomorphogenic response to UV-B. At 24hrs +UVB, green leaf area of *wt* was 6% smaller than under –UVB at the same time point ($P < 0.001$, Fig 4.2) and at 48hrs under +UVB green leaf area was 11% smaller than -UVB ($P < 0.001$, Fig 4.2). In the absence of UV-B, green leaf area of *sig5-1* and *sig5-2* at each time point did not differ significantly from wild type (Fig 4.2); which further confirms the observations by Nagashima et al. (2004) and Tsunoyama et al. (2004), who showed that under normal light conditions the mutants have similar phenotypes to wild type.

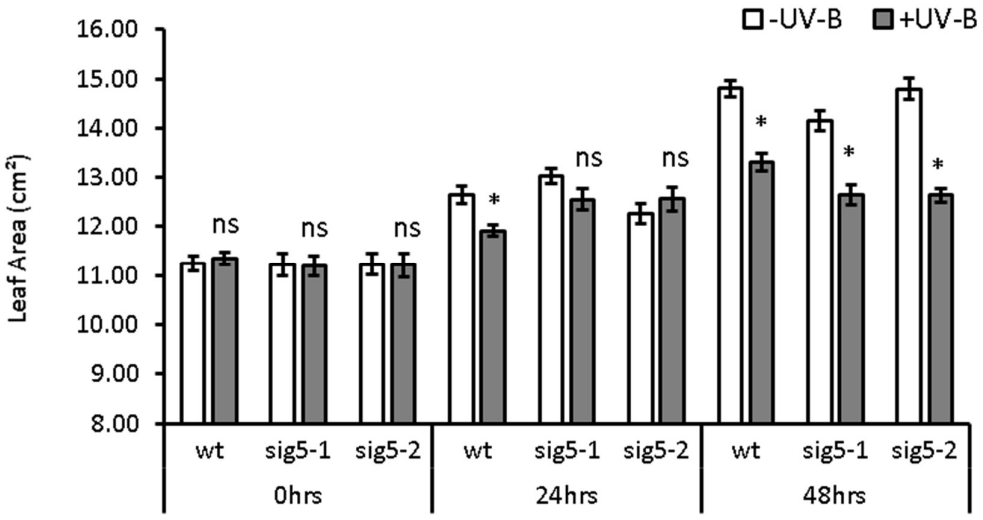

Figure 4.2 Changes in green leaf area (cm²) in *wt* (Col-0), *sig5-1* (Col) and *sig5-2* (Col) in response to irradiation with 0.5 µmol m^{-2} s^{-1} of UV-B (+UVB, grey) or without (-UVB, white) over 48 hours of exposure. 0hrs is 35 DAS and is leaf area prior to illumination with UV-B, while 24hrs is after 24 hours of exposure and so forth. In the +UVB condition the plants are exposed to 0.5 µmol m^{-2} s^{-1} and 220 µmol m^{-2} s^{-1} of PAR, in the –UVB condition the plants are exposed to 220 µmol m^{-2} s^{-1} of PAR only. *sig5-1 – sigma factor 5-1, sig5-2 - sigma factor 5-2*. Error bars represent ± S.E. (n = 16 biological repeats). Asterisks indicate statistically significant means ($P < 0.05$) between +UVB and –UVB treatments for a given time point and genotype; ns indicates not significant means.

The *sig5* mutants showed a similar response to UV-B exposure as wild type. Both mutants showed a significant increase in green leaf area between 0hrs and 24hrs +UVB ($P < 0.001$, Fig 4.2), and both mutants showed no significant difference in green leaf area between –UVB and +UVB conditions (Fig 4.2). While green leaf area still increased in both mutants between 24hrs

and 48hrs +UVB (Fig 4.2), in comparison to the increase observed in the absence of UV-B, the increase was much smaller. At 48hrs +UVB *sig5-1* was 18% smaller than under 48hrs –UVB ($P < 0.001$, Fig 4.2) and *sig5-2* was 17% at 48hrs +UVB compared to –UVB ($P < 0.001$, Fig 4.2). In summary, both mutants responded in a similar photomorphogenic manner to wild type.

In the absence of UV-B, both *sig5-1* and *sig5-2* showed a significant increase in green leaf area between each time point ($P < 0.001$, Fig 4.2). Furthermore, there were no observed differences in green leaf area between each mutant at each time point in both UV-B treated and no UV-B control plants. The absence of any difference between the two suggests that the different mutations do not affect green leaf area growth in both the presence and absence of UV-B.

4.2.3 Summary

Analysis of the photosynthesis response to low fluence UV-B in the *sig5* mutants showed that the UV-B dependent photosynthesis phenotype is reduced in the absence of functional SIG5 and is lost in the absence of the SIG5 sigma factor activity. Davey et al. (2012) showed that in response to 3 μmol m^{-2} s^{-1} of UV-B PS II efficiency in the *sig5* mutants was not affected and suggested that the increase in *psbD* in response to UV-B exposure was not required for maintaining photosynthetic efficiency under UV-B. While PS II efficiency was not measured, here the absence of SIG5 has been shown to affect photosynthesis in the presence of UV-B. The difference in observed response may be due to the lower UV-B fluence rate used in this research, which induces photomorphogenesis rather than a stress response in the mutant, and hence results in the variation in photosynthesis response as the loss of SIG5 negates the positive effect of UV-B. As green leaf area development is not negatively affected in response to UV-B exposure, it further suggests that the UV-B fluence rate is not damaging to the plant, but that exposure to UV-B limits growth both in the mutants and in the wild type.

The increase in photosynthetic rate is likely due to an increase in transcription of photosynthesis-associated chloroplast genes that are controlled by SIG5, such as *psbD* and *psbA*

(Nagashima et al., 2004; Tsunoyama et al., 2004; Noordally et al., 2013; Yamburenko et al., 2015). Higher transcription of these genes results in higher synthesis of D1 and D2 proteins (Mellenthin et al., 2014) and could thus increase photosynthetic rate. The loss of the photosynthesis phenotype in the *sig5* mutants suggests that the increase in photosynthetic rate in response to low fluence UV-B exposure is due to increased chloroplast transcription regulated by SIG5 and repair of UV-B damaged PS II.

4.3 EARLY LIGHT-INDUCIBLE PROTEIN 1 & 2 – ELIP1 (AT3G22840) & ELIP2 (AT4G14690)

ELIP1 and *ELIP2* are key light response genes involved in tolerance to photoinhibition and photooxidative stress (Rossini et al., 2006). They are part of a family of nuclear-encoded, thylakoid genes; related to the CAB proteins (Grimm et al., 1989; Adamska et al., 2001). ELIP proteins accumulate at different stages of plant development and show transient accumulation in response to environmental stress, especially in response to light stress (Adamska et al., 2001). Both the mRNA and the protein appear much earlier than other light-induced genes during the early stages of greening of etiolated seedlings and then disappear before the chloroplast development is complete (Pötter and Kloppstech, 1993). In mature plants, the proteins appear when the plant is exposed to photoinhibitory conditions such as high light or UV-B irradiance (Adamska et al., 1992; Rossini et al., 2006). Expression is meditated by the photoreceptors; such as cryptochrome and UVR8 (Brown et al., 2005; Kleine et al., 2007).

The physiological role of ELIPs *in planta* and their function in chloroplasts is uncertain (Rossini et al., 2006), although it is hypothesised that ELIPs protect the photosynthetic apparatus through altering chlorophyll accumulation and thus preventing overexcitation (Tzvetkova-Chevolleau et al., 2007). Evidence suggests that ELIPs have a photoprotective role under light stress conditions due to their ability to bind to pigments (Singh et al., 2008). This could be due to the proteins transiently binding to free chlorophyll, and thus preventing photooxidative stress, and/or by

participating in energy dissipation to protect the PS II reaction center from photoinhibition (Montané and Kloppstech, 2000; Adamska et al., 2001). While *ELIP1* and *ELIP2* transcripts are induced by both high and low fluence rates of UV-B, their role in the UV-B response is unknown (Brown et al., 2005; Oravecz et al., 2006; Kilian et al., 2007; Safrany et al., 2008; Favory et al., 2009; Davey et al., 2012; Hayami et al., 2015). Experiments have shown that UV-B exposure strongly induced *ELIP1* and *ELIP2* transcript levels, however, UV-B did not affect photosynthetic efficiency or plant viability of the *elip1,elip2* double mutant, and it has remained unclear why *ELIP1* and *ELIP2* are so highly induced by UV-B (Davey et al., 2012).

Here the response of the *elip1* and *elip2* mutants under 0.5 µmol m^{-2} s^{-1} UV-B was tested. *elip1* is a null mutant, with a T-DNA insertion in the third exon, which results in the absence of transcription of *ELIP1,* but does not show any difference to wild type under normal growth conditions (Casazza et al., 2005). *elip2* is a null mutant, with a T-DNA insertion at the beginning of the third exon (Casazza et al., 2005).

4.3.1 The UV-B dependent increase in photosynthesis is lower in *elip* mutants

In both *elip* mutants, the increase in photosynthetic rate observed in wild type at 24hrs of UV-B exposure is present, but the increase is significantly smaller than in wild type ($P < 0.001$, Fig 4.3). In *wt*, there was a 12% increase in photosynthetic rate at 24hrs UV-B compared to no UV-B ($P < 0.001$, Fig 4.3). *elip1* showed an increase of 6% at 24hrs +UVB compared to –UVB ($P < 0.001$, Fig 4.3), and *elip2* showed an increase of 3% at 24hrs +UVB compared to –UVB ($P < 0.001$, Fig 4.3). As the increase observed in the mutants is much lower than the increase observed in wild type, it suggests that the ELIPs play a role in the photosynthetic response to UV-B exposure, but the absence of either ELIP does not negatively affect photosynthesis at 24hrs of UV-B.

At 48hrs of UV-B, the increase in photosynthetic rate observed at 24hrs was lost in wild type. The same response was observed in *elip1*, which showed no significant difference between +UVB and –UVB at 48hrs (Fig 4.3). There was no significant decrease in rate between 24hrs +UVB

and 48hrs +UVB, suggesting that the absence of *elip1* does not negatively impact photosynthesis under UV-B exposure and that ELIP1 plays a role in maintaining photosynthetic efficiency under prolonged UV-B exposure. Interestingly, *elip1* exhibited a significantly lower photosynthetic rate than wild type in the absence of UV-B up to 24hrs, after which the photosynthetic rate was similar to wild type, suggesting that the loss of ELIP1 has an impact on photosynthetic rate.

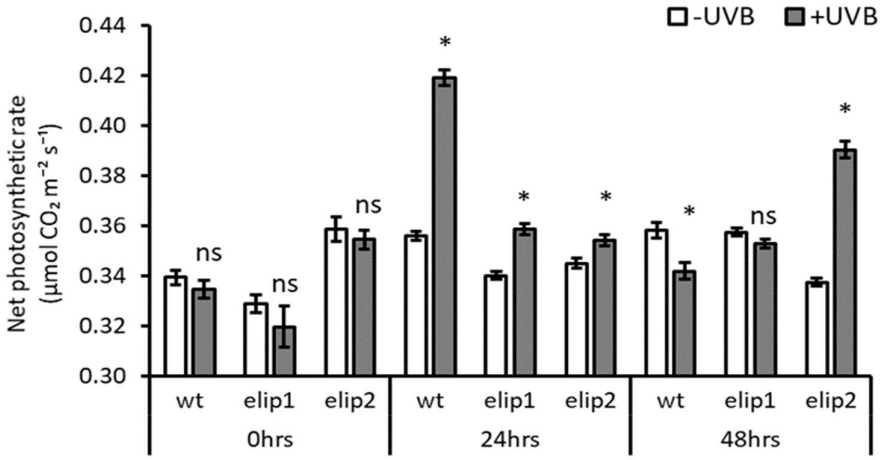

Figure 4.3 Changes in net photosynthetic rate (µmol CO_2 m^{-2} s^{-1}) normalised to leaf area in *wt* (Col-0), *elip1* (Col) and *elip2* (Col) in response to irradiation with 0.5 µmol m^{-2} s^{-1} of UV-B (+UVB, grey) or without (-UVB, white) over 48 hours of exposure. 0hrs is 35 DAS and is the net photosynthetic rate prior to illumination with UV-B, while 24hrs is after 24 hours of exposure and so forth. In the +UVB condition the plants are exposed to 0.5 µmol m^{-2} s^{-1} and 220 µmol m^{-2} s^{-1} of PAR, in the –UVB condition the plants are exposed to 220 µmol m^{-2} s^{-1} of PAR only. *elip1 – early light-inducible protein 1, elip2 – early light-inducible protein 2.* Error bars represent ± S.E. (n = 16 biological repeats). Asterisks indicate statistically significant means ($P < 0.05$) between +UVB and –UVB treatments for a given time point and genotype; ns indicates not significant means.

elip2, however, exhibited a different response as photosynthetic rate continued to increase under UV-B. At 48hrs +UVB the photosynthetic rate was 14% higher than under -UVB ($P < 0.001$, Fig 4.3), and at 48hrs of UV-B the rate was 10% higher than the rate observed at 24hrs of UV-B ($P < 0.001$, Fig 4.3). The response observed seems to be a delay in photosynthetic response to UV-B exposure as the increase in photosynthetic rate only occurs at 48hrs; although further measurements at later time points would be necessary to confirm this. The absence of the initial increase in photosynthetic rate at 24hrs of UV-B in *elip2* could suggest that ELIP2 is involved in the photosynthetic response to UV-B exposure and that the loss of ELIP2 results in the loss of

increase. However, as photosynthetic rate increased at 48hrs of UV-B exposure in *elip2,* it could suggest that the absence of ELIP2 delays the response to UV-B, and that ELIP2 is not directly involved in the increase in rate, but instead it maybe involved in terms of limiting the increase in photosynthetic rate after 24hrs of UV-B exposure.

elip1 and *elip2* differ considerably from one another in terms of photosynthesis both in the absence and presence of UV-B. Prior to UV-B exposure, the photosynthetic rate of *elip1* was significantly lower than the photosynthetic rate of *elip2* ($P < 0.001$, Fig 4.2). However, in the absence of UV-B at 24hrs and 48hrs, the mutants have similar photosynthetic rates. Also, the photosynthetic rate of *elip1* having increased significantly between 0hrs and 24hrs of UV-B ($P < 0.001$, Fig 4.2). The different responses to UV-B exposure show that the two ELIPs are involved in different parts of the photosynthesis response to UV-B.

4.3.2 Green leaf area development in *elip* mutants is limited by UV-B exposure

In wild type plants, green leaf area increased significantly between 0hrs, 24hrs and 48hrs both in the absence and in the presence of UV-B ($P < 0.001$, Fig 4.4). However, under UV-B the increase in green leaf area is lower than the increase observed in the absence of UV-B, indicating a UV-B photomorphogenic response. At 24hrs +UVB the green leaf area of *wt* was 7% than under –UVB at 24hrs ($P < 0.001$, Fig 4.4) and at 48hrs +UVB green leaf area was 9% smaller than under -UVB($P < 0.001$, Fig 4.4). Thus showing that wild type is responding to the presence of UV-B by limiting plant development and that the response increases in response to longer UV-B exposure.

In terms of green leaf area development, the *elip* mutants exhibited a similar phenotype to wild type plants in response to UV-B exposure. Both mutants showed significant increases in green leaf area in the absence of UV-B between 0hrs, 24hrs and 48hrs ($P < 0.001$, Fig 4.4). Under UV-B conditions, the increase in green leaf area slows, resulting in smaller plants under +UVB compared to –UVB. At 24hrs, both mutants did not show a significant difference in leaf area

between +UVB and –UVB (Fig 4.4). At 48hrs, however, *elip1* is 20% smaller under +UVB than under -UVB ($P < 0.05$, Fig 4.4), and *elip2* is 16% smaller ($P < 0.001$, Fig 4.4). Between 24hrs of UV-B and 48hrs of UV-B, there was no significant change in green leaf area in both mutants (Fig 4.4), which suggests that green leaf area development slows and perhaps even stops in response to prolonged UV-B exposure, which could hint at a possible interaction between the ELIPs and green leaf area development. The slowing of green leaf area development, rather than a distinct negative impact on green leaf area, suggests a photomorphogenic response to UV-B exposure, rather than a stress response. The significant difference in area at 48hrs of UV-B between wild type and the *elip* mutants further hints at an interaction between green leaf area development and ELIP1 and ELIP2.

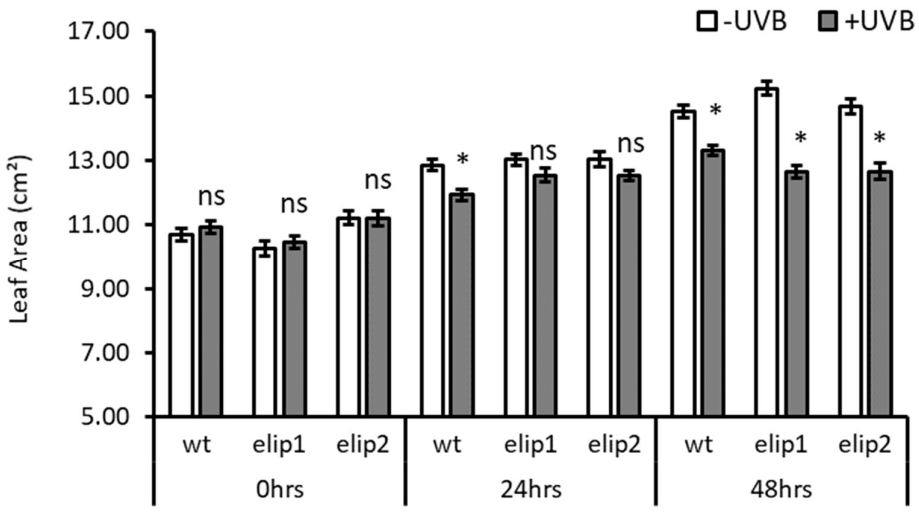

Figure 4.4 Changes in leaf area (cm²) in *wt* (Col-0), *elip1* (Col) and *elip2* (Col) in response to irradiation with 0.5 µmol m^{-2} s^{-1} of UV-B (+UVB, grey) or without (-UVB, white) over 48 hours of exposure. 0hrs is 35 DAS and is leaf area prior to illumination with UV-B, while 24hrs is after 24 hours of exposure and so forth. In the +UVB condition the plants are exposed to 0.5 µmol m^{-2} s^{-1} and 220 µmol m^{-2} s^{-1} of PAR, in the –UVB condition the plants are exposed to 220 µmol m^{-2} s^{-1} of PAR only. *elip1 – early light-inducible protein 1, elip2 – early light-inducible protein 2*. Error bars represent ± S.E. (n = 16 biological repeats). Asterisks indicate statistically significant means ($P < 0.05$) between +UVB and –UVB treatments for a given time point and genotype; ns indicates not significant means.

Prior to UV-B exposure, *elip1* and *elip2* differed in terms of green leaf area, as *elip2* was significantly larger than *elip1* ($P < 0.05$, Fig 4.4). The difference in green leaf area could explain

the difference in photosynthetic rate observed prior to UV-B exposure, as *elip1* exhibited a significantly lower photosynthetic rate ($P < 0.001$, Fig 4.4) at 0hrs than *elip2.* Less green leaf area and a smaller surface area in general (Data not shown), could result in the lower photosynthetic rate seen in *elip1*. As green leaf area increased significantly between 0hrs and 24hrs for *elip1* ($P < 0.001$, Fig 4.4), so did the photosynthetic rate ($P < 0.001$, Fig 4.4), which suggests that the lower green leaf area was the result of the lower photosynthetic rate. By 24hrs green leaf area no longer differed between *elip1* and *elip2* (Fig 4.4), suggesting that there is a difference in plant development between the mutants.

4.3.3 Summary

In *elip1* and *elip2* the photosynthesis phenotype in response to UV-B is altered. At 24hrs of UV-B exposure, both mutants exhibited lower photosynthetic rates than wild type, which suggests that both are involved in the photosynthesis phenotype observed in wild type at 24hrs of UV-B exposure. As the *ELIPs* are only induced early during plant development and in response to high light stress (Grimm and Kloppstech, 1987; Grimm et al., 1989; Adamska et al., 2001), the specific role of either in the response to low fluence UV-B exposure is unknown as their physiological role is unknown (Brown et al., 2005; Rossini et al., 2006). It has been hypothesized that ELIPs protect the photosynthetic apparatus through altering chlorophyll accumulation and thus preventing overexcitation (Tzvetkova-Chevolleau et al., 2007); thus the increase in photosynthetic rate may be due to an increase in chlorophyll accumulation; although the chlorophyll content analysis shown in Chapter 3 showed that chlorophyll content did not increase significantly in response to UV-B exposure.

Thus we can only hypothesise about the physiological mechanism behind the absence of the photosynthesis phenotype in *elip1* and *elip2*. However, the phenotype observed in both mutants suggests that both ELIPs are involved in the photosynthesis response to low fluence UV-B. Furthermore, that ELIP2 plays a role in the regulation of the photosynthesis response at 48hrs

of UV-B exposure as in the absence of *ELIP2* photosynthetic rate continues to increase under UV-B exposure, as to how this regulation may occur is unknown.

Other experiments have suggested that exposure to UV-B does not negatively impact photosynthetic efficiency in the *elip* mutants (Rossini et al., 2006; Davey et al., 2012); however, these experiments used high fluence UV-B and showed no negative impact on photosynthetic efficiency in the mutants. Whereas in this experiment, a photomorphogenic dose was used and there is no detrimental impact on photosynthesis rate. Instead, the increase in photosynthetic rate was reduced in the mutants.

In terms of green leaf area, both mutants behave much like wild type; with green leaf area development slowing in response to UV-B exposure. The slowing of development suggests that the response is photomorphogenic rather than a stress response, as stress would induce reductions in green leaf area. In the absence of UV-B, green leaf area develops in the mutants as it does in wild type, thus being in accordance with Casazza et al. (2005), who found that the *elip* mutants behave much like wild type under normal growth conditions.

4.4 REPRESSOR OF UV-B PHOTOMORPHOGENESIS 1 & 2 – RUP1 (AT5G52250) & RUP2 (AT5G23730)

RUP1 and RUP2 are negative regulators of UVR8 (Gruber et al., 2010). Both are transcriptionally activated by the UVR8/COP1/HY5 signalling complex (Gruber et al., 2010). RUP1 and RUP2 interact with UVR8 in a similar mechanism as COP1 (Gruber et al., 2010; Cloix et al., 2012; Yin et al., 2015) and are hypothesized to displace COP1 in the COP1-UVR8 complex to allow for redimerisation of UVR8 (Cloix et al., 2012; Heijde et al., 2013) and thus regulating the UVR8 mediated response to UV-B. Both RUP1 and RUP2 are needed to balance the need for UV-B damage response and plant growth (Gruber et al., 2010; Vanhaelewyn et al., 2016). The *rup1,rup2* double mutant showed a stronger response to UV-B stress and was better acclimated to UV-B exposure (Gruber et al., 2010).

Here the response of the *rup1,rup2* (*rup1,2)* double mutant under 0.5 µmol m^{-2} s^{-1} UV-B was tested (Chapter 2: Materials and Methods). The *rup1,2* double mutant was produced by crossing the single mutants *rup1-1* and *rup1-2* (Gruber et al., 2010). Both mutants are T-DNA insertion lines, which results in the absence of the respective mRNAs and hence shows reduced functionality (Gruber et al., 2010). In *rup1,2* the lack of transcripts of both genes makes it hypersensitive to UV-B exposure (Gruber et al., 2010).

4.4.1 The UV-B dependent increase in photosynthetic rate is prolonged in *rup1,2*

Under UV-B exposure photosynthetic rate increased by 14% in wild type compared to no UV-B at 24hrs ($P < 0.001$, Fig 4.5). *rup1,2* exhibited a similar photosynthesis response, as the photosynthetic rate of *rup1,2* increased by 10% under UV-B at 24hrs compared to no UV-B ($P < 0.001$, Fig 4.5), the photosynthetic rate at 24hrs of UV-B was 7% higher than the rate observed at 0hrs ($P < 0.001$, Fig 4.5). Unlike in *wt*, where photosynthetic rate decreased at 48hrs +UVB compared to both 48hrs –UVB ($P < 0.01$, Fig 4.5) and 24hrs +UVB ($P < 0.001$, Fig 4.5); in *rup1,2* photosynthetic rate continued to be higher under 48hrs +UVB compared to 48hrs –UVB ($P < 0.001$, Fig 4.5), the increase in rate still being at around 10%. In fact, there was no difference in photosynthetic rate between 24hrs +UVB and 48hrs +UVB (Fig 4.5).

As the amount of increase in rate was less in *rup1,2* at 24hrs of UV-B than in wild type under the same conditions, it could suggest that the RUPs are involved in the increase in rate, but are not essential. The continued upregulation of photosynthetic rate in *rup1,2* at 48hrs of UV-B suggests that the loss of negative regulation of UVR8 in the mutant results in the prolonged phenotype as UVR8 is not inactivated by RUP1 and RUP2. The results also show that inactivation of UVR8 likely plays a part in the decrease of photosynthetic rate observed at 48hrs in wild type.

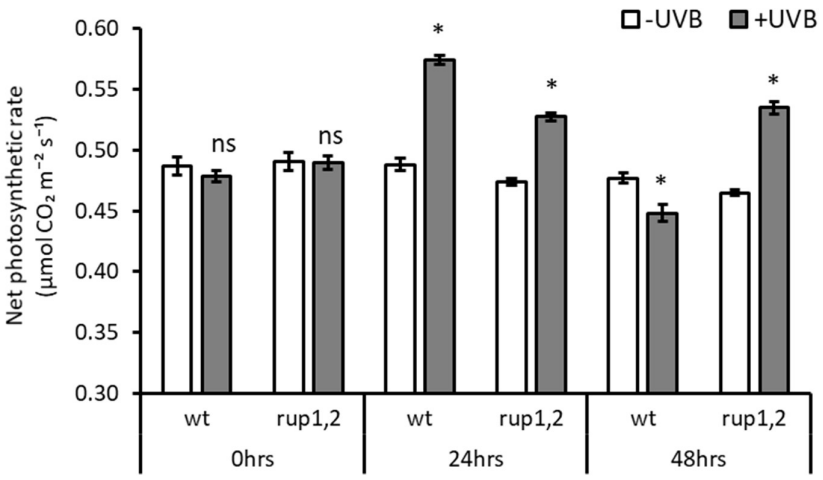

Figure 4.5 Changes in net photosynthetic rate (µmol CO_2 m^{-2} s^{-1}) normalised to leaf area in *wt* (Col-0) and *rup1,2* (Col) in response to irradiation with 0.5 µmol m^{-2} s^{-1} of UV-B (+UVB, grey) or without (-UVB, white) over 48 hours of exposure. 0hrs is 35 DAS and is the net photosynthetic rate prior to illumination with UV-B, while 24hrs is after 24 hours of exposure and so forth. In the +UVB condition the plants are exposed to 0.5 µmol m^{-2} s^{-1} and 220 µmol m^{-2} s^{-1} of PAR, in the –UVB condition the plants are exposed to 220 µmol m^{-2} s^{-1} of PAR only. *rup1,2 – repressor of UV—B photomorphogenesis 1,2*. Error bars represent ± S.E. (n = 16 biological repeats). Asterisks indicate statistically significant means ($P < 0.05$) between +UVB and –UVB treatments for a given time point and genotype; ns indicates not significant means.

4.4.2 Green leaf area growth is limited in *rup1,2* in response to UV-B

In the absence of UV-B exposure wild type and *rup1,2* did not differ in green leaf area (Fig 4.6). Over 48hrs of exposure, the rate of increase in green leaf area was maintained at an equal pace, as at each time point they do not differ significantly from each other. These observations suggest that the loss of RUP1 and RUP2 does not have an adverse effect on leaf area in a PAR only (-UVB) environment.

Under UV-B exposure there was a significant difference in leaf area; at 48hrs of UV-B wild type had a significantly larger green leaf area than *rup1,2* ($P < 0.001$, Fig 4.6). The difference in green leaf area suggests that the loss of RUP1 and RUP2 results in a slower growth rate in response to low doses of UV-B. UV-B exposure only significantly affected green leaf area at 48hrs in both wild type and *rup1,2.* The green leaf area of *rup1,2* was significantly lower ($P < 0.001$, Fig 4.6) in plants exposed to UV-B, compared to no UV-B.

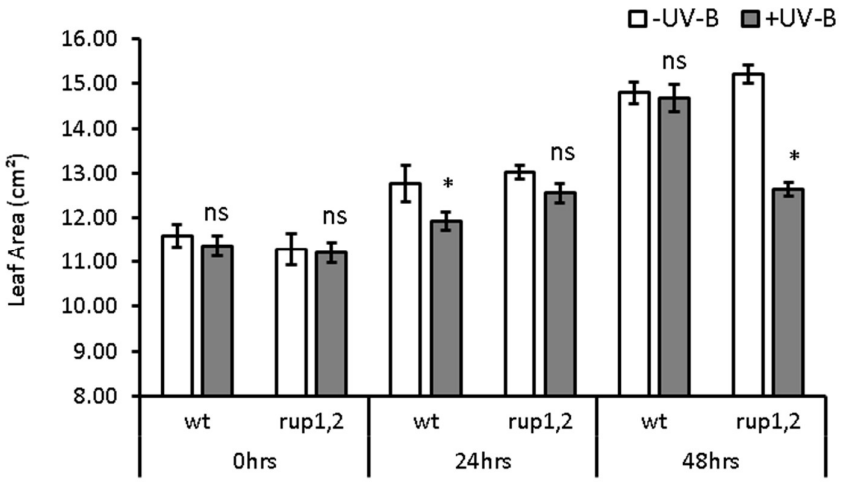

Figure 4.6 Changes in leaf area (cm²) in *wt* (Col-0) and *rup1,2* (Col) in response to irradiation with 0.5 µmol m⁻² s⁻¹ of UV-B (+UVB, grey) or without (-UVB, white) over 48 hours of exposure. 0hrs is 35 DAS and is leaf area prior to illumination with UV-B, while 24hrs is after 24 hours of exposure and so forth. In the +UVB condition the plants are exposed to 0.5 µmol m⁻² s⁻¹ and 220 µmol m⁻² s⁻¹ of PAR, in the –UVB condition the plants are exposed to 220 µmol m⁻² s⁻¹ of PAR only. *rup1,2 – repressor of UV-B photomorphogenesis 1,2*. Error bars represent ± S.E. (n = 16 biological repeats). Asterisks indicate statistically significant means ($P < 0.05$) between +UVB and –UVB treatments for a given time point and genotype, ns indicates not significant means.

Analysis showed that *rup1,2* experienced continuous increases in leaf area in the absence of UV-B as there was a significant increase in leaf area between each time point. Interestingly, *rup1,2* showed a significant increase in leaf area between 0hrs and 24hrs of UV-B exposure ($P < 0.001$, Fig 4.6), however, at 48hrs the increase in green leaf area is so small that is insignificant; suggesting that the absence of RUP1 and RUP2 affects growth rate in a UV-B environment.

4.4.3 Summary

In the absence of both RUP1 and RUP2 photosynthetic rate is elevated at 24hrs and 48hrs of UV-B exposure. This differs from wild type where photosynthetic rate was only increased at 24hrs of UV-B exposure. RUP1 and RUP2 are negative regulators of UVR8 (Gruber et al., 2010). Hence the prolonged increase in photosynthetic rate suggests that RUP1 and RUP2 negatively regulate UVR8 to limit the impact of low fluence UV-B exposure and that in the absence of both the negative regulation is lost. The observed phenotype also aligns with the observation that *rup1,2* is hypersensitive to UV-B (Gruber et al., 2010) as it shows a prolonged photosynthesis response

to UV-B exposure. The phenotype suggests that RUP1 and RUP2 are involved in regulating the decrease in photosynthetic rate at 48hrs UV-B exposure compared to 24hrs UV-B exposure, by inactivating UVR8 and thus limiting regulation of the genes involved in the phenotype. As RUP1 and RUP2 limit UVR8 induced photomorphogenesis (Gruber et al., 2010; Vanhaelewyn et al., 2016), the continued increase in photosynthetic rate in the mutants suggests that photosynthesis response to low fluence UV-B exposure is a photomorphogenic response.

As the photosynthetic rate increase in *rup1,2* is lower than the increase observed in wild type, it suggests that RUP1 and RUP2 are also involved in the initial increase in photosynthetic rate, but as to how this occurs is unknown. Green leaf area development is also limited in *rup1,2* under UV-B; which suggests that green leaf area development in the presence of UV-B involves RUP1 and RUP2 activity but as to how this occurs is unknown.

4.5 Chapter Summary

A number of genes have been identified as being regulated by the UVR8-COP1 signalling cascade that are associated with maintenance of the photosynthetic machinery in response to UV-B exposure; two of these are *SIG5* and the *ELIPs* (Davey et al., 2012). In this chapter, the photosynthesis responses to low fluence UV-B in mutants of these genes were characterised. As they are associated with maintenance of the photosynthetic machinery in response to UV-B and are upregulated under low fluence UV-B (Davey et al., 2012), it was expected that they might be involved in the response or drive the increase in net photosynthetic rate in some way. The results have shown that each of these genes is involved in the photosynthesis response, as the mutants exhibit lower increases in net photosynthetic rate. However, photosynthetic rate was not negatively impacted under UV-B exposure in their absence; which suggests that *SIG5*, *ELIP1* and *ELIP2*, are involved but not crucial to the increase in photosynthetic rate. This points to the regulation of photosynthesis in response to low fluence UV-B exposure being driven by other, as of yet unidentified factors. The differences in photosynthetic rate in each mutant also

suggests that the increase in net photosynthetic rate seen in wild type is due to an increase in chloroplast transcription.

To better understand the role of UVR8 in driving the photosynthesis response to UV-B, the photosynthesis response of the *rup1,2* mutant was also tested. The prolonged photosynthesis response to UV-B observed in *rup1,2* suggests that UVR8 does indeed mediate the increase in net photosynthetic rate and that the response maybe lost at 48hrs due to UVR8 inactivation by RUP1 and RUP2, in order to prevent overexcitation in response to UV-B exposure and to strike a metabolic balance between plant development and photomorphogenic response.

Changes in green leaf area in response to UV-B were also assessed, to determine if low fluence UV-B would have an impact on green leaf area development. In response to low fluence UV-B exposure, the development of green leaf area slows both in wild type and the mutants, but leaf area does not decrease. The mutants tested all showed a stronger response to UV-B than wild type, as green leaf area increased more slowly than wild type, which suggests that these genes may be involved in the response to UV-B in terms of green leaf area development and regulation.

Overall, the pre-identified UVR8 regulated UV-B induced genes appear to be underpinning the UV-B-photosynthetic interactions. However, none of these regulators appear to be completely required for the UV-B mediated increase in net photosynthetic rate. In order to determine a complete transcriptomic pattern during the initial 24hrs of UV-B exposure and search for novel regulators, we used RNA-seq for global expression profiling analysis, the results of which are presented in the next Chapter.

5 Analysis of transcriptome changes in response to 0.5 µmol m^{-2} s^{-1} of UV-B

5.1 Introduction

In Chapter 3 the UV-B dependent increase in photosynthetic rate was characterised. Photosynthetic rate increased by 12% at 24hrs. The increase in photosynthetic rate was transient; as at 48hrs of UV-B exposure, the rate of photosynthesis was no longer higher than the photosynthetic rate of plants not exposed to UV-B (-UVB). In the *uvr8* mutant, *uvr8-1,* the photosynthesis phenotype was absent, indicating that functional UVR8 is involved in the increase in photosynthetic rate. The increase in photosynthetic rate is likely due to changes in gene expression, thus to better understand what causes the increase, changes in gene expression were analysed through RNA-Seq.

Whole genome expression profiling studies using microarray have shown that exposure to UV-B results in the regulation of large number of genes (Green et al., 1991; Brosché et al., 2002; Ulm et al., 2004; Stracke et al., 2010); and that over a hundred genes involved in the UV-B response are regulated by UVR8 (Brown et al., 2005; Favory et al., 2009; Tilbrook et al., 2013; Jenkins, 2014b). However, at the time of conducting our study, no RNA-seq studies focused on UV-B responses had been published. As previously discussed the analysis of the Favory et al. (2009) microarray data by Wargent and Jordan (2013), shows that in response to low fluence UV-B exposure a number of photosynthesis-associated genes are upregulated. Whereas the analysis of the Brown et al. (2005) microarray data; in which high fluence UV-B was used, shows a trend of downregulation in photosynthesis-associated genes (Wargent and Jordan, 2013). Although genes such as *SIG5*, *ELIP1, ELIP2* and two *FtsH* (ATP-dependent metalloproteases) are upregulated; which suggests that not all photosynthesis-associated genes are negatively impacted by UV-B exposure. Since the photosynthesis phenotype was characterised using an even lower fluence rate of UV-B than the one used by Favory et al. (2009), it is expected that the

general pattern of upregulation in photosynthesis-associated genes will continue and that the analysis will allow for the identification of genes that are involved in the photosynthesis phenotype.

To gain a better understanding of what causes the increase in net photosynthetic rate at 24hrs of UV-B exposure, RNA-seq analysis focused on determining changes in gene expression at 6hrs and at 24hrs of UV-B exposure in the wild type, as the transcriptional regulation of the phenotype would be expected to begin as soon as UV-B exposure begins. The 6hrs time point was selected as a time point, rather than 12hrs, to reduce the detection of genes regulated by circadian rhythm. To determine what causes the absence of the photosynthesis phenotype in *uvr8-1,* the analysis focused on determining the differences in gene expression in the mutant (*uvr8-1*) versus the wild type (*wt* – L*er*) over 24hrs of UV-B exposure. *uvr8-1* samples in the absence of UV-B (-UVB) were not sequenced as the focus of the analysis was to determine what causes the increase in photosynthetic rate in the wild type, rather than determining what occurs in the mutant. under Together, the RNA-seq analysis should allow for the characterisation of changes on a transcriptional level in response to low fluence UV-B exposure that may be involved in the in the increase in photosynthetic rate at 24hrs of UV-B exposure.

5.2 General observations of RNA-seq data

RNA-seq was performed to identify differentially expressed genes in response to UV-B exposure. Wild type (L*er*) samples were collected at three time points: 0hrs, 6hrs and 24hrs, and the two different light conditions +UVB and –UVB. While, *uvr8-1* samples were collected at 0hrs, 6hrs and 24hrs, under +UVB only. RNA samples for 4 biological repeats were submitted to New Zealand Genomics Limited (NZGL; Otago, New Zealand) for processing and sequencing (Chapter 2: Materials and Methods).

Three lanes of Illumina HiSeq2500 sequencing generated an average number ~ 13 million reads (Q30 > 94.87%) per sample and ~40 million (Q30 > 94.4%) per biological replicate. Stability and

reproducibility of data is indicated by the Pearson correlation coefficients (> 0.95) between the biological replicates samples. Reads were mapped to the TAIR10 release of the *A. thaliana* genome using tophat2; which generated an average concordant mapping rate of 86.5%. Gene counts were generated from each aligned BAM file using the software HTSeq-count package. Differential expression was detected using the R-package DESeq2. The differential expression was performed in a pairwise fashion with the *wt* –UVB samples used as the control. The adjusted p-values (padj) represent False Discovery Rate (FDR) corrected values with a 5% FDR cut off used.

DESeq2 analysis showed a modest overall effect in response to UV-B exposure, as determined by the relatively small number of differentially expressed genes (DEGs). In a detailed analysis of the differential expression data, gene expression patterns can be seen in the following sections below which focus on particular comparisons of interest. To validate the RNA-seq results, 6 DEGs were selected for qRT-PCR analysis (Supplementary information Fig 9.4). The correlations between the RNA expression level from qRT-PCR and RNA-seq were relatively high, with Pearson correlation coefficients of 0.84 (P < 0.001) and Spearman coefficient of 0.97 (P < 0.001), validating the repeatability and reproducibility of gene expression data.

5.3 Analysis of transcriptome changes in response to +UVB exposure vs –UVB exposure at 6hrs and 24hrs

The previously established photosynthesis phenotype showed that at 24hrs there was a significant increase in photosynthetic rate under UV-B exposure compared to no UV-B in wild type. To determine what may drive the increase in photosynthetic rate on a transcript level, the analysis of the RNA-seq data focused on investigating the differences between +UVB and -UVB at 6hrs and 24hrs. Analysing differential gene expression between +UVB versus -UVB allows for a better understanding of changes that occur solely due to UV-B exposure. Differential gene expression analysis at 6hrs allows for the identification of genes that may be involved in the positive regulation of photosynthesis at 24hrs; the analysis of differential gene expression at

24hrs may allow the identification of genes resulting in the absence of the increase in photosynthetic rate at 48hrs of UV-B exposure. Comparing the gene expression patterns of 6hrs and 24hrs indicates as to how gene expression shifts over time under UV-B exposure, both specifically in relation to photosynthesis, and in general terms of UV-B photomorphogenesis.

5.3.1 Relative gene expression is higher at 6hrs of UV-B exposure than at 24hrs

To provide an overview of changes in overall gene expression in response to UV-B in wild type at 6hrs and 24hrs; volcano plots were used to show the distribution of all DEGs (Fig 5.1). In the volcano plots green dots represent significant DEGs (padj < 0.05) and a log2foldchange (LFC) > 1; red dots represent DEGs (padj < 0.05) and black dots represent genes that were not significantly different (padj > 0.05). The plots show that 6hrs +UVB:-UVB (Fig 5.1a) and 24hrs +UVB:-UVB (Fig 5.1b) have distinct transcriptional profiles. 6hrs +UVB:-UVB shows an even distribution of significantly changed DEGs (padj < 0.05, Fig 5.1a), whereas 24hrs +UVB:-UVB shows more positively changed DEGs (padj < 0.05, Fig 5.1b) than negative. In both comparisons the overall fold change is low, suggesting that the impact of the UV-B dose is relatively modest; as is to be expected given the low fluence rate of UV-B used.

At 6hrs +UVB:-UVB (Fig 5.1a), a total of 119 significantly changed genes (padj < 0.05) were detected; with an even split of both upregulated (59) and downregulated (60) genes. Of the 119 significantly changed genes; 109 are characterised genes, and 10 are uncharacterised genes (Details of all DEGs are shown in Supplementary Table 9.7). GO enrichment analysis using PANTHER (http://www.pantherdb.org/) (Mi et al., 2017) showed that there is an overrepresentation of genes associated with the thylakoid (FDR < 0.05) and chloroplast (FDR < 0.001) in the subset of significantly changed DEGs. Interestingly, there was also an overrepresentation of genes associated with intramolecular oxidoreductase activity (FDR < 0.001), which may explain the increase in photosynthetic rate at 24hrs of UV-B exposure; as oxidoreductase activity is involved in photosynthesis. The absence of DEGs associated with the

UV-B stress response suggests that at 6hrs the UV-B exposure is not yet damaging to the plant, but rather has a positive impact on plant performance.

At 24hrs +UVB:-UVB (Fig 5.1b), there were 43 significantly changed genes (padj < 0.05), and there were more upregulated genes (38) than there are downregulated genes (5). Of the 43 significantly changed genes, 41 are characterised genes, and 2 are uncharacterised genes (Details of all DEGs are shown in Supplementary Table 9.8). GO enrichment analysis using PANTHER (http://www.pantherdb.org/) shows that there is an overrepresentation of genes involved in the flavonoid biosynthesis pathway (FDR < 0.001), and genes involved in response to light stimulus (FDR < 0.001) and the UV-B response (FDR < 0.001). The absence of DEGs associated with photosynthesis shows that there is a shift in gene expression patterns at 24hrs of UV-B exposure; away from the positive regulation in response to UV-B regarding photosynthesis and towards a more stereotypical UV-B acclimation/photomorphogenic response. The absence of the upregulation of photosynthesis-associated genes may also explain the decrease in photosynthetic rate seen at 48hrs of UV-B exposure; as the loss of upregulation of photosynthesis-associated genes would arguably only become noticeable in phenotype later.

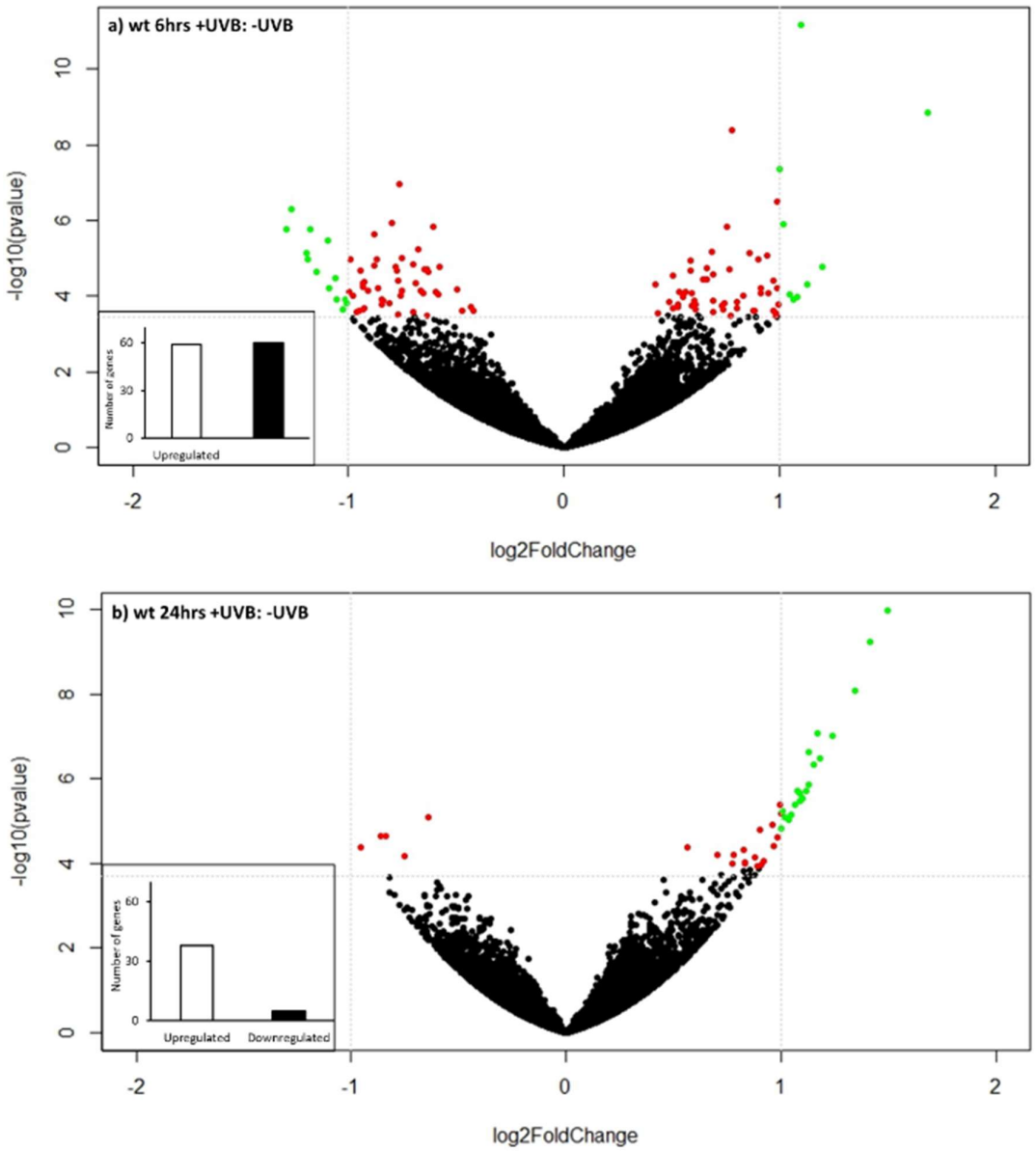

Figure 5.1 Volcano plot showing the magnitude of differential expression (log2FoldChange) compared to the measure of statistical significance (-log10 pvalue) at 6hrs and 24hrs of UV-B exposure in *wt* (L*er*). Individual dots represent genes differentially regulated in response to UV-B exposure (+UVB:-UVB). Red dots represent genes with a padj value < 0.05, green dots represents values genes with a padj value < 0.05 and a log2foldchange > 1. **a)** Differential gene expression at 6hrs in *wt* (L*er*) +UVB:-UVB. The bar graph represents the number of genes significantly up and down-regulated in response to UV-B exposure. **b)** Differential gene expression at 24hrs in *wt* (L*er*) +UVB:-UVB. The bar graph represents the number of genes significantly up and down regulated in response to UV-B exposure.

Furthermore, when comparing the significant DEGs for 6hrs +UVB:-UVB and 24hrs +UVB:-UVB (Fig 5.2), the only overlap is *ABCB13* (*ATP-BINDING CASSETTE B13*, AT1G27940); an ATP-binding cassette transporter (ABC transporter) gene involved in ATPase activity and transmembrane

movement (Martinoia et al., 2001; Geisler et al., 2003; Verrier et al., 2008). *ABCB13* is upregulated in both 6hrs +UVB:-UVB (LFC = 0.97, padj < 0.05) and 24hrs +UVB:-UVB (LFC = 1.00, padj < 0.01). The increase in photosynthetic rate at 24hrs is likely the cause of the upregulation of *ABCB13* expression, as the increase in photosynthetic rate over the first 24hrs of exposure increases the demand for detoxification and the associated transport functions that *ABCB13* is involved in (Sánchez-Fernández et al., 2001b; Sánchez-Fernández et al., 2001a; Verrier et al., 2008). Thus suggesting that rather than being involved in the upregulation of photosynthetic rate, it is upregulated as a result of the increase in photosynthetic rate.

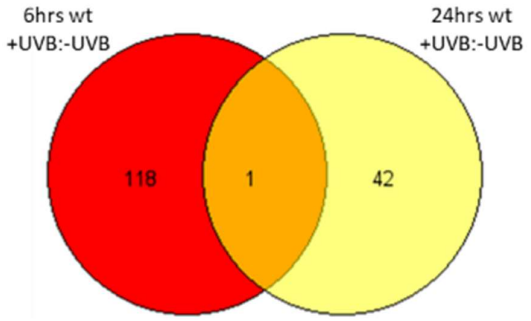

Figure 5.2 Venn diagram showing the number of significantly differentially expressed genes in *wt* (L*er*) 6hrs and 24hrs +UVB:-UVB. In red are the differentially expressed genes unique to *wt* (L*er*) 6hrs UV-B:-UVB. In yellow are the differentially expressed genes unique to *wt* (L*er*) 24hrs UV-B:-UVB. The threshold is padj < 0.05.

5.3.2 Upregulation of photosynthesis-associated genes occurs during the first 6hrs of UV-B exposure

Due to the small number of genes that were significantly changed in response to UV-B exposure, the focus here was on the overall impact of UV-B exposure on *Arabidopsis* metabolism by looking at all DEGs that have LFC > 0.5 and padj < 1. DEGs identified in *wt* 6hrs +UVB:-UVB and in *wt* 24hrs +UVB:-UVB where analysed using MapMan 3.6.0 (http://mapman.gabipd.org/web/guest/mapman) (Thimm et al., 2004; Usadel et al., 2009). In MapMan the DEGs are collected into functional categories and then associated with specific pathways using the mapping file for *Arabidopsis* (Ath_AFFY_ATH1_TAIR9_Jan2010 - Chapter 2: Materials and Methods). In each pathway analysis blue represents the positive LFC and hence

the upregulation under +UVB exposure compared to -UVB; red represents the negative LFC and hence the downregulation under +UVB exposure compared to -UVB.

The metabolism overview of wild type at 6hrs +UVB:-UVB (Fig 5.3a) shows that genes associated with the photosynthesis pathway demonstrate a general pattern of positive LFC; indicating that at 6hrs +UVB:-UVB there is an upregulation of photosynthesis-associated genes under UV-B that is not present in the absence of UV-B. Furthermore, analysis of the tetrapyrrole synthesis pathway demonstrates a pattern of positive LFC; indicating that UV-B exposure upregulates tetrapyrrole synthesis. As the chlorophylls are a subgroup of tetrapyrroles; the upregulation under UV-B could indicate downstream increases in chlorophyll; which may be involved in the increase in photosynthetic rate seen at 24hrs, albeit an increase in chlorophyll could not be characterised *in planta*. Also, the mixture of positive and negative LFC in the flavonoid associated pathway, suggests that at 6hrs the plant begins to respond to the presence of UV-B by increase flavonoid production; but a specific stress response appears to be absent.

The metabolism overview of wild type at 24hrs +UVB:-UVB (Fig 5.3b) shows a different pattern of LFC in the photosynthesis pathway. At 24hrs +UVB:-UVB there are still some genes that show a positive LFC in response to UV-B exposure; however, there are far fewer genes than at 6hrs +UVB:-UVB. The absence of large amounts of downregulation of photosynthesis-associated genes at 24hrs +UVB:-UVB is also of note. At 24hrs +UVB:-UVB there are a number of genes upregulated in the flavonoid and phenolics biosynthesis pathway; but there is no large increase in the number of genes being upregulated in the pathway compared to 6hrs +UVB:-UVB. The absence of a large increase in flavonoid biosynthesis genes being upregulated suggests that while the plant is responding to the presence of UV-B, it is not a stress response to UV-B.

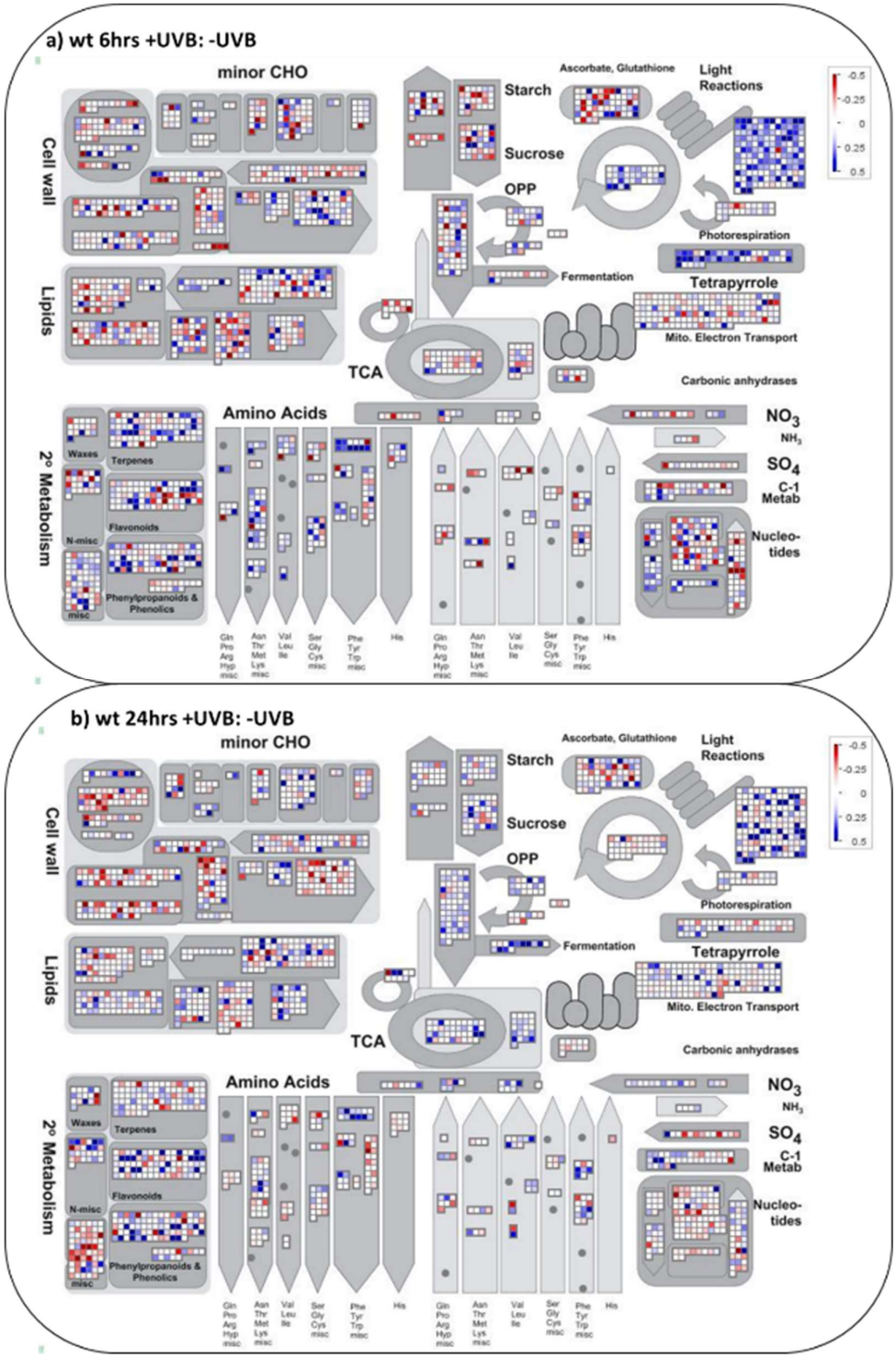

Figure 5.3 MapMan metabolism overview maps showing differences in transcript levels in *wt* (L*er*) during +UVB exposure versus -UVB exposure at 6hrs and 24hrs. Genes associated with metabolic pathways were analysed by the MapMan 3.6.0 software (http://mapman.gabipd.org/web/guest/mapman). On the colour scale, blue represents an increase in expression, while red represents a decrease in expression, with a threshold of 0.5. **a)** Differences in transcript levels at 6hrs in *wt* (L*er*) +UVB:-UVB**. b)** Differences in transcript levels at 24hrs in *wt* (L*er*) +UVB:-UVB.

The PageMan analysis (Fig 5.4) further illustrates the differences in gene regulation between 6hrs +UVB:-UVB and 24hrs +UVB:-UVB. PageMan provides an overview of significant (LFC > 0.5, padj < 1) MapMan categories (Thimm et al., 2004; Usadel et al., 2006), allowing for easy comparison of RNA-seq Data. The PageMan analysis (Fig 5.4) further demonstrates that at 6hrs +UVB:-UVB a larger number of photosynthesis-associated genes are upregulated; whereas at 24hrs +UVB:-UVB there are far less. The two groups upregulated at both time points are genes associated with cytochrome b6/f complex and chlororespiration; which are both associated with ATP synthesis (Peltier and Cournac, 2002; Rumeau et al., 2007; Yamori et al., 2011). This provides a link to *ABCB13*, which was the only significant DEG that was shared between 6hrs +UVB:-UVB and 24hrs +UVB:-UVB, which is involved in ATP synthase activity.

Genes associated with protein targeting to the chloroplast are also upregulated both at 6hrs +UVB:-UVB and 24hrs +UVB:-UVB. Interestingly, at 6hrs +UVB:-UVB genes associated with chloroplast synthesis are upregulated, which are not differentially expressed at 24hrs +UVB:-UVB. If the increase in chloroplast synthesis-associated genes results in the downstream increase in the number of chloroplasts that may explain the increase in photosynthetic rate seen at 24hrs UV-B. Furthermore, the upregulation in tetrapyrrole synthesis observed at 6hrs +UVB:-UVB is shown to be absent at 24hrs +UVB:-UVB. Of particular interest is the upregulation of genes associated with magnesium chelatase in the tetrapyrrole synthesis at 6hrs; as magnesium chelatase is involved in the biosynthesis of chlorophyll (Brzezowski et al., 2015; Brzezowski et al., 2016). This upregulation suggests that synthesis of chlorophyll increases in response to low fluence UV-B exposure; although this has not been confirmed in *planta.*.

The PageMan analysis (Fig 5.4) further confirms that the low fluence rate of UV-B used is not a major stressor to the plant. This is shown by the upregulation of genes associated with carbohydrate (CHO) metabolism at 24hrs of UV-B exposure; as under chronic UV-B stress, CHO metabolism has been shown to be downregulated (Gao et al., 2016). Furthermore, at 24hrs

+UVB:-UVB, there is upregulation of genes associated with flavonoid biosynthesis that is absent at 6hrs +UVB:-UVB, which suggests that at 24hrs +UVB radiation begins to negatively impact the plant, which would further explain the eventual decrease in photosynthetic rate.

Both the MapMan (Fig 5.3) and PageMan (Fig 5.4) analysis show the differences in transcription between 6hrs +UVB:-UVB and 24hrs +UVB:-UVB and the differences in response to UV-B over time. The differences in response indicate why photosynthetic rate decreases over 48hrs of UV-B exposure. At 6hrs +UVB:-UVB photosynthesis-associated genes are upregulated; whereas at 24hrs +UVB:-UVB the upregulation of photosynthesis-associated genes is largely absent, and there is not a general pattern of downregulation either. At 24hrs of UV-B, there is an increase in photosynthetic rate, which is lost at 48hrs; whereas the photosynthetic rate under UV-B is not significantly different from the photosynthetic rate in the absence of UV-B (-UVB). Further quantification of photosynthetic rate at 72hrs of UV-B exposure showed that photosynthetic rate is significantly lower under UV-B than it is in the absence of UV-B. The upregulation of photosynthesis-associated genes at 6hrs could explain the increase in photosynthetic rate seen at 24hrs; the loss of that increase in photosynthetic rate at 48hrs is reflected by the loss of upregulation of photosynthesis-associated genes at 24hrs. Perhaps at 48hrs of UV-B exposure, the pattern of gene regulation would show downregulation of photosynthesis-associated genes and more upregulation of genes associated with the UV-B stress response.

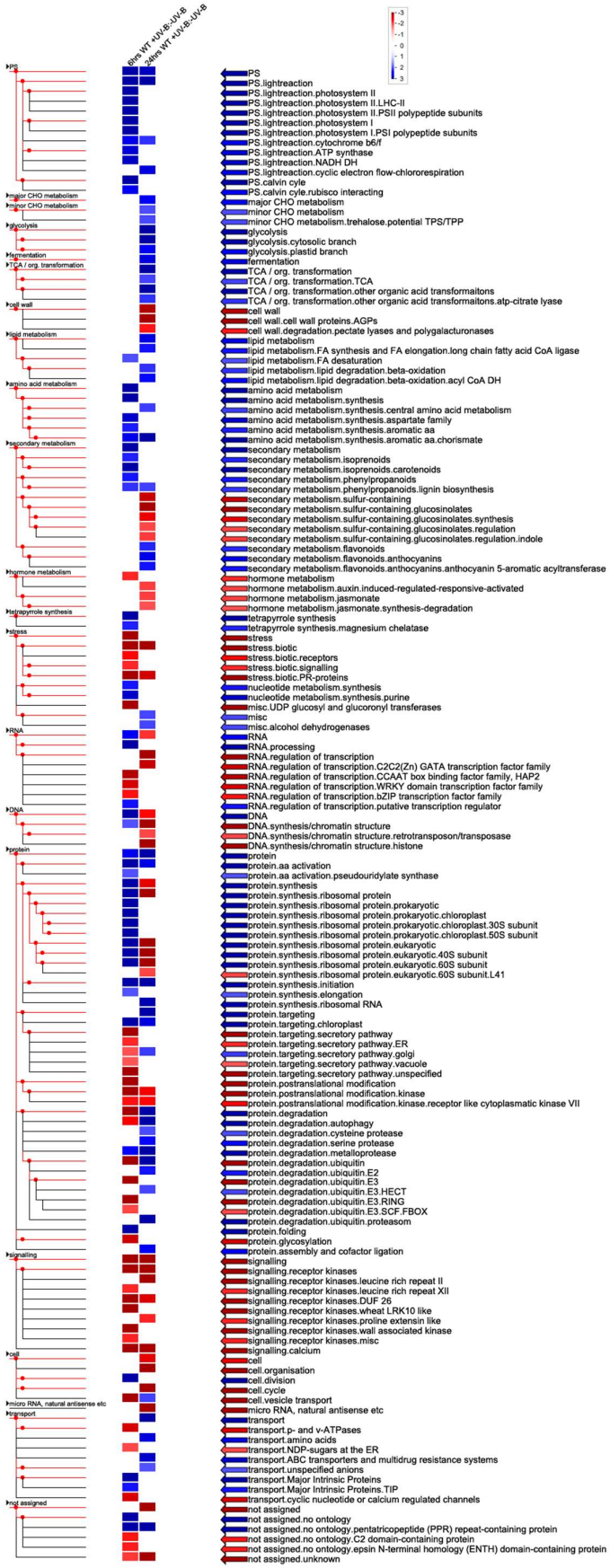
6hrs WT +UV-B:-UV-B
24hrs WT +UV-B:-UV-B
-3
-2
-1
0
1
2
3
PS
major CHO metabolism
minor CHO metabolism
glycolysis
fermentation
TCA / org. transformation
cell wall
lipid metabolism
amino acid metabolism
secondary metabolism
hormone metabolism
tetrapyrrole synthesis
stress
RNA
DNA
protein
signalling
cell
micro RNA, natural antisense etc
transport
not assigned
PS
PS.lightreaction
PS.lightreaction.photosystem II
PS.lightreaction.photosystem II.LHC-II
PS.lightreaction.photosystem II.PSII polypeptide subunits
PS.lightreaction.photosystem I
PS.lightreaction.photosystem I.PSI polypeptide subunits
PS.lightreaction.cytochrome b6/f
PS.lightreaction.ATP synthase
PS.lightreaction.NADH DH
PS.lightreaction.cyclic electron flow-chlororespiration
PS.calvin cyle
PS.calvin cyle.rubisco interacting
major CHO metabolism
minor CHO metabolism
minor CHO metabolism.trehalose.potential TPS/TPP
glycolysis
glycolysis.cytosolic branch
glycolysis.plastid branch
fermentation
TCA / org. transformation
TCA / org. transformation.TCA
TCA / org. transformation.other organic acid transformaitons
TCA / org. transformation.other organic acid transformaitons.atp-citrate lyase
cell wall
cell wall.cell wall proteins.AGPs
cell wall.degradation.pectate lyases and polygalacturonases
lipid metabolism
lipid metabolism.FA synthesis and FA elongation.long chain fatty acid CoA ligase
lipid metabolism.FA desaturation
lipid metabolism.lipid degradation.beta-oxidation
lipid metabolism.lipid degradation.beta-oxidation.acyl CoA DH
amino acid metabolism
amino acid metabolism.synthesis
amino acid metabolism.synthesis.central amino acid metabolism
amino acid metabolism.synthesis.aspartate family
amino acid metabolism.synthesis.aromatic aa
amino acid metabolism.synthesis.aromatic aa.chorismate
secondary metabolism
secondary metabolism.isoprenoids
secondary metabolism.isoprenoids.carotenoids
secondary metabolism.phenylpropanoids
secondary metabolism.phenylpropanoids.lignin biosynthesis
secondary metabolism.sulfur-containing
secondary metabolism.sulfur-containing.glucosinolates
secondary metabolism.sulfur-containing.glucosinolates.synthesis
secondary metabolism.sulfur-containing.glucosinolates.regulation
secondary metabolism.sulfur-containing.glucosinolates.regulation.indole
secondary metabolism.flavonoids
secondary metabolism.flavonoids.anthocyanins
secondary metabolism.flavonoids.anthocyanins.anthocyanin 5-aromatic acyltransferase
hormone metabolism
hormone metabolism.auxin.induced-regulated-responsive-activated
hormone metabolism.jasmonate
hormone metabolism.jasmonate.synthesis-degradation
tetrapyrrole synthesis
tetrapyrrole synthesis.magnesium chelatase
stress
stress.biotic
stress.biotic.receptors
stress.biotic.signalling
stress.biotic.PR-proteins
nucleotide metabolism.synthesis
nucleotide metabolism.synthesis.purine
misc.UDP glucosyl and glucoronyl transferases
misc
misc.alcohol dehydrogenases
RNA
RNA.processing
RNA.regulation of transcription
RNA.regulation of transcription.C2C2(Zn) GATA transcription factor family
RNA.regulation of transcription.CCAAT box binding factor family, HAP2
RNA.regulation of transcription.WRKY domain transcription factor family
RNA.regulation of transcription.bZIP transcription factor family
RNA.regulation of transcription.putative transcription regulator
DNA
DNA.synthesis/chromatin structure
DNA.synthesis/chromatin structure.retrotransposon/transposase
DNA.synthesis/chromatin structure.histone
protein
protein.aa activation
protein.aa activation.pseudouridylate synthase
protein.synthesis
protein.synthesis.ribosomal protein
protein.synthesis.ribosomal protein.prokaryotic
protein.synthesis.ribosomal protein.prokaryotic.chloroplast
protein.synthesis.ribosomal protein.prokaryotic.chloroplast.30S subunit
protein.synthesis.ribosomal protein.prokaryotic.chloroplast.50S subunit
protein.synthesis.ribosomal protein.eukaryotic
protein.synthesis.ribosomal protein.eukaryotic.40S subunit
protein.synthesis.ribosomal protein.eukaryotic.60S subunit
protein.synthesis.ribosomal protein.eukaryotic.60S subunit.L41
protein.synthesis.initiation
protein.synthesis.elongation
protein.synthesis.ribosomal RNA
protein.targeting
protein.targeting.chloroplast
protein.targeting.secretory pathway
protein.targeting.secretory pathway.ER
protein.targeting.secretory pathway.golgi
protein.targeting.secretory pathway.vacuole
protein.targeting.secretory pathway.unspecified
protein.postranslational modification
protein.postranslational modification.kinase
protein.postranslational modification.kinase.receptor like cytoplasmatic kinase VII
protein.degradation
protein.degradation.autophagy
protein.degradation.cysteine protease
protein.degradation.serine protease
protein.degradation.metalloprotease
protein.degradation.ubiquitin
protein.degradation.ubiquitin.E2
protein.degradation.ubiquitin.E3
protein.degradation.ubiquitin.E3.HECT
protein.degradation.ubiquitin.E3.RING
protein.degradation.ubiquitin.E3.SCF.FBOX
protein.degradation.ubiquitin.proteasom
protein.folding
protein.glycosylation
protein.assembly and cofactor ligation
signalling
signalling.receptor kinases
signalling.receptor kinases.leucine rich repeat II
signalling.receptor kinases.leucine rich repeat XII
signalling.receptor kinases.DUF 26
signalling.receptor kinases.wheat LRK10 like
signalling.receptor kinases.proline extensin like
signalling.receptor kinases.wall associated kinase
signalling.receptor kinases.misc
signalling.calcium
cell
cell.organisation
cell.division
cell.cycle
cell.vesicle transport
micro RNA, natural antisense etc
transport
transport.p- and v-ATPases
transport.amino acids
transport.NDP-sugars at the ER
transport.ABC transporters and multidrug resistance systems
transport.unspecified anions
transport.Major Intrinsic Proteins
transport.Major Intrinsic Proteins.TIP
transport.cyclic nucleotide or calcium regulated channels
not assigned
not assigned.no ontology
not assigned.no ontology.pentatricopeptide (PPR) repeat-containing protein
not assigned.no ontology.C2 domain-containing protein
not assigned.no ontology.epsin N-terminal homology (ENTH) domain-containing protein
not assigned.unknown

Figure 5.4 Summary of MapMan gene categories, as displayed by PageMan (Thimm et al., 2004; Usadel et al., 2006), representing relative transcriptomic responses to UV-B treatments in *wt* (L*er*). Data was subjected to Wilcoxon Rank-Sum testing within MapMan to identify significant differences in expression patterns within each functional gene group compared with each entire dataset per sample. Expression ratios are calculated on the basis of +UVB treatments compared with -UVB treatments. Columns are also annotated according to duration (6hrs, 24hrs). Coloured boxes indicate statistically significant groups (Benjamini & Hochberg-corrected P-value < 0.05), and colour scale represents z-transformed P-values, with blue indicating a trend within the group for the up-regulation of expression relative to -UVB controls, and red indicating a trend within the group for down-regulation. Arrows, shown with the same colour scheme, indicate MapMan annotation of differentially regulated gene classes (MapMan 3.6.0 software (http://mapman.gabipd.org/web/guest/mapman)).

5.3.2.1 At 6hrs of UV-B exposure genes associated with the light reactions are upregulated

A closer look at the changes in the MapMan photosynthesis pathway (Fig 5.5) and chloroplast pathway (Fig 5.6) in 6hrs +UVB:-UVB and 24hrs +UVB:-UVB further illustrates the differences in transcription profiles between the two time points. It shows the stark differences in patterns of expression in genes associated with the light reactions; at 6hrs +UVB:-UVB there is a general pattern of upregulation seen in almost all genes (Fig 5.5a), at 24hrs +UVB:-UVB (Fig 5.5b) there are far fewer genes that are upregulated, and more downregulated genes. MapMan analysis of the bins associated with the photosynthesis pathway show that at 6hrs +UVB:-UVB the four significant bins are the PS II polypeptide subunits ($P < 0.001$), LHC II ($P < 0.001$), PS I polypeptide subunits ($P < 0.001$) and ATP synthase ($P < 0.01$); suggesting that it is these parts of the photosynthesis pathway that are most upregulated by the presence of UV-B at 6hrs. At 24hrs +UVB:-UVB there are only two bins that are significant: cytochrome b6/f ($P < 0.05$) and ATP synthase ($P < 0.05$). These are the two bins that had also been identified through PageMan analysis. The upregulation of the pathways associated with PS II polypeptide subunits, the light-harvesting complex II and PS I polypeptide subunits are unique to 6hrs +UVB:-UVB. The genes associated with each of these pathways may be involved in the increase in photosynthetic rate seen at 24hrs UV-B exposure.

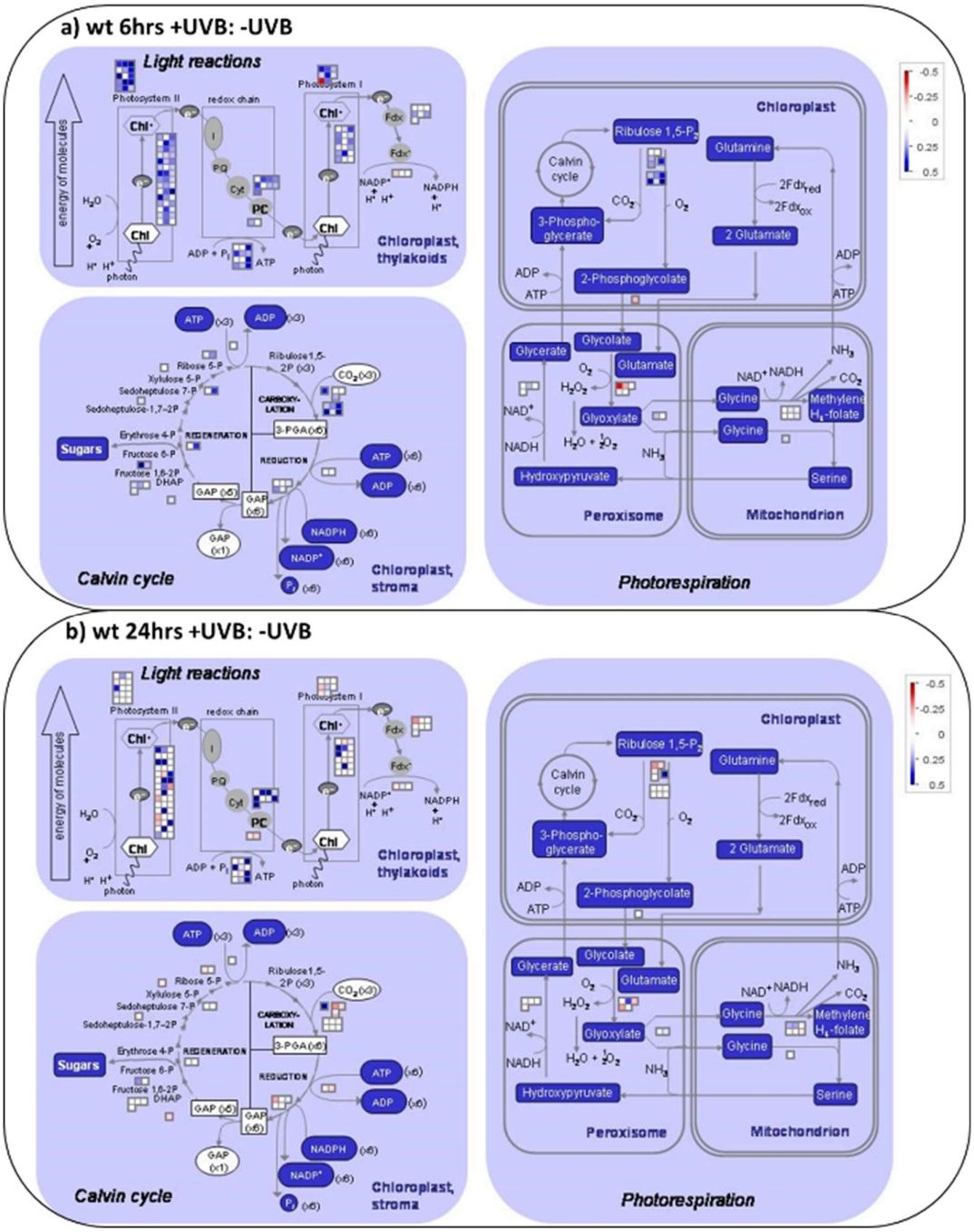

Figure 5.5 MapMan photosynthesis overview maps showing differences in transcript levels in *wt* (L*er*) during +UVB exposure versus -UVB exposure at 6hrs and 24hrs. Genes associated with the photosynthesis pathways were analysed by the MapMan 3.6.0 software (http://mapman.gabipd.org/web/guest/mapman). On the colour scale, blue represents an increase in expression, while red represents a decrease in expression, with a threshold of 0.5. **a)** Differences in transcript levels at 6hrs in *wt* (L*er*) +UVB:-UVB. **b)** Differences in transcript levels at 24hrs in *wt* (L*er*) +UVB:-UVB.

Analysis of the chloroplast pathway (Fig 5.6) shows a similar pattern of transcriptomic response to the photosynthesis pathway. At 6hrs +UVB:-UVB (Fig 5.6a) PS I and PS II, as well as ATP

synthase show a pattern of upregulation in the presence of +UVB that is absent in -UVB. Analysis of the MapMan bins shows that PS II ($P < 0.001$), PS I ($P < 0.001$), ATP synthase ($P < 0.01$) and cytochrome b6/f ($P < 0.01$) are significant. At 24hrs +UVB:-UVB (Fig 5.6b) regulation can be seen; a lot of the upregulation is lost; however, some are shown to be more upregulated at 24hrs. Analysis of the MapMan bins shows that the significantly changed bins are ATP synthase ($P < 0.05$) and cytochrome b6/f ($P < 0.05$).

MapMan analysis of the photosynthesis and chloroplast pathways showed that at 6hrs +UVB:-UVB genes associated with the light reactions of photosynthesis are upregulated; specifically PS I and PS II. At 24hrs +UVB:-UVB these genes are no longer significantly upregulated. Upregulation of these genes could be involved in the increase in photosynthetic rate seen at 24hrs of UV-B exposure; the subsequent decrease in photosynthetic rate at 48hrs may be the result of the absence of upregulation of these genes. 6hrs +UVB:-UVB and 24hrs +UVB:-UVB show an overlap in significantly upregulated bins: ATP synthase and cytochrome b6/f. The continued upregulation of these bins at 24hrs of UV-B may explain as to why photosynthetic rate under UV-B is the same as photosynthetic rate in the absence of UV-B at 48hrs.

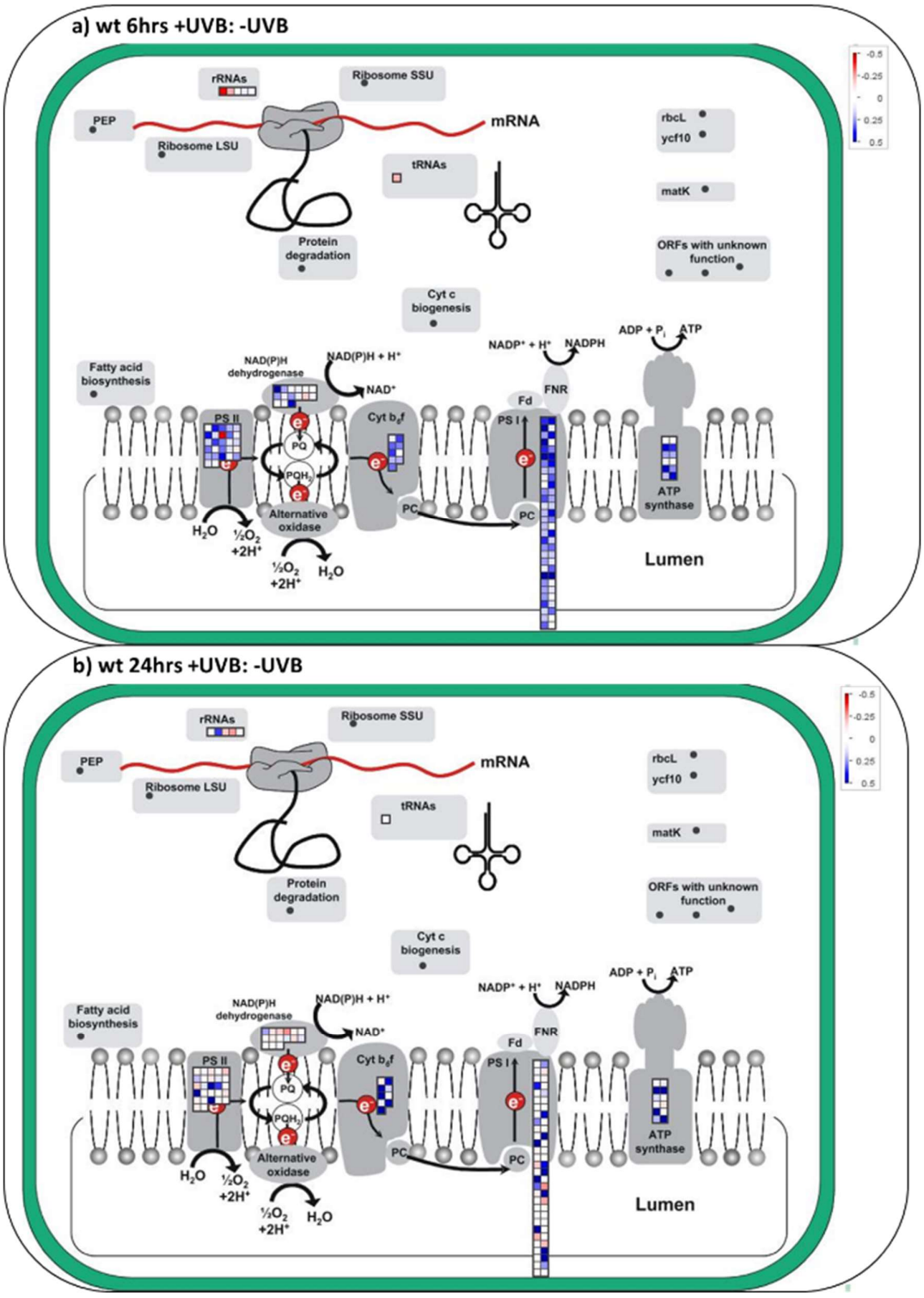

Figure 5.6 MapMan Chloroplast overview maps showing differences in transcript levels in *wt* (L*er*) during +UVB exposure versus -UVB exposure at 6hrs and 24hrs. Genes associated with the chloroplast pathway were analysed by the MapMan 3.6.0 software (http://mapman.gabipd.org/web/guest/mapman). On the colour scale, blue represents an increase in expression, while red represents a decrease in expression, with a threshold of 0.5. **a)** Differences in transcript levels at 6hrs in *wt* (L*er*) +UVB:-UVB. **b)** Differences in transcript levels at 24hrs in *wt* (L*er*) +UVB:-UVB.

5.3.2.2 Candidate genes of interest indicate significant regulation at 6hrs but are lost at 24hrs

To identify possible candidate genes involved in the photosynthesis phenotype observed at 24hrs UV-B exposure, the significantly changed DEGs ($P < 0.05$) at 6hrs +UVB:-UVB were further analysed for photosynthesis association using the functional classification tool in PANTHER (http://www.pantherdb.org/) (Mi et al., 2017). The top 10 significantly changed ($P < 0.05$) genes associated with photosynthesis were identified at 6hrs +UVB:-UVB and then tracked at 24hrs +UVB:-UVB (Table 5.1).

Table 5.1 Differential expression (Log2FoldChange, LFC) of the top 10 significantly changed photosynthesis-associated genes in response to 0.5 µmol m^{-2} s^{-1} of +UVB exposure versus –UVB at 6hrs and 24hrs in *wt* (L*er*). Log2FoldChange at 6hrs is 6hrs +UVB: 6hrs -UVB, for 24hrs is 24hrs +UVB: 24hrs -UVB. Genes were selected based on padj value < 0.05 and photosynthesis pathway association determined through the use of the functional classification tool in PANTHER (**http://www.pantherdb.org/**).

Gene of interest			6hrs *wt* +UVB:-UVB		24hrs *wt* +UVB:-UVB	
Identifier	**Name**	**Description**	**LFC**	**padj**	**LFC**	**padj**
AT4G34730	RBF1	Ribosome-binding factor 1	1.098	0.000	0.223	0.823
AT1G52990	TFP	Thioredoxin family protein	1.686	0.000	0.598	0.293
AT1G02280	TOC33	Translocon at the outer envelope membrane of chloroplasts 33	0.779	0.000	0.137	0.919
AT2G40400	BPG3	Putative DUF399 family protein	1.02	0.002	0.102	0.951
AT4G30720	PDE327	FAD/NAD(P)-binding oxidoreductase family protein	0.688	0.007	0.172	0.857
AT2G04270	RNEE/G	RNAse E/G-like	0.587	0.008	0.128	0.864
AT1G77510	PDIL1-2	Protein disulfide isomerase 1-2	-0.944	0.010	-0.023	0.990
AT4G20130	PTAC14	Plastid transcriptionally active 14	0.663	0.015	0.073	0.955
AT3G62910	APG3	Chloroplast ribosome release factor 1	0.536	0.022	0.062	0.950
AT4G28660	PSB28	Photosystem II reaction center PSB28 protein	0.562	0.022	-0.047	0.977

All of the genes identified are shown to be significantly changed at 6hrs +UVB:-UVB ($P < 0.05$, Table 5.1); but are no longer significantly changed at 24hrs +UVB:-UVB. All genes are upregulated at 6hrs +UVB:-UVB, apart from *PDIL1-2*, which is strongly downregulated (Fig 5.7). At 24hrs +UVB:-UVB all genes show the same pattern as they all show little LFC at 24hrs +UVB:-UVB. The loss of upregulation at 24hrs +UVB:-UVB seen in each of these genes furthers the notion that the decrease in photosynthetic rate seen at 48hrs of UV-B is driven by the loss of

upregulation in photosynthesis-associated genes rather than chronic damage to the photosynthetic apparatus.

The identified genes can be split into two groups – genes that are associated with chloroplast biogenesis and synthesis of chloroplastic proteins, and genes that are associated with chloroplastic oxidoreductase activity. Genes associated with the chloroplast biogenesis and synthesis of photosynthesis-associated proteins are *RBF1* (*RIBOSOME-BINDING FACTOR 1*), *TOC33 (TRANSLOCON AT THE OUTER ENVELOPE MEMBRANE OF CHLOROPLASTS 33)*, *BPG3 (BRZ-INSENSITIVE-PALE GREEN 3), RNEE/G (RNASE E/G-LIKE), PTAC14 (PLASTID TRANSCRIPTIONALLY ACTIVE 14), PSB28 (PHOTOSYSTEM II REACTION CENTRE PSB28)* and *APG3 (ALBINO AND PALE GREEN).* The genes associated with chloroplastic oxidoreductase activity are *TFP (THIOREDOXIN FAMILY PROTEIN), PDE327 (PIGMENT DEFECTIVE 327)* and *PDIL1-2 (PROTEIN DISULFIDE ISOMERASE 1-2).*

5.3.2.2.1 Genes associated with chloroplast biogenesis and photosynthesis-associated proteins

RBF1 encodes a thylakoid-associated protein, involved in the biogenesis of the 30S subunit of the chloroplast ribosome (Fristedt et al., 2014). Studies have shown that photosynthetic performance is reduced in the absence of RBF1 (Fristedt et al., 2014). *TOC33* encodes a homodimerizing GTPase (Oreb et al., 2011). Along with TOC159, it controls the recognition and translocation of pre-proteins into the chloroplast (Kessler and Schnell, 2004; Oreb et al., 2008; Oreb et al., 2011). *BPG3* encodes a novel chloroplast protein that is involved in the regulation of photosynthesis and plays an important role in electron transport in PS II (Yoshizawa et al., 2014). Furthermore, it involved in chloroplast regulation related to brassinosteroids signalling; however its specific function is unknown (Yoshizawa et al., 2014). *RNEE/G* encodes an endoribonuclease E/G present in chloroplasts and is required for RNA accumulation in the chloroplast and chloroplast development (Bollenbach et al., 2005; Mudd et al., 2008). The absence of RNEE/G results in the arrest of chloroplast development (Mudd et al., 2008). PTAC14

is a chloroplast-located plastid-encoded polymerase (PEP) (Rius et al., 2008; Gao et al., 2012). As a transcriptionally active chromosome (TAC) it makes up a fraction of the protein/DNA complex with RNA polymerase which is involved in gene expression in chloroplasts. Its specific function is still unknown, but it has been shown to regulate chloroplast gene expression, and it has been suggested that it is involved in the phytochrome-dependent gene expression in chloroplasts (Pfalz et al., 2006; Gao et al., 2011). PSB28 is a stroma/cytoplasm localised protein (Shi et al., 2012). In cyanobacteria, PSB28 is associated with the biogenesis and assembly of chlorophyll-containing proteins such as PsaA, and PsaB (Dobáková et al., 2009). However, the role of PSB28 in higher plants is not fully understood; but as it is evolutionarily conserved, it is predicted to function similarly (Lu, 2016). APG3 is a nuclear-encoded chloroplast protein (Motohashi et al., 2007). It is a ribosome release factor in chloroplasts and is associated with the termination of plastid protein translation (Motohashi et al., 2007; Satou et al., 2014). It has been shown to be essential to the chloroplast machinery, chloroplast development and thylakoid biogenesis (Motohashi et al., 2007).

5.3.2.2.2 Genes associated with chloroplastic oxidoreductase activity

TFP encodes a putative chloroplastic thioredoxin (Meyer et al., 2006). Thioredoxins are involved in the regulatory ferredoxin/thioredoxin system that is associated with oxygenic photosynthesis and light (Schürmann and Buchanan, 2001). *PDE327* encodes an oxidoreductase/electron carrier that is localised to the chloroplast (Zybailov et al., 2008; Vlad et al., 2010). It is essential for correct electron flow through the photosynthetic chain (Vlad et al., 2010), and hence for photosynthetic efficiency. *PDIL1-2* is the only gene of the top 10 identified that is downregulated in response to UV-B exposure at 6hrs +UVB:-UVB (Fig 5.7). PDIL1-2 is a protein disulphide isomerase that is targeted and localised to the chloroplast (Wittenberg et al., 2014). *pdil1-2* knockdowns show a higher resistance to photoinhibition when exposed to higher light intensity

(Wittenberg et al., 2014). Studies have also shown that D1 synthesis is increased in the *pdil1-2* knockdown (Wittenberg et al., 2014).

The subset of genes analysed suggests that the upregulation of photosynthetic rate at 24hrs of UV-B is likely due to an increase in chloroplast number and photosynthetic function, as well as an increase in chloroplastic oxidoreductases. As RBF1 and RNEE/G are involved in chloroplast biogenesis, their upregulation under UV-B could suggest an increase in the number of chloroplasts. TOC33 is involved in import into the chloroplast; while PTAC14, PSB28, BPG3 and APG3 are involved in the regulation and biosynthesis of chloroplast machinery. The upregulation of these genes further illustrates that the increase in photosynthetic rate may be due to an increase in chloroplast function. The upregulation of *TFP* and *PDE327* under UV-B suggests that photosynthetic efficiency is improved; which increases the photosynthetic rate at 24hrs UV-B. The downregulation of *PDIL1-2* suggests that the resistance to photoinhibition is increased in response to UV-B during the initial 6hrs of exposure; which suggests that the increase in photosynthetic rate may be due a decrease in photoinhibition. Although photoinhibition was not induced in this experiment; the downregulation of *PDIL1-2* in response to UV-B may explain the increased resistance to photoinhibition after UV-B exposure observed by Wargent et al. (2011) in *Lactuca sativa*.

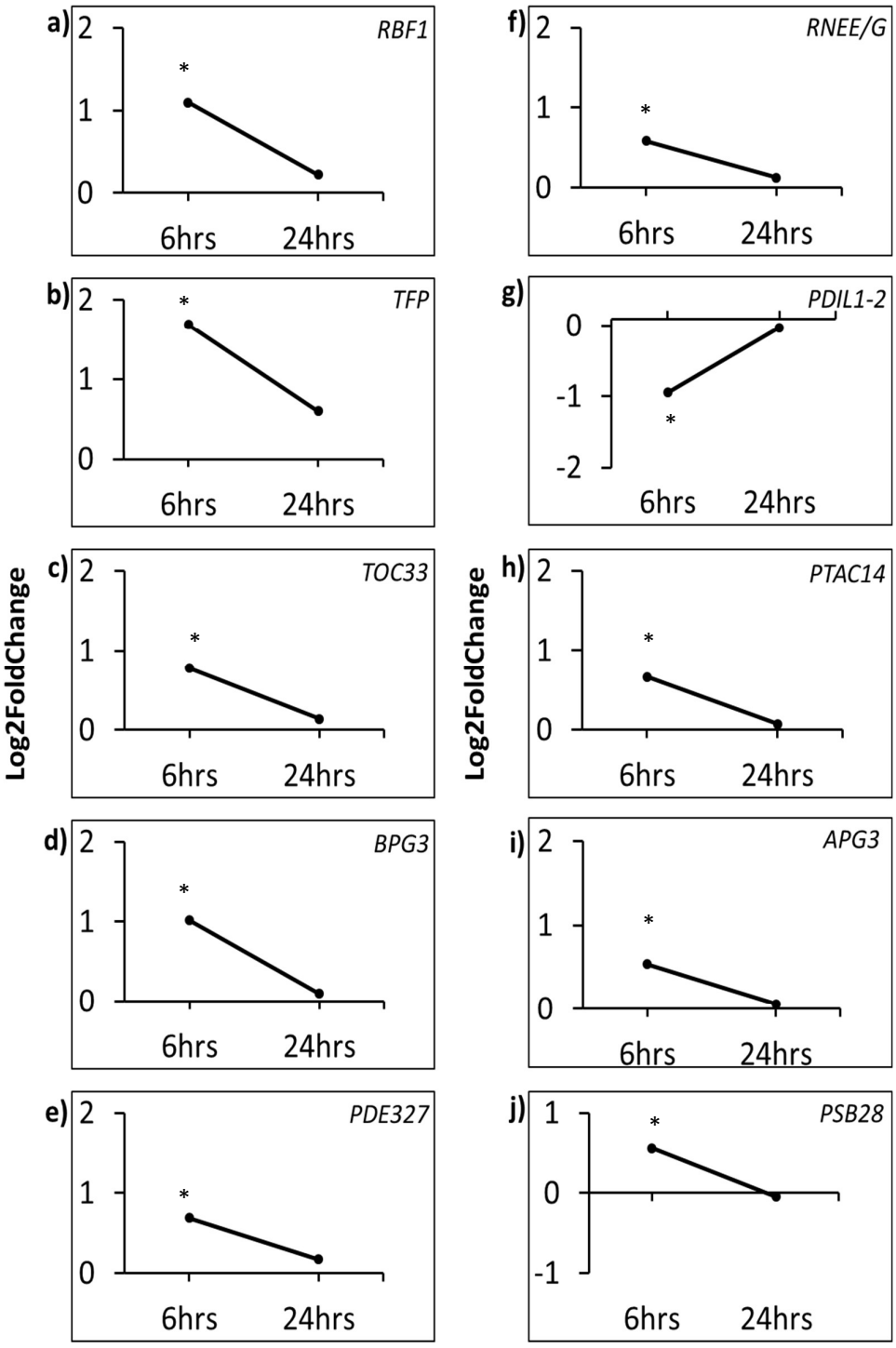
a)
RBF1
b)
TFP
c)
TOC33
d)
BPG3
e)
PDE327
f)
RNEE/G
g)
PDIL1-2
h)
PTAC14
i)
APG3
j)
PSB28
Log2FoldChange
Log2FoldChange
6hrs
24hrs
*

Figure 5.7 Differential expression (Log2FoldChange) of the top 10 significantly changed photosynthesis-associated genes in response to 0.5umol of +UVB exposure versus -UVB at 6hrs and 24hrs in *wt* (L*er*). Log2FoldChange at 6hrs is 6hrs +UVB: 6hrs -UVB, for 24hrs is 24hrs +UVB: 24hrs -UVB. Genes were selected based on padj value < 0.05 and photosynthesis pathway association determined through the use of the functional classification tool in PANTHER (**http://www.pantherdb.org/**). **a)** *RBF1* (*RIBOSOME-BINDING FACTOR 1,* AT4G34730). **b)** *TFP* (*THIOREDOXIN FAMILY PROTEIN,* AT1G52990). **c)** *TOC33* (*TRANSLOCON AT THE OUTER ENVELOPE MEMBRANE OF CHLOROPLASTS 33*, AT1G02280). **d)** *BPG3* (*BRZ-INSENSITIVE-PALE GREEN 3,* AT2G40400). **e)** *PDE327* (*PIGMENT DEFECTIVE 327,* AT4G30720) **f)** *RNEE/G* (*RNASE E/G-LIKE,* AT2G04270). **g)** *PDIL1-2* (*PROTEIN DISULFIDE ISOMERASE 1-2,* AT1G77510). **h)** *PTAC14* (*PEPTIDE CHAIN RELEASE FACTOR 1*, AT4G20130). **i)** *APG3* (*ALBINO AND PALE GREEN,* AT3G62910). **j)** *PSB28* (*PHOTOSYSTEM II REACTION CENTRE PSB28 PROTEIN,* AT4G28660). Asterisks denote significance (padj < 0.05).

5.3.2.3 Pre-identified candidate genes

In Chapter 4, the photosynthesis response under low fluence UV-B in mutants of *sig5, elip1, elip2* and the negative regulator of UVR8 *rup1*,*rup2* was characterised. Analysis of the photosynthesis phenotype showed that SIG5 and the ELIPs are involved in the UV-B dependent photosynthesis phenotype, but are not crucial to the response. Analysis of the *rup1,2* double mutant showed that the RUPs negatively regulate the photosynthesis response after prolonged UV-B exposure.

Analysis of DEGs at 6hrs +UVB:-UVB and 24hrs +UVB:-UVB found that none of these genes are significantly regulated in response to UV-B (Table 5.2). The absence of significant regulation in response to UV-B suggests that none of these genes are crucial to the photosynthesis phenotype and are not key regulators of the photosynthesis phenotype. However, Brown and Jenkins (2008) showed that in response to low fluence UV-B exposure (0.1 µmol m^{-2} s^{-1} UV-B) *SIG5* and *ELIP1* are significantly upregulated. This upregulation is absent in the RNA-seq data, suggesting that the regulation in response to UV-B may also be influenced by other factors such as the ratio of PAR: UV-B, which differs greatly between the two studies. Due to the absence of regulation, we chose not further investigated these genes as possible regulators of the UV-B dependent photosynthesis response.

Table 5.2 Differential expression (Log2FoldChange, LFC) of the pre-identified candidate regulators of UV-B dependent phenotype in response to 0.5 µmol m^{-2} s^{-1} of +UVB exposure versus –UVB at 6hrs and 24hrs in *wt* (L*er*). Log2FoldChange at 6hrs is 6hrs +UVB: 6hrs -UVB, for 24hrs is 24hrs +UVB: 24hrs -UVB.

		6hrs *wt* +UVB:-UVB		24hrs *wt* +UVB:-UVB	
Identifier	**Name**	**LFC**	**padj**	**LFC**	**padj**
AT5G24120	SIG5	0.149	0.945	0.515	0.471
AT3G22840	ELIP1	0.269	0.849	0.448	0.573
AT4G14690	ELIP2	0.195	0.871	0.879	0.067
AT5G52250	RUP1	0.238	0.884	0.895	0.052
AT5G23730	RUP2	0.725	0.267	0.324	0.794

5.4 Analysis of transcriptome changes in the absence of functional UVR8 under low fluence UV-B

In the absence of functional UVR8, the photosynthesis phenotype observed at 24hrs UV-B in wild type is absent; which suggests that UVR8 is involved in the regulation of photosynthesis in response to UV-B exposure. To better understand how UVR8 may be involved; RNA-seq analysis was performed on *uvr8-1* samples and DESeq2 analysis was performed to determine differential expression between mutant (*mt*, *uvr8-1*) and wild type (L*er*) under UV-B exposure was done.

Initial assessment of significant DEGs (padj < 0.05) shows that initially wild type and *uvr8-1* (*mt*) do not differ much; as there are only 8 differentially expressed genes (Fig 5.8, details of all DEGs in Supplementary Table 9.9). Functional analysis using PANTHER GO showed that these genes are not associated with photosynthesis; for most of the genes in this subset, their exact function is not known. This suggests that the absence of functional UVR8 does not affect photosynthesis-associated genes prior to exposure to UV-B. At 6hrs of UV-B exposure, *uvr8-1* and wild type begin to differ widely from another (588 DEGs) and at 24hrs of UV-B exposure the difference is even larger (993 DEGs). At 6hrs the photosynthesis-associated genes in the subset of significant DEGs are highly downregulated in *mt* +UVB versus *wt* +UVB; which is expected as the photosynthesis phenotype is absent in *uvr8-1*, and the high negative LFC will be due to the upregulation seen in wild type under UV-B. At 24hrs the LFC difference of photosynthesis-associated genes between *mt:wt* +UVB is considerably lessened, i.e., for *wt* +UVB 24hrs the

upregulation of photosynthesis-associated genes is absent. Interestingly, there are some photosynthesis-associated genes that are upregulated in *mt* 24hrs +UVB versus *wt* 24hrs +UVB. These are the CHLOROPHYLL A-B BINDING proteins (CAB proteins); which are the apoproteins of the light-harvesting complex of PS II (Liu et al., 2013), interestingly, other members of the CAB family (Green et al., 1991) the ELIPs are downregulated in *uvr8-1* versus wild type. As the upregulation of the CAB genes does not increase photosynthetic rate, it suggests that regulation of the light-harvesting complex is not involved in the photosynthesis phenotype.

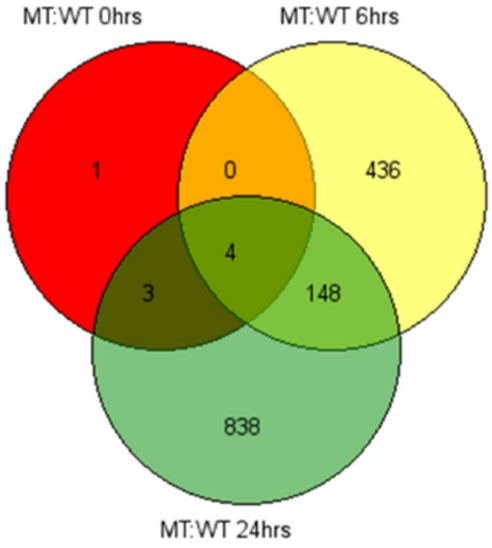

Figure 5.8 Venn diagram showing the differentially expressed genes in *mt* (*uvr8-1*) versus *wt* (L*er*) under +UVB at 0hrs, 6hrs and 24hrs. In red are the differentially expressed genes unique to 0hrs -UVB *mt (uvr8-1)* versus *wt* (L*er*). In green are the differentially expressed genes unique to 6hrs +UVB mt (*uvr8-1)* versus wt (L*er*), in blue are the differentially expressed genes unique to 24hrs +UV mt (*uvr8-1)* versus wt (L*er*). The threshold is padj < 0.05

5.4.1 In the absence of UVR8, photosynthesis-associated genes are downregulated under UV-B

To understand the overall changes in gene expression in response to UV-B in *mt*:*wt*, PageMan analysis was completed on all DEGs (Fig 5.9). When focusing on all DEGs, photosynthesis-associated genes are downregulated in *uvr8-1* compared to wild type prior to UV-B exposure (0hrs). However, this does not have an impact on photosynthetic rate. At 6hrs of UV-B photosynthesis-associated genes are highly downregulated in the *mt* versus *wt*; which explains

the absence of the UV-B dependent phenotype at 24hrs of UV-B in *uvr8-1*. At 24hrs differences in LFC are absent, suggesting that in terms of photosynthesis gene expression wild type and *uvr8-1* act similarly under prolonged UV-B exposure. As noted before at 24hrs, *uvr8-1* shows upregulation in the polypeptide subunits of PS I and PS II compared to wild type; suggesting that UVR8 may be involved in the regulation of these genes. Overall, this suggests that functional UVR8 is involved in the regulation of certain photosynthesis-associated genes, which are involved in the UV-B dependent photosynthesis phenotype.

Compared to wild type*, uvr8-1* exhibits downregulation of a large number of pathways in response to UV-B exposure that have been identified as being involved in the photosynthesis response. *uvr8-1* shows downregulation in genes involved in ribosomal protein synthesis in the chloroplast as well as protein targeting to the chloroplast; which were identified as genes involved in the photosynthesis phenotype. This downregulation further illustrates the role these genes may play in the increase in photosynthetic rate at 24hrs of UV-B in wild type as well as suggesting that these genes are partially regulated by UVR8 in response to UV-B.

The absence of a general pattern of downregulation in response to UV-B in *uvr8-1* compared to wild type further suggests that our chosen fluence rate was not a major stressor; but rather elicits a photomorphogenic response in the first 24hrs of UV-B exposure.

It should be noted that there was a disparity in the number of significant DEGs identified in Fig 5.8 at 0hrs mt:wt and the number of significantly changed bins shown at the same time point in Fig 5.9. This difference is likely due to how genes are associate with certain MapMan bins, and that there are genes present in multiple bins.

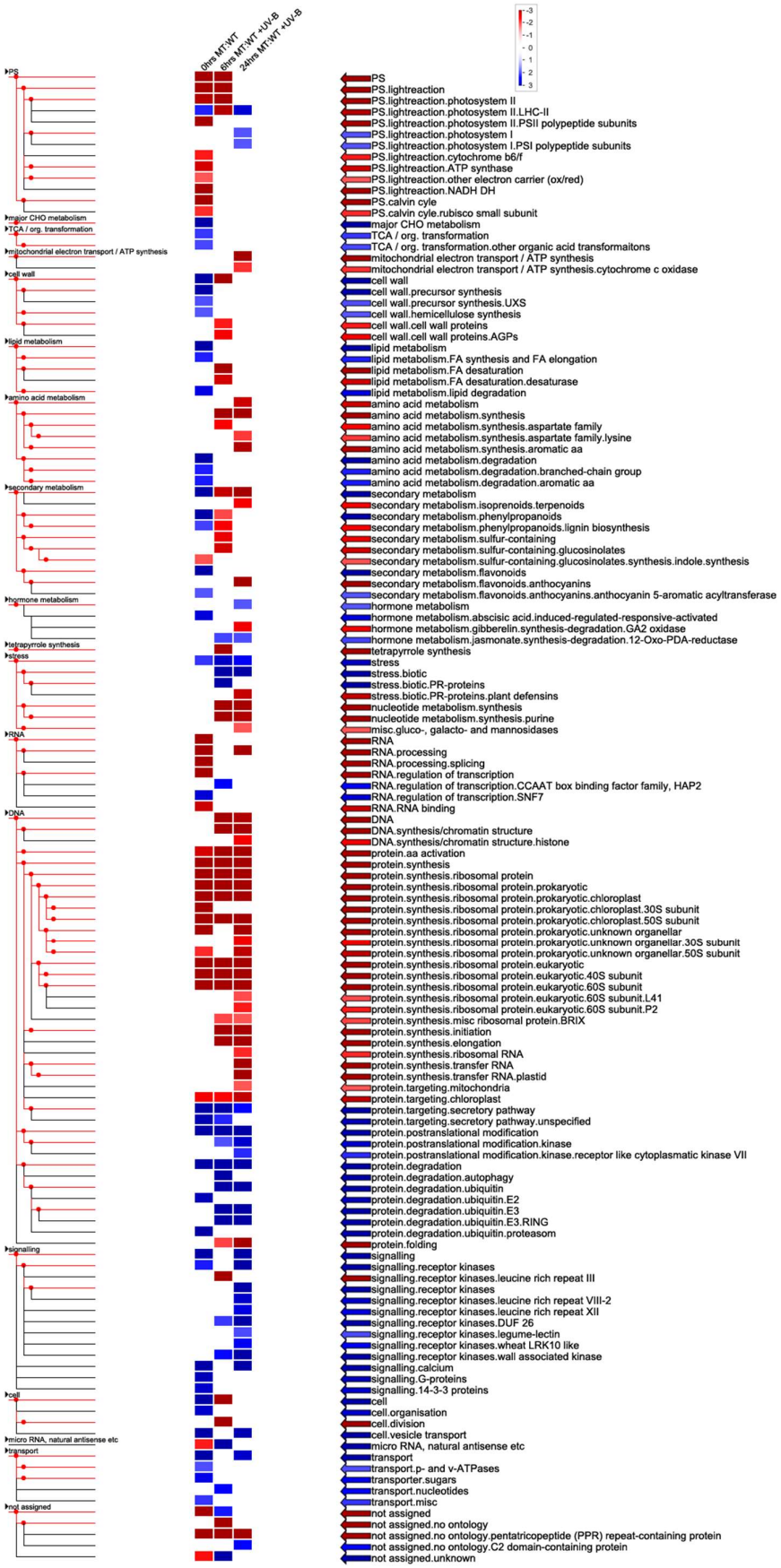
0hrs MT:WT
6hrs MT:WT +UV-B
24hrs MT:WT +UV-B
-3
-2
-1
0
1
2
3
PS
major CHO metabolism
TCA / org. transformation
mitochondrial electron transport / ATP synthesis
cell wall
lipid metabolism
amino acid metabolism
secondary metabolism
hormone metabolism
tetrapyrrole synthesis
stress
RNA
DNA
signalling
cell
micro RNA, natural antisense etc
transport
not assigned
PS
PS.lightreaction
PS.lightreaction.photosystem II
PS.lightreaction.photosystem II.LHC-II
PS.lightreaction.photosystem II.PSII polypeptide subunits
PS.lightreaction.photosystem I
PS.lightreaction.photosystem I.PSI polypeptide subunits
PS.lightreaction.cytochrome b6/f
PS.lightreaction.ATP synthase
PS.lightreaction.other electron carrier (ox/red)
PS.lightreaction.NADH DH
PS.calvin cyle
PS.calvin cyle.rubisco small subunit
major CHO metabolism
TCA / org. transformation
TCA / org. transformation.other organic acid transformaitons
mitochondrial electron transport / ATP synthesis
mitochondrial electron transport / ATP synthesis.cytochrome c oxidase
cell wall
cell wall.precursor synthesis
cell wall.precursor synthesis.UXS
cell wall.hemicellulose synthesis
cell wall.cell wall proteins
cell wall.cell wall proteins.AGPs
lipid metabolism
lipid metabolism.FA synthesis and FA elongation
lipid metabolism.FA desaturation
lipid metabolism.FA desaturation.desaturase
lipid metabolism.lipid degradation
amino acid metabolism
amino acid metabolism.synthesis
amino acid metabolism.synthesis.aspartate family
amino acid metabolism.synthesis.aspartate family.lysine
amino acid metabolism.synthesis.aromatic aa
amino acid metabolism.degradation
amino acid metabolism.degradation.branched-chain group
amino acid metabolism.degradation.aromatic aa
secondary metabolism
secondary metabolism.isoprenoids.terpenoids
secondary metabolism.phenylpropanoids
secondary metabolism.phenylpropanoids.lignin biosynthesis
secondary metabolism.sulfur-containing
secondary metabolism.sulfur-containing.glucosinolates
secondary metabolism.sulfur-containing.glucosinolates.synthesis.indole.synthesis
secondary metabolism.flavonoids
secondary metabolism.flavonoids.anthocyanins
secondary metabolism.flavonoids.anthocyanins.anthocyanin 5-aromatic acyltransferase
hormone metabolism
hormone metabolism.abscisic acid.induced-regulated-responsive-activated
hormone metabolism.gibberelin.synthesis-degradation.GA2 oxidase
hormone metabolism.jasmonate.synthesis-degradation.12-Oxo-PDA-reductase
tetrapyrrole synthesis
stress
stress.biotic
stress.biotic.PR-proteins
stress.biotic.PR-proteins.plant defensins
nucleotide metabolism.synthesis
nucleotide metabolism.synthesis.purine
misc.gluco-, galacto- and mannosidases
RNA
RNA.processing
RNA.processing.splicing
RNA.regulation of transcription
RNA.regulation of transcription.CCAAT box binding factor family, HAP2
RNA.regulation of transcription.SNF7
RNA.RNA binding
DNA
DNA.synthesis/chromatin structure
DNA.synthesis/chromatin structure.histone
protein.aa activation
protein.synthesis
protein.synthesis.ribosomal protein
protein.synthesis.ribosomal protein.prokaryotic
protein.synthesis.ribosomal protein.prokaryotic.chloroplast
protein.synthesis.ribosomal protein.prokaryotic.chloroplast.30S subunit
protein.synthesis.ribosomal protein.prokaryotic.chloroplast.50S subunit
protein.synthesis.ribosomal protein.prokaryotic.unknown organellar
protein.synthesis.ribosomal protein.prokaryotic.unknown organellar.30S subunit
protein.synthesis.ribosomal protein.prokaryotic.unknown organellar.50S subunit
protein.synthesis.ribosomal protein.eukaryotic
protein.synthesis.ribosomal protein.eukaryotic.40S subunit
protein.synthesis.ribosomal protein.eukaryotic.60S subunit
protein.synthesis.ribosomal protein.eukaryotic.60S subunit.L41
protein.synthesis.ribosomal protein.eukaryotic.60S subunit.P2
protein.synthesis.misc ribosomal protein.BRIX
protein.synthesis.initiation
protein.synthesis.elongation
protein.synthesis.ribosomal RNA
protein.synthesis.transfer RNA
protein.synthesis.transfer RNA.plastid
protein.targeting.mitochondria
protein.targeting.chloroplast
protein.targeting.secretory pathway
protein.targeting.secretory pathway.unspecified
protein.postranslational modification
protein.postranslational modification.kinase
protein.postranslational modification.kinase.receptor like cytoplasmatic kinase VII
protein.degradation
protein.degradation.autophagy
protein.degradation.ubiquitin
protein.degradation.ubiquitin.E2
protein.degradation.ubiquitin.E3
protein.degradation.ubiquitin.E3.RING
protein.degradation.ubiquitin.proteasom
protein.folding
signalling
signalling.receptor kinases
signalling.receptor kinases.leucine rich repeat III
signalling.receptor kinases
signalling.receptor kinases.leucine rich repeat VIII-2
signalling.receptor kinases.leucine rich repeat XII
signalling.receptor kinases.DUF 26
signalling.receptor kinases.legume-lectin
signalling.receptor kinases.wheat LRK10 like
signalling.receptor kinases.wall associated kinase
signalling.calcium
signalling.G-proteins
signalling.14-3-3 proteins
cell
cell.organisation
cell.division
cell.vesicle transport
micro RNA, natural antisense etc
transport
transport.p- and v-ATPases
transporter.sugars
transport.nucleotides
transport.misc
not assigned
not assigned.no ontology
not assigned.no ontology.pentatricopeptide (PPR) repeat-containing protein
not assigned.no ontology.C2 domain-containing protein
not assigned.unknown

Figure 5.9 Summary of MapMan gene categories, as displayed by PageMan (Thimm et al., 2004; Usadel et al., 2006), representing relative transcriptomic responses to UV-B treatments in *mt* (*uvr8-1*) versus *wt* (L*er*). Data was subjected to Wilcoxon Rank-Sum testing within MapMan to identify significant differences in expression patterns within each functional gene group compared with each entire dataset per sample. Expression ratios are calculated on the basis of +UVB treatments of *uvr8-1* compared with +UVB treatments of *wt* (L*er*). Columns are also annotated according to duration of treatment (0hrs, 6hrs, 24hrs). Coloured boxes indicate statistically significant groups (Benjamini & Hochberg-corrected P-value < 0.05), and colour scale represents z-transformed P-values, with blue indicating a trend within the group for the up-regulation of expression relative to *wt* +UVB controls, and red indicating a trend within the group for down-regulation. Arrows, shown with the same colour scheme, indicate MapMan annotation of differentially regulated gene classes. (MapMan 3.6.0 software (http://mapman.gabipd.org/web/guest/mapman)).

5.4.2 Candidate genes show a pattern of downregulation in *uvr8-1*

To understand how the candidate genes, identified in section 5.3.2.2, respond to UV-B exposure in the absence of functional UVR8, their expression in the *mt*:*wt* comparison for each time point was analysed (Fig 5.10). Each of the candidates shows little to no change in expression at 0hrs *mt*:*wt,* suggesting that in the absence of UV-B the loss of functional UVR8 does not impact their transcription levels significantly. All genes show negative LFC in *mt*:*wt* at 6hrs and 24hrs; apart from *PDIL1-2*, which shows positive LFC at 6hrs and 24hrs. This negative LFC shows that in *uvr8-1* expression of each candidate gene is the opposite to the expression in wild type; suggesting that functional UVR8 is involved in the regulation of each of these genes in response to UV-B exposure.

At 6hrs *RBF1* shows a high negative LFC in *mt*:*wt* (Fig 5.10, padj < 0.01); and while *RBF1* still shows negative LFC at 48hrs it is no longer significant, this shows that *RBF1* expression is downregulated in *uvr8-1* versus wild type. The significant negative LFC change at 6hrs illustrates that the upregulation of *RBF1* at 6hrs UV-B in wild type is lost in the absence of UVR8 and that *RBF1* is downregulated in *uvr8-1* in response to UV-B. The not significant LFC at 24hrs shows that expression in wild type is still lower in *uvr8-1*, but as upregulation also decreases in the wild type the differences in expression are no longer as large. It suggests that *RBF1* expression is linked to the initial response to UV-B exposure; within the first 6 to 12 hours of exposure, and becomes less regulated after longer exposure.

TFP indicates a not-significant negative LFC at 6hrs (Fig 5.10, padj > 0.05) in *mt*:*wt*, but at 24hrs is significantly downregulated (Fig 5.10, padj < 0.01), showing that *TFP* expression is downregulated in *uvr8-1* in response to prolonged UV-B exposure. The continued downward trend of *TFP* expression in *uvr8-1* suggests UVR8 is involved in the regulation of *TFP* under UV-B exposure.

In *uvr8-1, TOC33, PDE327, RNEE/G, PTAC14* and *APG3* exhibit similar expression profiles to *TFP* in *mt*:*wt* at 6hrs and 24hrs. Each gene shows not significant LFC at 6hrs (Fig 5.10, padj > 0.05) in *mt*:*wt*, and significant negative LFC at 24hrs (Fig 5.10, padj < 0.05). The pattern suggests that the initial increase in expression seen in wild type is linked to functional UVR8 being present; and that the over prolonged UV-B exposure expression in the absence of UVR8 becomes further downregulated.

BPG3 and *PSB28* show similar expression patterns in *mt*:*wt* at 6hrs and 24hrs; each gene exhibits a higher negative LFC (Fig 5.10, padj < 0.05) at 6hrs, and a lower negative LFC (Fig 5.10, padj < 0.01) at 24hrs. The high LFC at 6hrs between *uvr8-1* and wild type suggests that the presence of functional UVR8 is required for the increase in expression observed in wild type; and that prolonged exposure to UV-B in the absence of UVR8 results in downregulation.

PDIL1-2 was the only gene that exhibited a positive LFC *mt*:*wt* at 6hrs and 24hrs. It was shown to be downregulated in response to UV-B exposure in wild type at 6hrs of UV-B and shows no change in expression at 24hrs of UV-B. As expression of *PDIL1-2* in the absence of UVR8 increases under UV-B exposure, it suggests that UVR8 negatively regulates *PDIL1-2* in response to low fluence UV-B at 6hrs and that over prolonged exposure to UV-B UVR8 ceases to alter *PDIL1-2* expression. The increase in *PDIL1-2* expression may also explain the reduction in photosynthetic

rate as upregulation of *PDIL1-2* may make the plants more susceptible to UV-B induced photoinhibition.

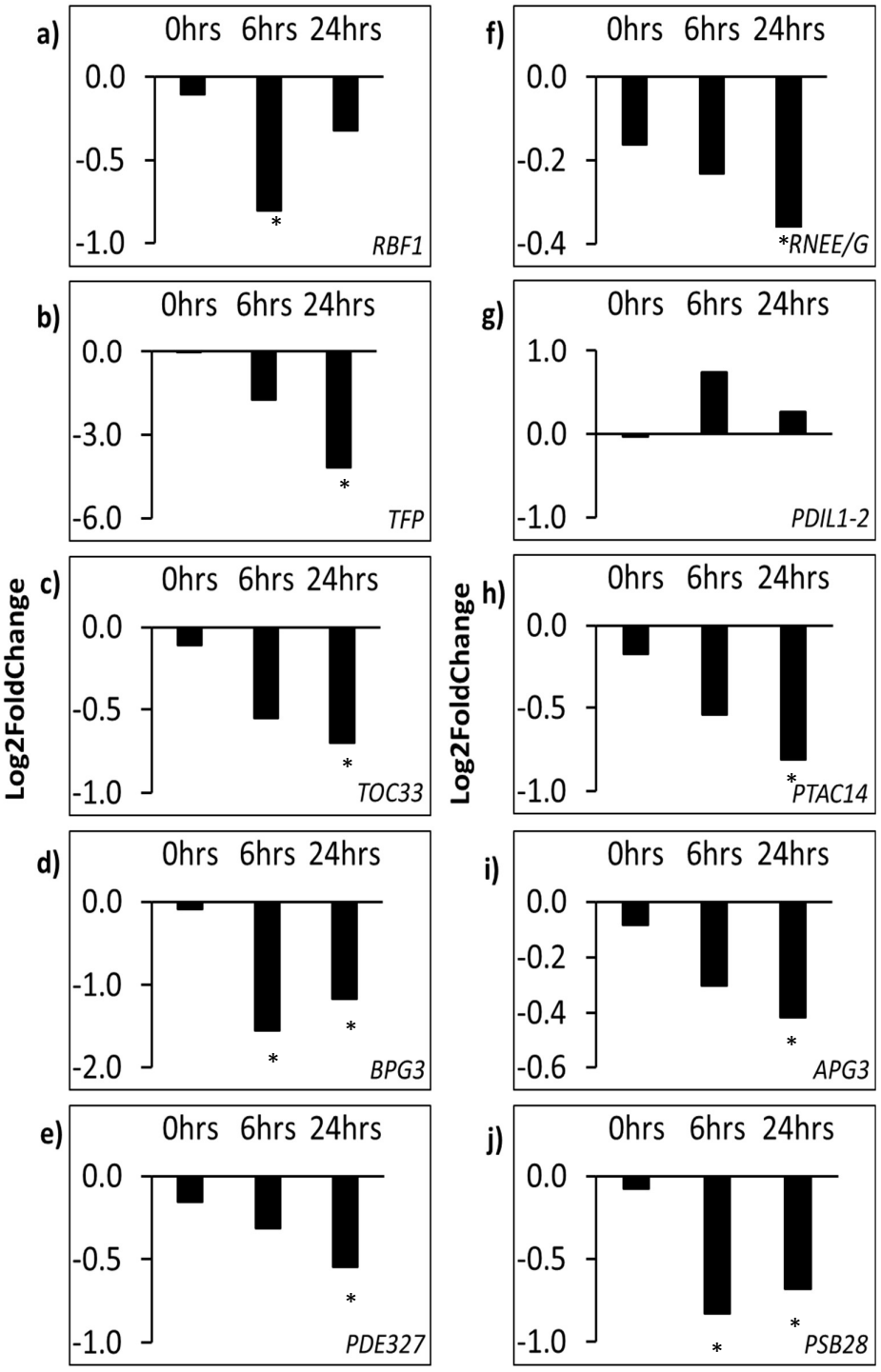

Figure 5.10 Differential expression (Log2FoldChange) of the previously identified photosynthesis-associated genes in *mt* (*uvr8-1*) +UVB compared to *wt* (L*er*) +UVB at 0hrs, 6hrs and 24hrs. Log2FoldChange at 0hrs is 0hrs –UVB *mt*:*wt* -UVB, for 6hrs is 6hrs +UVB *mt:wt* and for 24hrs is 24hrs +UVB *mt:wt* . Genes of interested had been identified in +UVB 6hrs *wt*: -UVB 6hrs *wt* and were selected based on padj value < 0.05 and photosynthesis pathway association determined by MapMan bins (MapMan 3.6.0 software (http://mapman.gabipd.org/web/guest/mapman)). **a)** *RBF1* (*RIBOSOME-BINDING FACTOR 1,* AT4G34730). **b)** *TFP (THIOREDOXIN FAMILY PROTEIN*, AT1G52990). **c)** *TOC33 (TRANSLOCON AT THE OUTER ENVELOPE MEMBRANE OF CHLOROPLASTS 33*, AT1G02280). **d)** *BPG3* (*BRZ-INSENSITIVE-PALE GREEN 3*, AT2G40400). **e)** *PDE327* (*PIGMENT DEFECTIVE 327,* AT4G30720). **f)** *RNEE/G* (*RNASE E/G-LIKE,* AT2G04270). **g)** *PDIL1-2* (*PROTEIN DISULFIDE ISOMERASE 1-2,* AT1G77510). **h)** *PTAC14 (PEPTIDE CHAIN RELEASE FACTOR 1,* AT4G20130). **i)** *APG3* (*ALBINO AND PALE GREEN* AT3G62910). **j)** *PSB28 (PHOTOSYSTEM II REACTION CENTRE PSB28,* AT4G28660). Asterisks denotes significance (padj < 0.05).

5.5 Chapter summary

RNA-seq analysis was undertaken to determine what changes occur in the transcriptome in response to low fluence UV-B exposure that may explain the increase in photosynthetic rate seen at 24hrs of UV-B exposure in wild type compared to no UV-B exposure. The analysis showed that low UV-B exposure has a modest overall effect on gene expression in wild type plants. As in response to UV-B exposure compared to no UV-B exposure relatively few genes are significantly differentially expressed; both at 6hrs and 24hrs, and the LFC change was low.

The 6hr time point shows that during the initial exposure to UV-B genes associated with the chloroplast and thylakoid are upregulated; as well as genes associated with chloroplastic oxidoreductases. This suggests that the increase in photosynthetic rate seen at 24hrs of UV-B exposure in wild type is driven by an increase in chloroplast biogenesis and synthesis of proteins in the chloroplast, as well as an increase in chloroplastic oxidoreductases. Further investigation of the transcript profile at 6hrs showed that in response to UV-B exposure tetrapyrrole synthesis is upregulated; which may suggest an upregulation in chlorophyll in response to UV-B exposure. PageMan analysis showed that at 6hrs synthesis of chloroplast proteins and targeting to the chloroplast are upregulated. Detailed analysis of the photosynthesis pathway and chloroplast in MapMan illustrated that in response to UV-B exposure at 6hrs the light reactions; specifically PS I and PS II-associated genes are upregulated. Many of the candidate photosynthetic genes

identified here have not been previously associated with UV-B response, and/or downstream UVR8-mediated UV-B signalling.

Gene expression at 24hrs differs much from expression seen at 6hrs. At 24hrs of UV-B the upregulation of photosynthesis-associated genes is absent, and the genes associated with the flavonoid biosynthesis pathway become upregulated. The absence of downregulation of photosynthesis-associated genes may explain why photosynthetic rate at 48hrs of UV-B is the same as the photosynthetic rate at 48hrs in the absence of UV-B, rather than being lower. The increase in flavonoid biosynthesis associated genes suggests that the plant begins to respond to negative impact of UV-B and begins increasing photoprotective pigments.

The analysis of significant DEGs in wild type at 6hrs +UVB:-UVB identified 10 candidate genes that may be involved in the photosynthesis phenotype at 24hrs of UV-B. The identified genes can be split into two categories; genes associated with the chloroplast (*RBF1, TOC33, BPG3, RNEE/G, PTAC14, PSB28* and *APG3*) and chloroplastic oxidoreductase activity associated genes (*TFP, PDE327* and *PDIL1-2*). Each of these genes, apart from *PDIL1-2*, are significantly upregulated at 6hrs, and at 24hrs show little to no upregulation and are not significant. Upregulation of these genes suggests that the photosynthesis phenotype is due to an increase in chloroplast biogenesis and synthesis of proteins within chloroplast as well as an increase in chloroplastic oxidoreductase activity. The analysis also showed that none of the pre-identified genes investigated in Chapter 4 are significantly changed under UV-B, and hence are not key to the photosynthesis phenotype.

To further understand the photosynthesis phenotype the differences in gene expression between wild type and the *uvr8-1* mutant were investigated. In the absence of functional UVR8, the photosynthesis phenotype is absent, which suggests that the increase in photosynthetic rate is regulated by UVR8. Analysis showed that prior to UV-B exposure wild type and *uvr8-1* do not differ significantly from each other in terms of gene expression; however, at 6hrs of UV-B

exposure downregulation of a large number of genes is seen in *uvr8-1* compared to wild type; continuing at 24hrs as UV-B exposure continues. The analysis showed that in response to UV-B exposure the *uvr8-1* showed decreased expression in chloroplast biogenesis and chloroplastic protein associated genes as well as decreased expression of chloroplastic oxidoreductase associated genes. The downregulation of these genes suggests that UVR8 plays a key part in their regulation in response to UV-B exposure. The candidate genes showed a pattern of downregulation in *uvr8-1* compared to wild type in the presence of UV-B, which further illustrates that UVR8 may be involved in the regulation of these genes in response to UV-B exposure.

In summary, the RNA-seq analysis illustrates that the increase in photosynthetic rate observed in the wild type at 24hrs under UV-B coincides with the upregulation of photosynthesis-associated genes; specifically, genes associated with chloroplast biogenesis and synthesis of chloroplastic proteins as well chloroplastic oxidoreductase activity. This increase suggests that an increase in chloroplast number and synthesis of photosynthetic proteins within the chloroplast, as well as an increase in chloroplastic oxidoreductase activity, results in the increase in photosynthetic rate observed. The analysis further showed that in the absence of functional UVR8 the upregulation of these genes is absent, which suggests UVR8 is involved in the regulation of these genes in response to UV-B and thus functional UVR8 is required for the photosynthesis phenotype.

6 Response to low fluence UV-B in mutants of candidate regulators of photosynthesis phenotype

6.1 Introduction

In Chapter 5 the RNA-seq analysis found that in the first 6hrs of UV-B exposure a number of photosynthesis-associated genes are upregulated and that at 24hrs these genes are no longer significantly regulated; suggesting that the photosynthesis phenotype, characterised in Chapter 3, is a result of upregulation of photosynthesis-associated genes in response to UV-B exposure. To further characterise the molecular basis of the photosynthesis phenotype in response to low fluence UV-B exposure; the three most highly significantly changed photosynthesis-associated genes; *RBF1, TFP* and *TOC33,* were selected for further analysis.

Each of these genes showed statistically significant upregulation at 6hrs of UV-B exposure compared to 6hrs of no UV-B, and at 24hrs +UVB are no longer significantly regulated compared to 24hrs –UVB. When the experiments were undertaken, none of these genes had been previously associated with UV-B response, and very little was known about their role in response to both high and low fluence rates of UV-B.

Here, the aim is to gain a greater understanding as to how these genes are involved in the UV-B dependent photosynthesis response. To assess their role in the photosynthesis phenotype, a knockout or knockdown mutant of the gene was selected, and their response to low fluence UV-B was assessed. Both photosynthetic rate and green leaf area size was measured under the established UV-B fluence rate and conditions to determine if the absence of each of these factors changed compared to the wild type response previously characterised. qRT-PCR was then used to determine UV-B induced changes in gene expression in wild type (Col-0) and *uvr8-6* (Col) as well as confirming the RNA-seq results obtained in *wt* (L*er*) and *uvr8-1* (L*er*) in the previous chapter. Together, these analyses provide a better understanding as to how these

genes are involved in the UV-B dependent photosynthesis phenotype and how they may interact with each other.

6.2 RBF1 - RIBOSOME-BINDING FACTOR 1 (AT4G34730)

RBF1 is a putative ribosome biogenesis factor involved in thylakoid membrane biogenesis (Fristedt et al., 2014). It is a homolog of the *E.coli* ribosome binding factor A (RbfA), which is a bacterial 30S subunit binding protein that is required for the 5' processing of the 16S rRNA (Jones and Inouye, 1996; Xia et al., 2003; Datta et al., 2007; Fristedt et al., 2014). In *Arabidopsis thaliana* RBF1 is nuclear encoded, localised to the thylakoid membrane and involved in the 59 and 39 end processing of 16s rRNA (Fristedt et al., 2014). In the *rbf1* mutants; *rbf1-1* (SALK_008178) and *rbf1-2* (SALK_058490), chloroplast ribosomal accumulation is reduced, and the unprocessed precursors (1.7-kb species) accumulate (Fristedt et al., 2014). *rbf1-1* is a partial loss of function mutant; it has T-DNA insertion in the lowly conserved 39 portion of the *RBF1* coding region, while *rbf1-2* is a leaky mutant, as residual expression may occur due to the T-DNA insertion being in the 59 untranslated region, outside the coding region (Fristedt et al., 2014). The null allele *rbf1-3* dies as a young seedling.

Little is known about the impact of reduced *RBF1* expression on photosynthesis; Fristedt et al. (2014) showed reduced PS II efficiency (Fv/Fm) in young leaves in *rbf1-1* and *rbf1-2,* but in mature, fully expanded leaves Fv/Fm values were similar to wild type. The recovery of the PS II efficiency as the plant matures suggests that the translationary machinery in the mutants catch up and restores levels of chloroplast proteins to wild type-like as the plant ages (Fleischmann et al., 2011).

The impact of UV-B exposure on *RBF1* expression is not well studied, as so far it has only been shown to be upregulated in a whole genome transcriptomic screen looking at the response to narrowband UV-B in *Chlamydomonas reinhardtii* (Tilbrook et al., 2016). Apart from the RNA-seq

analysis, we have performed, there have been no other studies linking UV-B exposure to increases in *RBF1* expression.

6.2.1 Photosynthetic rate in *rbf1* mutants decreases at 24hrs UV-B exposure

To determine if the loss of *RBF1* would alter the photosynthesis response to UV-B; the photosynthetic rate of *rbf1* mutants was assessed under the same conditions as were used to characterise the UV-B dependent photosynthesis phenotype in wild type. After a 7-day PAR acclimation period, *rbf1-1* and *rbf1-2* plants were exposed to 0.5 µmol m^{-2} s^{-1} of UV-B, and their photosynthesis response was characterised (Chapter 2: Materials and Methods).

The UV-B dependent increase in photosynthetic rate observed in wild type is absent in both *rbf1* mutants. In fact, both mutants exhibited a significant decrease in photosynthetic rate at 24hrs of UV-B compared to no UV-B (Fig 6.1). *rbf1-1* had a photosynthetic rate 10% lower under +UVB compared to –UVB ($P < 0.001$, Fig 6.1); while *rbf1-2* showed a decrease of 20% in the same comparison ($P < 0.05$, Fig 6.1). The impact of UV-in the *rbf1* mutants is further illustrated by the observed decrease in rate between 0hrs and 24hrs of UV-B as *rbf1-1* exhibited a 15% decrease ($P < 0.001$, Fig 6.1) and *rbf1-2* exhibited a 17% decrease ($P < 0.001$, Fig 6.1). The decrease in rate suggests that RBF1 is a key player in the UV-B dependent increase in photosynthetic rate observed in wild type as well as playing an important role in maintaining photosynthetic function in the presence of UV-B.

The importance of RBF1 in maintaining photosynthetic rate is further illustrated by the continued decrease in photosynthetic rate observed at 48hrs under UV-B compared to 24hrs of UV-B (Fig 6.1). At 48hrs of UV-B the photosynthetic rate of *rbf1-1* was 14% lower than at 24hrs of UV-B ($P < 0.001$, Fig 6.1); however, *rbf1-2* showed no significant decrease in rate between 24hrs and 48hrs of UV-B, suggesting that the different RBF1 levels in the mutants have different effects on photosynthetic efficiency under longer UV-B exposure. The importance of RBF1 to photosynthesis under UV-B is demonstrated by the continued decrease in photosynthetic rate

observed at 48hrs of +UVB exposure compared to –UVB. Photosynthetic rate at 48hrs +UVB was significantly lower than 48hrs –UVB (Fig 6.1), as both *rbf1-1* showed a 23% decrease in photosynthetic rate between +UVB and –UVB ($P < 0.001$, Fig 6.1) and *rbf1-2* showed a decrease of 21% ($P < 0.01$, Fig 6.1). The continued decrease suggests that the reduced RBF1 levels have a detrimental effect on photosynthesis function under UV-B exposure and that it plays a key role in maintaining photosynthetic function in wild type under UV-B.

The importance of RBF1 to photosynthetic function becomes more evident when comparing the decrease in photosynthetic rate observed in *uvr8-6* and the *rbf1* mutants. In *uvr8-6* the decrease in photosynthetic rate observed at 24hrs between +UVB and –UVB was only 4% ($P < 0.001$), whereas in the same comparison the photosynthetic rate of the *rbf1* mutants was between 10% and 20%. This difference in magnitude shows that the presence of functional *RBF1* is required for maintaining photosynthetic function in response to UV-B exposure, as well as being involved in the UV-B dependent photosynthesis phenotype. The importance of functional RBF1 in maintaining photosynthetic efficiency is also demonstrated by the difference in photosynthetic rates at 48hrs +UVB and –UVB in the *rbf1* mutants and *uvr8-6*; as the decrease in rate in *rbf1-1* and *rbf1-2* is between 21% and 23%; whereas in *uvr8-6* the rate of decrease is only 12% ($P < 0.001$).

Both *rbf1* mutants behaved similarly in terms of net photosynthetic rate under UV-B exposure and were not significantly different from one another at 24hrs and 48hrs of UV-B (Fig 6.1). *rbf1-2* is a leaky mutant, which exhibits low RBF1 levels, and *rbf1-1* is a partial loss of function mutant (Fristedt et al., 2014). As the photosynthetic rate under UV-B was so similar, it suggests that the functional activity of RBF1 is key to maintaining photosynthetic function in response to low fluence UV-B exposure.

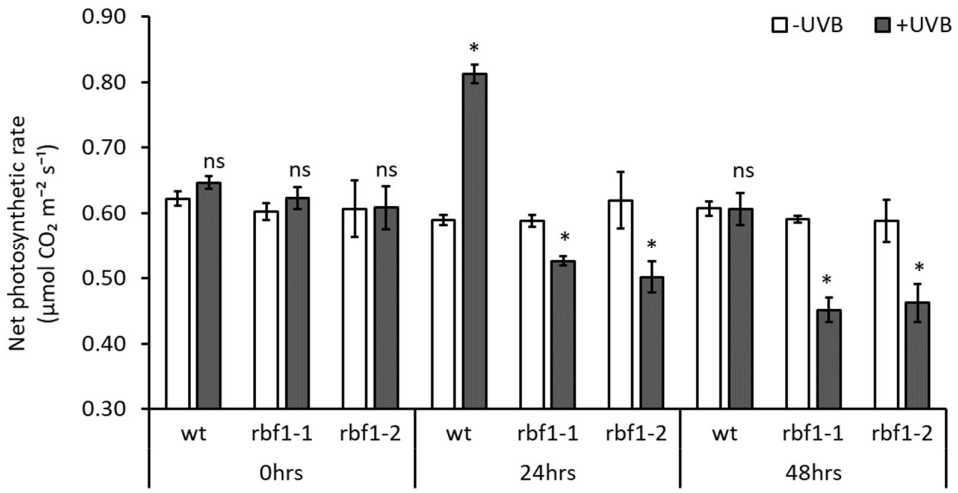

Figure 6.1 Changes in net photosynthetic rate (µmol CO_2 m^{-2} s^{-1}) normalised to leaf area in *wt* (Col-0), *rbf1-1* (Col) and *rbf1-2* (Col) in response to irradiation with 0.5 µmol m^{-2} s^{-1} of UV-B (+UVB, grey) or without (-UVB, white) over 48 hours of exposure. 0hrs is 35 DAS and is the net photosynthetic rate prior to commencement of illumination with UV-B, while 24hrs is after 24 hours of exposure and so forth. In the +UVB condition the plants are exposed to 0.5 µmol m^{-2} s^{-1} and 220 µmol m^{-2} s^{-1} of PAR, in the –UVB condition the plants are exposed to 220 µmol m^{-2} s^{-1} of PAR only. *rbf1-1 - ribosome-binding factor 1-1, rfb1-2 - ribosome-binding factor 1-2.* Error bars represent ± S.E. (n = 16 biological repeats). Asterisks indicate statistically significant means ($P < 0.05$) between +UVB and -UVB treatments for a given time point and genotype; ns indicates not significant means.

Interestingly, both *rbf1* mutants had similar photosynthetic rates to wild type in the absence of UV-B (Fig 6.1), which suggests that RBF1 is key to maintaining photosynthetic function under UV-B exposure, but the reduction of RBF1 levels is not detrimental to photosynthetic function in the absence of UV-B. Studies by Fristedt et al. (2014) found that reduction of RBF1 is most detrimental to PS II efficiency in young leaves, but that in mature leaves PS II efficiency is not significantly different from wild type, suggesting that as the plants mature the translationary machinery involved in chloroplast biogenesis catches up and the impact of the reduced RBF1 levels decreases. The findings suggest that in the absence of UV-B, the response observed by Fristedt et al. (2014) holds true and that the reduced activity of RBF1 only becomes detrimental to photosynthetic function in response to UV-B exposure.

The decrease in photosynthetic rate suggests that not only does RBF1 plays a key role in the UV-B dependent increase seen in photosynthetic rate at 24hrs in wild type, but also plays a role in maintaining photosynthetic function in response to low fluence UV-B exposure. The absence of

the UV-B dependent photosynthesis phenotype in the *rbf1* mutants suggests that in wild type low fluence UV-B exposure may result in an increase in chloroplast biogenesis; which could underpin the photosynthesis phenotype.

6.2.2 UV-B exposure limits increases in green leaf area in *rbf1* mutants

Not only does low fluence UV-B negatively affect photosynthetic function in the *rbf1* mutants; it also limits the increase in green leaf area development over time (Fig 6.2). Green leaf area development was assessed to determine if the presence of low fluence UV-B had a photomorphogenic response in the mutants, or induced a stress response, resulting in leaf purpling due to flavonoid induction.

Under UV-B conditions, the reduced levels of RBF1 affect the rate of increase in green leaf area compared to no UV-B exposure. In the absence of UV-B green leaf area increases in both *rbf1-1* and *rbf1-2*; with green leaf area having increased by 7% - 9% between 0hrs and 24hrs, as well as increasing at the same rate between 24hrs and 48hrs in the absence of UV-B for *rbf1-1* ($P < 0.001$; Fig 6.2); and increased between 5% - 10% for *rbf1-2* ($P < 0.001$; Fig 6.2). However, the rate of increase was much slower under UV-B conditions; as the rate of increase for *rbf1-1* was only 4% between 0hrs and 24hrs of UV-B ($P < 0.05$; Fig 6.2); and 5% for *rbf1-2* ($P < 0.01$; Fig 6.2). Between 24hrs and 48hrs of UV-B exposure, green leaf area did not increase significantly in the *rbf1* mutants; suggesting that functional RBF1 plays an important role in the plant's response to UV-B; especially over longer exposure times.

The role of RBF1 in the UV-B response is further illustrated when comparing the changes in green leaf area of the *rbf1* mutants to the changes in area in wild type. In the absence of UV-B, green leaf area of wild type and the *rbf1* mutants did not differ significantly from one another; suggesting that in the absence of UV-B the reduction of RBF1 levels does not impact green leaf area development. However, under UV-B conditions green leaf area continued to increase in wild type, increasing between by 13% between 0hrs and 24hrs of UV-B ($P < 0.01$; Fig 6.2); and

continuing to increase by 6% between 24hrs and 48hrs of UV-B ($P < 0.001$; Fig 6.2). In the *rbf1* mutants there was no increase; further illustrating the importance of RBF1 in the UV-B response.

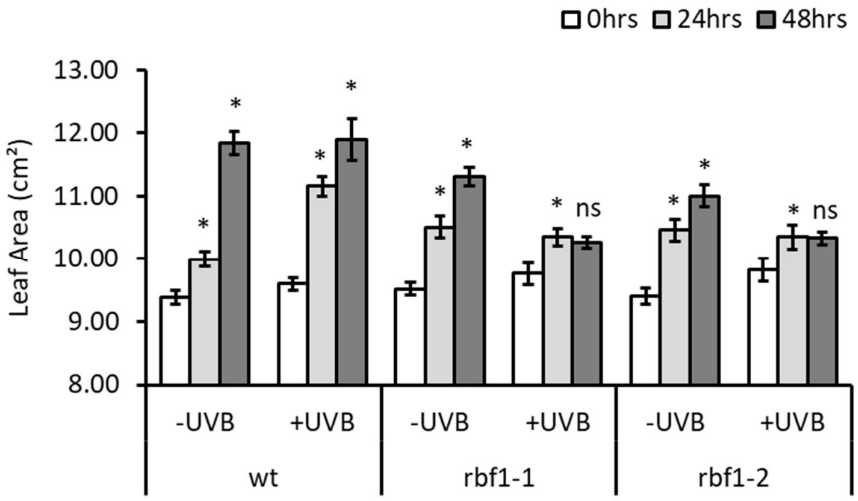

Figure 6.2 Changes in green leaf area (cm²) in *wt* (Col-0), *rbf1-1* (Col) and *rbf1-2* (Col) in response to irradiation with 0.5µmol m^{-2} s^{-1} of UV-B (+UVB) or without (-UVB) over 48 hours of exposure. 0hrs (white) is 35 DAS and is leaf area prior to commencement of illumination with UV-B, while 24hrs (light grey) is after 24 hours of exposure, 48hrs (dark grey) is after 48 hours of exposure. In the +UVB condition the plants are exposed to 0.5 µmol m^{-2} s^{-1} and 220 µmol m^{-2} s^{-1} of PAR, in the -UVB condition the plants are exposed to 220 µmol m^{-2} s^{-1} of PAR only. *rbf1-1 - ribosome-binding factor 1-1, rfb1-2 - ribosome-binding factor 1-2.* Error bars represent ± S.E. (n = 16 biological repeats). Asterisks indicate statistically significant means ($P < 0.05$) between time point and 0hr control for a treatment and genotype; ns indicates not significant means.

It is also of note that prior to UV-B exposure, the reduction of RBF1 does not affect green leaf area as both *rbf1* mutants have a similar green leaf area to wild type. As the green leaf area is the same in both wild type and *rbf1* mutants, this suggests that reduction of RBF1 does not limit plant growth. Fristedt et al. (2014) suggested that in mature leaves, the translationary machinery involved in chloroplast biogenesis catches up and the lower RBF1 levels are no longer limiting to the plant; which may explain the absence of the *rbf1* specific phenotype. The slowing of green leaf area development under UV-B in the mutants suggests that the addition of UV-B to the spectrum stresses the translationary machinery in the *rbf1* mutants, resulting in the limiting of green leaf development under prolonged exposure.

The impact of high fluence UV-B exposure (3 µmol m^{-2} s^{-1}) was also assessed over 5 days of exposure (Fig 6.3), to determine if the mutations altered plant viability in response to UV-B.

Viability was assessed through measuring of green leaf area over time as well survival rate of the plants at 5 days of high fluence UV-B exposure (Chapter 2: Materials and Methods).

The analysis showed that on Day 5 both *rbf1* mutants, *rbf1-1* and *rbf1-2*, exhibited a significant decrease in green leaf area in response to UV-B exposure compared Day 0 ($P < 0.01$; Fig 6.3). At Day 5 of UV-B *rbf1-1* showed a 14% decrease in green leaf area compared to Day 0 ($P < 0.001$; Fig 6.3); while *rbf1-2* showed an 18% decrease in green leaf area in the same comparison ($P < 0.001$; Fig 6.3). The decrease in leaf area suggests that in high fluence rate UV-B exposure has a negative impact of plant growth in the reduction of functional RBF1. This is further illustrated when comparing the changes in green leaf area in wild type and the mutants green leaf area continues to increase in response to UV-B exposure; as there was a 43% increase in green leaf area in wild type between Day 0 to Day 5 of UV-B ($P < 0.001$; Fig 6.3).

Not only was the green leaf area significantly reduced in mutants under UV-B compared to no UV-B; in comparison to wild type under UV-B at Day 5 both *rbf1* mutants showed 40% decrease in green leaf area ($P < 0.001$; Fig 6.3). Suggesting that high fluence UV-B exposure has a more detrimental effect on the *rbf1* mutants than it has on wild type. The decrease in green leaf area observed in both mutants suggests that the loss of RBF1 activity affects the plant's response to high fluence UV-B and that it may play a role in plant survival in response to high fluence UV-B. The higher fluence rate used is likely to further aggravate the negative impact on photosynthetic rate in the *rbf1* mutants; which is likely to have an impact on the viability of the mutants.

The effect of the reduced levels of RBF1 on green leaf area under high UV-B exposure is further illustrated when comparing differences in green leaf area between *uvr8-6* and *rbf1* mutants. When comparing the green leaf area of *rbf1-1* at Day 5 of UV-B exposure and *uvr8-6* at the same time point; there was only a 1% difference in area, with *rbf1-1* being 1% smaller than *uvr8-6* (Fig 6.3). However, *rfb1-2* 6% smaller than *uvr8-6* ($P < 0.01$; Fig 6.3) suggesting that the reduction of

RBF1 levels is more detrimental to the plant than the absence of UVR8 under high fluence UV-B.

Together both the changes in green leaf area in response to UV-B exposure in the mutants show that the reduction of RBF1 has a detrimental effect on the plant and its ability to cope with long-term exposure to UV-B; which further illustrates the importance of RBF1 in the plant's response to UV-B exposure.

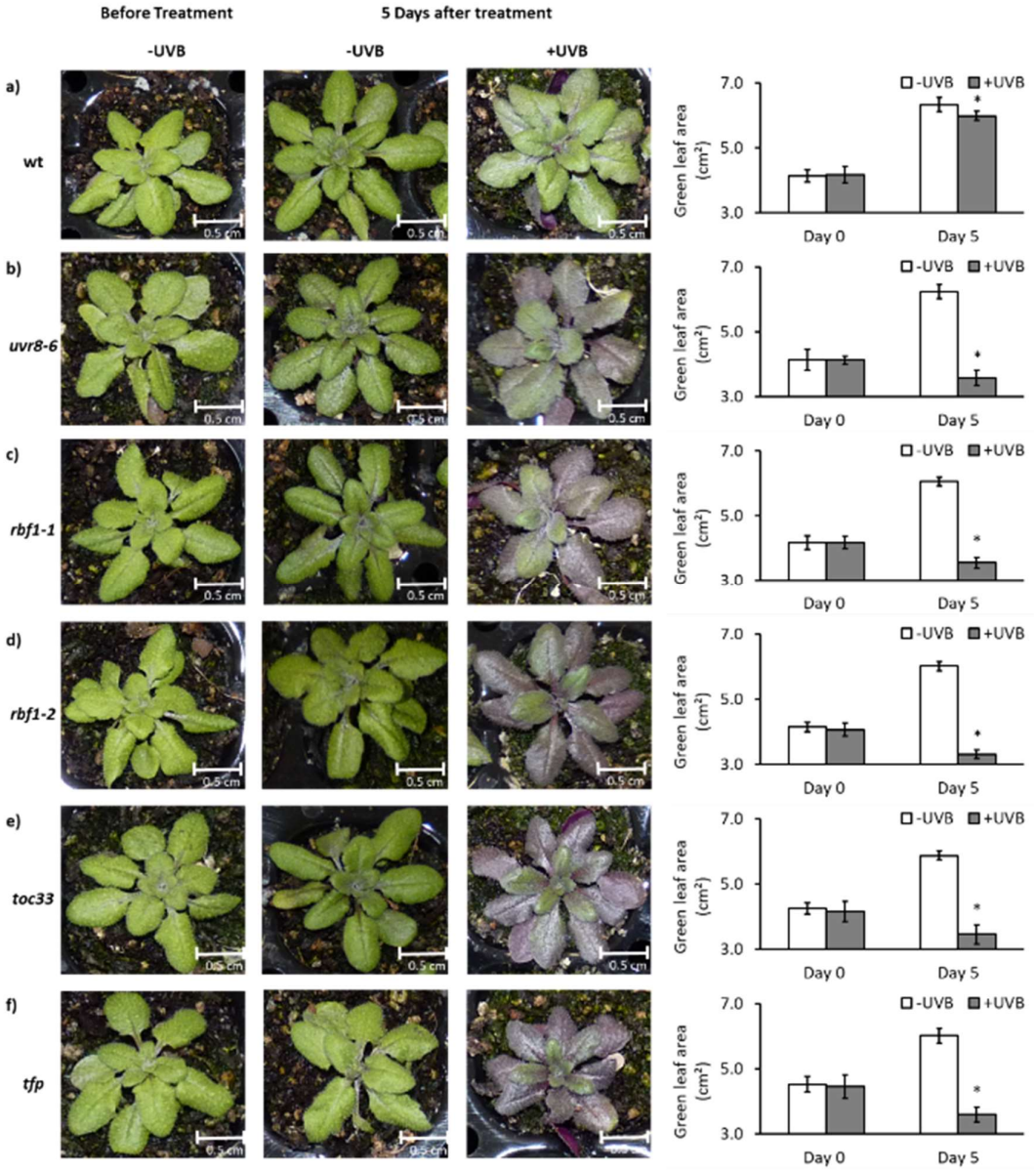

Figure 6.3 Changes in green leaf area in *wt* (Col-0) and various mutants in response to 3 µmol m^{-2} s^{-1} of UV-B (+UVB, grey) or without (-UVB, white) over 5 days of exposure. Day 0 is 21 DAS and is prior to commencement of illumination with UV-B, while Day 5 is 5 days after exposure. In the +UVB condition the plants are exposed to 3 µmol m^{-2} s^{-1} of UVB and 220 µmol m^{-2} s^{-1} of PAR, in the -UVB condition the plants are exposed to 220 µmol m^{-2} s^{-1} of PAR only. **a)** *wt* - Col-0, **b)** *uvr8-6* (Col) – *UV-B resistance locus 8-6* , **c)** *rbf1-1* (Col)- *ribosome-binding factor 1-1,* **d)** *rbf1-2* (Col) - *ribosome-binding factor 1-2,* **e)** *toc33* (Col) - *translocon at the outer envelope membrane of chloroplasts 33 ,* **f)** *tfp* (Col) - *thioredoxin family protein*. Error bars represent ± S.E. (n = 6 biological repeats). Asterisks indicate statistically significant means ($P < 0.05$) between +UVB and -UVB treatments for a given time point.

6.2.3 *RBF1* expression is upregulated at 6hrs UV-B exposure in Col-0

To determine if *RBF1* exhibits a similar expression pattern in Col-0 compared to L*er*; relative gene expression of *RBF1* was measured in Col-0 using qRT-PCR, under the same experimental conditions as used for the RNA-seq analysis (Chapter 2: Materials and Methods).

In response to initial UV-B exposure, *RBF1* expression is upregulated in wild type. At 6hrs of UV-B exposure relative expression of *RBF1* exhibited a 34% increase compared to 0hrs ($P < 0.03$, Fig 6.4a); as well as a significant increase at 6hrs +UVB compared to 6hrs –UVB ($P < 0.01$, Fig 6.4b). The increase in relative expression at 6hrs suggests that *RBF1* is upregulated in response to low fluence UV-B. Expression of *RBF1* decreased significantly between 6hrs and 24hrs of UV-B exposure ($P < 0.001$, Fig 6.4a); suggesting that the initial increase in expression is driven by UV-B, but UV-B exposure does not affect continued expression. The lack differential expression levels between 24hrs of UV-B and 0hrs (Fig 6.4a) further illustrates this as it suggests that under longer UV-B exposure *RBF1* is no longer upregulated. This pattern is similar to the expression pattern observed in L*er* through RNA-seq.

However, *RBF1* expression analysis in Col-0 revealed that in the absence of UV-B at 6hrs and 24hrs relative expression *RBF1* was significantly decreased compared to 0hrs ($P < 0.001$, Fig 6.4a). The cause of this decrease in expression is unknown. The lower levels of expression at 24hrs in the absence of UV-B may explain as to why there was significantly higher *RBF1* expression at 24hrs +UVB when compared to 24hrs –UVB ($P < 0.001$, Fig 6.3b). *RBF1* expression at 24hrs +UVB is higher than at 24hrs –UVB, which suggests that *RBF1* is still upregulated at 24hrs of UV-B exposure. But as the comparison to 0hrs shows the levels of expression at 24hrs of UV-B are the same as the levels observed pre-treatment, suggesting that UV-B does not, in fact, continue to regulated *RBF1* expression after the initial 6hrs period. However, to better understand if UV-B continues to regulate expression of *RBF1* after the initial 6hrs of exposure, expression at later time points would need to be measured.

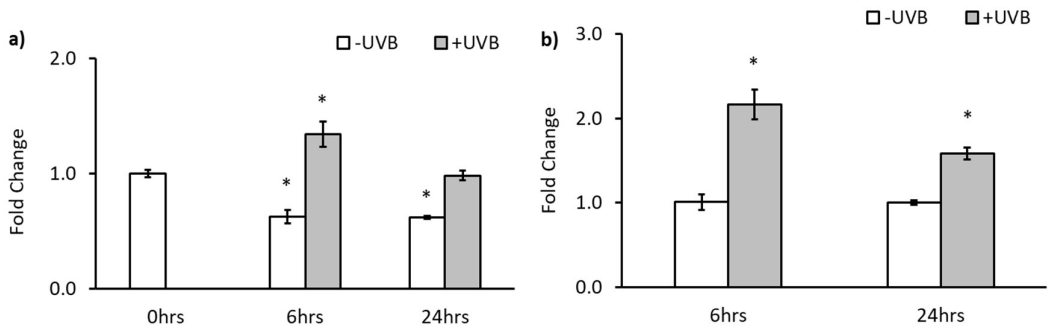

Figure 6.4 Changes in relative transcript levels of *RBF1* in *wt* (Col-0) in response to irradiation with 0.5 µmol m^{-2} s^{-1} of UV-B (+UVB, grey) or without (-UVB, white) over 24 hours of exposure. Relative transcript abundance (fold change) was determined by qRT-PCR and was normalised to control treatment using two internal reference genes *UBC9* and *AT2G32170*. 0hrs is 35 DAS and is prior to commencement of illumination with UV-B, while 6hrs is after 6 hours of exposure and so forth. In the +UVB condition the plants are exposed to 0.5 µmol m^{-2} s^{-1} and 220 µmol m^{-2} s^{-1} of PAR, in the -UVB condition the plants are exposed to 220 µmol m^{-2} s^{-1} of PAR only. RBF1 - RIBOSOME-BINDING FACTOR 1 (AT4G34730). Error bars represent ± S.E. (n = 3 biological repeats). **a)** Changes in relative transcript levels of *RBF1* in *wt* (Col-0) normalised to 0hrs control. Asterisks indicate statistically significant means ($P < 0.05$) and each following time point and treatment. **b)** Changes in relative transcript levels of *RBF1* in *wt* (Col-0) normalised to the -UVB control at 6hrs and 24hrs. Asterisks indicate statistically significant means ($P < 0.05$) between +UVB and -UVB treatments for a given time point.

6.2.4 *RBF1* expression in response to UV-B is lower in *uvr8-6* compared to wt

To determine if UVR8 plays a role in the regulation of *RBF1* expression in response to UV-B, relative expression was measured in *uvr8-6* in response to UV-B exposure using qRT-PCR (Chapter 2: Materials and Methods).

In the *uvr8* mutant, *uvr8-6,* relative expression of *RBF1* was not changed in response to UV-B exposure (Fig 6.4a). At 6hrs and 24hrs of UV-B composure compared to relative expression in *uvr8-6* at 0hrs showed no change, suggesting that UVR8 may regulate expression of *RBF1* in response to UV-B exposure; as hypothesised in Chapter 4.

When compared to expression in wild type at 0hrs (Fig 6.5b) and expression in wild type in the absence of UV-B (Table 6.1) no upregulation of *RBF1* in response to UV-B was observed in *uvr8-6*. At 0hrs expression of *RBF1* was significantly lower in *uvr8-6* than it was in Col-0 ($P < 0.01$; Fig 6.5b, Table 6.1) suggesting that UVR8 may mediate regulation of *RBF1* even in the absence of UV-B exposure. However, expression of *RBF1* decreased in *wt* in the absence of UV-B at 6hrs and 24hrs; and after the decrease in expression; levels of *RBF1* in wild type and *uvr8-6* were no

longer significantly different from each other (Table 6.1). The reason for the decrease of expression observed in wild type is unknown, hence one cannot conclude if UVR8 is involved in expression of *RBF1* in the absence of UV-B.

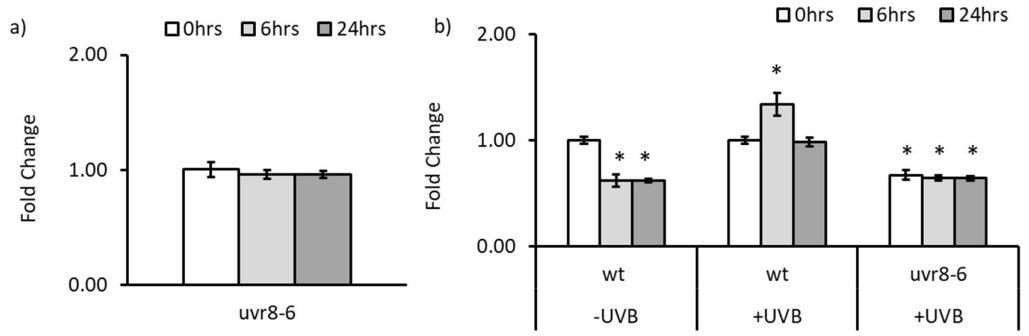

Figure 6.5 Changes in relative transcript levels of *RBF1* in *uvr8-6* (Col) in response to irradiation with 0.5µmol m^{-2} s^{-1} of UV-B (+UVB) over 24 hours of exposure. Relative transcript abundance (fold change) was determined by qRT-PCR and was normalised to control treatment using two internal reference genes *UBC9* and *AT2G32170*. 0hrs is 35 DAS and is prior to commencement of illumination with UV-B, while 6hrs is after 6 hours of exposure and so forth. In the +UVB condition the plants are exposed to 0.5 µmol m^{-2} s^{-1} and 220 µmol m^{-2} s^{-1} of PAR, in the -UVB condition the plants are exposed to 220 µmol m^{-2} s^{-1} of PAR only. RBF1 - RIBOSOME-BINDING FACTOR 1 (AT4G34730), *uvr8-6 – UV-B resistance locus 8 - 6*. Error bars represent ± S.E. (n = 3 biological repeats). **a)** Changes in relative transcript levels of *RBF1* in *uvr8-6* (Col) normalised to 0hrs as control; 0hrs (white), 6hrs (light grey) and 24hrs (dark grey). **b)** Changes in relative transcript levels of *RBF1* in *wt* (Col-0) and *uvr8-6* normalised to *wt* (Col-0) 0hrs. Asterisks indicate statistically significant means ($P < 0.05$) between *wt* 0hrs and the given treatment.

The decrease in *rbf1* expression observed in the RNA-seq in Chapter 4 between *uvr8-1* and L*er* is likely due to the lower expression of *RBF1* observed in the *uvr8* mutant under UV-B. Expression of *RBF1* in *uvr8-6* relative to *wt* 0hrs (Fig 6.5b) as well as relative to *wt* –UVB (Table 6.1) showed much lower expression in the mutant compared to expression in wild type under UV-B. The difference of expression further illustrates the role of UVR8 in regulating expression of *RBF1* in response to UV-B exposure.

Table 6.1 Changes in relative *RBF1* expression in *wt* (Col-0) and *uvr8-6* normalised to *wt* (Col-0) –UVB for each time point over 24hrs of 0.5 µmol m^{-2} s^{-1} UV-B exposure.

Genotype	Treatment	Time point		
		0hrs	6hrs	24hrs
wt (Col-0)	-UVB	1.00±0.03	1.01±0.09	1.00±0.03
wt (Col-0)	+UVB	1.00±0.03 NS	2.17±0.18 **	1.59±0.07 **
uvr8-6 (Col)	+UVB	0.67±0.04 **	1.04±0.04 NS	1.04±0.03 NS

*$P < 0.05$, **$P < 0.01$, ***$P < 0.001$, NS - not significant

6.2.5 Summary

Reduction of RBF1 levels downregulates photosynthetic function under low fluence UV-B, as well as green leaf area development. This suggests that RBF1 plays a key role in the UV-B dependent photosynthesis phenotype observed in wild type and that the increase in photosynthetic rate observed at 24hrs is partially due to increased chloroplast biogenesis. Furthermore, *RBF1* expression in Col-0 is upregulated in the presence of UV-B, and the most significant increase in expression is observed at 6hrs of UV-B exposure. However, it is unknown as to what caused the decrease in expression observed at 6hrs and 24hrs in the absence of UV-B compared to 0hrs, and further experimental work is required to determine the role of UV-B in regulating the expression of *RBF1* over time. Further expression analysis in *uvr8-6* has determined that UVR8 regulates the increase in *RBF1* expression in response to low fluence UV-B, and it may also be involved in *RBF1* expression in the absence of UV-B.

6.3 TOC33 - TRANSLOCON AT THE OUTER ENVELOPE MEMBRANE OF CHLOROPLASTS 33 (AT1G02280)

As most chloroplast proteins are nuclear-encoded, chloroplast biogenesis requires large-scale import of pre-proteins from the cytosol into the chloroplast (Viro and Kloppstech, 1980; Hiltbrunner et al., 2001). Protein import into the chloroplast is facilitated by the TOC (Translocon at the outer envelope membrane of chloroplasts) complex; made up of two homologous GTP-binding proteins (TOC33 and TOC159) and a channel protein (TOC75) (Hiltbrunner et al., 2001; Aronsson and Jarvis, 2011). TOC33 is one of the two isoforms of TOC34 present in *Arabidopsis* (Jarvis et al., 1998); first identified in *Pisum sativum* (Kubis et al., 2003; Ivanova et al., 2004). TOC33 is the key GTPase involved in the import of photosynthetic pre proteins into the chloroplast in *Arabidopsis*, whereas TOC34 is involved in the import of non-photosynthetic pre proteins (Bauer et al., 2000; Kubis et al., 2003; Hiltbrunner et al., 2004; Ivanova et al., 2004; Smith et al., 2004).

The most well-known *toc33* mutant is *ppi1* (*plastid protein import 1*) (Jarvis et al., 1998). *ppi1* presents as pale green seedlings due to being chlorophyll deficient due to limited chloroplast biogenesis (Jarvis et al., 1998; Hiltbrunner et al., 2004). *ppi1* has been shown to be deficient in photosynthetic proteins (Jarvis et al., 1998; Bauer et al., 2000; Kubis et al., 2003; Smith et al., 2004). However, the pale green phenotype is lost in mature plants (Jarvis et al., 1998).

The impact of UV-B exposure on *TOC33* expression has not been studied, and no interactions between *TOC33,* UV-B exposure, and photosynthesis have been characterised. As the *toc33* mutant shows reduced levels of chlorophyll in early development, this suggests that the rate of photosynthesis may be affected in young plants. However, as the pale green phenotype is lost in mature leaves (Jarvis et al., 1998), the import machinery in mature leaves is less affected by the absence of TOC33, and hence the impact of UV-B on the photosynthetic rate of *toc33* is expected to be minimal.

6.3.1 UV-B dependent photosynthesis phenotype is lost in the absence of TOC33

Photosynthetic rate for *toc33* was determined in the same manner as for the *rbf1* mutants (Chapter 2: Materials and Methods).

In the absence of TOC33, the increase in photosynthetic rate observed in wild type at 24hrs is absent. At 24hrs, there was no significant increase in photosynthetic rate between +UVB and -UVB in *toc33* plants (Fig 6.6). The absence of the UV-B dependent increase in photosynthetic rate in *toc33* suggests that TOC33 is required for the increase in photosynthetic rate in response to UV-B. At 48hrs of UV-B exposure, there was no significant decrease in photosynthetic rate between +UVB and –UVB (Fig 6.6), suggesting that the absence of TOC33 does not affect photosynthetic function in response to longer-term UV-B exposure.

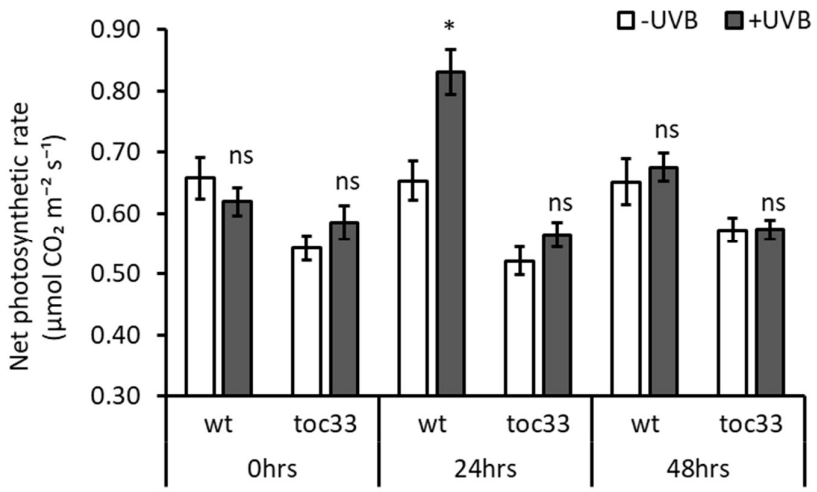

Figure 6.6 Changes in net photosynthetic rate (µmol CO_2 m^{-2} s^{-1}) normalised to leaf area in *wt* (Col-0) and *toc33* (Col) in response to irradiation with 0.5 µmol m^{-2} s^{-1} of UV-B (+UVB, grey) or without (-UVB, white) over 48 hours of exposure. 0hrs is 35 DAS and is the net photosynthetic rate prior to commencement of illumination with UV-B, while 24hrs is after 24 hours of exposure and so forth. In the +UVB condition the plants are exposed to 0.5 µmol m^{-2} s^{-1} and 220 µmol m^{-2} s^{-1} of PAR, in the –UVB condition the plants are exposed to 220 µmol m^{-2} s^{-1} of PAR only. *toc33 - translocon at the outer envelope membrane of chloroplasts 33*. Error bars represent ± S.E. (n = 16 biological repeats). Asterisks indicate statistically significant means ($P < 0.05$) between +UVB and -UVB treatments for a given time point and genotype; ns indicates not significant means.

Interestingly, net photosynthetic rate of *toc33* was significantly lower than wild type both in the absence and presence of UV-B (Fig 6.6). At 0hrs, the photosynthetic rate of *toc33* was 12% lower than that of the wild type ($P < 0.01$; Fig 6.6); and in the absence of UV-B, the photosynthetic rate was continuously lower in *toc33* compared to wild type. The significantly lower photosynthetic rate observed in *toc33* suggests that the absence of TOC33 affects the chloroplast import machinery sufficiently to reduce photosynthetic rate even in mature plants. However, the loss of *TOC33* does not have a detrimental impact on photosynthetic rate under UV-B. Hence, while the chloroplast import machinery is affected in *toc33* resulting in a lower photosynthetic rate, UV-B exposure does not further reduce photosynthetic rate in *toc33.* As the photosynthesis phenotype is absent in *toc33,* it suggests that UV-B may induce increased chloroplast biogenesis resulting in the photosynthesis phenotype.

Much like the phenotype observed in wild type at 48hrs, there was no negative impact on photosynthetic rate in *toc33* over longer exposure; as the rate of photosynthesis stayed the same in the presence and absence of UV-B at 48hrs. This suggests that TOC33 is not required for maintaining photosynthetic competency under prolonged UV-B exposure, unlike UVR8 and RBF1, both of which are required for the UV-B-photosynthesis phenotype.

6.3.2 *toc33* exhibits reduced green leaf area development under UV-B exposure

Although the photosynthetic rate is lower in *toc33* even in the absence of UV-B, green leaf area was not significantly smaller than wild type (Fig 6.7). Thus suggesting that the lower photosynthetic rate is not due to a lower green leaf area.

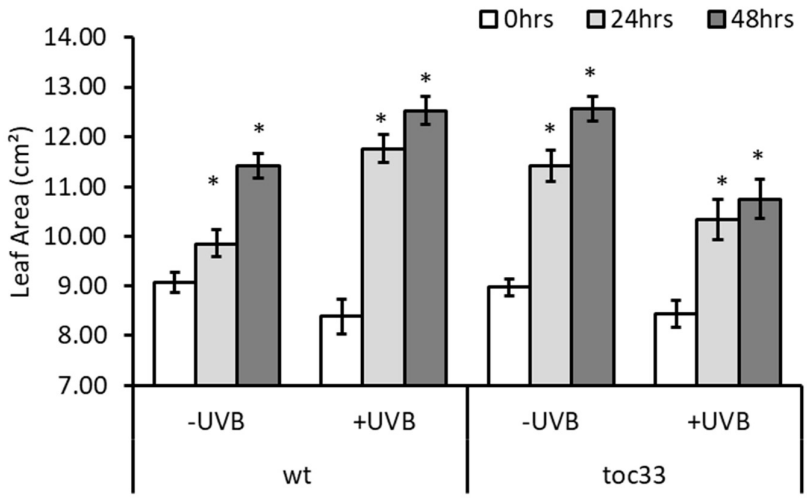

Figure 6.7 Changes green leaf area (cm²) in *wt* (Col-0) and *toc33* (Col) in response to irradiation with 0.5 µmol m^{-2} s^{-1} of UV-B (+UVB) or without (-UVB) over 48 hours of exposure. 0hrs (white) is 35 DAS and is leaf area prior to commencement of illumination with UV-B, while 24hrs (light grey) is after 24 hours of exposure, 48hrs (dark grey) is after 48 hours of exposure. In the +UVB condition the plants are exposed to 0.5 µmol m^{-2} s^{-1} and 220 µmol m^{-2} s^{-1} of PAR, in the -UVB condition the plants are exposed to 220 µmol m^{-2} s^{-1} of PAR only. *toc33* - *translocon at the outer envelope membrane of chloroplasts 33*. Error bars represent ± S.E. (n = 16 biological repeats). Asterisks indicate statistically significant means ($P < 0.05$) between time point and 0hr control for a treatment and genotype; ns indicates not significant means

It is only after the beginning of UV-B exposure that changes in green leaf area development were observed. At 24hrs of UV-B exposure *toc33* had a 12% smaller green leaf area than wild type ($P < 0.001$; Fig 6.7); and at 48hrs of UV-B *toc33* was 14% smaller than wild type ($P < 0.001$; Fig 6.7). The difference in green leaf area suggests that the presence of UV-B limits green leaf area

development, but that the fluence rate supplied does not result in damage to the plant by 48hrs of exposure.

Under UV-B exposure, *toc33* showed a slower increase in green leaf area development than in the absence of UV-B (Fig 6.7). Under UV-B exposure green leaf area increased by 10% between 0hrs and 24hrs ($P < 0.001$, Fig 6.7), whereas in the absence of UV-B green leaf area increased by 27% ($P < 0.001$, Fig 6.2). This difference in green leaf area shows that in the presence of UV-B green leaf area development in *toc33* is impaired. This suggests that in the presence of UV-B and the absence of TOC33, import of photosynthetic proteins is affected and the plant undergoes stress as a consequence. Furthermore, the rate of green leaf area development slows over time under UV-B exposure. While there was a significant increase in green leaf area between 0hrs and 24hrs UV-B ($P < 0.001$, Fig 6.7); the rate of increase slowed between 24hrs and 48hrs of UV-B exposure, as between the two there was only a 2% increase in green leaf area ($P < 0.001$, Fig 6.7). The slowing of green leaf area development suggests that over prolonged UV-B exposure, the absence of TOC33 limits the development of green leaf area; which may be due to stress.

Under high fluence UV-B (3 µmol m^{-2} s^{-1}) green leaf area of *toc33* decreased over the 5 days of exposure (Fig 6.3). At Day 5 of UV-B exposure green leaf area of *toc33* was 17% smaller compared to Day 0 ($P < 0.001$, Fig 6.3) and 41% smaller at Day 5 of UV-B exposure compared to no UV-B ($P < 0.001$, Fig 6.3). The decrease in green leaf area under UV-B exposure suggests that the loss of TOC33 results in the plant being more susceptible to damage by high UV-B fluence rates. This is further illustrated by the differences in green leaf area of *toc33* relative to wild type; as prior to UV-B exposure *wt* and *toc33* do not differ significantly in terms of green leaf area as well as there being no difference in the absence of UV-B, but at Day 5 of UV-B *toc33* is 42% smaller than *wt* ($P < 0.001$, Fig 6.3).

The effect of the loss of TOC33 on green leaf area under high UV-B exposure is also evident when comparing differences in green leaf area between *uvr8-6* and *toc33*. In terms of green leaf area,

toc33 was 3% smaller than *uvr8-6* ($P < 0.05$; Fig 6.3) suggesting that the loss of TOC33 is more detrimental to the plant than the absence of UVR8 under high fluence UV-B.

The changes in green leaf area in response to UV-B exposure highlight the different responses of *toc33* under different fluence rates of UV-B. Under low fluence rate UV-B, green leaf area development slows but continues, while under high fluence UV-B green leaf area decreases; suggesting that the mutant is more susceptible to damage under high fluence and that the absence of TOC33 only has a detrimental impact over longer exposure times at high fluence rates.

6.3.3 Low fluence UV-B increases *TOC33* expression in Col-0 at 6hrs and 24hrs

qRT-PCR confirmed the TOC33 response to UV-B, observed in L*er*, in Col-0, and showed that in response to UV-B exposure TOC33 was upregulated at 6hrs. qRT-PCR analysis showed that between 0hrs and 6hrs of UV-B exposure there was a 36% increase in relative expression ($P < 0.001$, Fig 6.8a), as well as being a 96% increase in relative expression at 6hrs +UVB compared to 6hrs –UVB ($P < 0.001$, Fig 6.8b). This response is similar to the response observed in the RNA-seq.

Of interest is that relative expression of TOC33 at 24hrs of UV-B exposure, as when compared to 0hrs *TOC33* expression was still significantly upregulated at 24hrs of UV-B exposure ($P < 0.001$, Fig 6.8a). The continued upregulation was not observed in the RNA-seq results. However, when comparing expression levels at 24hrs +UVB and –UVB there was no evidence of upregulation, which suggests that the continued upregulation may not be a result of the sustained exposures to UV-B, but rather suggests that there are as of yet unidentified factors inducing *TOC33* expression. This is further illustrated by the significant increase in relative expression observed at 24hrs –UVB compared to 0hrs ($P < 0.001$, Fig 6.8a). The upregulation of *TOC33* in the absence of UV-B further suggests that regulation of *TOC33* may not be solely due to the presence of UV-B and that there may be other factors involved.

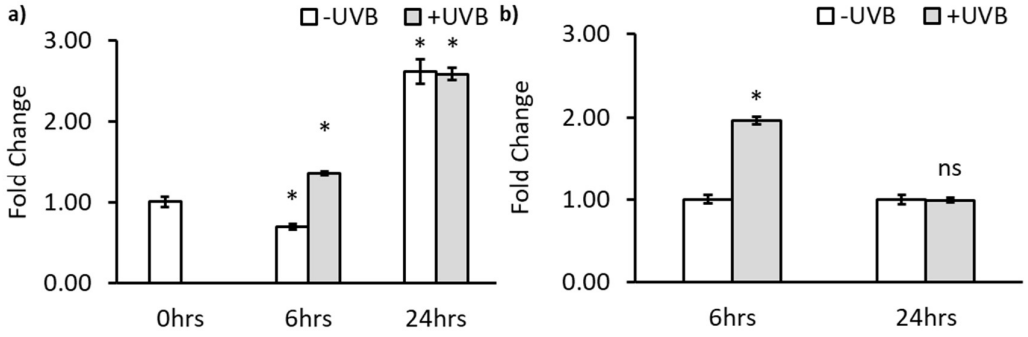

Figure 6.8 Changes in relative transcript levels of *TOC33* in *wt* (Col-0) in response to irradiation with 0.5 µmol m^{-2} s^{-1} of UV-B (+UVB, grey) or without (-UVB, white) over 24 hours of exposure. Relative transcript abundance (fold change) was determined by qRT-PCR and was normalised to control treatment using two internal reference genes *UBC9* and *AT2G32170*. 0hrs is 35 DAS and is prior to commencement of illumination with UV-B, while 6hrs is after 6 hours of exposure and so forth. In the +UVB condition the plants are exposed to 0.5 µmol m^{-2} s^{-1} and 220 µmol m^{-2} s^{-1} of PAR, in the -UVB condition the plants are exposed to 220 µmol m^{-2} s^{-1} of PAR only. TOC33 - TRANSLOCON AT THE OUTER ENVELOPE MEMBRANE OF CHLOROPLASTS 33 (AT1G02280). Error bars represent ± S.E. (n = 3 biological repeats). **a)** Changes in relative transcript levels of *TOC33* in *wt* (Col-0) normalised to 0hrs control. Asterisks indicate statistically significant means ($P < 0.05$) between 0hr control and each following time point and treatment. **b)** Changes in relative transcript levels of *TOC33* in *wt* (Col-0) normalised to the -UVB control at 6hrs and 24hrs. Asterisks indicate statistically significant means ($P < 0.05$) between +UVB and -UVB treatments for a given time point and genotype; ns indicates not significant means.

Relative expression of *TOC33* was reduced at 6hrs –UVB compared to 0hrs ($P < 0.001$, Fig 6.8a); which suggests that other factors may be involved in the regulation of *TOC33*. However, as there was a significant increase in relative expression between 0hrs and 6hrs +UVB, as well as 6hrs –UVB and 6hrs +UVB, UV-B may upregulate the expression of TOC33 initially, and any changes in expression are due to other factors regulating expression.

6.3.4 *TOC33* expression is lower in *uvr8-6* under UV-B compared to *wt*

In *uvr8-6* the upregulation of relative expression of *TOC33,* observed in wild type at 6hrs of UV-B exposure, was absent (Fig 6.9a). In *uvr8-6* relative expression of *TOC33* was significantly lower at 24hrs of UV-B exposure compared to 0hrs ($P < 0.001$, Fig 6.9a). Furthermore, in *uvr8-6* relative expression of *TOC33* was 85% lower at 24hrs +UVB compared to *wt* 24hrs +UVB ($P < 0.01$, Table 6.2). The decrease in expression is the opposite of the response observed in wild type where relative expression increased significantly at 6hrs +UVB compared to –UVB, and increased even further at 24hrs of UV-B. The absence of the response in *uvr8-6* plus the decrease in relative

expression at 24hrs +UVB suggests that UVR8 is involved in the regulation of *TOC33* under UV-B exposure.

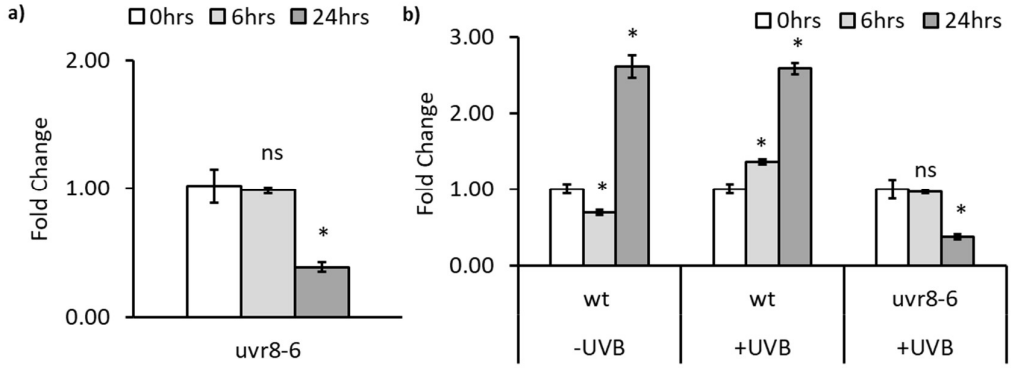

Figure 6.9 Changes in relative transcript levels of *TOC33* in *uvr8-6* (Col) response to irradiation with 0.5 µmol m^{-2} s^{-1} of UV-B (+UVB) over 24 hours of exposure. Relative transcript abundance (fold change) was determined by qRT-PCR and was normalised to control treatment using two internal reference genes *UBC9* and *AT2G32170*. 0hrs is 35 DAS and is prior to commencement of illumination with UV-B, while 6hrs is after 6 hours of exposure and so forth. In the +UVB condition the plants are exposed to 0.5 µmol m^{-2} s^{-1} and 220 µmol m^{-2} s^{-1} of PAR, in the -UVB condition the plants are exposed to 220 µmol m^{-2} s^{-1} of PAR only. TOC33 - TRANSLOCON AT THE OUTER ENVELOPE MEMBRANE OF CHLOROPLASTS 33 (AT1G02280), *uvr8-6 – UV-B resistance locus 8-6*. Error bars represent ± S.E. (n = 3 biological repeats). **a)** Changes in relative transcript levels of *TOC33* in *uvr8-6* (Col) normalised to 0hrs as control; 0hrs (white), 6hrs (light grey) and 24hrs (dark grey). Asterisks indicate statistically significant means ($P < 0.05$) between treatment and 0hr control; ns indicates not significant means. **b)** Changes in relative *TOC33* expression *wt* (Col-0) and *uvr8-6* normalised to *wt* (Col-0) 0hrs. Asterisks indicate statistically significant means ($P < 0.05$) between *wt* 0hrs and the given treatment; ns indicates not significant means.

As the initial upregulation at 6hrs is absent, as well as the upregulation at 24hrs, UVR8 plays a role in the expression of *TOC33* in response to UV-B exposure. It is unlikely that UVR8 regulates expression of *TOC33* in the absence of UV-B as expression levels do not differ prior to UV-B exposure (Table 6.2, Fig 6.9b). However, it is worth noting that at 24hrs of UV-B the upregulation of expression observed in *wt* in both –UVB and +UVB conditions is absent in *uvr8-6* which may suggest that UVR8 plays are a role in *TOC33* expression even in the absence of UV-B. It may also be that the absence of UVR8 results a stressed plant, which leads to further downregulation of *TOC33* at 24hrs of UV-B. To better determine what occurs in terms of expression, one would have to observe *TOC33* expression in *uvr8-6* in the absence of UV-B.

Table 6.2 Changes in relative TOC33 expression in *wt* (Col-0) and uvr8-6 normalised to *wt* (Col-0) –UVB for each time point over 24hrs of 0.5 µmol m^{-2} s^{-1} UV-B exposure.

Genotype	Treatment	Time point		
		0hrs	6hrs	24hrs
wt (Col-0)	-UVB	1.00±0.06	1.00±0.05	1.00±0.06
wt (Col-0)	+UVB	1.00±0.06	1.96±0.04 ***	0.99±0.03 NS
uvr8-6 (Col)	+UVB	1.00±0.13 NS	1.39±0.04 **	0.15±0.01 ***

*$P < 0.05$, **$P < 0.01$, ***$P < 0.001$, NS - not significant

6.4 Summary

In the *TOC33* mutant, the photosynthesis phenotype observed in wild type in response to UV-B is absent. In fact, the presence of UV-B does not have an effect on photosynthetic rate over the 48hrs measured, but the photosynthetic rate of *toc33* is significantly lower than wild type even in the absence of UV-B, suggesting that *TOC33* plays an important role in maintaining photosynthetic efficiency. However, even though *toc33* has a lower photosynthetic rate than wild type in the absence of UV-B, there are no discernible differences in terms of green leaf area under the same conditions. Under UV-B exposure, increases in green leaf area are limited in *toc33* compared to no UV-B as well as wild type under UV-B, suggesting that plant development under UV-B exposure is affected in the mutant. The decrease in green leaf area observed in *toc33* under high fluence UV-B further illustrates this, as the rate of leaf area development decreases in *toc33* is much more than the rate of decrease observed in wild type and *uvr8-6*, suggesting that TOC33 plays a role in maintaining green leaf area under UV-B exposure.

qRT-PCR analysis confirmed the RNA-seq results which showed the upregulation of *TOC33* at 6hrs of UV-B exposure in wild type, as well as the absence of upregulation at 24hrs +UVB compared to –UVB. However, the analysis also showed that there is a lot of variation in *TOC33* expression over 24hrs in the absence of UV-B exposure. The variation in relative expression suggests that the initial upregulation in expression is driven by UV-B exposure, but the further upregulation observed is due to the cyclical nature of *TOC33* expression. The qRT-PCR analysis also showed that UVR8 is likely involved in the upregulation of *TOC33* at 6hrs of UV-B as well as

the playing a role in the regulation of *TOC33* after the initial period of upregulation, and hence may be involved in the regulation of *TOC33* expression in the absence of UV-B.

6.5 TFP - THIOREDOXIN FAMILY PROTEIN (AT1G52990)

TFP encodes a putative chloroplastic thioredoxin, with no orthologues in any other plants (Meyer et al., 2006). TFP has not been well characterised, and little is understood regarding function. It is known to encode a thioredoxin with a WCGPC redox site and has a large N-terminal extension of unknown function (Meyer et al., 2006). The WCGPC redox site is highly conserved and has two redox-active Cys residues (Holmgren, 1989), and is able to reduce the disulphide bridges in target proteins (Collet and Messens, 2010).

Chloroplasts contain a large variety of thioredoxins, which are involved in the regulatory ferredoxin/thioredoxin system that is associated with oxygenic photosynthesis and light (Schürmann and Buchanan, 2001; Schürmann and Buchanan, 2008). Studies have shown that a number of chloroplastic thioredoxins are involved in photosynthetic electron transport, as they catalyse the light-dependent reduction of target enzymes (Trost et al., 2006; Schürmann and Buchanan, 2008; Naranjo et al., 2016). Due to the large variety of thioredoxins present, they are involved in many different processes in the chloroplast; from chloroplast biogenesis, gene expression to photosynthesis; illustrating the vital role thioredoxins play in the chloroplast (Gelhaye et al., 2005; Schürmann and Buchanan, 2008; Geigenberger and Fernie, 2014; Nikkanen and Rintamäki, 2014; Brzezowski et al., 2015; Rouhier et al., 2015; Nikkanen et al., 2017). However, as so little is known about TFP; little can be said about what its role is in photosynthesis or the UV-B response. The RNA-seq experiment performed in Chapter 4 showed for the first time that TFP was upregulated in response to UV-B, and hence little is known about its role in the UV-B dependent photosynthesis phenotype observed in wild type.

In order to further study the role of TFP in the photosynthesis phenotype, the *tfp* knockout line SALK_009687C was selected, as it was in a Columbia background and homozygosity could be confirmed through PCR.

6.5.1 UV-B dependent photosynthesis phenotype is lost in the absence of *TFP*

Photosynthetic rate for *tfp* was determined in the same manner as for the *rbf1* mutants (Chapter 2: Materials and Methods).

In the *tfp* mutant, the UV-B dependent increase in photosynthetic rate seen at 24hrs in the wild type was absent (Fig 6.10). There was no significant difference in photosynthetic rate in *tfp* at 24hrs between +UVB and –UVB; which indicates that TFP is required for the upregulation of photosynthesis at 24hrs. When comparing *tfp* at 0hrs and 24hrs of UV-B, there was also no significant increase in rate. However, there was a significant decrease in photosynthetic rate at 48hrs +UVB in *tfp* compared to -UVB ($P < 0.001$, Fig 6.10). At 48hrs the photosynthetic rate of *tfp* under +UVB was 33% lower compared to –UVB ($P < 0.001$, Fig 6.10), and it was also 36% lower than the photosynthetic rate of *tfp* at 24hrs +UVB ($P < 0.001$, Fig 6.10).

At 48hrs of UV-B exposure, the photosynthetic rate was also 24% lower than at 0hrs ($P < 0.001$, Fig 6.10). The decrease in photosynthetic rate at 48hrs showed that chronic exposure to UV-B has a higher impact on the photosynthetic rate in *tfp*; which illustrates the importance of TFP under UV-B stress. Because there was no difference in photosynthetic rate prior to UV-B exposure, this suggests that TFP is not required for photosynthetic function unless the plant is stressed, in addition to the requirement of TFP for the UV-B dependent increase in photosynthetic rate seen in wild type at 24hrs.

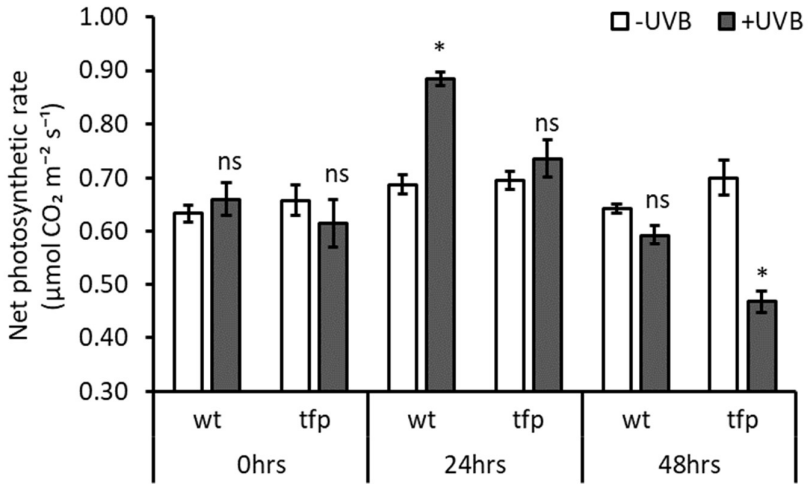

Figure 6.10 Changes in net photosynthetic rate (µmol CO_2 m^{-2} s^{-1}) normalised to leaf area in *wt* (Col-0) and *tfp* (Col) in response to irradiation with 0.5 µmol m^{-2} s^{-1} of UV-B (+UVB, grey) or without (-UVB, white) over 48 hours of exposure. 0hrs 35 DAS and is the net photosynthetic rate prior to commencement of illumination with UV-B, while 24hrs is after 24 hours of exposure and so forth. In the +UVB condition the plants are exposed to 0.5 µmol m^{-2} s^{-1} and 220 µmol m^{-2} s^{-1} of PAR, in the -UVB condition the plants are exposed to 220µmol m^{-2} s^{-1} of PAR only. *tfp - thioredoxin family protein*. Error bars represent ± S.E. (n = 16 biological repeats). Asterisks indicate statistically significant means ($P < 0.05$) between +UVB and -UVB treatments for a given time point and genotype; ns indicates not significant means.

It is also worth noting that the decrease in photosynthetic rate observed in *tfp* at 48hrs of UV-B was much larger than the decrease in rate observed in *uvr8-6.* At 48hrs of UV-B the photosynthetic rate of *uvr8-6* was 12% lower compared to no UV-B ($P < 0.01$, Fig 9.3), whereas the rate in *tfp* showed a 33% reduction for the same comparison. This difference in magnitude of reduction suggests that the absence of TFP is more detrimental to photosynthetic efficiency under UV-B than is the absence of UVR8.

6.5.2 Green leaf area development is limited in the *tfp* mutant

The increase in green leaf area development is limited in *tfp*. In the absence of UV-B green leaf area increased in *tfp*; by 31% ($P < 0.001$, Fig 6.11) between 0hrs and 24hrs, and by another 12% between 24hrs and 48hrs ($P < 0.001$, Fig 6.11). However, under UV-B exposure, green leaf area increased by 20% between 0hrs and 24hrs ($P < 0.001$, Fig 6.11), while there was no observable increase in green leaf area between 24hrs and 48hrs. As green leaf area did not increase between 24hrs and 48hrs, it suggests that longer exposure to UV-B limits growth in the *tfp*

mutant; which works in tandem with the significant decrease in photosynthetic rate at 48hrs of UV-B suggesting that *tfp* is more susceptible to damage under prolonged exposure to UV-B.

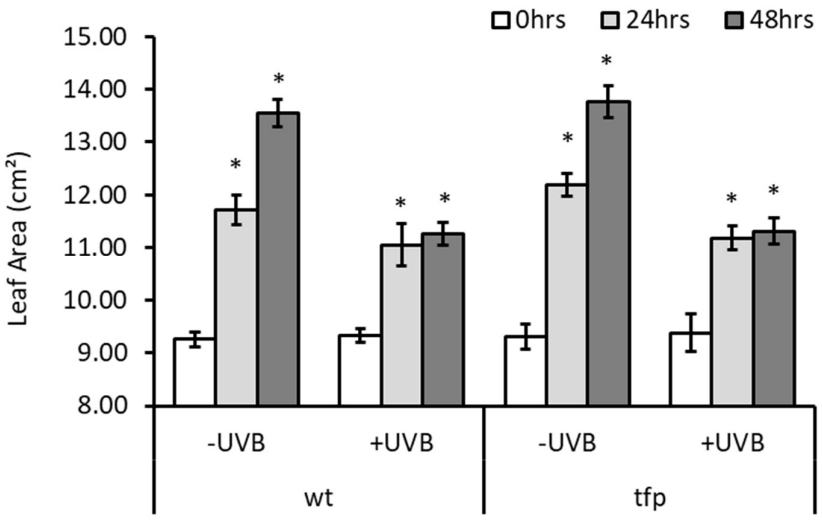

Figure 6.11 Changes in green leaf area (cm²) in *wt* (Col-0) and *tfp* (Col) in response to irradiation with 0.5 µmol m^{-2} s^{-1} of UV-B (+UVB) or without (-UVB) over 48 hours of exposure. 0hrs (white) 35 DAS and is leaf area prior to illumination with UV-B, while 24hrs (light grey) is after 24 hours of exposure, 48hrs (dark grey) is after 48 hours of exposure. In the +UVB condition the plants are exposed to 0.5 µmol m^{-2} s^{-1} and 220 µmol m^{-2} s^{-1} of PAR, in the –UV-B condition the plants are exposed to 220 µmol m^{-2} s^{-1} of PAR only. *tfp* - *thioredoxin family protein*. Error bars represent ± S.E. (n = 16 biological repeats). Asterisks indicate statistically significant means ($P < 0.05$) between time point and 0hr control for a treatment and genotype.

Under high fluence UV-B (3µmol m^{-2} s^{-1}) green leaf area development is adversely affected in *tfp* over 5 days of UV-B exposure. Under –UVB conditions green leaf area of *tfp* increased by 33% between Day 0 and Day 5 ($P < 0.001$, Fig 6.3); whereas under UV-B green leaf decreased by 19% between Day 0 and Day 5 ($P < 0.001$, Fig 6.3). The impact of high fluence UV-B on *tfp* is further illustrated by the difference in area at Day 5 +UVB compared to –UVB; as the mutant was 40% smaller under +UVB compared to –UVB ($P < 0.01$, Fig 6.3). Whereas the decrease in wild type under +UVB was only 5% ($P < 0.001$, Fig 6.3).

Interestingly there was no significant difference in green leaf area between *uvr8-6* and *tfp*, which suggests that there under high fluence UV-B the absence of either protein has a similar effect on green leaf area development.

6.5.3 Low fluence UV-B increases *TFP* expression in Col-0 at 6hrs

The qRT-PCR analysis confirmed the *TFP* expression pattern observed in RNA-seq and showed that in response to UV-B exposure *TFP* is significantly upregulated at 6hrs. At 6hrs of UV-B exposure, there was a 232% increase in expression compared to 0hrs ($P < 0.001$, Fig 6.12a); and there was a 237% increase at 6hrs +UVB compared to 6hrs –UVB ($P < 0.001$, Fig 6.12b). As relative expression of *TFP* does not increase between 0hrs and 6hrs –UVB; the increase of expression observed under +UVB conditions suggests that UV-B drives the upregulation of *TFP*.

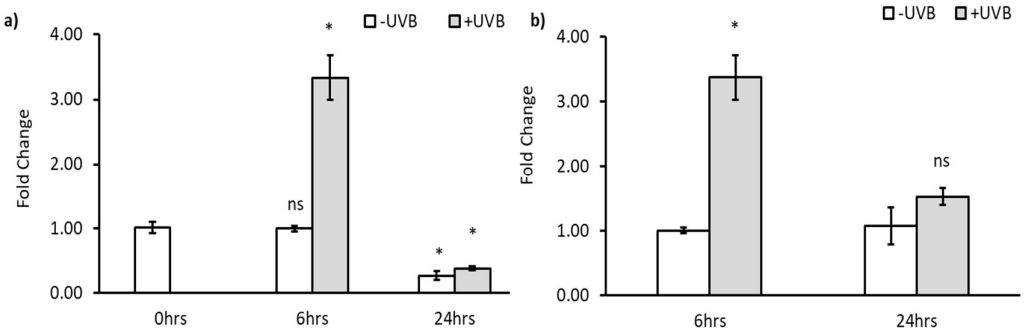

Figure 6.12 Changes in relative transcript levels of *TFP* in *wt* (Col-0) in response to irradiation with 0.5 µmol m^{-2} s^{-1} of UV-B (+UVB, grey) or without (-UVB, white) over 24 hours of exposure. Relative transcript abundance (fold change) was determined by qRT-PCR and was normalised to control treatment using two internal reference genes *UBC9* and *AT2G32170*. 0hrs is 35 DAS and is prior to commencement of illumination with UV-B, while 6hrs is after 6 hours of exposure and so forth. In the +UVB condition the plants are exposed to 0.5 µmol m^{-2} s^{-1} and 220 µmol m^{-2} s^{-1} of PAR, in the -UVB condition the plants are exposed to 220µmol m^{-2} s^{-1} of PAR only. TFP – THIOREDOXIN FAMILY PROTEIN (AT1G52990). Error bars represent ± S.E. (n = 3 biological repeats). **a)** Changes in relative transcript levels of *TFP* in *wt* (Col-0) normalised to 0hrs control. Asterisks indicate statistically significant means ($P < 0.05$) between treatment and 0hr control; ns indicates not significant means. **b)** Changes in relative transcript levels of *TFP* in *wt* (Col-0) normalised to the -UVB control at 6hrs and 24hrs. Asterisks indicate statistically significant means ($P < 0.05$) between +UVB and -UVB treatments for a given time point; ns indicates not significant means.

However, at 24hrs relative expression of *TFP* decreases in both –UVB and +UVB conditions. At 24hrs –UVB relative expression was decreased by 74% ($P < 0.01$, Fig 6.12a) compared to 0hrs, and in +UVB conditions, expression decreased 63% compared to 0hrs ($P < 0.01$, Fig 6.12a). As the downregulation is observed under both conditions, this suggests that the decrease is not due to UV-B exposure, but rather that expression decreases over time. This is further illustrated by the fact that there is no significant difference in expression between +UVB and -UVB at 24hrs

(Fig 6.12b); which shows that the presence of UV-B does not affect *TFP* expression after the initial up regulatory phase

The decrease in relative expression at 24hrs both in the presence and absence of UV-B suggests that there *TFP* is also regulated by other factors and not just the UV-B exposure. However, it is unknown as to what these factors may be, and further analysis would have to be undertaken to developing a better understanding of the regulation and expression of *TFP.*

6.5.4 Under low fluence UV-B *TFP* expression is lower in *uvr8-6*

In *uvr8-6* the upregulation observed in wild type at 6hrs of UV-B exposure was absent. At 6hrs of UV-B there is no significant increase in *TFP* expression compared to 0hrs (Fig 6.13a). The absence of the increased expression suggests that UVR8 is involved in the initial upregulation of *TFP* in response to UV-B exposure.

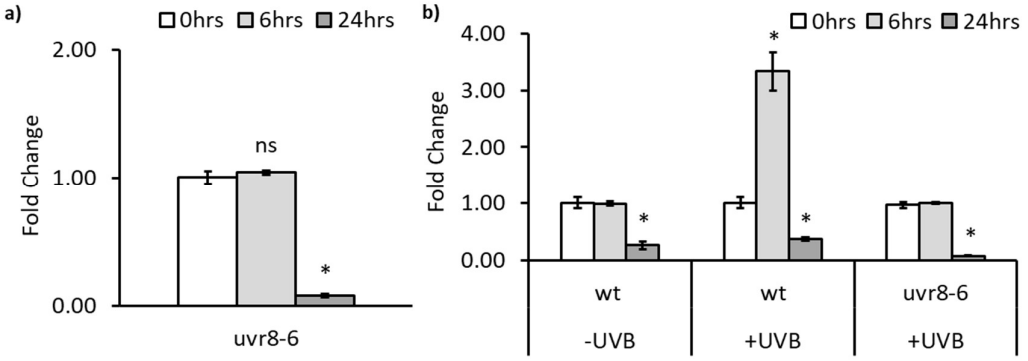

Figure 6.13 Changes in relative transcript levels of *TFP* in *uvr8-6* (Col) in response to irradiation with 0.5 µmol m^{-2} s^{-1} of UV-B (+UVB) over 24 hours of exposure. Relative transcript abundance (fold change) was determined by qRT-PCR and was normalised to control treatment using two internal reference genes *UBC9* and *AT2G32170*. 0hrs is 35 DAS and is prior to commencement of illumination with UV-B, while 6hrs is after 6 hours of exposure and so forth. In the +UVB condition the plants are exposed to 0.5 µmol m^{-2} s^{-1} and 220 µmol m^{-2} s^{-1} of PAR, in the -UVB condition the plants are exposed to 220 µmol m^{-2} s^{-1} of PAR only. TFP - THIOREDOXIN FAMILY PROTEIN (AT1G52990), *uvr8-6 – UV-B resistance locus 8-6.* Error bars represent ± S.E. (n = 3 biological repeats). **a)** Changes in relative transcript levels of *TFP* in *uvr8-6* (Col) normalised to 0hrs as control; 0hrs (white), 6hrs (light grey) and 24hrs (dark grey). Asterisks indicate statistically significant means ($P < 0.05$) between treatment and 0hr control. **b)** Changes in relative transcript levels of *TFP* in *wt* (Col-0) and *uvr8-6* (Col) normalised to *wt* (Col-0) 0hrs. Asterisks indicate statistically significant means ($P < 0.05$) between *wt* 0hrs and the given treatment.

However, at 24hrs of UV-B exposure *TFP* expression decreased by 92% compared to 0hrs ($P < 0.001$, Fig 6.13a); which is similar to the downregulation observed in wild type. The decrease of

TFP expression observed at 24hrs of UV-B in *uvr8-6* was higher than the downregulation observed in wild type (Fig 6.13b). Whereas the decrease observed in *uvr8-6* was 92% ($P < 0.01$, Fig 6.13a), for wild type 24hrs of UV-B the decrease compared to 0hrs was 63% ($P < 0.01$, Fig 6.13a), and even in the absence of UV-B the decrease was only 74% ($P < 0.01$, Fig 6.13a); suggesting that UVR8 may play a role in the downregulation of *TFP* at 24hrs. To further test this hypothesis, *TFP* expression in *uvr8-6* in the absence of UV-B would have to be characterised.

6.5.5 Summary

In the absence of TFP, the UV-B dependent increase in photosynthetic rate is absent, suggesting that TFP is required for the photosynthetic phenotype. Furthermore, as UV-B exposure continues, photosynthetic rate decreases, thus indicating that TFP is required to maintain photosynthetic function under prolonged UV-B exposure. This is further illustrated by the limiting effect UV-B has on green leaf area development in the *tfp* mutant; as green leaf area ceases to increase significantly after the initial 24hrs of UV-B exposure. Also, high fluence UV-B exposure showed that green leaf area development in the *tfp* mutant is adversely affected over prolonged exposure, to a similar degree as uvr8-*6.*

qRT-PCR analysis showed that UV-B exposure results in a significant increase in *TFP* expression; similarly to the increase in expression observed in the RNA-seq results. The increase in expression at 6hrs UV-B suggests that increased chloroplastic oxidoreductase activity may result in the increased photosynthetic rate observed at 24hrs as hypothesised in Chapter 4. Furthermore, qRT-PCR further showed that UVR8 plays a part in the upregulation of *TFP* in response to UV-B exposure, but that it is not involved in regulating *TFP* expression in the absence of UV-B.

The analysis of *TFP* expression also showed that *TFP* expression is likely regulated by other factors as well as UV-B exposure, and more experimental work has to be done to determine how *TFP* expression is regulated.

6.6 Chapter Summary

RNA-seq analysis identified a number of genes that were altered in expression pattern in response to UV-B exposure at 6hrs compared to no UV-B. The three most significantly changed genes identified were *RBF1*, *TOC33* and *TFP.* Here it has been shown that each of these genes plays a critical role in the increase in photosynthetic rate observed in wild type at 24hrs, as the mutants of these genes lack the UV-B-dependent photosynthesis phenotype.

RBF1 is shown to play an important role in the photosynthesis response to UV-B exposure as the reduction of RBF1 levels results in a decrease in photosynthetic rate upon illumination with UV-B. This suggests that RBF1 is key to maintaining photosynthetic competency under UV-B exposure as well as playing a part in the increase in photosynthetic rate observed in the wild type.

TOC33 is shown to be involved in the increase in response, as well as playing a role in photosynthetic efficiency in the absence of UV-B as the photosynthetic rate of the *toc33* mutant was significantly lower than that of wild type even in the absence of UV-B. *TFP*, on the other hand, is shown to play a part both in the increase in rate in wild type as well as in maintaining photosynthetic efficiency under prolonged UV-B exposure as it showed a decrease in photosynthetic rate over longer exposure times. As each of these genes plays a role in the increase in photosynthetic rate, it suggests that the increase in photosynthetic rate may be due to both an increase in chloroplast number as well as due to an increase in oxidoreductase activity in the chloroplast.

Each of the genes is also shown to potentially play a role in UV-B stress acclimation. When green leaf area was assessed in response to low fluence UV-B, all mutants were shown to be limited in green leaf area development over prolonged UV-B exposure, whereas wild type was not as limited. This suggests that all of these genes play a role in acclamatory responses to longer UV-B exposure. This is further illustrated by the decrease in green leaf area over time observed

under high fluence UV-B, where each of the mutants showed a significant decrease in leaf area. Often showing significantly more decrease in area than the *uvr8* mutant, *uvr8-6,* showing that the mutants were more affected and hence more critical to maintaining green leaf area development than uvr8.

qRT-PCR analysis of expression of *RBF1*, *TOC33* and *TFP*¸ showed that the expression patterns observed in L*er* and *uvr8-1* in the RNA-seq also occur in Col-0 and *uvr8-6*. Analysis of *RBF1* expression showed that it is upregulated in response to UV-B exposure in wild type; being highly upregulated at 6hrs of exposure and less upregulated at 24hrs of UV-B exposure. Expression in *uvr8-6* also showed that the initial upregulation at 6hrs is regulated by UVR8. Expression analysis of *TOC33* in wild type showed that it is upregulated in response to UV-B exposure at 6hrs, however, at 24hrs upregulation is likely due to other factors as expression also increases in the absence of UV-B. Analysis in *uvr8-6* also showed that the increase in *TOC33* expression at 6hrs is controlled by UVR8 and that UVR8 may play a role in expression even in the absence of UVB exposure. Analysis of *TFP* expression in wild type also showed that the initial upregulation is due to UV-B exposure, but that regulation of expression after initial exposure is not affected UV-B exposure. Upregulation of *TFP* at 6hrs is also controlled by the presence of UVR8, as in *uvr8-6* the increase of expression is absent.

These results show that RBF1, TOC33 and TFP play an important role in the increase in photosynthetic rate at 24hrs of UV-B seen in wild type and that each gene also plays a role in response to prolonged UV-B exposure. Each gene is upregulated by the presence of UV-B during initial exposure (6hrs), but during longer exposure UV-B is not necessarily a regulating factor. The initial upregulation is also likely to be controlled by the presence of UVR8; whereas regulation by UVR8 seems to be absent after prolonged exposure to UV-B.

7 Discussion and Conclusion

Photosynthetic competency and performance have been a focus for UV-B response studies since the birth of the discipline itself. Many historical UV-B experiments have been performed in the presence of high fluence rate UV-B, and low fluence rates of PAR, and showed that exposure to high fluence UV-B severely impedes photosynthetic performance (Allen et al., 1997; Mackerness et al., 1998; Takahashi et al., 2010). High fluence rates of UV-B damage the photosystems and lower photosynthetic efficiency (Tyystjärvi, 2008; Davey et al., 2012; Dobrikova et al., 2013), as well as inhibiting net photosynthetic rate (Jansen et al., 1998). The focus on high fluence rates of UV-B has arguably resulted in a somewhat skewed view of the photosynthetic responses of plants exposed to UV-B. In nature, plants are exposed to a variety of fluence rates of UV-B, and no visible damage is detected. Thus, plants are capable of coping with UV-B exposure at low and moderate levels in nature, suggesting that photosynthesis should not always be dramatically impeded by UV-B exposure.

In recent years, studies have begun to focus on the impact of low fluence UV-B on the plant, and understanding the photomorphogenic response elicited by lower UV-B levels (Kliebenstein et al., 2002; Brown et al., 2005; Brown and Jenkins, 2008; Favory et al., 2009; Jenkins, 2014a). There is evidence to suggest that exposure to low levels of UV-B can be beneficial to photosynthetic performance (Vidović et al., 2015), and result in the upregulation of photosynthesis-associated genes (Davey et al., 2012; Wargent and Jordan, 2013; Tilbrook et al., 2016).

This PhD thesis focused on the impact of 0.5 µmol m^{-2} s^{-1} UV-B supplemented with 220 µmol m^{-2} s^{-1} of PAR; thus characterising the UV-B dependent increase in photosynthetic rate in wild type. Furthermore, it characterised the transcriptomic response to the fluence rate, and through it identified a number of candidate regulators involved in the response. Thus allowing us to develop a model of how low fluence UV-B exposure results in the increase in net photosynthetic rate through the UVR8-dependent UV-B signalling cascade inducing increases in chloroplast

biogenesis and synthesis of photosynthetic proteins within the chloroplast and increasing levels of chloroplastic oxidoreductases.

7.1 The UV-B dependent photosynthesis phenotype

Initial experiments focused on measuring photosynthetic rate in plants exposed to 1.5 µmol m^{-2} s^{-1} UV-B. This fluence rate had been established previously as photomorphogenesis-inducing by Favory et al. (2009). PageMan analysis by Wargent and Jordan (2013) of the Favory et al. (2009) microarray data showed that a number of photosynthesis-associated genes are upregulated in response to this fluence rate of UV-B. The upregulation of photosynthesis-associated genes hinted at a UV-B induced change in photosynthesis. However, our results show that in response to 1.5 µmol m^{-2} s^{-1}, UV-B photosynthetic rate does not increase (Fig 3.1). This is similar to the response observed in other studies showing no effect of low fluence UV-B exposure on photosynthesis and the photosynthetic machinery (Hectors et al., 2007; Ballaré et al., 2011; Hideg et al., 2013).

During prolonged exposure, over 48hrs, photosynthetic rate decreases under UV-B exposure, compared to no UV-B exposure, suggesting that even the low fluence rate of 1.5 µmol m^{-2} s^{-1} UV-B may result in dynamic or chronic damage to the photosynthetic machinery after prolonged exposure. This confirms the suggestion by Favory et al. (2009) that the fluence rate of 1.5 µmol m^{-2} s^{-1} UV-B induces both a photomorphogenic response as well as a stress response. It is possible that photosynthesis rate does not change under 1.5 µmol m^{-2} s^{-1} of UV-B, as the increase in photosynthesis-associated genes allow the plant to adapt to UV-B exposure, and thus prevents the build-up of UV-B induced damage, which may reduce photosynthetic efficiency at higher fluence rates. Hence, photosynthetic rate remains the same during initial exposure of UV-B, and only decreases after prolonged exposure, as damage to the photosynthetic machinery accrues. The upregulation of photosynthesis-associated genes may result in increased turnover of damaged proteins as well as increasing the initial synthesis of photosynthesis-associated

proteins; which prevents the accumulation of damage to the photosynthetic apparatus. Moreover, the decrease in photosynthetic rate at 48hrs of UV-B exposure is likely due to the loss of regulation of these genes resulting in the accumulation of damage to the photosynthetic machinery.

As the exposure to 1.5 µmol m^{-2} s^{-1} UV-B did not result in an increase in photosynthetic rate, we decided to use a lower fluence rate. Exposure to 0.5 µmol m^{-2} s^{-1} UV-B resulted in an increase of 10% in photosynthetic rate at 24hrs of exposure in wild type L*er* (Fig 3.2), and by 12% in wild type Col-0 (Fig 3.8). The increase in photosynthetic rate shows that low fluence UV-B exposure can be beneficial to photosynthesis in *Arabidopsis;* which has not been shown before. The increase in photosynthetic rate under UV-B exposure is transient as at 48hrs of UV-B exposure the increase in photosynthetic rate is lost (Fig 3.2). The absence of a deleterious effect on photosynthetic rate confirms that the fluence rate used is photomorphogenic rather than stress-inducing. It further shows that the length of exposure to UV-B alters the plant's response to UV-B, as plants have to adapt to prolonged UV-B exposure, and the accumulation of UV-B induced damage. Part of the photomorphogenic response in *Arabidopsis* is the induction of flavonoid biosynthesis in response to UV-B exposure (Favory et al., 2009; Tilbrook et al., 2013; Vandenbussche et al., 2014). At 48hrs of UV-B exposure, wild type showed an increase in flavonoid content (Fig 3.4), showing the shift in the response to UV-B exposure to damage prevention through a photomorphogenic response. Previous studies have suggested that UV-B exposure results in damage to PS II, resulting in a lower PS II efficiency (Tyystjärvi, 2008; Davey et al., 2012; Dobrikova et al., 2013). The decrease in photosynthetic rate observed in wild type at 48hrs under 0.5 µmol m^{-2} s^{-1} of UV-B does not result in a lower PS II efficiency (Fig 3.5) suggesting that the fluence rate used does not induce damage in PS II and the decrease is due to other factors.

In response to illumination with 0.5 µmol m^{-2} s^{-1} of UV-B, the net photosynthetic rate of wild type *Arabidopsis* increases at 24hrs of exposure. However, after a further 24hrs of exposure; at 48hrs, the increase in photosynthetic rate is lost, and net photosynthetic rate is the same under UV-B as it is in the absence of UV-B. In order for us to determine what causes the initial increase in photosynthetic rate, transcriptomic analysis was undertaken.

7.2 Transcriptome changes in response to low fluence UV-B exposure

The transcriptomic analysis using RNA-seq identified a number of photosynthesis-associated genes that are upregulated in response to low fluence UV-B exposure at 6hrs, similarly to the transcriptomic response seen in Favory et al. (2009) microarray data analysed by Wargent and Jordan (2013). However, unlike the microarray analysis by Favory et al. (2009) and many other whole genome expression profiling (Green et al., 1991; Brosché et al., 2002; Ulm et al., 2004; Stracke et al., 2010); the RNA-seq identified only a small number of genes significantly changed under UV-B exposure. At 6hrs of UV-B exposure, there were 119 significantly changed genes, and at 24hrs there were only 43 significantly changed genes. This further illustrates that the fluence rate used has a much smaller effect on the plant than other higher doses, and thus the response of the plant is more photomorphogenic rather than a stress response that would induce a large number of genes (Brown et al., 2005).

At 6hrs of UV-B exposure overrepresentation analysis showed that a large number of the genes significantly regulated are associated with the chloroplast and the thylakoid as well as being associated with intramolecular oxidoreductase activity. This suggests that the increase in photosynthetic rate is driven by an increase in chloroplast biogenesis, and synthesis of proteins within the chloroplast, as well as chloroplastic oxidoreductase activity. At 24hrs of exposure overrepresentation analysis showed that a large number of the genes significantly regulated are associated with flavonoid biosynthesis and the response to light stimulus. The absence of photosynthesis-associated genes at 24hrs shows that there is a shift in gene expression patterns;

away from the regulation of photosynthesis in response to UV-B and towards a traditional UV-B acclimation/photomorphogenic response. The increase in flavonoid biosynthesis pathway associated genes likely results in the increase in flavonoid content observed at 48hrs of UV-B exposure (Fig 3.4); and the absence of photosynthesis-associated genes likely results in the absence of the increase in photosynthetic rate at 48hrs (Fig3.2).

7.2.1 Regulation of photosynthesis-associated genes under UV-B exposure

At 6hrs of UV-B exposure, a number of photosynthesis-associated genes are upregulated. The term photosynthesis-associated is broad and includes a large number of different genes. Analysis of the RNA-seq data showed that the upregulated genes at 6hrs fall predominately into two groups; (1) chloroplast biogenesis and synthesis of chloroplastic proteins and (2) chloroplastic oxidoreductase associated.

7.2.1.1 Chloroplast biogenesis and synthesis of chloroplastic proteins

The impact of UV-B exposure on chloroplasts and the photosynthetic machinery contained therein is broad and varied. Studies have shown that UV-B exposure affects the number and accumulation of chloroplasts (Izumi et al., 2017), results in loss of integrity of the thylakoid membrane (Gupta et al., 2008), reduced chlorophyll content (Fagerberg, 2007; van Rensen et al., 2007) among others. Furthermore, UV-B exposure also changes the expression of chloroplast proteins, which also limits photosynthesis (Jordan et al., 1992). As UV-B exposure has such a broad impact on the chloroplast, the upregulation of chloroplast biogenesis associated genes, as well as genes associated with the synthesis chloroplastic proteins under low fluence UV-B, is likely an adaptive response. Therefore, the upregulation of chloroplast and photosynthesis-associated genes initially results in an increase in photosynthetic rate, but in the long term allows the plant to acclimate to UV-B exposure and better cope with UV-B induced damage in the long term.

The RNA-seq analysis identified a number of chloroplast associated genes that are upregulated in response to UV-B. *RBF1* and *RNEE/G* are involved in chloroplast biogenesis (Bollenbach et al., 2005; Mudd et al., 2008; Fristedt et al., 2014), suggesting that in response to low fluence UV-B, the number of chloroplasts may increase. Further studies assessing chloroplast number could give a better indication if the upregulation of these genes drives an increase in chloroplast number, and may also give an indication of how localisation changes occur in response to low fluence UV-B exposure. TOC33 is the transporter involved in the import of pre-proteins into the chloroplast (Kessler and Schnell, 2004; Oreb et al., 2008; Oreb et al., 2011), which could indicate that import of photosynthetic pre-proteins for synthesis within chloroplast increases in response to UV-B exposure. Higher levels of pre-proteins in the chloroplast may account for the increase in photosynthetic rate as it could allow for the presence of more photosynthesis-associated proteins. The increase in proteins could increase photosynthetic rate, as well as, allowing for a higher turnover rate of damaged proteins to allow for acclimation to UV-B exposure. Upregulation of the chloroplast located PEP *PTAC14* and the ribosome release factor *APG3*, further strengthens this hypothesis, as they are involved in transcription of chloroplast proteins (Rius et al., 2008; Gao et al., 2012). Suggesting that increased import of chloroplast pre-proteins and transcription of these proteins allow for a higher photosynthetic rate in response to UV-B exposure. However, further study assessing protein levels in the chloroplast is required, to give a better indication of the impact the upregulation has on a proteomic level. This was outside of the achievable scope of this thesis.

The upregulation of *BPG3,* which encodes a chloroplast protein involved in the electron transport in PS II, and has been implicated in the stabilization of chlorophyll (Yoshizawa et al., 2014), suggests that UV-B exposure may also drive a direct increase in electron transport efficiency in the photosystems by increasing the amounts of proteins involved in electron transport and to enable stabilization of chlorophyll under UV-B. PSB28, a protein involved in the

biogenesis and assembly of chlorophyll-containing proteins such as *PsaA* and *PsaB* in PS II (Dobáková et al., 2009), may also have a direct impact on photosynthetic rate through increasing the amounts of photosystem associated genes. Increasing amount of photosystem associated genes may also allow for higher turnover rates in response to damage and hence prevent a UV-B induced reduction in photosynthetic rate, as the ratio of damaged to functional proteins arguably remains low. This may explain why photosynthetic rate at 48hrs is not significantly lower under UV-B than in the absence of UV-B, as there would still be sufficient functional photosystem proteins to allow for a "normal" photosynthesis levels.

7.2.1.1.1 Tetrapyrrole synthesis:

At 6hrs of UV-B exposure, tetrapyrrole synthesis is upregulated; and a subgroup of tetrapyrroles are the chlorophylls. An increase in chlorophyll content could result in the increase in photosynthetic rate observed in wild type at 24hrs of exposure, although non-destructive measurements of chlorophyll content did not show a UV-B specific increase in chlorophyll content (Fig 3.3). However, measuring chlorophyll destructively may show a different response and reveal an increase in chlorophyll in response to low fluence UV-B exposure. Destructive measuring would give a better indication of the amount of chlorophyll in the entire plant rather than the amount present only in one leaf and measured by absorbance within the leaf. UV-B exposure has been shown to reduce chlorophyll content (Quan et al., 2018) via damage to the chlorophylls by alterations in composition (Strid and Porra, 1992) and through photobleaching (Zvezdanović et al., 2009), and inhibition of synthesis of chlorophyll (Sakaki et al., 1983; Trošt Sedej and Gaberščik, 2008). The upregulation of chlorophyll synthesis genes may result in higher chlorophyll synthesis to replace any chlorophyll degraded by UV-B exposure, which in turn may increase net photosynthetic rate.

7.2.1.2 Chloroplastic oxidoreductases

Exposure to UV-B damages many of the key oxidoreductases involved in the electron transport chain in the chloroplast, such as the D1 and D2 proteins of PS II and Rubisco (Jansen et al., 1998; Caldwell et al., 2003; Caldwell et al., 2007), resulting in the inactivation of PS II and lower photosynthetic efficiency. However, in response to low fluence rate UV-B exposure, a number of genes associated with chloroplastic oxidoreductases were found to be upregulated at 6hrs of UV-B exposure; suggesting that low fluence rate UV-B may increase photosynthetic efficiency through increased levels of oxidoreductases in the chloroplast as well as via increased activity. Two of the most significantly upregulated genes by low fluence UV-B are *TFP* and *PDE327.* These two genes represent two types of oxidoreductases that are involved in photosynthesis. *TFP* encodes a putative chloroplastic thioredoxin (Meyer et al., 2006). Thioredoxins play an important part in the various processes in chloroplasts; such as regulating proteins linked to the photosynthetic reactions and Calvin Cycle, as well as biogenesis of chloroplasts and chlorophyll synthesis (Chi et al., 2008; Jiang et al., 2012; Cheng et al., 2014; Brzezowski et al., 2015). While *PDE327* encodes a chloroplast-localized oxidoreductase/electron carrier (Zybailov et al., 2008; Vlad et al., 2010). The electron carriers are vital for the correct electron flow through the photosynthetic chain (Vlad et al., 2010), and hence for photosynthetic efficiency.

Under low fluence UV-B exposure, genes upregulated are associated with chloroplastic oxidoreductases involved in the photosynthesis pathway; suggesting that the response is more in the direction of higher photosynthetic yield than as a stress response to ROS production (Hideg et al., 2013). Studies examining photosynthesis-associated chloroplastic oxidoreductases have shown that a reduction in genes associated with these proteins resulted in decreased expression of genes involved in the Calvin Cycle and decreased activity of the associated enzymes (Chi et al., 2008; Jiang et al., 2012; Cheng et al., 2014). This suggests that upregulation would increase expression of these genes and could thus drive the increase in photosynthetic rate observed in wild type. Furthermore, some chloroplastic thioredoxins have also been

associated with non-photochemical quenching in response to light stress (Naranjo et al., 2016); suggesting that in response to low UV-B exposure increased levels of thioredoxins may aide in photochemical quenching to prevent damage by UV-B exposure. Additionally, silencing of certain thioredoxins has also shown to decrease levels of chlorophyll biosynthesis related genes and decrease photosynthetic efficiency (Luo et al., 2012). This suggests that there may be an interplay between the upregulation of chloroplastic oxidoreductases associated genes and genes associated with the synthesis of photosynthetically active chloroplast proteins.

In summary, this suggests that low fluence UV-B exposure results in an increase in chloroplast biogenesis and synthesis of photosynthetically active proteins within the chloroplast, as well as affecting the oxidoreductase enzyme activity to affect electron transport within the chloroplast and thus increase photosynthetic efficiency. Together, these drive the increase in photosynthetic rate at 24hrs and may aid in the adaptive response to UV-B exposure by increasing turnover of damaged proteins or acting as protectants against UV-B damage through non-photochemical quenching.

7.2.1.3 Regulation of genes associated with ATP synthase and cytochrome b6/f

Both at 6hrs and 24hrs of UV-B exposure, RNAseq analysis showed upregulation of genes associated with ATP synthase and the cytochrome b6/f complex. Under high fluence UV-B exposure both of these complexes are negatively affected and damaged; with ATP synthase is the most adversely affected and cytochrome b6/f being the least adversely affected (Strid et al., 1990; Zhang et al., 1994; Lidon et al., 2012; Kataria et al., 2014). High UV-B exposure has also been shown to downregulate genes associated with ATP synthase (Babele et al., 2015). UV-B exposure has also been shown to reduce cytochrome b6/f content, which is associated with a lower Chl *a*: Chl *b* ratio, and a reduction in electron transport capacity (Eichhorn et al., 1994; Watanabe et al., 1994). Both complexes are associated with the electron flow in the electron transport chain resulting in the generation of ATP. Upregulation of genes associated with these

complexes under UV-B exposure suggests that under low fluence UV-B exposure the plant adapts to UV-B exposure; which entails increasing biosynthesis of key proteins, increasing efficiency and allowing for increased turnover of UV-B damaged proteins, and stabilising the present proteins to delay the accumulation of damage in response to UV-B. As genes associated with both groups are upregulated at both 6hrs and 24hrs of exposure, it may explain the absence of a negative impact on photosynthetic rate at 48hrs in wild type, as increased synthesis and turnover would continue; preventing accumulation of damage which would decrease the photosynthetic rate. Further transcriptomic analysis focusing on later time points; as UV-B exposure continues, would likely show that these genes are no longer upregulated and that damage to the photosynthetic machinery would accrue, resulting in the decrease in photosynthetic rate seen at later time points.

7.2.1.4 Summary

In response to low fluence UV-B exposure, a number of photosynthesis-associated genes become upregulated. The majority of those genes are upregulated during initial exposure; prior to the 24hr mark, and are associated with chloroplast biogenesis and biosynthesis of photosynthetically active proteins in the chloroplast, or are involved in regulating the enzymatic activity of chloroplastic oxidoreductases. The upregulation of these genes is likely to be an adaptive response to UV-B exposure, allowing the plant to acclimate to UV-B exposure, increase efficiency and prevent the accumulation of damage by increasing biosynthesis and turnover of key proteins usually damaged by UV-B exposure, as well as stabilizing some of these key proteins such as chlorophyll.

At 24hrs the upregulation of many of these genes is absent; suggesting that the plant shifts to a different acclimation response, as seen by the increase in genes associated with the flavonoid biosynthesis pathway. The plant begins to adapt to prolonged UV-B exposure and beings to synthesise proteins associated with a response to prevent chronic damage. At 24hrs, only a few

photosynthesis-associated genes remain upregulated, but most that were previously upregulated are no longer significantly changed in comparison to no UV-B conditions. This suggests that the plant is still engaging in an acclimation response, as if the plant was stressed, the photosynthesis-associated genes would arguably be downregulated to limit energy expenditure. The continued acclimation response also explains why there is no negative impact on photosynthetic rate at 48hrs; instead, photosynthetic rate is the same under UV-B as it is in the absence of it. Damage to the photosynthetic machinery begins to accrue; which lowers the photosynthetic rate from the higher rate at 24hrs, but the damage is not severe enough to reduce photosynthetic rate below 'normal'. Even longer exposure, at 72hrs likely results in more damage accumulating, which then further lowers photosynthetic rate under UV-B exposure.

7.3 Candidate regulators of the UV-B dependent photosynthesis phenotype

The transcriptomic analysis plus prior literature revealed a number of possible regulators that may play key roles in the UV-B dependent increase in photosynthetic rate in wild type at 24hrs. These are the UV-B photoreceptor UVR8, the negative regulators of UVR8 RUP1 and RUP2, as well as the previously identified SIG5, ELIP1 and ELIP2; as well as the three most significantly changed genes in the RNA-seq screen at 6hrs of UV-B exposure; *RBF1*, *TOC33* and *TFP*. For each of these, their role in the photosynthesis phenotype was assessed by measuring photosynthetic rate and green leaf area development in mutants under low fluence UV-B exposure

7.3.1 UVR8 and literature identified candidate regulators

UVR8 and the signalling cascade it induces upon UV-B exposure play a key part in the photosynthetic response to low fluence UV-B exposure. Analysis of the photosynthesis screen showed that functional UVR8 is required for the increase in photosynthetic rate at 24hrs of UV-B; as this is absent in both *uvr8* mutants. However, photosynthetic rate does not decrease under UV-B at 24hrs compared to in the absence of UV-B. This indicates that the rate used is indeed

more photomorphogenically active than chronic stress-inducing. At 48hrs of UV-B, photosynthetic rate in the *uvr8* mutants is decreased compared to the no UV-B, which further suggests that prolonged exposure results in damage to the photosynthetic machinery and the loss of UVR8 leads to increased susceptibility to stress.

In the RNA-seq screen, photosynthesis-associated genes were significantly lower in *uvr8-1* compared to wild type at 6hrs of UV-B exposure. This further exemplifies that UVR8 regulates the increase in photosynthetic genes in response to UV-B exposure during initial exposure. At 24hrs, there is no difference in regulation between wild type and *uvr8-1*. The absence of regulation of these genes at 24hrs suggests that UVR8 ceases to regulate those genes after initial exposure, and it is likely that UVR8 begins the regulation of other genes; such as flavonoid biosynthesis.

7.3.1.1 RUP1 & RUP2

Analysis of the photosynthetic rate in the *rup1,2* double mutant showed that photosynthetic rate is continuously increased in response to UV-B exposure in the absence of the negative regulation of UVR8 by RUP1 and RUP2. This further shows that UVR8 is involved in the initial increase in photosynthetic rate at 24hrs of UV-B exposure and that the alteration in photosynthetic rate back to 'normal' levels at 48hrs may be partly due to UVR8 being negatively regulated by RUP1 and RUP2. RUP1 and RUP2 bind to UVR8 in place of COP1 to limit the photomorphogenic response elicited by the UVR8 signalling cascade (Gruber et al., 2010; Cloix et al., 2012; Heijde et al., 2013; Yin et al., 2015). Hence, the negative regulation of UVR8 by RUP1 and RUP2 may be to limit the response to UV-B or to allow for the regulatory shift towards a more photomorphogenic response to UV-B exposure.

7.3.1.2 SIG5

SIG5 is a responsive sigma factor involved in chloroplast transcription (Tsunoyama et al., 2002; Nagashima et al., 2004; Tsunoyama et al., 2004) and is regulated by UVR8 in response to UV-B

(Brown and Jenkins, 2008; Mellenthin et al., 2014). In my experiments, *sig5* mutants exposed to low fluence UV-B lack the UV-B dependent increase in photosynthetic rate. In fact, the *sig5-2* mutant, lacking sigma factor activity, shows a reduction in photosynthetic rate under UV-B compared to no UV-B at 24hrs. Thus suggesting that sigma factor activity is crucial to maintaining photosynthesis in the presence of UV-B. The absence of the UV-B dependent increase in photosynthetic rate in the *sig5* mutants suggests that the increase in photosynthetic rate may be due to an increase in transcription of photosynthesis-associated chloroplast genes controlled by SIG5, such as *psbD* and *psbA* (Nagashima et al., 2004; Tsunoyama et al., 2004; Noordally et al., 2013; Yamburenko et al., 2015). Higher transcription of these genes results would result in higher synthesis of D1 and D2 proteins (Mellenthin et al., 2014) and could thus increase photosynthetic rate. However, in the RNA-seq screen SIG5 is not significantly regulated in response to UV-B exposure, contrary to other studies that have shown it to be upregulated even in the presence of very low UV-B doses (0.1 µmol m^{-2} s^{-1}) (Davey et al., 2012). The photosynthesis response of the *sig5* mutants suggest that SIG5 plays a role in the increase in photosynthetic rate in response to UV-B, but the absence of upregulation at 6hrs and 24hrs UV-B, suggests that SIG5 does not need to be upregulated to affect the UV-B dependent photosynthesis response.

7.3.1.3 ELIP1 and ELIP2

ELIP1 and *ELIP2* are light response genes involved in tolerance to photoinhibition and photooxidative stress (Rossini et al., 2006). ELIPs are expressed in mature plants in response to UV-B exposure, and their expression is mediated by UVR8 (Adamska et al., 1992; Brown et al., 2005; Rossini et al., 2006). In the photosynthesis screen, the *elip* mutants showed an increase in photosynthetic rate at 24hrs UV-B exposure compared to no UV-B; but the increase is much lower than in wild type. Interestingly, *elip2* showed an increase in photosynthetic rate in at 48hrs of UV-B exposure. The photosynthetic response to UV-B in both mutants suggests that both

ELIPs play a role in the UV-B dependent photosynthesis response, but neither is significantly upregulated in response to UV-B exposure at 6hrs in wild type in the RNA-seq screen; suggesting that they are not key to the photosynthesis phenotype.

As the physiological roles of the ELIPs are unknown, and as they were not upregulated in response to UV-B exposure, in contrast to prior work showing them to be upregulated in response to UV-B exposure (Brown et al., 2005; Oravecz et al., 2006; Kilian et al., 2007; Safrany et al., 2008; Favory et al., 2009; Davey et al., 2012; Hayami et al., 2015), it still remains unknown as to what role the ELIPs may play in the photosynthesis phenotype. Although it may be hypothesised that ELIPs aid chlorophyll accumulation in some manner, and may prevent overexcitation in response to UV-B exposure (Tzvetkova-Chevolleau et al., 2007), a clear mechanistic understanding remains elusive.

7.3.2 RNA-seq identified candidate regulators

7.3.2.1 RBF1

RBF1 was identified in the RNA-seq screen and is significantly upregulated in response to UV-B exposure. It is localised to the thylakoid membrane and involved in the biogenesis of the thylakoid membrane (Fristedt et al., 2014). The two *rbf1* mutants exhibit much lower photosynthetic rates at 24hrs under UV-B than in the absence of UV-B, and the photosynthetic rate continues to decrease in response to UV-B exposure. This suggests that RBF1 plays a key role in the UV-B dependent increase in photosynthetic rate at 24hrs, and in maintaining photosynthetic rate under UV-B. As RBF1 is involved in thylakoid membrane biogenesis and is UV-B has been shown to affect thylakoid membrane integrity (Strid et al., 1994), it stands to reason that RBF1 plays a key role in the maintaining thylakoid membrane integrity under UV-B exposure. Analysis of expression in the *uvr8* mutant shows that in response to UV-B exposure RBF1 is regulated by UVR8, as upregulation is absent in both *uvr8* mutants. This leads to the hypothesis that in response to low fluence UV-B exposure, UVR8 upregulates expression of

RBF1. This results in increased thylakoid biogenesis, increasing photosynthetic rate through increased thylakoid and chloroplast numbers.

7.3.2.2 TOC33

TOC33 was identified as significantly upregulated in response to UV-B exposure at 6hrs in the RNA-seq screen. TOC33 is a vital part of the chloroplast import machinery involved in the large-scale import of photosynthetic pre proteins into the chloroplast (Bauer et al., 2000; Kubis et al., 2003; Hiltbrunner et al., 2004; Ivanova et al., 2004; Smith et al., 2004). In response to low fluence UV-B exposure, the *toc33* mutant exhibited no change in photosynthetic rate at 24hrs of exposure compared to no UV-B exposure; suggesting that it is required for the UV-B dependent increase in photosynthetic rate. Analysis of *TOC33* expression in *uvr8-6* showed that upregulation in response to UV-B is regulated by UVR8 and that UVR8 continues to regulate *TOC33* expression under UV-B exposure, likely resulting in the continued increase in relative expression observed in wild type in qRT-PCR analysis (which was not seen in RNA-seq experiments). However, as indicated by the absence of continuously higher photosynthetic rate in wild type, continued upregulation does not continue to increase photosynthetic rate. This suggests that the initial upregulation of *TOC33* in response to UV-B is involved in the increase in photosynthetic rate, but this does not affect photosynthetic rate in the medium-long term.

As TOC33 is a key factor in the import of photosynthetic pre-proteins into the chloroplast, it may be that the upregulation of *TOC33* by UVR8 results in more import of photosynthetic pre-proteins into the chloroplast resulting in a higher photosynthetic rate and improving photosynthetic efficiency. However, continued exposure to UV-B limits expression of pre-proteins or damages proteins in the chloroplast, negating the impact of higher TOC33 levels, hence the absence of the UV-B dependent increase in photosynthetic rate at 48hrs of UV-B exposure.

7.3.2.3 TFP

TFP was also identified as a significantly upregulated gene in response to UV-B exposure at 6hrs in the RNA-seq screen. TFP is a chloroplastic thioredoxin (Meyer et al., 2006), but little is known about it, apart from that it is likely involved in the ferredoxin/thioredoxin system that is associated with oxygenic photosynthesis and light (Schürmann and Buchanan, 2001; Schürmann and Buchanan, 2008). The photosynthesis screen of the *tfp* mutant showed that in response to low fluence UV-B exposure, the UV-B dependent increase in photosynthetic rate is absent at 24hrs. At 48hrs photosynthetic rate is significantly lower under UV-B than in the absence of UV-B; suggesting that the loss of *tfp* results in stress to the photosynthetic machinery over prolonged exposure. Both the RNA-seq screen and qRT-PCR analysis showed that in response to UV-B, relative expression of *TFP* increases at 6hrs of UV-B exposure, and expression decreases at 24hrs UV-B exposure. The upregulation of *TFP* at 6hrs suggests that increased thioredoxin activity increases photosynthetic rate in response to UV-B exposure at 24hrs and that the reduction in photosynthetic rate at 48hrs UV-B compared to 24hrs UV-B is in part a result of the decrease in expression of *TFP* after 24hrs. qRT-PCR analysis of relative expression of *TFP* in *uvr8-6* also showed that UVR8 is involved in the upregulation of *TFP* in response to UV-B exposure at 6hrs, but that at 24hrs it is no longer involved in the regulation, as both in wild type and *uvr8-1* *TFP* expression decreases. Hence it can be hypothesised that in response to low fluence UV-B, UVR8 upregulates *TFP*, resulting in an increase in thioredoxin activity in the chloroplast during the first 24hrs of UV-B exposure. This results in an increase in photosynthetic rate, but the specific interaction of TFP in the regulation of photosynthetic rate is unknown. After 24hrs, expression of *TFP* decreases both under UV-B, and in the absence of UV-B, suggesting that another regulatory factor is involved in *TFP* regulation and that increased thioredoxin activity in the chloroplast is likely regulated by a large number of factors.

7.4 Conclusion

Based on the results of these experiments, as well as our existing knowledge, a model of the early-stage, UV-B-dependent increase in photosynthesis, is suggested (Fig 7.1). During initial exposure, low fluence UV-B is perceived by the UV-B photoreceptor UVR8. The UVR8 homodimer monomerises upon illumination with UV-B, and initiates the UVR8/COP1 signalling cascade resulting in the upregulation of photosynthesis-associated genes; among them *RBF1, TOC33* and *TFP.* Upregulation of genes such as *RBF1* and *TOC33* results in increased biosynthesis and activity within the chloroplast through increased thylakoid biosynthesis and import of photosynthetic pre-proteins into the chloroplast. Upregulation of genes such as *TFP* result in increased oxidoreductase activity, increasing photosynthetic efficiency in response to UV-B. Together, the increase in photosynthetically active proteins in the chloroplast and the increased oxidoreductase activity in the chloroplast result in increased net photosynthetic rate at 24hrs of UV-B exposure.

Other UV-B responsive genes such as *SIG5* and the *ELIPs* play a part in the photosynthesis phenotype but are not upregulated in response to UV-B exposure. Lack of regulation in response to UV-B exposure suggests that while these may be involved in the photosynthesis response, their specific role in the phenotype is unknown and remains to be elucidated. The role of RUP1 and RUP2 are not clear in terms of how they are involved in the photosynthesis response. However, RUP1 and RUP2 could interact with UVR8 after the initial exposure to UV-B and negatively regulate UVR8 resulting less regulation of photosynthesis-associated genes.

Following the initial exposure response, around 24hrs after UV-B is first perceived by UVR8, the UVR8/COP1/HY5 signalling cascade shifts regulation from photosynthesis-associated genes towards a photomorphogenic response by upregulating the phenylpropanoid pathway, resulting in the induction of flavonoids and anthocyanins and other pathways associated with UV-B mediated morphogenesis. The shift in response also results in reduced autotrophic growth in

response to UV-B exposure, as illustrated by the slower green leaf area development seen in the various mutants and wild type in response to UV-B exposure. The shift in regulation away from photosynthesis-associated genes results in the absence of increased photosynthetic rate at 48hrs of UV-B exposure.

In Conclusion, we have fulfilled the aims laid out in the introduction of this thesis. We characterised the photosynthetic response to low fluence UV-B in wild type Arabidopsis and in the uvr8 mutants; showing a UVR8 dependent increase in photosynthetic rate in response to low fluence UV-B exposure in the first 24hrs of UV-B (Aim 1). Through RNA-seq analysis we identified several candidate genes; *RFB1, TFP* and *TOC33*; which are significantly upregulated in response to low fluence UV-B exposure at 6hrs of exposure (Aim 2). Through further analysis of these genes, we have shown that each of these genes plays a role in the photosynthesis response to low fluence UV-B exposure and are likely to be regulated by UVR8 during UV-B exposure (Aim 3).

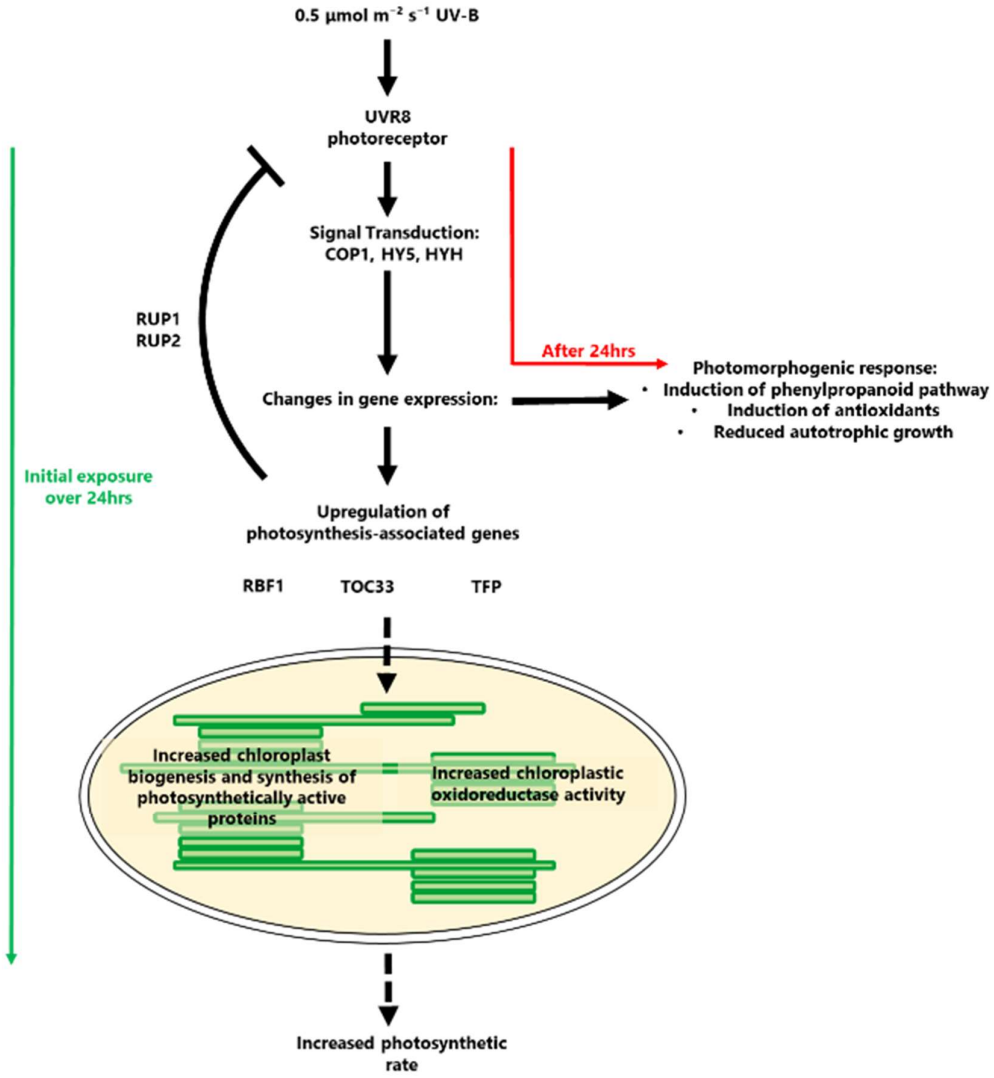

Figure 7.1 Proposed model of the response to 0.5 µmol m^{-2} s^{-1} UV-B exposure resulting in increase in photosynthetic rate at 24 hours. Plants perceive UV-B through the UVR8 photoreceptor, a homodimer, which monomerises upon illumination with UV-B. The monomer then interacts with COP1 and stabilises HY5 and HYH. This results in the induction of a large number of genes. During the initial illumination period the UVR8/COP1/HY5 pathway induces a number of photosynthesis-associated genes. The most highly upregulated are *RBF1, TOC33* and *TFP*. The upregulation of these genes results in increased biosynthesis of photosynthetically active proteins in the chloroplast and increase chloroplast biogenesis and increased chloroplastic oxidoreductase activity, which results in higher a higher photosynthetic rate in response to UV-B exposure. After 24hrs of exposure gene expression shifts toward a photomorphogenic response; such as increased flavonoid content and reduced autotrophic growth. Black arrows denote interactions established in literature, dashed black arrow denotes possible interactions identified in this work. Green arrow denotes response to initial exposure over 24hrs, red arrow denotes response after 24hrs. Chloroplast image adapted from Höhner et al. (2016).

7.5 Future directions

The work presented in this thesis shows that in response to low fluence UV-B exposure, net photosynthetic rate increases in the wild type at 24hrs of UV-B exposure, and that the increase in rate is due to the upregulation in photosynthesis-associated genes; especially related to chloroplast biogenesis and synthesis of chloroplastic proteins and chloroplastic oxidoreductase activity. These genes have not been associated with UV-B exposure previously.

Future experiments could focus on further characterising the genes identified as key genes through RNA-seq; thus doing further biochemical characterisation of RBF1, TOC33 and TFP. Identifying if these genes are regulated by UV-B signalling pathways acting downstream of UVR8; by examining expression by UV-B in known UV-B responsive mutants such as *cop1-4* and the *hy5* mutants. Furthermore, analysis of changes on the proteomic level would provide a better understanding of the impact of low fluence UV-B and how the transcriptomic changes impact protein levels.

Due to the volume of data produced by the RNA-seq screen, further analysis of the data, as well as further investigation into many of the significantly regulated genes, would provide an enhanced understanding of what drives the UV-B dependent increase in photosynthetic rate. Analysis of the expression of UVR8-independent genes would provide a better understanding of how the UVR8-independent response to UV-B modulates the photomorphogenic response. There has been a paucity of whole-genome transcriptomic studies of acclamatory UV-B responses to date, despite the availability of RNAseq tools for some time. Along with further analysis of the transcriptomic response, analysis of the proteomic response would also provide a deeper insights, as such approaches would determine if the increase in transcription of photosynthesis-associated genes at 6hrs of UV-B exposure translates into a change of protein levels associated with the genes; as increased transcription does not necessarily result in increased translation. Proteomic analysis would also show which factors are specifically involved

in the response. Furthermore, further analysis of the chloroplasts under UV-B exposure; determining the impact of low fluence rate UV-B on chloroplast number and accumulation, as well as biosynthesis within the chloroplast. This would allow for a better understanding of how the exposure to low fluence UV-B affects chloroplast development and integrity. While older studies often examined chloroplast structure and performance in response to higher fluence UV-B, there are very few contemporary studies focused on this aspect of biochemistry.

In addition to focusing on increased understanding of the regulatory mechanism of the UV-B dependent increase in photosynthetic rate, it would be interesting to determine if the increase in photosynthetic rate in response to low fluence UV-B exposure translates into a similar response in other plant species. If a similar response can be produced in other plant species, use of low fluence UV-B may be a useful tool in terms of increasing crop productivity in agriculture. Increasing crop yields through the use of light 'treatments', with reduced reliance upon genetic modification, chemical applications, or long-term breeding programs, offers a sustainable method to close crop yield gaps and satisfy the growing global demand for food.

8 References

Abramoff, M., Magalhães, P., and Ram, S.J. (2003). Image Processing with ImageJ. Biophotonics International **11,** 36-42.

Adamska, I., Ohad, I., and Kloppstech, K. (1992). Synthesis of the early light-inducible protein is controlled by blue light and related to light stress. Proc. Natl. Acad. Sci. USA **89,** 2610-2613.

Adamska, I., Kruse, E., and Kloppstech, K. (2001). Stable insertion of the early light-induced proteins into etioplast membranes requires chlorophyll *a*. J. Biol. Chem. **276,** 8582-8587.

Ahmad, M., Jarillo, J.A., Klimczak, L.J., Landry, L.G., Peng, T., Last, R.L., and Cashmore, A.R. (1997). An enzyme similar to animal type II photolyases mediates photoreactivation in Arabidopsis. Plant Cell **9,** 199-207.

Allen, D.J., McKee, I.F., Farage, P.K., and Baker, N.R. (1997). Analysis of limitations to CO2 assimilation on exposure of leaves of two *Brassica napus* cultivars to UV-B. Plant Cell Environ **20,** 633-640.

Aphalo, P.J. (2003). Do current levels of UV-B radiation affect vegetation? The importance of long-term experiments. New Phytol. **160,** 273-276.

Aphalo, P.J., Albert, A., Björn, L.O., McLeod, A., Robson, T.M., and Rosenqvist, E. (2012). Beyond the Visible - Handbook of best practices in plant UV photobiology. (Helsinki: University of Helsinki, Division of Plant Biology).

Aronsson, H., and Jarvis, P. (2011). Dimerization of TOC receptor GTPases and its implementation for the control of protein import into chloroplasts. Biochem. J. **436,** e1-2.

Babele, P.K., Singh, G., Kumar, A., and Tyagi, M.B. (2015). Induction and differential expression of certain novel proteins in *Anabaena* L31 under UV-B radiation stress. Front Microbiol **6**.

Ballaré, C.L., Caldwell, M.M., Flint, S.D., Robinson, S.A., and Bornman, J.F. (2011). Effects of solar ultraviolet radiation on terrestrial ecosystems. Patterns, mechanisms, and interactions with climate change. Photochem Photobiol Sci **10,** 226-241.

Balmford, A., Green, R.E., and Scharlemann, J.P.W. (2005). Sparing land for nature: exploring the potential impact of changes in agricultural yield on the area needed for crop production. Global Change Biol. **11,** 1594-1605.

Bauer, J., Chen, K., Hiltbunner, A., Wehrli, E., Eugster, M., Schnell, D., and Kessler, F. (2000). The major protein import receptor of plastids is essential for chloroplast biogenesis. Nature **403,** 203-207.

Belbin, F.E., Noordally, Z.B., Wetherill, S.J., Atkins, K.A., Franklin, K.A., and Dodd, A.N. (2017). Integration of light and circadian signals that regulate chloroplast transcription by a nuclear-encoded sigma factor. New Phytol. **213,** 727-738.

Boccalandro, H.E., Mazza, C.A., Mazzella, M.A., Casal, J.J., and Ballaré, C.L. (2001). Ultraviolet B radiation enhances a phytochrome-B-mediated photomorphogenic response in Arabidopsis. Plant Physiol. **126,** 780-788.

Bolink, E.M., van Schalkwijk, I., Posthumus, F., and van Hasselt, P.R. (2001). Growth under UV-B radiation increases tolerance to high-light stress in pea and bean plants. Plant Ecol. **154,** 147-156.

Bollenbach, T.J., Lange, H., Gutierrez, R., Erhardt, M., Stern, D.B., and Gagliardi, D. (2005). RNR1, a 3'-5' exoribonuclease belonging to the RNR superfamily, catalyzes 3' maturation of chloroplast ribosomal RNAs in *Arabidopsis thaliana*. Nucleic Acids Res. **33,** 2751-2763.

Booij-James, I.S., Dube, S.K., Jansen, M.A.K., Edelman, M., and Mattoo, A.K. (2000). Ultraviolet-B radiation impacts light-mediated turnover of the photosystem II reaction center heterodimer in Arabidopsis mutants altered in phenolic metabolism. Plant Physiol. **124,** 1275-1284.

Booij, I.S., Callahan, F.E., Jansen, M.A.K., Edelman, M., and Mattoo, A.K. (1999). Photoregulation and photoprotection of the photosystem II reaction center heterodimer. In Concepts in Photobiology : Photosynthesis and Photomorphogenesis, G.S. Singhal, G. Renger, S.K. Sopory, I. K.-D., and Govindjee, eds (New Delhi: Narosa Publishing House), pp. 549-571.

Bornman, J.F. (1994). Interaction of UV-B radiation and the photosynthetic process. In Stratospheric Ozone Depletion/UV-B Radiation in the Biosphere, R.H. Biggs and M.E.B. Joyner, eds (Springer Berlin Heidelberg), pp. 63-63.

Bornman, J.F., Reuber, S., Cen, Y.P., and Weissenböck, G. (1997). Ultraviolet radiation as a stress factor and the role of protective pigments. In Plants and UV-B: Responses to Environmental Change, P. Lumsden, ed (Cambridge: Cambridge University Press), pp. 157-168.

Braun, J., and Tevini, M. (1993). Regulation of Uv-Protective Pigment Synthesis in the Epidermal Layer of Rye Seedlings (*Secale-Cereale* L-Cv Kustro). Photochem. Photobiol. **57,** 318-323.

Britt, A.B. (1999). Molecular genetics of DNA repair in higher plants. Trends Plant Sci. **4,** 20-25.

Britt, A.B. (2004). Repair of DNA damage induced by solar UV. Photosynth Res **81,** 105-112.

Britt, A.B., and May, G.D. (2003). Re-engineering plant gene targeting. Trends Plant Sci. **8,** 90-95.

Britt, A.B., Chen, J.J., Wykoff, D., and Mitchell, D. (1993). A UV-sensitive mutant of *Arabidopsis* defective in the repair of pyrimidine-pyrimidinone(6-4) dimers. Science **261,** 1571-1574.

Brosché, M., and Strid, Å. (2003). Molecular events following perception of ultraviolet-B radiation by plants. Physiol. Plant. **117,** 1-10.

Brosché, M., Schuler, M.A., Kalbina, I., Connor, L., and Strid, Å. (2002). Gene regulation by low level UV-B radiation: identification by DNA array analysis. Photochem Photobiol Sci **1,** 656-664.

Brown, B.A., and Jenkins, G.I. (2008). UV-B signaling pathways with different fluence-rate response profiles are distinguished in mature Arabidopsis leaf tissue by requirement for UVR8, HY5, and HYH. Plant Physiol. **146,** 576-588.

Brown, B.A., Cloix, C., Jiang, G.H., Kaiserli, E., Herzyk, P., Kliebenstein, D.J., and Jenkins, G.I. (2005). A UV-B-specific signaling component orchestrates plant UV protection. Proc. Natl. Acad. Sci. USA **102,** 18225-18230.

Brzezowski, P., Richter, A.S., and Grimm, B. (2015). Regulation and function of tetrapyrrole biosynthesis in plants and algae. Bba-Bioenergetics **1847,** 968-985.

Brzezowski, P., Sharifi, M.N., Dent, R.M., Morhard, M.K., Niyogi, K.K., and Grimm, B. (2016). Mg chelatase in chlorophyll synthesis and retrograde signaling in *Chlamydomonas reinhardtii*: CHLI2 cannot substitute for CHLI1. J. Exp. Bot. **67,** 3925-3938.

Caldwell, M.M. (1971). Solar UV irradiation and the growth and development of higher plants. In Photophysiology, A.C. Giese, ed (New York: Academic Press), pp. 131-177.

Caldwell, M.M., and Flint, S.D. (1994). Stratospheric Ozone Reduction, Solar Uv-B Radiation and Terrestrial Ecosystems. Clim. Change **28,** 375-394.

Caldwell, M.M., Teramura, A.H., and Tevini, M. (1989). The changing solar ultraviolet climate and the ecological consequences for higher plants. Trends Ecol. Evol **4,** 363-367.

Caldwell, M.M., Bornman, J.F., Ballaré, C.L., Flint, S.D., and Kulandaivelu, G. (2007). Terrestrial ecosystems, increased solar ultraviolet radiation, and interactions with other climate change factors. Photochem Photobiol Sci **6,** 252-266.

Caldwell, M.M., Ballaré, C.L., Bornman, J.F., Flint, S.D., Björn, L.O., Teramura, A.H., Kulandaivelu, G., and Tevini, M. (2003). Terrestrial ecosystems, increased solar ultraviolet radiation and interactions with other climatic change factors. Photochem Photobiol Sci **2,** 29-38.

Casazza, A.P., Rossini, S., Rosso, M.G., and Soave, C. (2005). Mutational and expression analysis of ELIP1 and ELIP2 in *Arabidopsis thaliana*. Plant Mol. Biol **58,** 41-51.

Cerovic, Z.G., Masdoumier, G., Ghozlen, N.B., and Latouche, G. (2012). A new optical leaf-clip meter for simultaneous non-destructive assessment of leaf chlorophyll and epidermal flavonoids. Physiol. Plant. **146,** 251-260.

Chen, J.J., Mitchell, D.L., and Britt, A.B. (1994). A light-dependent pathway for the elimination of UV-Induced Pyrimidine (6-4) Pyrimidinone photoproducts in Arabidopsis. Plant Cell **6,** 1311-1317.

Cheng, F., Zhou, Y.H., Xia, X.J., Shi, K., Zhou, J., and Yu, J.Q. (2014). Chloroplastic thioredoxin-*f* and thioredoxin-*m*1/4 play important roles in brassinosteroids-induced changes in CO2 assimilation and cellular redox homeostasis in tomato. J. Exp. Bot. **65,** 4335-4347.

Chi, W., He, B., Mao, J., Jiang, J., and Zhang, L. (2015). Plastid sigma factors: Their individual functions and regulation in transcription. Bba-Bioenergetics **1847,** 770-778.

Chi, Y.H., Moon, J.C., Park, J.H., Kim, H.S., Zulfugarov, I.S., Fanata, W.I., Jang, H.H., Lee, J.R., Lee, Y.M., Kim, S.T., Chung, Y.Y., Lim, C.O., Kim, J.Y., Yun, D.J., Lee, C.H., Lee, K.O., and Lee, S.Y. (2008). Abnormal chloroplast development and growth inhibition in rice thioredoxin *m* knock-down plants. Plant Physiol. **148,** 808-817.

Cho, R.J., and Campbell, M.J. (2000). Transcription, genomes, function. Trends Genet. **16,** 409-415.

Christie, J.M., and Jenkins, G.I. (1996). Distinct UV-B and UV-A/blue light signal transduction pathways induce chalcone synthase gene expression in Arabidopsis cells. Plant Cell **8,** 1555-1567.

Christie, J.M., Blackwood, L., Petersen, J., and Sullivan, S. (2015). Plant flavoprotein photoreceptors. Plant Cell Physiol. **56,** 401-413.

Christie, J.M., Arvai, A.S., Baxter, K.J., Heilmann, M., Pratt, A.J., O'Hara, A., Kelly, S.M., Hothorn, M., Smith, B.O., Hitomi, K., Jenkins, G.I., and Getzoff, E.D. (2012). Plant UVR8 photoreceptor senses UV-B by tryptophan-mediated disruption of cross-dimer salt bridges. Science **335,** 1492-1496.

Christopher, D.A., and Mullet, J.E. (1994). Separate photosensory pathways co-regulate blue light/ultraviolet-A-activated *psbD-psbC* transcription and light-induced D2 and CP43 degradation in barley (*Hordeum vulgare*) chloroplasts. Plant Physiol. **104,** 1119-1129.

Cloix, C., and Jenkins, G.I. (2008). Interaction of the *Arabidopsis* UV-B-specific signaling component UVR8 with chromatin. Molecular plant **1,** 118-128.

Cloix, C., Kaiserli, E., Heilmann, M., Baxter, K.J., Brown, B.A., O'Hara, A., Smith, B.O., Christie, J.M., and Jenkins, G.I. (2012). C-terminal region of the UV-B photoreceptor UVR8 initiates

signaling through interaction with the COP1 protein. Proc. Natl. Acad. Sci. USA **109,** 16366-16370.

Cnossen, I., Sanz-Forcada, J., Favata, F., Witasse, O., Zegers, T., and Arnold, N.F. (2007). Habitat of early life: Solar X-ray and UV radiation at Earth's surface 4–3.5 billion years ago. J. Geophys. Res. **112**.

Collet, J.F., and Messens, J. (2010). Structure, function, and mechanism of thioredoxin proteins. Antioxid. Redox Signal. **13,** 1205-1216.

Crutzen, P.J. (1970). The influence of nitrogen oxides on the atmospheric ozone content. Quart. J. R. Met. Soc **96,** 320-325.

Datta, P.P., Wilson, D.N., Kawazoe, M., Swami, N.K., Kaminishi, T., Sharma, M.R., Booth, T.M., Takemoto, C., Fucini, P., Yokoyama, S., and Agrawal, R.K. (2007). Structural aspects of RbfA action during small ribosomal subunit assembly. Mol. Cell **28,** 434-445.

Davey, M.P., Susanti, N.I., Wargent, J.J., Findlay, J.E., Paul Quick, W., Paul, N.D., and Jenkins, G.I. (2012). The UV-B photoreceptor UVR8 promotes photosynthetic efficiency in *Arabidopsis thaliana* exposed to elevated levels of UV-B. Photosynth Res **114,** 121-131.

Dobáková, M., Sobotka, R., Tichý, M., and Komenda, J. (2009). Psb28 protein is involved in the biogenesis of the photosystem II inner antenna CP47 (PsbB) in the cyanobacterium *Synechocystis* sp. PCC 6803. Plant Physiol. **149,** 1076-1086.

Dobrikova, A.G., Krasteva, V., and Apostolova, E.L. (2013). Damage and protection of the photosynthetic apparatus from UV-B radiation. I. Effect of ascorbate. J. Plant Physiol. **170,** 251-257.

Eichhorn, M., Augsten, H., and Döhler, G. (1994). Impact of UV-B radiation on photosynthetic electron transport of *Wolffia arrhiza*. Photosynthetica **29,** 613-618.

Endo, M., Araki, T., and Nagatani, A. (2016). Tissue-specific regulation of flowering by photoreceptors. Cell. Mol. Life Sci. **73,** 829-839.

Fagerberg, W.R. (2007). Below-ambient levels of UV induce chloroplast structural change and alter starch metabolism. Protoplasma **230,** 51-59.

FAO. (2014). Food and Nutrition in Numbers. 2014. (Rome: FAO).

FAO. (2016). The State of Food and Agriculture 2016. Climate change, agriculture and food security (Rome: FAO).

FAO. (2017). The State of Food and Agriculture 2017. Leveraging food systems for inclusive rural transformation (Rome: FAO).

FAO, WFP, and IFAD. (2012). The State of Food Insecurity in the World 2012. Economic growth is necessary but not sufficient to accelerate reduction of hunger and malnutrition. (Rome: FAO).

FAO, IFAD, and WFP. (2015). The State of Food Insecurity in the World 2015. Meeting the 2015 international hunger targets: taking stock of uneven progress, F.a.A.O.o.t.U. Nations, ed (Rome: FAO).

FAO, IFAD, UNICEF, WFP, and WHO. (2017). The State of Food Security and Nutrition in the World 2017. Building resilience for peace and food security (Rome: FAO).

Farman, J.C., Gardiner, B.G., and Shanklin, J.D. (1985). Large Losses of Total Ozone in Antarctica Reveal Seasonal Clox/Nox Interaction. Nature **315,** 207-210.

Favory, J.J., Stec, A., Gruber, H., Rizzini, L., Oravecz, A., Funk, M., Albert, A., Cloix, C., Jenkins, G.I., Oakeley, E.J., Seidlitz, H.K., Nagy, F., and Ulm, R. (2009). Interaction of COP1 and UVR8

regulates UV-B-induced photomorphogenesis and stress acclimation in *Arabidopsis*. EMBO J. **28,** 591-601.

Fernández, M.B., Tossi, V., Lamattina, L., and Cassia, R. (2016). A comprehensive phylogeny reveals functional conservation of the UV-B photoreceptor UVR8 from green algae to higher plants. Front Plant Sci **7,** 1698.

Fleischmann, T.T., Scharff, L.B., Alkatib, S., Hasdorf, S., Schöttler, M.A., and Bock, R. (2011). Nonessential plastid-encoded ribosomal proteins in tobacco: a developmental role for plastid translation and implications for reductive genome evolution. Plant Cell **23,** 3137-3155.

Fristedt, R., Scharff, L.B., Clarke, C.A., Wang, Q., Lin, C., Merchant, S.S., and Bock, R. (2014). RBF1, a plant homolog of the bacterial ribosome-binding factor RbfA, acts in processing of the chloroplast 16S ribosomal RNA. Plant Physiol. **164,** 201-215.

Frohnmeyer, H. (1999). In or out - photoreceptors in motion. Trends Plant Sci. **4,** 294-295.

Frohnmeyer, H., and Staiger, D. (2003). Ultraviolet-B radiation-mediated responses in plants. Balancing damage and protection. Plant Physiol. **133,** 1420-1428.

Frohnmeyer, H., Loyall, L., Blatt, M.R., and Grabov, A. (1999). Millisecond UV-B irradiation evokes prolonged elevation of cytosolic-free Ca2+ and stimulates gene expression in transgenic parsley cell cultures. Plant J. **20,** 109-117.

Fuglevand, G., Jackson, J.A., and Jenkins, G.I. (1996). UV-B, UV-A, and blue light signal transduction pathways interact synergistically to regulate chalcone synthase gene expression in Arabidopsis. Plant Cell **8,** 2347-2357.

Gao, C., Yang, B., Zhang, D., Chen, M., and Tian, J. (2016). Enhanced metabolic process to indole alkaloids in *Clematis terniflora* DC. after exposure to high level of UV-B irradiation followed by the dark. BMC Plant Biol. **16**.

Gao, W., Zheng, Y., Slusser, J.R., Heisler, G.M., Grant, R.H., Xu, J., and He, D. (2004). Effects of supplementary ultraviolet-B irradiance on maize yield and qualities: a field experiment. Photochem. Photobiol. **80,** 127-131.

Gao, Z.P., Chen, G.X., and Yang, Z.N. (2012). Regulatory role of Arabidopsis pTAC14 in chloroplast development and plastid gene expression. Plant Signal. Behav **7,** 1354-1356.

Gao, Z.P., Yu, Q.B., Zhao, T.T., Ma, Q., Chen, G.X., and Yang, Z.N. (2011). A functional component of the transcriptionally active chromosome complex, Arabidopsis pTAC14, interacts with pTAC12/HEMERA and regulates plastid gene expression. Plant Physiol. **157,** 1733-1745.

Gartia, S., Pradhan, M.K., Joshi, P.N., Biswal, U.C., and Biswal, B. (2003). UV-A irradiation guards the photosynthetic apparatus against UV-B-induced damage. Photosynthetica **41,** 545-549.

Geigenberger, P., and Fernie, A.R. (2014). Metabolic control of redox and redox control of metabolism in plants. Antioxid. Redox Signal. **21,** 1389-1421.

Geisler, M., Kolukisaoglu, H.Ü., Bouchard, R., Billion, K., Berger, J., Saal, B., Frangne, N., Koncz-Kálmán, Z., Koncz, C., Dudler, R., Blakeslee, J.J., Murphy, A.S., Martinoia, E., and Schulz, B. (2003). TWISTED DWARF1, a unique plasma membrane-anchored immunophilin-like protein, interacts with *Arabidopsis* multidrug resistance-like transporters AtPGP1 and AtPGP19. Mol Biol Cell **14,** 4238-4249.

Gelhaye, E., Rouhier, N., Navrot, N., and Jacquot, J.P. (2005). The plant thioredoxin system. Cell. Mol. Life Sci. **62,** 24-35.

Godfray, H.C.J., Beddington, J.R., Crute, I.R., Haddad, L., Lawrence, D., Muir, J.F., Pretty, J., Robinson, S., Thomas, S.M., and Toulmin, C. (2010). Food security: The challenge of feeding 9 billion people. Science **327,** 812-818.

Götz, M., Albert, A., Stich, S., Heller, W., Scherb, H., Krins, A., Langebartels, C., Seidlitz, H.K., and Ernst, D. (2010). PAR modulation of the UV-dependent levels of flavonoid metabolites in *Arabidopsis thaliana* (L.) Heynh. leaf rosettes: cumulative effects after a whole vegetative growth period. Protoplasma **243,** 95-103.

Green, B.R., Pichersky, E., and Kloppstech, K. (1991). Chlorophyll a/b-binding proteins: an extended family. Trends Biochem. Sci. **16,** 181-186.

Grimm, B., and Kloppstech, K. (1987). The early light-inducible proteins of barley. Characterization of two families of 2-h-specific nuclear-coded chloroplast proteins. Eur. J. Biochem. **167,** 493-499.

Grimm, B., Kruse, E., and Kloppstech, K. (1989). Transiently expressed early light-inducible thylakoid proteins share transmembrane domains with light-harvesting chlorophyll binding proteins. Plant Mol. Biol **13,** 583-593.

Gruber, H., Heijde, M., Heller, W., Albert, A., Seidlitz, H.K., and Ulm, R. (2010). Negative feedback regulation of UV-B-induced photomorphogenesis and stress acclimation in *Arabidopsis*. Proc. Natl. Acad. Sci. USA **107,** 20132-20137.

Gupta, R., Bhadauriya, P., Chauhan, V.S., and Bisen, P.S. (2008). Impact of UV-B radiation on thylakoid membrane and fatty acid profile of *Spirulina platensis*. Curr. Microbiol. **56,** 156-161.

Hahlbrock, K., and Scheel, D. (1989). Physiology and Molecular-Biology of Phenylpropanoid Metabolism. Annu Rev Plant Physiol Plant Mol Bio **40,** 347-369.

Haque, E., Taniguchi, H., Hassan, M.M., Bhowmik, P., Karim, M.R., Smiech, M., Zhao, K., Rahman, M., and Islam, T. (2018). Application of CRISPR/Cas9 genome editing technology for the improvement of crops cultivated in tropical climates: recent progress, prospects, and challenges. Front Plant Sci **9,** 617.

Hayami, N., Sakai, Y., Kimura, M., Saito, T., Tokizawa, M., Iuchi, S., Kurihara, Y., Matsui, M., Nomoto, M., Tada, Y., and Yamamoto, Y.Y. (2015). The Responses of Arabidopsis *Early Light-Induced Protein2* to Ultraviolet B, High Light, and Cold Stress Are Regulated by a Transcriptional Regulatory Unit Composed of Two Elements. Plant Physiol. **169,** 840-855.

Hayes, S., Velanis, C.N., Jenkins, G.I., and Franklin, K.A. (2014). UV-B detected by the UVR8 photoreceptor antagonizes auxin signaling and plant shade avoidance. Proc. Natl. Acad. Sci. USA **111,** 11894-11899.

Hayes, S., Sharma, A., Fraser, D.P., Trevisan, M., Cragg-Barber, C.K., Tavridou, E., Fankhauser, C., Jenkins, G.I., and Franklin, K.A. (2017). UV-B perceived by the UVR8 photoreceptor inhibits plant thermomorphogenesis. Curr. Biol. **27,** 120-127.

Hectors, K., Prinsen, E., De Coen, W., Jansen, M.A.K., and Guisez, Y. (2007). *Arabidopsis thaliana* plants acclimated to low dose rates of ultraviolet B radiation show specific changes in morphology and gene expression in the absence of stress symptoms. New Phytol. **175,** 255-270.

Heijde, M., and Ulm, R. (2012). UV-B photoreceptor-mediated signalling in plants. Trends Plant Sci. **17,** 230-237.

Heijde, M., Binkert, M., Yin, R., Ares-Orpel, F., Rizzini, L., Van De Slijke, E., Persiau, G., Nolf, J., Gevaert, K., De Jaeger, G., and Ulm, R. (2013). Constitutively active UVR8 photoreceptor variant in *Arabidopsis*. Proc. Natl. Acad. Sci. USA **110,** 20326-20331.

Hideg, É., Jansen, M.A.K., and Strid, Å. (2013). UV-B exposure, ROS, and stress: inseparable companions or loosely linked associates? Trends Plant Sci. **18,** 107-115.

Hiltbrunner, A., Grünig, K., Alvarez-Huerta, M., Infanger, S., Bauer, J., and Kessler, F. (2004). AtToc90, a new GTP-binding component of the *Arabidopsis* chloroplast protein import machinery. Plant Mol. Biol **54,** 427-440.

Hiltbrunner, A., Bauer, J., Vidi, P.A., Infanger, S., Weibel, P., Hohwy, M., and Kessler, F. (2001). Targeting of an abundant cytosolic form of the protein import receptor at Toc159 to the outer chloroplast membrane. J. Cell Biol. **154,** 309-316.

Hoffman, P.D., Batschauer, A., and Hays, J.B. (1996). PHH1, a novel gene from *Arabidopsis thaliana* that encodes a protein similar to plant blue-light photoreceptors and microbial photolyases. Mol. Gen. Genet. **253,** 259-265.

Höhner, R., Aboukila, A., Kunz, H.H., and Venema, K. (2016). Proton gradients and proton-dependent transport processes in the Chloroplast. Front Plant Sci **7,** 218.

Hollósy, F. (2002). Effects of ultraviolet radiation on plant cells. Micron **33,** 179-197.

Holmgren, A. (1989). Thioredoxin and glutaredoxin systems. J. Biol. Chem. **264,** 13963-13966.

Hornitschek, P., Kohnen, M.V., Lorrain, S., Rougemont, J., Ljung, K., López-Vidriero, I., Franco-Zorrilla, J.M., Solano, R., Trevisan, M., Pradervand, S., Xenarios, I., and Fankhauser, C. (2012). Phytochrome interacting factors 4 and 5 control seedling growth in changing light conditions by directly controlling auxin signaling. Plant J. **71,** 699-711.

Hu, Z., Li, H., Chen, S., and Yang, Y. (2013). Chlorophyll content and photosystem II efficiency in soybean exposed to supplemental ultraviolet-B radiation. Photosynthetica **51,** 151-157.

IPCC. (2007). Climate Change 2007 – Impacts, Adaptation and Vulnerability: Contribution of Working Group II to the Fourth Assessment Report of the IPCC. (Cambridge, UK: Cambridge University Press).

Ivanova, Y., Smith, M.D., Chen, K., and Schnell, D.J. (2004). Members of the Toc159 import receptor family represent distinct pathways for protein targeting to plastids. Mol Biol Cell **15,** 3379-3392.

Izumi, M., Ishida, H., Nakamura, S., and Hidema, J. (2017). Entire Photodamaged Chloroplasts Are Transported to the Central Vacuole by Autophagy. Plant Cell **29,** 377-394.

Jaganathan, D., Ramasamy, K., Sellamuthu, G., Jayabalan, S., and Venkataraman, G. (2018). CRISPR for crop improvement: An update review. Front Plant Sci **9,** 985.

Jansen, M.A.K., and Bornman, J.F. (2012). UV-B radiation: from generic stressor to specific regulator. Physiol. Plant. **145,** 501-504.

Jansen, M.A.K., Gaba, V., and Greenberg, B.M. (1998). Higher plants and UV-B radiation: balancing damage, repair and acclimation. Trends Plant Sci. **3,** 131-135.

Jarvis, P., Chen, L.J., Li, H., Peto, C.A., Fankhauser, C., and Chory, J. (1998). An *Arabidopsis* mutant defective in the plastid general protein import apparatus. Science **282,** 100-103.

Jenkins, G.I. (2009). Signal transduction in responses to UV-B radiation. Annu. Rev. Plant Biol. **60,** 407-431.

Jenkins, G.I. (2014a). The UV-B photoreceptor UVR8: from structure to physiology. Plant Cell **26,** 21-37.

Jenkins, G.I. (2014b). Structure and function of the UV-B photoreceptor UVR8. Curr. Opin. Struct. Biol. **29,** 52-57.

Jenkins, G.I. (2017). Photomorphogenic responses to ultraviolet-B light. Plant Cell Environ **40,** 2544-2557.

Jenkins, G.I., Long, J.C., Wade, H.K., Shenton, M.R., and Bibikova, T.N. (2001). UV and blue light signalling: pathways regulating chalcone synthase gene expression in *Arabidopsis*. New Phytol. **151,** 121-131.

Jiang, Y.P., Cheng, F., Zhou, Y.H., Xia, X.J., Mao, W.H., Shi, K., Chen, Z., and Yu, J.Q. (2012). Cellular glutathione redox homeostasis plays an important role in the brassinosteroid-induced increase in CO2 assimilation in *Cucumis sativus*. New Phytol. **194,** 932-943.

Jones, P.G., and Inouye, M. (1996). RbfA, a 30S ribosomal binding factor, is a cold-shock protein whose absence triggers the cold-shock response. Mol. Microbiol. **21,** 1207-1218.

Jordan, B.R. (1996). The effects of ultraviolet-B radiation on plants: A molecular perspective. In Advances in Botanical Research, J.A. Callow, ed (London: Academic Press), pp. 97-162.

Jordan, B.R., He, J., Chow, W.S., and Anderson, J.M. (1992). Changes in mRNA levels and polypeptide subunits of ribulose 1,5-bisphosphate carboxylase in response to supplementary ultraviolet-B radiation. Plant Cell Environ **15,** 91-98.

Joshi, P.N., Ramaswamy, N.K., Raval, M.K., Desai, T.S., Nair, P.M., and Biswal, U.C. (1997). Response of senescing leaves of wheat seedlings to UVA radiation: inhibition of PSII activity in light and darkness. Environ Exper Bot **38,** 237-242.

Jung, J.H., Domijan, M., Klose, C., Biswas, S., Ezer, D., Gao, M., Khattak, A.K., Box, M.S., Charoensawan, V., Cortijo, S., Kumar, M., Grant, A., Locke, J.C., Schäfer, E., Jaeger, K.E., and Wigge, P.A. (2016). Phytochromes function as thermosensors in *Arabidopsis*. Science **354,** 886-889.

Kaiser, T., and Batschauer, A. (1995). *Cis*-acting elements of the *CHS1* gene from white mustard controlling promoter activity and spatial patterns of expression. Plant Mol. Biol **28,** 231-243.

Kaiserli, E., and Jenkins, G.I. (2007). UV-B promotes rapid nuclear translocation of the *Arabidopsis* UV-B specific signaling component UVR8 and activates its function in the nucleus. Plant Cell **19,** 2662-2673.

Kanamaru, K., and Tanaka, K. (2004). Roles of chloroplast RNA polymerase sigma factors in chloroplast development and stress response in higher plants. Biosci Biotechnol Biochem **68,** 2215-2223.

Kataria, S., Jajoo, A., and Guruprasad, K.N. (2014). Impact of increasing Ultraviolet-B (UV-B) radiation on photosynthetic processes. J Photochem Photobiol B **137,** 55-66.

Kendrick, R.E., and Kronenberg, G.H.M. (1994). Photomorphogenesis in Plants. (Dordrecht: Springer).

Kessler, F., and Schnell, D.J. (2004). Chloroplast protein import: solve the GTPase riddle for entry. Trends Cell Biol. **14,** 334-338.

Kilian, J., Whitehead, D., Horak, J., Wanke, D., Weinl, S., Batistic, O., D'Angelo, C., Bornberg-Bauer, E., Kudla, J., and Harter, K. (2007). The AtGenExpress global stress expression data set: protocols, evaluation and model data analysis of UV-B light, drought and cold stress responses. Plant J. **50,** 347-363.

Kim, B.C., Tennessen, D.J., and Last, R.L. (1998). UV-B-induced photomorphogenesis in *Arabidopsis thaliana*. Plant J. **15,** 667-674.

Kim, W.Y., Fujiwara, S., Suh, S.S., Kim, J., Kim, Y., Han, L., David, K., Putterill, J., Nam, H.G., and Somers, D.E. (2007). ZEITLUPE is a circadian photoreceptor stabilized by GIGANTEA in blue light. Nature **449,** 356-360.

Kleine, T., Kindgren, P., Benedict, C., Hendrickson, L., and Strand, Å. (2007). Genome-wide gene expression analysis reveals a critical role for CRYPTOCHROME1 in the response of *Arabidopsis* to high irradiance. Plant Physiol. **144,** 1391-1406.

Kliebenstein, D.J., Lim, J.E., Landry, L.G., and Last, R.L. (2002). Arabidopsis *UVR8* regulates Ultraviolet-B signal transduction and tolerance and contains sequence similarity to Human *Regulator of Chromatin Condensation 1*. Plant Physiol. **130,** 234-243.

Kong, S.G., and Okajima, K. (2016). Diverse photoreceptors and light responses in plants. J. Plant Res. **129,** 111-114.

Königer, M., Delamaide, J.A., Marlow, E.D., and Harris, G.C. (2008). *Arabidopsis thaliana* leaves with altered chloroplast numbers and chloroplast movement exhibit impaired adjustments to both low and high light. J. Exp. Bot. **59,** 2285-2297.

Kubis, S., Baldwin, A., Patel, R., Razzaq, A., Dupree, P., Lilley, K., Kurth, J., Leister, D., and Jarvis, P. (2003). The Arabidopsis *ppi1* mutant is specifically defective in the expression, chloroplast import, and accumulation of photosynthetic proteins. Plant Cell **15,** 1859-1871.

Legris, M., Klose, C., Burgie, E.S., Rojas, C.C., Neme, M., Hiltbrunner, A., Wigge, P.A., Schäfer, E., Vierstra, R.D., and Casal, J.J. (2016). Phytochrome B integrates light and temperature signals in *Arabidopsis*. Science **354,** 897-900.

Li, J., Li, G., Wang, H., and Wang Deng, X. (2011a). Phytochrome signaling mechanisms. Arabidopsis Book **9,** e0148.

Li, L., Ljung, K., Breton, G., Schmitz, R.J., Pruneda-Paz, J., Cowing-Zitron, C., Cole, B.J., Ivans, L.J., Pedmale, U.V., Jung, H.S., Ecker, J.R., Kay, S.A., and Chory, J. (2012). Linking photoreceptor excitation to changes in plant architecture. Genes Dev. **26,** 785-790.

Li, X., Wang, Q., Yu, X., Liu, H., Yang, H., Zhao, C., Liu, X., Tan, C., Klejnot, J., Zhong, D., and Lin, C. (2011b). Arabidopsis cryptochrome 2 (CRY2) functions by the photoactivation mechanism distinct from the tryptophan (trp) triad-dependent photoreduction. Proc. Natl. Acad. Sci. USA **108,** 20844-20849.

Lidon, J.C.F., Reboredo, F.H., Leitão, A.E., Silva, M.M.A., Duarte, M.P., and Ramalho, J.C. (2012). Impact of UV-B radiation on photosynthesis – an overview. Emir. J. Food. Agric **24,** 546-556.

Liu, R., Xu, Y.H., Jiang, S.C., Lu, K., Lu, Y.F., Feng, X.J., Wu, Z., Liang, S., Yu, Y.T., Wang, X.F., and Zhang, D.P. (2013). Light-harvesting chlorophyll *a/b*-binding proteins, positively involved in abscisic acid signalling, require a transcription repressor, WRKY40, to balance their function. J. Exp. Bot. **64,** 5443-5456.

Liu, Z., Hossain, G.S., Islas-Osuna, M.A., Mitchell, D.L., and Mount, D.W. (2000). Repair of UV damage in plants by nucleotide excision repair: *Arabidopsis UVH1* DNA repair gene is a homolog of *Saccharomyces cerevisiae Rad1*. Plant J. **21,** 519-528.

Loll, B., Kern, J., Saenger, W., Zouni, A., and Biesiadka, J. (2007). Lipids in photosystem II: interactions with protein and cofactors. Bba-Bioenergetics **1767,** 509-519.

Love, M.I., Huber, W., and Anders, S. (2014). Moderated estimation of fold change and dispersion for RNA-seq data with DESeq2. Genome Biol **15,** 550.

Lu, Y. (2016). Identification and roles of photosystem II assembly, stability, and repair factors in Arabidopsis. Front Plant Sci **7**.

Luo, T., Fan, T., Liu, Y., Rothbart, M., Yu, J., Zhou, S., Grimm, B., and Luo, M. (2012). Thioredoxin redox regulates ATPase activity of magnesium chelatase CHLI subunit and modulates redox-

mediated signaling in tetrapyrrole biosynthesis and homeostasis of reactive oxygen species in pea plants. Plant Physiol. **159,** 118-130.

Mackerness, S.A.H., Surplus, S.L., Jordan, B.R., and Thomas, B. (1998). Effects of supplementary ultraviolet-B radiation on photosynthetic transcripts at different stages of leaf development and light levels in Pea (*Pisum sativum* L.): role of active oxygen species and antioxidant enzymes. Photochem. Photobiol. **68,** 88-96.

Martinoia, E., Klein, M., Geisler, M., Bovet, L., Forestier, C., Kolukisaoglu, Ü., Müller-Röber, B., and Schulz, B. (2001). Multifunctionality of plant ABC transporters – more than just detoxifiers. Planta **214,** 345-355.

Mattoo, A.K., Marder, J.B., and Edelman, M. (1989). Dynamics of the photosystem II reaction center. Cell **56,** 241-246.

Mattoo, A.K., Giardi, M.T., Raskind, A., and Edelman, M. (1999). Dynamic metabolism of photosystem II reaction center proteins and pigments. Physiol. Plant. **107,** 454-461.

Mazza, C.A., and Ballare, C.L. (2015). Photoreceptors UVR8 and phytochrome B cooperate to optimize plant growth and defense in patchy canopies. New Phytol. **207,** 4-9.

Mazza, C.A., Boccalandro, H.E., Giordano, C.V., Battista, D., Scopel, A.L., and Ballaré, C.L. (2000). Functional significance and induction by solar radiation of ultraviolet-absorbing sunscreens in field-grown soybean crops. Plant Physiol. **122,** 117-126.

Mellenthin, M., Ellersiek, U., Börger, A., and Baier, M. (2014). Expression of the *Arabidopsis* sigma factor SIG5 is photoreceptor and photosynthesis controlled. Plants **3,** 359-391.

Meyer, Y., Riondet, C., Constans, L., Abdelgawwad, M.R., Reichheld, J.P., and Vignols, F. (2006). Evolution of redoxin genes in the green lineage. Photosynth Res **89,** 179-192.

Mi, H., Muruganujan, A., Casagrande, J.T., and Thomas, P.D. (2013). Large-scale gene function analysis with the PANTHER classification system. Nature protocols **8,** 1551-1566.

Mi, H., Huang, X., Muruganujan, A., Tang, H., Mills, C., Kang, D., and Thomas, P.D. (2017). PANTHER version 11: expanded annotation data from Gene Ontology and Reactome pathways, and data analysis tool enhancements. Nucleic Acids Res. **45,** D183-D189.

Molina, M.J., and Rowland, F.S. (1974). Stratospheric sink for chlorofluoromethanes: chlorine atomc-atalysed destruction of ozone. Nature **249,** 810-812.

Montané, M.H., and Kloppstech, K. (2000). The family of light-harvesting-related proteins (LHCs, ELIPs, HLIPs): was the harvesting of light their primary function? Gene **258,** 1-8.

Monte, E., Tepperman, J.M., Al-Sady, B., Kaczorowski, K.A., Alonso, J.M., Ecker, J.R., Li, X., Zhang, Y., and Quail, P.H. (2004). The phytochrome-interacting transcription factor, PIF3, acts early, selectively, and positively in light-induced chloroplast development. Proc. Natl. Acad. Sci. USA **101,** 16091-16098.

Morales, L.O., Brosché, M., Vainonen, J.P., Sipari, N., Lindfors, A.V., Strid, Å., and Aphalo, P.J. (2015). Are solar UV-B- and UV-A-dependent gene expression and metabolite accumulation in *Arabidopsis* mediated by the stress response regulator RADICAL-INDUCED CELL DEATH1? Plant Cell Environ **38,** 878-891.

Morales, L.O., Brosché, M., Vainonen, J., Jenkins, G.I., Wargent, J.J., Sipari, N., Strid, Å., Lindfors, A.V., Tegelberg, R., and Aphalo, P.J. (2013). Multiple roles for UV RESISTANCE LOCUS8 in regulating gene expression and metabolite accumulation in Arabidopsis under solar ultraviolet radiation. Plant Physiol. **161,** 744-759.

Motohashi, R., Yamazaki, T., Myouga, F., Ito, T., Ito, K., Satou, M., Kobayashi, M., Nagata, N., Yoshida, S., Nagashima, A., Tanaka, K., Takahashi, S., and Shinozaki, K. (2007). Chloroplast

ribosome release factor 1 (AtcpRF1) is essential for chloroplast development. Plant Mol. Biol **64,** 481-497.

Mudd, E.A., Sullivan, S., Gisby, M.F., Mironov, A., Kwon, C.S., Chung, W.I., and Day, A. (2008). A 125 kDa RNase E/G-like protein is present in plastids and is essential for chloroplast development and autotrophic growth in *Arabidopsis*. J. Exp. Bot. **59,** 2597-2610.

Murashige, T., and Skoog, F. (1962). A revised medium for rapid growth and bio assays with tobacco tissue cultures. Physiol. Plant. **15,** 473-497.

Murchie, E.H., and Niyogi, K.K. (2011). Manipulation of photoprotection to improve plant photosynthesis. Plant Physiol. **155,** 86-92.

Nagashima, A., Hanaoka, M., Shikanai, T., Fujiwara, M., Kanamaru, K., Takahashi, H., and Tanaka, K. (2004). The multiple-stress responsive plastid sigma factor, SIG5, directs activation of the *psbD* blue light-responsive promoter (BLRP) in *Arabidopsis thaliana*. Plant Cell Physiol. **45,** 357-368.

Naranjo, B., Mignée, C., Krieger-Liszkay, A., Hornero-Méndez, D., Gallardo-Guerrero, L., Cejudo, F.J., and Lindahl, M. (2016). The chloroplast NADPH thioredoxin reductase C, NTRC, controls non-photochemical quenching of light energy and photosynthetic electron transport in *Arabidopsis*. Plant Cell Environ **39,** 804-822.

Nellemann, C., MacDevette, M., Manders, T., Eickhout, B., Svihus, B., Prins, A.G., and Kaltenborn, P.B. (2009). The environmental food crisis: the environment's role in averting future food crises: a UNEP rapid response assessment. (Norway: UNEP/Earthprint).

Nikkanen, L., and Rintamäki, E. (2014). Thioredoxin-dependent regulatory networks in chloroplasts under fluctuating light conditions. Philosophical transactions of the Royal Society of London. Series B, Biological sciences **369,** 20130224.

Nikkanen, L., Toivola, J., Diaz, M.G., and Rintamäki, E. (2017). Chloroplast thioredoxin systems: prospects for improving photosynthesis. Philosophical transactions of the Royal Society of London. Series B, Biological sciences **372,** 20160474.

Noordally, Z.B., Ishii, K., Atkins, K.A., Wetherill, S.J., Kusakina, J., Walton, E.J., Kato, M., Azuma, M., Tanaka, K., Hanaoka, M., and Dodd, A.N. (2013). Circadian control of chloroplast transcription by a nuclear-encoded timing signal. Science **339,** 1316-1319.

Nordborg, M., Hu, T.T., Ishino, Y., Jhaveri, J., Toomajian, C., Zheng, H., Bakker, E., Calabrese, P., Gladstone, J., Goyal, R., Jakobsson, M., Kim, S., Morozov, Y., Padhukasahasram, B., Plagnol, V., Rosenberg, N.A., Shah, C., Wall, J.D., Wang, J., Zhao, K., Kalbfleisch, T., Schulz, V., Kreitman, M., and Bergelson, J. (2005). The pattern of polymorphism in *Arabidopsis thaliana*. PLoS Biol. **3,** e196.

Onda, Y., Yagi, Y., Saito, Y., Takenaka, N., and Toyoshima, Y. (2008). Light induction of Arabidopsis *SIG1* and *SIG5* transcripts in mature leaves: differential roles of cryptochrome 1 and cryptochrome 2 and dual function of SIG5 in the recognition of plastid promoters. Plant J. **55,** 968-978.

Oravecz, A., Baumann, A., Máté, Z., Brzezinska, A., Molinier, J., Oakeley, E.J., Adám, E., Schäfer, E., Nagy, F., and Ulm, R. (2006). CONSTITUTIVELY PHOTOMORPHOGENIC1 is required for the UV-B response in *Arabidopsis*. Plant Cell **18,** 1975-1990.

Oreb, M., Tews, I., and Schleiff, E. (2008). Policing Tic 'n' Toc, the doorway to chloroplasts. Trends Cell Biol. **18,** 19-27.

Oreb, M., Höfle, A., Koenig, P., Sommer, M.S., Sinning, I., Wang, F., Tews, I., Schnell, D.J., and Schleiff, E. (2011). Substrate binding disrupts dimerization and induces nucleotide exchange of the chloroplast GTPase Toc33. Biochem. J. **436,** 313-319.

Ort, D.R., Merchant, S.S., Alric, J., Barkan, A., Blankenship, R.E., Bock, R., Croce, R., Hanson, M.R., Hibberd, J.M., Long, S.P., Moore, T.A., Moroney, J., Niyogi, K.K., Parry, M.A., Peralta-Yahya, P.P., Prince, R.C., Redding, K.E., Spalding, M.H., van Wijk, K.J., Vermaas, W.F., von Caemmerer, S., Weber, A.P., Yeates, T.O., Yuan, J.S., and Zhu, X.G. (2015). Redesigning photosynthesis to sustainably meet global food and bioenergy demand. Proc. Natl. Acad. Sci. USA **112,** 8529-8536.

Passardi, F., Dobias, J., Valério, L., Guimil, S., Penel, C., and Dunand, C. (2007). Morphological and physiological traits of three major *Arabidopsis thaliana* accessions. J. Plant Physiol. **164,** 980-992.

Paul, N. (2001). Plant responses to UV-B: time to look beyond stratospheric ozone depletion? New Phytol. **150,** 5-8.

Pedmale, U.V., Huang, S.C., Zander, M., Cole, B.J., Hetzel, J., Ljung, K., Reis, P.A.B., Sridevi, P., Nito, K., Nery, J.R., Ecker, J.R., and Chory, J. (2016). Cryptochromes Interact Directly with PIFs to Control Plant Growth in Limiting Blue Light. Cell **164,** 233-245.

Peltier, G., and Cournac, L. (2002). Chlororespiration. Annu. Rev. Plant Biol. **53,** 523-550.

Pfalz, J., Liere, K., Kandlbinder, A., Dietz, K.J., and Oelmüller, R. (2006). pTAC2, -6, and -12 are components of the transcriptionally active plastid chromosome that are required for plastid gene expression. Plant Cell **18,** 176-197.

Pötter, E., and Kloppstech, K. (1993). Effects of light stress on the expression of early light-inducible proteins in barley. Eur. J. Biochem. **214,** 779-786.

Poulson, M.E., Boeger, M.R., and Donahue, R.A. (2006). Response of photosynthesis to high light and drought for *Arabidopsis thaliana* grown under a UV-B enhanced light regime. Photosynth Res **90,** 79-90.

Pretty, J. (2008). Agricultural sustainability: concepts, principles and evidence. Philosophical transactions of the Royal Society of London. Series B, Biological sciences **363,** 447-465.

Pyle, J.A. (1997). Global ozone depletion: observation and theory. In Plants and UV-B: Responses to Environmental Change, P.J. Lumbsden, ed (Cambridge: Cambridge University Press), pp. 3-12.

Quail, P.H. (1997). An emerging molecular map of the phytochromes. Plant Cell Environ **20,** 657-665.

Quan, J., Song, S., Abdulrashid, K., Chai, Y., Yue, M., and Liu, X. (2018). Separate and combined response to UV-B radiation and jasmonic acid on photosynthesis and growth characteristics of *Scutellaria baicalensis*. Int J Mol Sci **19,** 1194.

Ranjbarfordoei, A., Samson, R., and Van Damme, P. (2011). Photosynthesis performance in sweet almond [*Prunus dulcis* (Mill) D. Webb] exposed to supplemental UV-B radiation. Photosynthetica **49,** 107-111.

Rastogi, R.P., Richa, Kumar, A., Tyagi, M.B., and Sinha, R.P. (2010). Molecular mechanisms of ultraviolet radiation-induced DNA damage and repair. J Nucleic Acids **2010,** 592980.

Reed, J.W., Nagpal, P., Poole, D.S., Furuya, M., and Chory, J. (1993). Mutations in the gene for the red/far-red light receptor phytochrome B alter cell elongation and physiological responses throughout Arabidopsis development. Plant Cell **5,** 147-157.

Reinking, L. (2007). Examples of Image Analysis Using ImageJ.

Ries, G., Buchholz, G., Frohnmeyer, H., and Hohn, B. (2000a). UV-damage-mediated induction of homologous recombination in *Arabidopsis* is dependent on photosynthetically active radiation. Proc. Natl. Acad. Sci. USA **97,** 13425-13429.

Ries, G., Heller, W., Puchta, H., Sandermann, H., Seidlitz, H.K., and Hohn, B. (2000b). Elevated UV-B radiation reduces genome stability in plants. Nature **406,** 98-101.

Rius, S.P., Casati, P., Iglesias, A.A., and Gomez-Casati, D.F. (2008). Characterization of Arabidopsis lines deficient in GAPC-1, a cytosolic NAD-dependent glyceraldehyde-3-phosphate dehydrogenase. Plant Physiol. **148,** 1655-1667.

Rizzini, L., Favory, J.J., Cloix, C., Faggionato, D., O'Hara, A., Kaiserli, E., Baumeister, R., Schafer, E., Nagy, F., Jenkins, G.I., and Ulm, R. (2011). Perception of UV-B by the *Arabidopsis* UVR8 protein. Science **332,** 103-106.

Rossel, J.B., Wilson, I.W., and Pogson, B.J. (2002). Global changes in gene expression in response to high light in Arabidopsis. Plant Physiol. **130,** 1109-1120.

Rossini, S., Casazza, A.P., Engelmann, E.C., Havaux, M., Jennings, R.C., and Soave, C. (2006). Suppression of both ELIP1 and ELIP2 in Arabidopsis does not affect tolerance to photoinhibition and photooxidative stress. Plant Physiol. **141,** 1264-1273.

Rouhier, N., Cerveau, D., Couturier, J., Reichheld, J.P., and Rey, P. (2015). Involvement of thiol-based mechanisms in plant development. Biochimica et biophysica acta **1850,** 1479-1496.

Rozema, J., Björn, L.O., Bornman, J.F., Gaberscik, A., Hader, D.P., Trost, T., Germ, M., Klisch, M., Groniger, A., Sinha, R.P., Lebert, M., He, Y.Y., Buffoni-Hall, R., de Bakker, N.V., van de Staaij, J., and Meijkamp, B.B. (2002). The role of UV-B radiation in aquatic and terrestrial ecosystems - an experimental and functional analysis of the evolution of UV-absorbing compounds. J Photochem Photobiol B **66,** 2-12.

Ruijter, J.M., Ramakers, C., Hoogaars, W.M., Karlen, Y., Bakker, O., van den Hoff, M.J., and Moorman, A.F. (2009). Amplification efficiency: linking baseline and bias in the analysis of quantitative PCR data. Nucleic Acids Res. **37,** e45.

Rumeau, D., Peltier, G., and Cournac, L. (2007). Chlororespiration and cyclic electron flow around PSI during photosynthesis and plant stress response. Plant Cell Environ **30,** 1041-1051.

Safrany, J., Haasz, V., Máté, Z., Ciolfi, A., Feher, B., Oravecz, A., Stec, A., Dallmann, G., Morelli, G., Ulm, R., and Nagy, F. (2008). Identification of a novel cis-regulatory element for UV-B-induced transcription in Arabidopsis. Plant J. **54,** 402-414.

Sakaki, T., Kondo, N., and Sugahara, K. (1983). Breakdown of photosynthetic pigments and lipids in spinach leaves with ozone fumigation - Role of active oxygens. Physiol. Plant. **59,** 28-34.

Sánchez-Fernández, R., Rea, P.A., Emyr Davies, T.G., and Coleman, J.O.D. (2001a). Do plants have more genes than humans? Yes, when it comes to ABC proteins. Trends Plant Sci. **6,** 347-348.

Sánchez-Fernández, R., Davies, T.G., Coleman, J.O., and Rea, P.A. (2001b). The *Arabidopsis thaliana* ABC protein superfamily, a complete inventory. J. Biol. Chem. **276,** 30231-30244.

Sarvikas, P., Hakala, M., Pätsikkä, E., Tyystjärvi, T., and Tyystjärvi, E. (2006). Action spectrum of photoinhibition in leaves of wild type and *npq1-2* and *npq4-1* mutants of *Arabidopsis thaliana*. Plant Cell Physiol. **47,** 391-400.

Satou, M., Enoki, H., Oikawa, A., Ohta, D., Saito, K., Hachiya, T., Sakakibara, H., Kusano, M., Fukushima, A., Saito, K., Kobayashi, M., Nagata, N., Myouga, F., Shinozaki, K., and Motohashi, R. (2014). Integrated analysis of transcriptome and metabolome of *Arabidopsis albino or pale green* mutants with disrupted nuclear-encoded chloroplast proteins. Plant Mol. Biol **85,** 411-428.

Schmittgen, T.D., and Livak, K.J. (2008). Analyzing real-time PCR data by the comparative C(T) method. Nature protocols **3,** 1101-1108.

Schneider, C.A., Rasband, W.S., and Eliceiri, K.W. (2012). NIH Image to ImageJ: 25 years of image analysis. Nat. Methods **9,** 671-675.

Schoefs, B. (2005). Plant Pigments: Properties, Analysis, Degradation. In Advances in Food and Nutrition Research (Academic Press), pp. 41-91.

Schürmann, P., and Buchanan, B.B. (2001). The structure and function of the ferredoxin/thioredoxin system in photosynthesis. In Regulation of Photosynthesis, E.M. Aro and B. Andersson, eds (Dordrecht: Springer Netherlands), pp. 331-361.

Schürmann, P., and Buchanan, B.B. (2008). The ferredoxin/thioredoxin system of oxygenic photosynthesis. Antioxid. Redox Signal. **10,** 1235-1274.

Searles, P.S., Flint, S.D., and Caldwell, M.M. (2001). A meta-analysis of plant field studies simulating stratospheric ozone depletion. Oecologia **127,** 1-10.

Shi, L.X., Hall, M., Funk, C., and Schröder, W.P. (2012). Photosystem II, a growing complex: Updates on newly discovered components and low molecular mass proteins. Bba-Bioenergetics **1817,** 13-25.

Singh, P., Kaloudas, D., and Raines, C.A. (2008). Expression analysis of the *Arabidopsis* CP12 gene family suggests novel roles for these proteins in roots and floral tissues. J. Exp. Bot. **59,** 3975-3985.

Smith, H., and Whitelam, G.C. (1997). The shade avoidance syndrome: Multiple responses mediated by multiple phytochromes. Plant Cell Environ **20,** 840-844.

Smith, M.D., Rounds, C.M., Wang, F., Chen, K., Afitlhile, M., and Schnell, D.J. (2004). atToc159 is a selective transit peptide receptor for the import of nucleus-encoded chloroplast proteins. J. Cell Biol. **165,** 323-334.

Somers, D.E., Devlin, P.F., and Kay, S.A. (1998). Phytochromes and cryptochromes in the entrainment of the *Arabidopsis* circadian clock. Science **282,** 1488-1490.

Soriano, G., Cloix, C., Heilmann, M., Nunez-Olivera, E., Martinez-Abaigar, J., and Jenkins, G.I. (2018). Evolutionary conservation of structure and function of the UVR8 photoreceptor from the liverwort *Marchantia polymorpha* and the moss *Physcomitrella patens*. New Phytol. **217,** 151-162.

Stracke, R., Favory, J.J., Gruber, H., Bartelniewoehner, L., Bartels, S., Binkert, M., Funk, M., Weisshaar, B., and Ulm, R. (2010). The *Arabidopsis* bZIP transcription factor HY5 regulates expression of the *PFG1/MYB12* gene in response to light and ultraviolet-B radiation. Plant Cell Environ **33,** 88-103.

Strid, Å., and Porra, R.J. (1992). Alterations in pigment content in leaves of *Pisum sativum* after exposure to supplementary UV-B. Plant Cell Physiol. **33,** 1015-1023.

Strid, Å., Chow, W.S., and Anderson, J.M. (1990). Effects of Supplementary Ultraviolet-B Radiation on Photosynthesis in *Pisum Sativum*. Bba-Bioenergetics **1020,** 260-268.

Strid, Å., Chow, W.S., and Anderson, J.M. (1994). UV-B damage and protection at the molecular level in plants. Photosynth Res **39,** 475-489.

Suesslin, C., and Frohnmeyer, H. (2003). An *Arabidopsis* mutant defective in UV-B light-mediated responses. Plant J. **33,** 591-601.

Surabhi, G.K., Reddy, K.R., and Singh, S.K. (2009). Photosynthesis, fluorescence, shoot biomass and seed weight responses of three cowpea (*Vigna unguiculata* (L.) Walp.) cultivars with contrasting sensitivity to UV-B radiation. Environ Exper Bot **66,** 160-171.

Takahashi, S., Milward, S.E., Yamori, W., Evans, J.R., Hillier, W., and Badger, M.R. (2010). The solar action spectrum of photosystem II damage. Plant Physiol. **153,** 988-993.

Teramura, A.H. (1983). Effects of ultraviolet-B radiation on the growth and yield of crop plants. Physiol. Plant. **58,** 415-427.

Teramura, A.H., and Sullivan, J.H. (1994). Effects of UV-B radiation on photosynthesis and growth of terrestrial plants. Photosynth Res **39,** 463-473.

Terry, M.J. (1997). Phytochrome chromophore-deficient mutants. Plant Cell Environ **20,** 740-745.

Tester, M., and Langridge, P. (2010). Breeding technologies to increase crop production in a changing world. Science **327,** 818-822.

Thimm, O., Bläsing, O., Gibon, Y., Nagel, A., Meyer, S., Kruger, P., Selbig, J., Müller, L.A., Rhee, S.Y., and Stitt, M. (2004). MAPMAN: a user-driven tool to display genomics data sets onto diagrams of metabolic pathways and other biological processes. Plant J. **37,** 914-939.

Tilbrook, K., Arongaus, A.B., Binkert, M., Heijde, M., Yin, R., and Ulm, R. (2013). The UVR8 UV-B Photoreceptor: Perception, Signaling and Response. Arabidopsis Book **11,** e0164.

Tilbrook, K., Dubois, M., Crocco, C.D., Yin, R., Chappuis, R., Allorent, G., Schmid-Siegert, E., Goldschmidt-Clermont, M., and Ulm, R. (2016). UV-B Perception and Acclimation in *Chlamydomonas reinhardtii*. Plant Cell **28,** 966-983.

Trost, P., Fermani, S., Marri, L., Zaffagnini, M., Falini, G., Scagliarini, S., Pupillo, P., and Sparla, F. (2006). Thioredoxin-dependent regulation of photosynthetic glyceraldehyde-3-phosphate dehydrogenase: autonomous vs. CP12-dependent mechanisms. Photosynth Res **89,** 263-275.

Trošt Sedej, T., and Gaberščik, A. (2008). The effects of enhanced UV-B radiation on physiological activity and growth of Norway spruce planted outdoors over 5 years. Trees **22,** 423-435.

Tsunoyama, Y., Morikawa, K., Shiina, T., and Toyoshima, Y. (2002). Blue light specific and differential expression of a plastid sigma factor, Sig5 in *Arabidopsis thaliana*. FEBS Lett. **516,** 225-228.

Tsunoyama, Y., Ishizaki, Y., Morikawa, K., Kobori, M., Nakahira, Y., Takeba, G., Toyoshima, Y., and Shiina, T. (2004). Blue light-induced transcription of plastid-encoded *psbD* gene is mediated by a nuclear-encoded transcription initiation factor, AtSig5. Proc. Natl. Acad. Sci. USA **101,** 3304-3309.

Turcsányi, E., and Vass, I. (2000). Inhibition of photosynthetic electron transport by UV-A radiation targets the photosystem II complex. Photochem. Photobiol. **72,** 513-520.

Tyystjärvi, E. (2008). Photoinhibition of Photosystem II and photodamage of the oxygen evolving manganese cluster. Coordin Chem Rev **252,** 361-376.

Tzvetkova-Chevolleau, T., Franck, F., Alawady, A.E., Dall'Osto, L., Carrière, F., Bassi, R., Grimm, B., Nussaume, L., and Havaux, M. (2007). The light stress-induced protein ELIP2 is a regulator of chlorophyll synthesis in *Arabidopsis thaliana*. Plant J. **50,** 795-809.

Ulm, R., Baumann, A., Oravecz, A., Máté, Z., Ádám, É., Oakeley, E.J., Schäfer, E., and Nagy, F. (2004). Genome-wide analysis of gene expression reveals function of the bZIP transcription factor HY5 in the UV-B response of *Arabidopsis*. Proc. Natl. Acad. Sci. USA **101,** 1397-1402.

UN, D.o.E.a.S.A. (2017). World Population Prospects: The 2017 Revision, Key Findings and Advance Tables. , P.D. Department of Economic and Social Affairs, ed (New York: United Nations, Department of Economic and Social Affairs, Population Division).

Usadel, B., Poree, F., Nagel, A., Lohse, M., Czedik-Eysenberg, A., and Stitt, M. (2009). A guide to using MapMan to visualize and compare Omics data in plants: a case study in the crop species, Maize. Plant Cell Environ **32,** 1211-1229.

Usadel, B., Nagel, A., Steinhauser, D., Gibon, Y., Bläsing, O.E., Redestig, H., Sreenivasulu, N., Krall, L., Hannah, M.A., Poree, F., Fernie, A.R., and Stitt, M. (2006). PageMan: an interactive ontology tool to generate, display, and annotate overview graphs for profiling experiments. BMC Bioinformatics **7,** 535.

van Rensen, J.J., Vredenberg, W.J., and Rodrigues, G.C. (2007). Time sequence of the damage to the acceptor and donor sides of photosystem II by UV-B radiation as evaluated by chlorophyll *a* fluorescence. Photosynth Res **94,** 291-297.

Vandenbussche, F., Tilbrook, K., Fierro, A.C., Marchal, K., Poelman, D., Van Der Straeten, D., and Ulm, R. (2014). Photoreceptor-mediated bending towards UV-B in Arabidopsis. Molecular plant **7,** 1041-1052.

Vanhaelewyn, L., Schumacher, P., Poelman, D., Fankhauser, C., Van Der Straeten, D., and Vandenbussche, F. (2016). *REPRESSOR OF ULTRAVIOLET-B PHOTOMORPHOGENESIS* function allows efficient phototropin mediated ultraviolet-B phototropism in etiolated seedlings. Plant Sci. **252,** 215-221.

Verrier, P.J., Bird, D., Burla, B., Dassa, E., Forestier, C., Geisler, M., Klein, M., Kolukisaoglu, Ü., Lee, Y., Martinoia, E., Murphy, A., Rea, P.A., Samuels, L., Schulz, B., Spalding, E.J., Yazaki, K., and Theodoulou, F.L. (2008). Plant ABC proteins - a unified nomenclature and updated inventory. Trends Plant Sci. **13,** 151-159.

Vidović, M., Morina, F., Milić, S., Zechmann, B., Albert, A., Winkler, J.B., and Veljović Jovanović, S. (2015). Ultraviolet-B component of sunlight stimulates photosynthesis and flavonoid accumulation in variegated *Plectranthus coleoides* leaves depending on background light. Plant Cell Environ **38,** 968-979.

Viro, M., and Kloppstech, K. (1980). Differential expression of the genes for ribulose-1,5-bisphosphate carboxylase and light-harvesting chlorophyll a/b protein in the developing barley leaf. Planta **150,** 41-45.

Vlad, D., Rappaport, F., Simon, M., and Loudet, O. (2010). Gene transposition causing natural variation for growth in *Arabidopsis thaliana*. PLoS Genet. **6,** e1000945.

Wade, H.K., Bibikova, T.N., Valentine, W.J., and Jenkins, G.I. (2001). Interactions within a network of phytochrome, cryptochrome and UV-B phototransduction pathways regulate chalcone synthase gene expression in *Arabidopsis* leaf tissue. Plant J. **25,** 675-685.

Wargent, J.J., and Jordan, B.R. (2013). From ozone depletion to agriculture: understanding the role of UV radiation in sustainable crop production. New Phytol. **197,** 1058-1076.

Wargent, J.J., Elfadly, E.M., Moore, J.P., and Paul, N.D. (2011). Increased exposure to UV-B radiation during early development leads to enhanced photoprotection and improved long-term performance in *Lactuca sativa*. Plant Cell Environ **34,** 1401-1413.

Watanabe, N., Evans, J.R., and Chow, W.S. (1994). Changes in the Photosynthetic Properties of Australian Wheat Cultivars over the Last Century. Aust. J. Plant Physiol. **21,** 169-183.

Waterworth, W.M., Jiang, O., West, C.E., Nikaido, M., and Bray, C.M. (2002). Characterization of *Arabidopsis* photolyase enzymes and analysis of their role in protection from ultraviolet-B radiation. J. Exp. Bot. **53,** 1005-1015.

Wittenberg, G., Levitan, A., Klein, T., Dangoor, I., Keren, N., and Danon, A. (2014). Knockdown of the *Arabidopsis thaliana* chloroplast protein disulfide isomerase 6 results in reduced levels of photoinhibition and increased D1 synthesis in high light. Plant J. **78,** 1003-1013.

Wu, D., Hu, Q., Yan, Z., Chen, W., Yan, C., Huang, X., Zhang, J., Yang, P., Deng, H., Wang, J., Deng, X., and Shi, Y. (2012). Structural basis of ultraviolet-B perception by UVR8. Nature **484,** 214-219.

Wu, M., Strid, Å., and Eriksson, L.A. (2013). Interactions and stabilities of the UV RESISTANCE LOCUS8 (UVR8) protein dimer and its key mutants. J Chem Inf Model **53,** 1736-1746.

Xia, B., Ke, H., Shinde, U., and Inouye, M. (2003). The role of RbfA in 16S rRNA processing and cell growth at low temperature in *Escherichia coli*. J. Mol. Biol. **332,** 575-584.

Xiong, F.S., and Day, T.A. (2001). Effect of solar ultraviolet-B radiation during springtime ozone depletion on photosynthesis and biomass production of Antarctic vascular plants. Plant Physiol. **125,** 738-751.

Xu, J., and Gao, K. (2010). UV-A enhanced growth and UV-B induced positive effects in the recovery of photochemical yield in *Gracilaria lemaneiformis* (Rhodophyta). J Photochem Photobiol B **100,** 117-122.

Yamburenko, M.V., Zubo, Y.O., and Börner, T. (2015). Abscisic acid affects transcription of chloroplast genes via protein phosphatase 2C-dependent activation of nuclear genes: repression by guanosine-3'-5'-bisdiphosphate and activation by sigma factor 5. Plant J. **82,** 1030-1041.

Yamori, W., Takahashi, S., Makino, A., Price, G.D., Badger, M.R., and von Caemmerer, S. (2011). The roles of ATP synthase and the cytochrome *b6/f* complexes in limiting chloroplast electron transport and determining photosynthetic capacity. Plant Physiol. **155,** 956-962.

Yao, J., Roy-Chowdhury, S., and Allison, L.A. (2003). AtSig5 is an essential nucleus-encoded Arabidopsis sigma-like factor. Plant Physiol. **132,** 739-747.

Yao, Y.N., Xuan, Z.Y., Li, Y.A., He, Y.M., Korpelainen, H., and Li, C.Y. (2006). Effects of ultraviolet-B radiation on crop growth, development, yield and leaf pigment concentration of tartary buckwheat (*Fagopyrum tataricum*) under field conditions. Eur J Agron **25,** 215-222.

Ye, J., Coulouris, G., Zaretskaya, I., Cutcutache, I., Rozen, S., and Madden, T.L. (2012). Primer-BLAST: a tool to design target-specific primers for polymerase chain reaction. BMC Bioinformatics **13,** 134.

Yi, C., and Deng, X.W. (2005). COP1 - from plant photomorphogenesis to mammalian tumorigenesis. Trends Cell Biol. **15,** 618-625.

Yin, R., Arongaus, A.B., Binkert, M., and Ulm, R. (2015). Two distinct domains of the UVR8 photoreceptor interact with COP1 to initiate UV-B signaling in Arabidopsis. Plant Cell **27,** 202-213.

Yoshizawa, E., Kaizuka, M., Yamagami, A., Higuchi-Takeuchi, M., Matsui, M., Kakei, Y., Shimada, Y., Sakuta, M., Osada, H., Asami, T., and Nakano, T. (2014). BPG3 is a novel chloroplast protein that involves the greening of leaves and related to brassinosteroid signaling. Biosci Biotechnol Biochem **78,** 420-429.

Yu, G.H., Li, W., Yuan, Z.Y., Cui, H.Y., Lv, C.G., Gao, Z.P., Han, B., Gong, Y.Z., and Chen, G.X. (2012). The effects of enhanced UV-B radiation on photosynthetic and biochemical activities in super-high-yield hybrid rice Liangyoupeijiu at the reproductive stage. Photosynthetica **51,** 33-44.

Yu, X., Liu, H., Klejnot, J., and Lin, C. (2010). The Cryptochrome Blue Light Receptors. Arabidopsis Book **8,** e0135.

Zhang, J.W., Hu, X., Henkow, L., Jordan, B.R., and Strid, Å. (1994). The Effects of Ultraviolet-B Radiation on the CF0F1-ATPase. Bba-Bioenergetics **1185,** 295-302.

Zhu, X.G., Long, S.P., and Ort, D.R. (2008). What is the maximum efficiency with which photosynthesis can convert solar energy into biomass? Curr. Opin. Biotechnol. **19,** 153-159.

Zhu, X.G., Long, S.P., and Ort, D.R. (2010). Improving photosynthetic efficiency for greater yield. Annu. Rev. Plant Biol. **61,** 235-261.

Ziolkowski, P.A., Koczyk, G., Galganski, L., and Sadowski, J. (2009). Genome sequence comparison of Col and Ler lines reveals the dynamic nature of *Arabidopsis* chromosomes. Nucleic Acids Res. **37,** 3189-3201.

Zvezdanović, J., Cvetić, T., Veljović-Jovanović, S., and Marković, D. (2009). Chlorophyll bleaching by UV-irradiation in vitro and in situ: Absorption and fluorescence studies. Radiat. Phys. Chem **78,** 25-32.

Zybailov, B., Rutschow, H., Friso, G., Rudella, A., Emanuelsson, O., Sun, Q., and van Wijk, K.J. (2008). Sorting signals, N-terminal modifications and abundance of the chloroplast proteome. *PLoS One* **3,** e1994.

9 Supplementary Information

9.1 Supplementary information for Materials and Methods

9.1.1 PCR – Primers and Conditions

Table 9.1 Primers for PCR

Primer name	Sequence	Annealing Temperature (°C)	Product size (bp)	
Actin_F	CAAGGCCGAGTATGATGAGG	58	228	
Actin_R	GAAACGCAGACGTAAGTAAAAAC			
SALK lines				
Left border LBb1.3	ATTTTGCCGATTTCGGAAC	60		
uvr8-6_L	TTTGCTTGAACCATCCGTTAG	60	wt	900 - 1100
uvr8-6_R	AATGGCATTGACTTCAGATGG		hm	564 - 864
lug444_L	AGGACCAATGAGAAGCATTCC	60	wt	900 - 1100
lug444_R	CAGGAAGTTGCTGATTTCGAG		hm	530 - 830
luh4_L	ATTAGCAATTGATGCACCTGG	60	wt	900 - 1100
luh4_R	TCCTTCACAAGGGACAAACAC		hm	537 - 837
seu-4_L	TTTCCGTGGTGTTTACGACTC	60	wt	900 - 1100
seu-4_R	TTTTTGGCATTAGGAGCAAAG		hm	609 - 909
sig5-1_L	TGACCATTCTCTAGTGTCAGCC	60	wt	900 - 1100
sig5-1_R	AGATGTTGATGGTGTTGGAGC		hm	433 - 733
elip2_L	GAACCCTTTTGACTTTGCCTC	60	wt	900 - 1100
elip2_R	TGAGGAAACTTTTTCTTCCCC		hm	436 - 736
rbf1-1_L	GATTTGTGTGCTGGACCTAGC	60	wt	900 - 1100
rbf1-1_R	GTTCTCCATTCCGCCTTAGTC		hm	439 - 739
rbf1-2_L	AACCACCTACAACCCCAAAAG	60	wt	900 - 1100
rbf1-2_R	TAGCTGTGTTTTGCATCCATC		hm	507 - 807
toc33_L	TTGGTTATGCCGAGTTTTCTG	60	wt	900 - 1100
toc33_R	TAGCAATCACCCAAACCTTTG		hm	432 - 732
tfp_L	AAATAACGTCCTTCCAAACCC	60	wt	900 - 1100
tfp_R	AAAACCAATGTGCTGATACGC		hm	493 - 793
SAIL lines				
Left border LB1	GCCTTTTCAGAAATGGATAAATAGCCTTGCTTCC	60		
sig5-2_L	ATGGGACACGAGTGAAGTTTG	60	wt	900 - 1100
sig5-2_R	AACGATCTTTTGACACATCGG		hm	601 - 901
GABI KAT lines				
o2588	CGCCAGGGTTTTCCCAGTCACGACG	60	hm	680
o3269	GAAGGCGGGAAACGACAATCTG			
Elip1_ F	AACACACAGTAGGCCTAACACAGA	60	wt	870
Elip1_R	ACAACTCGACCTAATGACCTATCA			

wt – wild type; hm – homozygous; bp – base pairs

Table 9.2 PCR set up

Component	Volume for 25 µl
PCR master mix 2x	12.5 µl
Upstream Primer 10 µM	2.0 µl
Downstream primer 10 µM	2.0 µl
DNA template	1 µl
Nuclease-free water	7.5 µl

Table 9.3 PCR conditions

Step	Temperature	Time	Cycle number
Initial Denaturation	95°C	2 min	1
Denaturation	95°C	1 min	35
Annealing	Primer dependent	1 min	
Extension	72°C	1 min	
Final Extension	72°C	5 min	1
Soaking	4°C		Indefinitely

9.1.2 qRT-PCR – Primers and Conditions

Table 9.4 Primers for qRT-PCR

Primer name	Sequence	Annealing Temperature (°C)	Product size (bp)
Housekeeping			
UBC9_q_F	TCACAATTTCCAAGGTGCTGC	60	61
UBC9_q_R	TCATCTGGGTTTGGATCCGT		
AT2G_q_F	ATCGAGCTAAGTTTGGAGGATGTAA	60	61
AT2G_q_R	TCTCGATCACAAACCCAAAATG		
Genes of Interest			
TFP_q_F	TGATTGGTCTGGCCTCATTGCG	60	96
TFP_q_R	CGGGCTGTGAACATAACCATTACG		
TOC33_q_F	ATCCGGGCTGGTTCTAAGATGC	60	60
TOC33_q_R	GACTACCGCGATTGCAGAATCCTC		
RBF1_q_F	AAGCCGTTTAAGCAACGAGTGC	60	68
RBF1_q_R	GCCTTAGTCTTGTCCAACAACGC		
SIG5_q_F	CGAGGTAGTTGAGAGACTCA	60	210
SIG5_q_R	TCAATGAATCGAGCACATCG		
ELIP1_q_F	CATGGCTGAGGGAGGAC	60	192
ELIP1_q_R	AACGCTAGCAAGTCGCTAA		
CP12-2_q_F	ACAACTAACCGGATGATGAAA	60	201
CP12-2_q_R	ATCAGCCTTCTTCTTGTCTCTA		

Table 9.5 qRT-PCR set up

Component	Volume for 10 µl
SYBR Green master mix 2x	5 µl
Upstream Primer 10 µM	0.5 µl
Downstream primer 10 µM	0.5 µl
cDNA template	2.5 µl
Nuclease free water	1.5 µl

Table 9.6 qRT-PCR conditions

Step		Temperature	Time	Cycle number
Pre-Incubation		95 °C	5 min	1
Amplification	Denaturation	95 °C	10 sec	45
	Annealing	Primer dependent	10 sec	
	Extension	72 °C	10 sec	
Melting curve		95 °C	5 min	1
Cooling		40 °C		Indefinitely

9.2 Supplementary data for Chapter 3: Identification of photosynthesis phenotype in response to low fluence rates of UV-B

9.2.1 Net photosynthetic rate in *wt* (L*er*) and *uvr8-1* (L*er*) over 5 days of 1.5 µmol m^{-2} s^{-1} UV-B exposure

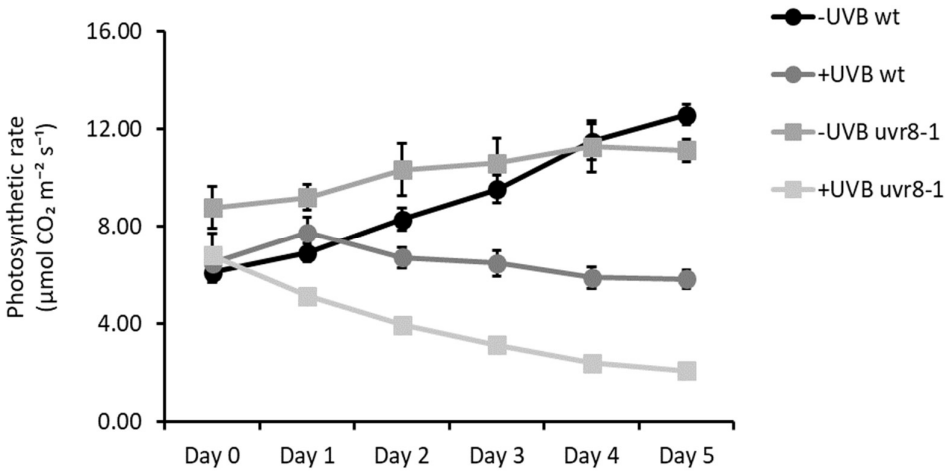

Figure 9.1 Changes in net photosynthetic rate (µmol CO_2 m^{-2} s^{-1}) in *wt* (L*er*) and *uvr8-1* (L*er*) in response to irradiation with 1.5 µmol m^{-2} s^{-1} of UV-B over 5 days. *wt* (L*er*) –UVB is represented as the black circles, *wt* (L*er*) +UVB is represented as the dark grey circles; while *uvr8-1* (L*er*) –UVB is represented as medium grey squares, *uvr8-1* (L*er*) +UVB is represented as light grey squares. Day 0 is 35 DAS and is the net photosynthetic rate prior to commencement of illumination with UV-B, while Day 1 is after 24 hours of exposure and so forth. In the +UVB condition the plants are exposed to 1.5 µmol m^{-2} s^{-1} and 220 µmol m^{-2} s^{-1} of PAR, in the -UVB condition the plants are exposed to 220 µmol m^{-2} s^{-1} of PAR only. Error bars represent ± S.E. (n = 8 biological repeats).

9.2.2 Dry weight of *wt* (L*er*) and *uvr8-1* after 5 days of 1.5 µmol m^{-2} s^{-1} UV-B exposure

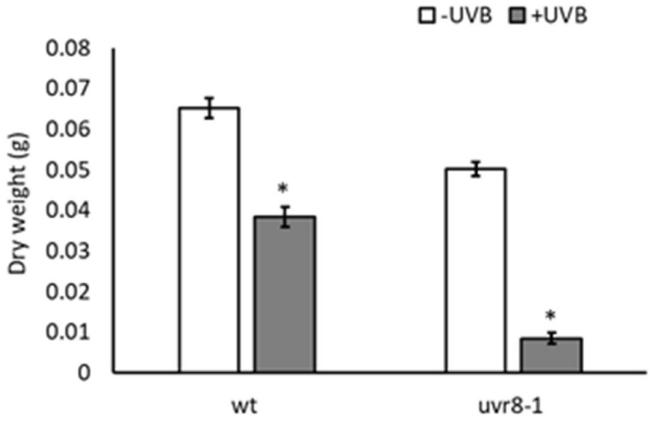

Figure 9.2 Changes in dry weight (g) in *wt* (L*er*) and *uvr8-1* (L*er*) in response to irradiation with 1.5 µmol m^{-2} s^{-1} of UV-B (+UVB, dark grey) or without (-UVB, white) at 5 days of exposure. In the +UVB condition the plants are exposed to 1.5 µmol m^{-2} s^{-1} and 220 µmol m^{-2} s^{-1} of PAR, in the -UVB condition the plants are exposed to 220 µmol m^{-2} s^{-1} of PAR only. Error bars represent ± S.E. (n = 8 biological repeats). Asterisks indicate statistically significant means (P < 0.05) between +UVB and -UVB treatments for a given time point and genotype.

9.2.3 Net photosynthesis rate of *wt* (Col-0) and *uvr8-6* (Col)

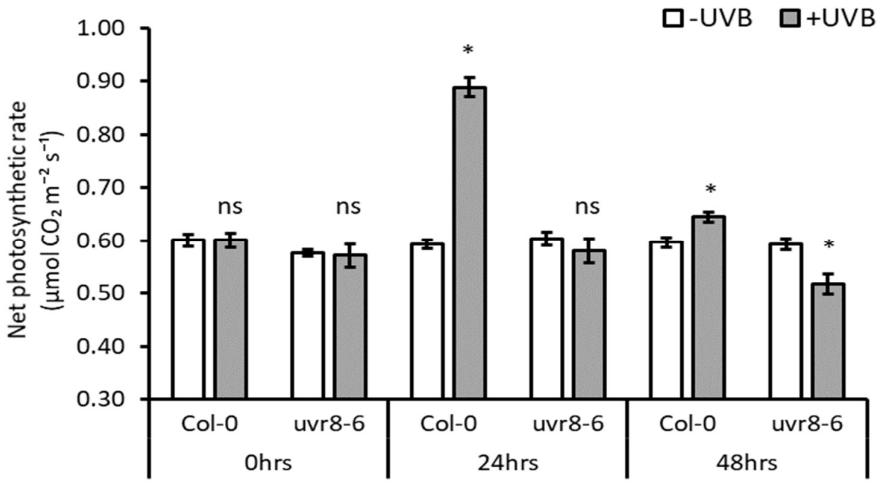

Figure 9.3 Changes in net photosynthetic rate (µmol CO_2 m^{-2} s^{-1}) normalised to leaf area in Col-0 and *uvr8-6* (Col) in response to irradiation with 0.5 µmol m^{-2} s^{-1} of UV-B (+UVB, dark grey) or without (-UVB, white) over 48 hours of exposure. 0hrs is 35 DAS and is the net photosynthetic rate prior to commencement of illumination with UV-B, while 24hrs is after 24 hours of exposure and so forth. In the +UVB condition the plants are exposed to 0.5 µmol m^{-2} s^{-1} and 220 µmol m^{-2} s^{-1} of PAR, in the -UVB condition the plants are exposed to 220 µmol m^{-2} s^{-1} of PAR only. Error bars represent ± S.E. (n = 16 biological repeats). Asterisks indicate statistically significant means (P < 0.05) between +UVB and -UVB treatments for a given time point and genotype; ns indicates not significant means.

9.3 Supplementary data for Chapter 5: Analysis of transcriptome changes in response to 0.5 µmol m^{-2} s^{-1} of UV-B

9.3.1 Confirmation of RNA-seq through qPCR analysis

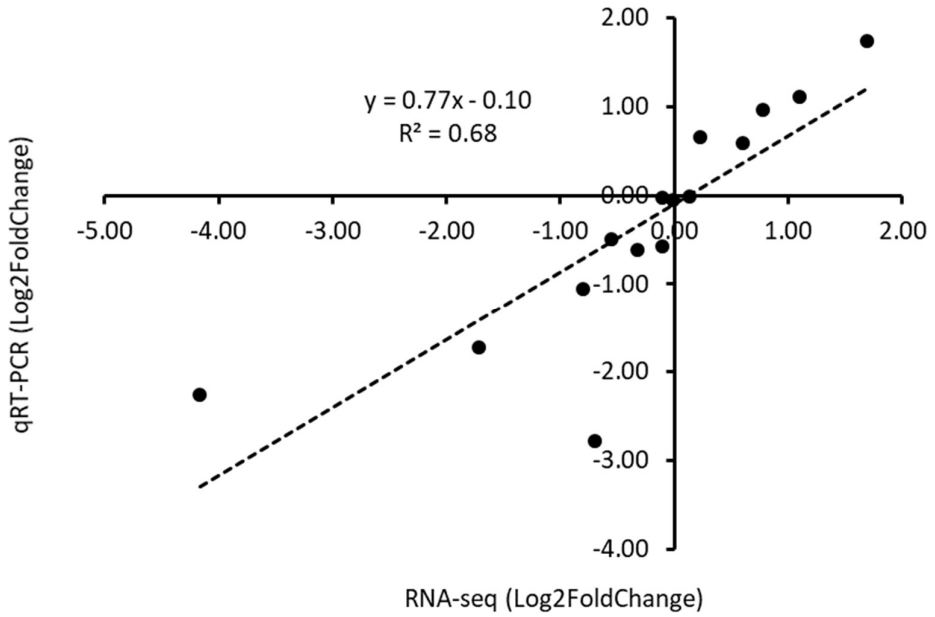

Figure 9.4 Correlation between RNA-seq and quantitative real-time PCR (qRT-PCR). Comparison of log2foldchange of 6 DEGs at different time points (0hrs, 6hrs, 24hrs) in *wt* (L*er*) obtained by RNA-seq and qRT-PCR. Strong, statistically significant Pearson correlation is shown between the expression levels measured using qRT-PCR and RNA-seq. Pearson correlation coefficients of 0.84 ($P < 0.001$) and Spearman coefficient of 0.97 ($P < 0.001$). DEGs used *CP12-2, ELIP1, SIG5, RBF1, TOC33* and *TFP.*

9.3.2 Differentially expressed genes identified in RNA-seq

Table 9.7 Significant DEGs identified at 6hrs +UVB:-UVB in *wt* (L*er*). Significance is determined by padj < 0.05. LFC – log2fold change, padj – adjusted p-value

Identifier	LFC	padj	Short Description
AT4G34730	1.10	0.00	ribosome-binding factor A family protein
AT1G52990	1.69	0.00	thioredoxin family protein
AT1G02280	0.78	0.00	translocon at the outer envelope membrane of chloroplasts 33
AT1G22550	1.00	0.00	Major facilitator superfamily protein
AT1G14010	-0.76	0.00	emp24/gp25L/p24 family/GOLD family protein
AT1G49650	0.99	0.00	alpha/beta-Hydrolases superfamily protein
AT3G57260	-1.26	0.00	beta-1,3-glucanase 2
AT2G40400	1.02	0.00	Protein of unknown function (DUF399 and DUF3411)
AT4G25570	0.76	0.00	Cytochrome b561/ferric reductase transmembrane protein family
AT4G33140	-0.60	0.00	Haloacid dehalogenase-like hydrolase (HAD) superfamily protein
AT5G50460	-0.80	0.00	secE/sec61-gamma protein transport protein
AT1G66960	-1.18	0.00	Terpenoid cyclases family protein

AT4G10500	-1.29	0.00	2-oxoglutarate (2OG) and Fe(II)-dependent oxygenase superfamily protein
AT1G27330	-0.88	0.00	Ribosome associated membrane protein RAMP4
AT3G60540	-1.09	0.00	Preprotein translocase Sec, Sec61-beta subunit protein
AT2G25110	-0.67	0.01	stromal cell-derived factor 2-like protein precursor
AT1G11670	0.86	0.01	MATE efflux family protein
AT4G30720	0.69	0.01	FAD/NAD(P)-binding oxidoreductase family protein
AT3G15536	-1.19	0.01	
AT3G51870	0.94	0.01	Mitochondrial substrate carrier family protein
AT5G54280	0.90	0.01	myosin 2
AT4G24920	-0.75	0.01	secE/sec61-gamma protein transport protein
AT1G56120	-0.87	0.01	Leucine-rich repeat transmembrane protein kinase
AT5G58940	-0.99	0.01	calmodulin-binding receptor-like cytoplasmic kinase 1
AT2G44380	-1.19	0.01	Cysteine/Histidine-rich C1 domain family protein
AT2G04270	0.59	0.01	RNAse E/G-like
AT4G08230	-0.70	0.01	glycine-rich protein
AT2G46140	-0.88	0.01	Late embryogenesis abundant protein
AT1G32780	1.20	0.01	GroES-like zinc-binding dehydrogenase family protein
AT2G43850	-0.58	0.01	Integrin-linked protein kinase family
AT1G27350	-0.78	0.01	Ribosome associated membrane protein RAMP4
AT4G21190	0.66	0.01	Pentatricopeptide repeat (PPR) superfamily protein
AT1G53250	0.77	0.01	
AT2G40890	0.59	0.01	cytochrome P450, family 98, subfamily A, polypeptide 3
AT2G47470	-0.64	0.01	thioredoxin family protein
AT3G56950	-0.65	0.01	small and basic intrinsic protein 2;1
AT3G62600	-0.78	0.01	DNAJ heat shock family protein
AT1G77510	-0.94	0.01	PDI-like 1-2
AT1G68470	-0.63	0.01	Exostosin family protein
AT5G52740	-1.15	0.01	Copper transport protein family
AT5G13360	0.69	0.01	Auxin-responsive GH3 family protein
AT5G20040	0.51	0.01	isopentenyltransferase 9
AT5G64000	-1.06	0.01	Inositol monophosphatase family protein
AT3G12930	0.65	0.01	Lojap-related protein
AT4G33110	0.97	0.01	S-adenosyl-L-methionine-dependent methyltransferases superfamily protein
AT4G20130	0.66	0.01	plastid transcriptionally active 14
AT1G21750	-0.77	0.01	PDI-like 1-1
AT1G65040	-0.69	0.02	RING/U-box superfamily protein
AT3G45290	-0.92	0.02	Seven transmembrane MLO family protein
AT1G04980	-0.93	0.02	PDI-like 2-2
AT1G68725	1.13	0.02	arabinogalactan protein 19
AT1G09490	0.42	0.02	NAD(P)-binding Rossmann-fold superfamily protein
AT1G04600	-0.94	0.02	myosin XI A
AT1G75030	0.99	0.02	thaumatin-like protein 3
AT1G70430	0.91	0.02	Protein kinase superfamily protein
AT4G22840	-0.86	0.02	Sodium Bile acid symporter family

AT1G21240	-1.09	0.02	wall associated kinase 3
AT5G58710	-0.49	0.02	rotamase CYP 7
AT3G50210	-0.66	0.02	2-oxoglutarate (2OG) and Fe(II)-dependent oxygenase superfamily protein
AT1G14880	-0.91	0.02	PLANT CADMIUM RESISTANCE 1
AT1G14360	-0.75	0.02	UDP-galactose transporter 3
AT2G18660	-1.00	0.02	plant natriuretic peptide A
AT3G62910	0.54	0.02	Peptide chain release factor 1
AT5G27830	-0.59	0.02	
AT2G22650	0.91	0.02	FAD-dependent oxidoreductase family protein
AT4G28660	0.56	0.02	photosystem II reaction center PSB28 protein
AT1G76720	0.95	0.02	eukaryotic translation initiation factor 2 (eIF-2) family protein
AT3G05410	0.59	0.02	Photosystem II reaction center PsbP family protein
AT5G47420	-0.65	0.02	Tryptophan RNA-binding attenuator protein-like
AT1G18810	1.05	0.02	phytochrome kinase substrate-related
AT2G45790	-0.58	0.02	phosphomannomutase
AT5G10740	-0.76	0.02	Protein phosphatase 2C family protein
AT5G18470	-0.98	0.02	Curculin-like (mannose-binding) lectin family protein
AT2G31830	0.83	0.02	endonuclease/exonuclease/phosphatase family protein
AT5G20130	0.55	0.02	
AT3G14395	1.08	0.02	
AT1G49490	1.07	0.03	Leucine-rich repeat (LRR) family protein
AT1G80130	-1.02	0.03	Tetratricopeptide repeat (TPR)-like superfamily protein
AT5G11920	-1.06	0.03	6-&1-fructan exohydrolase
AT4G39210	-0.84	0.03	Glucose-1-phosphate adenylyltransferase family protein
AT5G08050	0.69	0.03	Protein of unknown function (DUF1118)
AT1G16790	0.60	0.03	ribosomal protein-related
AT1G15790	-0.84	0.03	
AT5G55580	0.80	0.03	Mitochondrial transcription termination factor family protein
AT1G06690	0.74	0.03	NAD(P)-linked oxidoreductase superfamily protein
AT1G50450	0.49	0.03	Saccharopine dehydrogenase
AT4G29520	-0.81	0.03	
AT1G09932	-1.01	0.03	Phosphoglycerate mutase family protein
AT4G11175	0.53	0.03	Nucleic acid-binding, OB-fold-like protein
AT3G26230	-0.84	0.03	cytochrome P450, family 71, subfamily B, polypeptide 24
AT1G57770	0.61	0.03	FAD/NAD(P)-binding oxidoreductase family protein
AT5G03700	0.99	0.03	D-mannose binding lectin protein with Apple-like carbohydrate-binding domain
AT1G66840	0.59	0.03	Plant protein of unknown function (DUF827)
AT3G28460	0.53	0.03	methyltransferases
AT3G03630	0.73	0.03	cysteine synthase 26
AT3G07680	-0.43	0.04	emp24/gp25L/p24 family/GOLD family protein
AT5G34850	0.53	0.04	purple acid phosphatase 26
AT5G57345	0.80	0.04	
AT4G14510	0.50	0.04	CRM family member 3B
AT4G25000	-0.93	0.04	alpha-amylase-like

AT5G02860	0.74	0.04	Pentatricopeptide repeat (PPR) superfamily protein
AT1G58225	-0.94	0.04	
AT3G29250	-1.02	0.04	NAD(P)-binding Rossmann-fold superfamily protein
AT2G31750	0.88	0.04	UDP-glucosyl transferase 74D1
AT4G38160	0.61	0.04	Mitochondrial transcription termination factor family protein
AT1G78410	-0.95	0.04	VQ motif-containing protein
AT1G27940	0.97	0.04	P-glycoprotein 13
AT2G45400	0.88	0.04	NAD(P)-binding Rossmann-fold superfamily protein
AT4G05320	-0.47	0.04	polyubiquitin 10
AT3G50920	-0.42	0.04	Phosphatidic acid phosphatase (PAP2) family protein
AT3G07580	-0.70	0.04	
AT4G23150	-0.96	0.04	cysteine-rich RLK (RECEPTOR-like protein kinase) 7
AT3G14330	0.69	0.04	Tetratricopeptide repeat (TPR)-like superfamily protein
AT5G24150	0.98	0.04	FAD/NAD(P)-binding oxidoreductase family protein
AT1G11430	0.43	0.05	plastid developmental protein DAG, putative
AT5G10380	-0.77	0.05	RING/U-box superfamily protein
AT3G15620	0.98	0.05	DNA photolyase family protein
AT5G57180	0.77	0.05	chloroplast import apparatus 2
AT3G08870	-0.63	0.05	Concanavalin A-like lectin protein kinase family protein

Table 9.8 Significant DEGs identified at 24hrs +UVB:-UVB in *wt* (L*er*). Significance is determined by padj < 0.05. LFC – log2fold change, padj – adjusted p-value

Identifier	LFC	padj	Short description
AT5G17030	1.49	0.00	UDP-glucosyl transferase 78D3
AT2G22960	1.42	0.00	alpha/beta-Hydrolases superfamily protein
AT5G62210	1.34	0.00	Embryo-specific protein 3, (ATS3)
AT2G47460	1.24	0.00	myb domain protein 12
AT4G27570	1.17	0.00	UDP-Glycosyltransferase superfamily protein
AT2G23180	1.13	0.00	cytochrome P450, family 96, subfamily A, polypeptide 1
AT1G78440	1.18	0.00	Arabidopsis thaliana gibberellin 2-oxidase 1
AT2G22590	1.15	0.00	UDP-Glycosyltransferase superfamily protein
AT2G36750	1.13	0.00	UDP-glucosyl transferase 73C1
AT1G65560	1.12	0.00	Zinc-binding dehydrogenase family protein
AT5G08640	1.08	0.00	flavonol synthase 1
AT5G17040	1.09	0.00	UDP-Glycosyltransferase superfamily protein
AT4G30470	1.10	0.00	NAD(P)-binding Rossmann-fold superfamily protein
AT1G02205	1.09	0.00	Fatty acid hydroxylase superfamily
AT1G64340	0.99	0.00	
AT2G30300	1.07	0.00	Major facilitator superfamily protein
AT3G62610	1.07	0.00	myb domain protein 11
AT1G27940	1.00	0.01	P-glycoprotein 13
AT1G78570	1.00	0.01	rhamnose biosynthesis 1
AT3G13790	1.05	0.01	Glycosyl hydrolases family 32 protein
AT1G45207	-0.64	0.01	Remorin family protein

AT4G15480	1.02	0.01	UDP-Glycosyltransferase superfamily protein
AT4G25850	1.04	0.01	OSBP(oxysterol binding protein)-related protein 4B
AT5G49330	0.96	0.01	myb domain protein 111
AT5G65165	1.00	0.01	succinate dehydrogenase 2-3
AT3G24750	0.90	0.01	
AT2G42380	-0.86	0.01	Basic-leucine zipper (bZIP) transcription factor family protein
AT4G14560	-0.84	0.01	indole-3-acetic acid inducible
AT1G65060	0.98	0.02	4-coumarate:CoA ligase 3
AT5G44110	0.96	0.02	P-loop containing nucleoside triphosphate hydrolases superfamily protein
AT1G23440	0.56	0.02	Peptidase C15, pyroglutamyl peptidase I-like
AT3G10185	-0.96	0.02	Gibberellin-regulated family protein
AT3G20360	0.83	0.03	TRAF-like family protein
AT1G12570	0.78	0.03	Glucose-methanol-choline (GMC) oxidoreductase family protein
AT5G01520	0.70	0.03	RING/U-box superfamily protein
AT4G17680	-0.75	0.03	SBP (S-ribonuclease binding protein) family protein
AT1G64400	0.88	0.03	AMP-dependent synthetase and ligase family protein
AT4G02360	0.92	0.04	Protein of unknown function, DUF538
AT1G36160	0.83	0.04	acetyl-CoA carboxylase 1
AT3G19450	0.83	0.04	GroES-like zinc-binding alcohol dehydrogenase family protein
AT2G35770	0.77	0.04	serine carboxypeptidase-like 28
AT5G09930	0.91	0.05	ABC transporter family protein
AT4G21200	0.89	0.05	gibberellin 2-oxidase 8

Table 9.9 Significant DEGs identified at 0hrs *mt*:*wt* +UVB. Significance is determined by padj < 0.05. LFC – log2fold change, padj – adjusted p-value

Identifier	LFC	padj	Short Description
AT4G16215	2.21	0.00	
AT5G46760	1.05	0.00	Basic helix-loop-helix (bHLH) DNA-binding family protein
AT5G46750	0.98	0.00	ARF-GAP domain 9
AT1G54360	-1.10	0.00	tbp-associated factor 6b
AT3G43340	-1.09	0.00	Pseudouridine synthase family protein
AT3G30700	-0.94	0.00	transposable element gene
AT4G21090	0.65	0.00	mitochondrial ferredoxin 2
AT3G02520	0.48	0.00	general regulatory factor 7
AT1G22170	0.62	0.05	Phosphoglycerate mutase family protein